KOMUNIKÁCIE
COMMUNICATIONS

OPERATION AND ECONOMICS

MECHANICAL ENGINEERING

ELECTRICAL ENGINEERING

Dewi Budhiartini Juli Isnaini

CONSUMER PERSPECTIVE ON PUBLIC TRANSPORT: THE MEDAN–PEMATANG SIANTAR ROUTE AS A CASE STUDY

Development of public transportation is meant to bridge the divide between cities and encourage development results. The inter-city transportation opens up opportunities for the inter-city trade, reduces costs and increases labor mobility, thereby promoting the inter-city development opportunities. This study uses the factor and cluster analyses. Analysis of factors is performed to determine the most dominant factors. The cluster analysis is used to identify the advantages and disdvantages of five modes of transport, namely taxi, trade rail, economy bus, mini bus, and executive bus. This study aims to determine the perception of users of Medan-Pematang Siantar route service. The results of this study show that there are five dominant factors that are considered before the service users decide on the mode of transport to use, namely the comfort factor, which is the most important consideration, followed by the time factor, cost factor, accessibility factor and safety factor.

Keyword: *consumer's perspective, public transportation, inter-city trade*

1 Introduction

Development is a continuous process and it involves a plan to improve people's lives in various aspects. Transportation is an important aspect of development. Most aspects of human life involve transportation. Transportation develops along with the progress in human life and culture.

Development of the public transportation bridges the gap between cities and promotes development. The inter-city transportation provides opportunities for trade between cities and increases labor mobility, thereby promoting inter-city development opportunities.

In cities, transportation supports the achievement of labor or workplace needs, school needs, public needs and rural needs. In addition to meeting the needs of people, transportation is required to move goods from one place to another. Transportation has a direct impact on trade. It results in increased trade and inter-regional communications [1].

A study [2] mentions the development objectives of the land transportation department from 2005-2009, which focused on the preservation and development of transportation: (1) rehabilitation of roads is a priority in the development of road transportation; (2) development of municipal transportation, especially in major cities, is primarily concerned with the development of rail-based road transport, enabling the reduction of using the private cars and improving the efficiency of public transport; (3) development of the railway transportation is primarily concerned with the restoration of railway infrastructure to the normal state level, which involves maintenance activities to improve safety and ensure smooth operation.

Standard transportation facilities and good highway network are required to achieve efficient modes of transportation. The Medan-Pematang Siantar route connects two cities located in the North Sumatra region, with a distance of 120 km between them. The population of Medan City is estimated at two million people and it is a city that functions as the center of trade, tourism and government of North Sumatra. Pematang Siantar City has a population of around 300 thousand people and it is a city that functions as a trade center; the city is a transit to tourist attraction sites in cities such as Parapat, Berastagi and Samosir Island. Both cities are closely linked, both economically and culturally.

Medan-Pematang Siantar transportation route is crowded with various modes of public transportation, but the most common is bus transportation. Buses full of passengers are often seen since many people depend on the bus transportation, which is an economical mode of transport. Taxis are also common along the Medan–Pematang Siantar route, but they are often involved in accidents due to speed exceeding the limits stipulated by traffic regulations. However, other modes of transportation, such as executive trains and buses, are not considered by many passengers. In addition, the movement of people and goods between the cities of Medan and Pematang Siantar is increasing from year to year. This causes the public transportation needs to increase, as well.

The phenomenon described above attracts the attention of researchers. This study evaluates the transportation services between the cities of Medan and Pematang Siantar, as well as the perception of users of public transportation services regarding the reason for choosing a particular

Dewi Budhiartini Juli Isnaini
University of Amir Hamzah, Indonesia
E-mail of corresponding author: dewibudhiartinijuliisnaini@gmail.com

public transportation mode along the Medan-Pematang Siantar route.

2 Conceptual framework

2.1 Consumer perception

To understand a person's perception in the selection of any of the transport services listed in this chapter, it is important to understand consumer behavior towards other services. Therefore, the user's perception of public transport services is described based on the knowledge of the consumer behavior.

2.1.1 Understanding consumer perception

A study suggests that companies that truly understand consumer perceptions of external properties, pricing and different ad approaches have a great advantage over their competitors [3]. Some studies indicate that understanding the consumer and the process of consumption of goods are important in analyzing user decisions [4-5].

The ability to keep the user (consumer supremacy) is the underlying principle of all the marketing activities [6]. This principle emphasizes that the consumer is the goal of marketing. A study [7], derived from [4-5], pointed out that marketing is the whole business dealings seen from the point of view of the end-user.

User behavior is defined as a person's decision-making process and physical activity involving the processes of assessing, acquiring and using goods and services [8]. Furthermore from [9], indicated that a persons behavior is shaped by planning, buying and usage of economic goods and services.

In addition, [8] stated that individuals always choose the goods or services they deem to be capable of providing maximum satisfaction in the process of evaluating goods and services.

Consumer perception is also defined as the study of buying and exchange processes involving procurement and disposal of goods, services, experiences and ideas. A user cannot avoid the exchange process, i.e. all the resources are exchanged between the two parties [4-5]. The American Marketing Association, as cited by [10], defines the user behavior as the dynamic interaction of affect and cognition, behavior and surrounding events by which people carry out the exchange aspects of their lives.

From the explanations of experts, one can conclude that the behavior of a person, group or organization, related to obtaining and using goods or services, may be affected by the environment.

According to [11], the most appropriate source of marketing in a service output tends to be on personal resources. The personal resources are more important in influencing the purchase of a single service.

2.2 Transport services

2.2.1 Understanding public transport

The public transport refers to public service vehicles used to transport passengers who pay certain fares as payment for the trip. Vehicles used in public transport may be owned and maintained independently or by public bodies, such as local governments, municipalities and private companies, either for social or profit-making purposes.

The public transport is one of the the most important parts of a society, as transport is closely related to community locations and activities, as well as the availability of goods and services. Transport is defined as the transfer of persons and goods from one place to another for a particular purpose. Therefore, it is clear that transport is only a tool to overcome distance, which geographically separates human needs.

Transportation services provided by transportation services company is a type of service output. In general, service outputs have four basic forms: real, holdable, inseparable from entrepreneurs and cannot be saved.

Transport is defined as a process of transfer and this process cannot be separated from the need for supporting tools to ensure smooth transition at the desired time [12].

2.2.2 Transport service level

The service level is a measure of the overall performance of a service and it influences the perceptions of service users. Service level is a basic element of transport, since users are attracted to use a transport service based on travel behavior. The main factor used in assessing the level of transport services can be divided into three groups, namely [13]:

Elements that affect service users, such as operating speed, trust and safety.

Elements of quality of service account for qualitative services, including comfort, passenger perception, beauty and cleanliness.

Fares that must be paid by the service user for the service.

2.3 Transport modes

2.3.1 Definition of the transport mode

To analyze the transportation demands, [5] reviewed three key components of the transport mode: Transport mode as a representative of various transport elements (T), activity modes as a representative of socioeconomic activity (A), and transport flow pattern as a representative of movement of goods and persons according to origin (F). The interactions of the three components are shown in Figure 1.

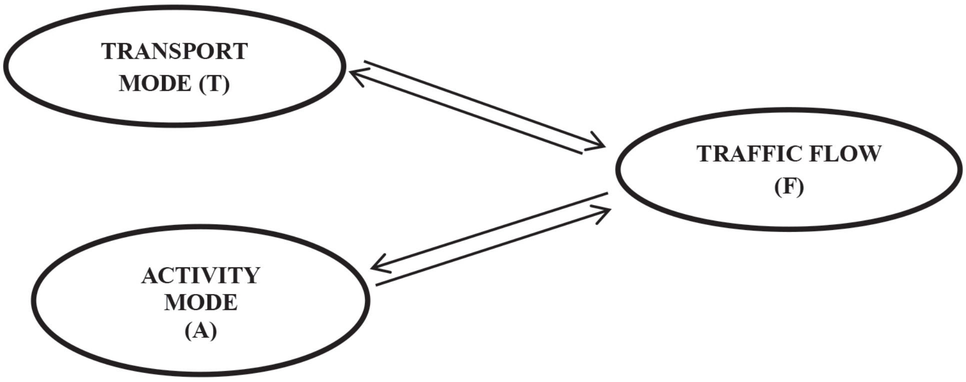

***Figure 1** Basic Relationship between the Components of Mode of Transport [5], (A) stands for Activity Mode, (T) stands for Transport Mode, (F) stands for Traffic Flow*

Figure 1 shows that traffic flow pattern (F) is strongly influenced by the transport mode (T) as supply and activity mode (A) as demand. In contrast, (F) through its serviceability may also affect (A) in providing the service.

Likewise, (T) changes based on (F), for example by building a new road. An issue that attracts attention while analyzing transport problems is that there is no direct relationship between (T) and (A). If they influence each other, then a change in (T) or (A) would result in a change in (F), which in turn affects one or both of them. This situation will result in balance and at all times lead to a state of mutual influence.

Transport service users, in selecting a particular mode of transportation, may be influenced by the situation or personal impulse [14]. Influence of the situation can be explained by the service level of the modes of transport and environmental factors at ta ravel time. On the contrary, personal impulses are heavily influenced by lifestyle aspirations and basic needs that make up a person's motivation to travel. Further, regarding situational influence, there is a direct factor that influences the service level of the transport service operator. According to [12], this factor is called factor of consideration in determining the level of services, i.e. time factor, travel cost factor, distance factor and societal income.

Environmental factors, such as place factor (comprising distance and facilities needed for transport services), are indirect factors influencing service operators and users of transport services [15]. The place factor is an added value offered by transport operators to transport service users according to the mode of transportation provided. The ecommerce environment factor is also categorized as an external factor because of the nature of the operators of the transport services.

From the above explanations, to obtain with certainty the reason for choosing the various transport modes in the Medan-Pematang Siantar route by passengers, it is necessary to consider the form of service offered by each passenger transport mode (as part of the internal factors), as well as the travel requirements and motivation influenced by the socio-economic level of the passenger (as part of the external factor).

2.3.2 Modes of public transport

The available modes of public transport in various places in Indonesia are categorized as follows:

- Big Bus (city bus)
- Simple bus (micro bus)
- Inter city bus
- Rental car
- Public passenger vehicles (taxis)
- Freight transport vehicles

In operation, public transport, according to Government Regulation of the Republic of Indonesia No. 44 of 1993, can be distinguished as follows:

- Transport of people in regular and irregular routes;
- Transport of people that are not in the path.

Intercity transport takes place from one city to another using public buses that have organized routes. Some transport service operators pick up passengers from door to door. The big bus is a bus equipped with 35 to 102 seats excluding the seat of the driver and without the carriage of goods. The simple bus is a bus equipped with 24 seats excluding the driver's premises and without freight services. The small bus is a bus equipped with 9 to 20 seats excluding the seat of the driver and without the carriage of goods.

3 Analysis of public transportation facilities along the Medan-Pematang Siantar route

Analysis of the Medan-Pematang Siantar route's public transport facilities is done under the following subheadings.

3.1 Dominant factors

Result of the data processing regarding the service perception of users is obtained by collecting users' data before taking a trip using public passenger transport from Medan to Pematang Siantar. From that data, there are 5 factors comprising a set of initial variables.

***Table 1** Matrix factor loading analysis*

Variable	Factor				
	Comfort	Accessibility	Cost	Time	Safety
X1	.4829	-.0799	.2075	-.3117	.0352
X2	.0332	.7077	.2121	.0869	.1696
X3	.5261	.0910	.1367	.3615	.1204
X4	.0019	.7114	.0645	-.3272	-.0488
X5	.5776	-.0831	.2654	-.0521	-.0100
X6	-.1308	-.1226	-.0186	.7817	-.0529
X7	.6409	.1163	.2898	-.1420	.0701
X8	.5629	.3467	-.2804	.1505	.0841
X9	-.1895	-.0296	.2866	.7444	-.0227
X10	.5574	.1776	-.1842	-.0909	.0448
X11	.1651	.5405	.2029	.2767	.0103
X12	.3636	.0705	.4813	-.1823	.1036
X13	.1745	.5911	-.0414	-.2073	-.1892
X14	-.0265	.1073	.6379	.0033	.1304
X15	.1668	.3247	.5802	.1632	-.0857
X16	.1253	-.0018	.6093	.1828	-.0568
X17	.4835	-.0311	-.0950	-.0957	-.5758
X18	.4518	.0398	-.0399	-.0131	.7016
X19	.3812	-.1136	.1067	-.1533	.6550

Source: Data Processing Results

The next step is to determine the dominant variables that form factors in succession, to be considered and renewed on the perception of a user's desire before they travel using public passenger transport from Medan to Pematang Siantar . Each factor has been identified and named based on the factor loading of the variable. The number of factors shows a correlation between one variable and another when a factor is formed. The magnitude of the factor loading of each variable is shown in Table 1.

An initial variable is said to be significant and can be grouped into a factor when it has an absolute value of factor loading ≥ 0.3. Variables that make up the factor with the highest factor loading are the most dominant variables in that factor. Likewise, the greatest-value factor of the two factors indicates the dominant variables of the two factors, thus the last variable. When a distortion has an absolute value of factor loading ≤ 0.3, then the variable will be ignored because it is considered insignificant.

3.1.1 Comfort factor

This factor is the most important factor influencing passenger's judgment regarding the transport mode to use from Medan to Pematang Siantar. It involves 6 initial variables having an absolute value of factor loading ≥ 0.3.

The dominant variables that make up this factor, as shown in Table 1 above, are the employee's hospitality at the terminal and vehicle workers on the route (X_{14}), airflow system and temperature regulation in the vehicle (X_{16}), seat comfort ($X_1$2) in the vehicle (X_{15}).

Values in Table 1 above show that these six initial variables have a high level of interdependence on each other. These six initial variables were taken from the comfort factor, namely X_{14}, X_{16}, X_{12}, X_{15}, X_{13}, and X_{17}. A study [13] states that one of the main traits of transport is comfort and pleasure. In this study, there are several initial variables that show the fun factor combined with other factors. The comfort factor has the highest variance of 3.7398%. This means that 3.7398% of the respondents' responses about the route were influenced by the comfort factor.

The overall average value of the comfort factor shown by the initial variable is $\frac{X_{14}+X_{16}+X_{12}+X_{15}+X_{18}+X_{17}}{6}=3.7787$. This indicates that the comfort factor is very important for every passenger. Therefore, passenger transport service operators who pass through the Medan-Pemantar Siantar route should consider and pay attention to the comfort factor of the service.

3.1.2 Accessibility factor

This factor is the fourth most important factor influencing an individual's judgment regarding the transport mode to be used from Medan to Pematang Siantar . It involves 2 initial variables that have absolute value of factor loading ≥ 0.3.

The dominant variables that make up this factor are described as follows:

X_{18}: Convenience to the departure point is the convenience to get to the terminal at the departure point. It has a factor loading of 0.398 (Table 1).

X_{19}: Facilities that reach the final destination from the terminal at the end of the route. It has a factor loading of 0.1136.

These values indicate that the two initial variables have high dependence on each other. Both variables are derived from the comfort and accessibility factors, associated with the convenience of access to transport services (both infrastructure and transport facilities) from origin to destination and from vehicle stopping to final destination. These two factors are also called convenience factors.

The accessibility factor has a variance of 1.9508%, obtained from the assessments carried out by passengers influenced by convenience factors (Table 1). The overall average value of the accessibility factor shown by the initial variables is $\frac{X_{18}+X_{19}}{2}=3.9336$ and indicates that this factor is considered to be very important for passengers.

3.1.3 Cost factor

This factor is the third most important factor influencing an individual's judgment regarding the transport mode to use from Medan to Pematang Siantar. It involves two initial variables that have an absolute value of the factor loading ≥ 0.3.

The dominant variables that form this third factor are described:

X_6: The cost of the main route is the total cost that the service user must pay for the journey from Medan to Pematang Siantar. It has a factor loading of 0.186 (Table 1).

X_7: The additional cost is the total cost incurred by travellers such as the cost of transport within the city from the original destination to another, parking and so on. It has a factor loading of 0.2898.

This means that the above variables are the third most important factor that can influence the respondents' decision while travelling through the Medan-Pematang Siantar route. These values indicate that the two variables have a high degree of mutual dependence on each other, and it appears that they are more dominated by cost factor, such as the cost incurred by the passenger from departure to the end destination.

The cost factor has a variance of 5.4330% derived from assessment of respondents influenced by the cost factor. The overall average value of the cost factor shown by the initial variables is $\frac{X_6+X_7}{2}=4.1638$ which indicates that this factor is considered important for travellers.

3.1.4 Time factor

This factor is the second most important factor influencing an individual's judgment regarding the transport mode to use from Medan to Pematang Siantar. It involves four initial variables that have absolute value of factor loading ≥ 0.3.

The dominant variables that make up this factor are shown:

X_4: The passage of time is either found to deviate from the average travel time or not. It has a factor loading of 0.3272

X_2: The additional route time is the time it takes to travel from home to departure (in Medan) and from transit (in Pematang Siantar) to the final destination. It has a factor loading of 0.0869.

X_1: The main route time is the time taken to travel from the departure point to the transit point. It has a factor loading of 0.3117.

X_3: The transfer time is the time taken during the change of vehicle and while waiting for the vehicle to depart. It has a factor loading of 0.3615.

This means that the above four variables are the second most important factor that can influence the respondents' decision when travelling through the Medan–Pematang Siantar route.

This suggests that these four initial variables have high interdependence on each other. These four initial variables are taken from the time factor, which is related to the total travel period (from departure to the final destination).

This factor has a variance of 18.6220%, obtained from responses of respondents influenced by time factor. The overall average value of the time factor shown by the initial variables is $\frac{X_4+X_2+X_1+X_3}{4}=4.0830$ which indicates that this factor is very important for travellers.

Therefore, passenger transport service operators on the Medan–Pematang Siantar route should consider and pay attention to the time factor of their service product.

3.1.5 Safety factor

This factor is the last factor influencing an individual's judgment regarding the transport mode to take from Medan to Pematang Siantar. It involves five initial variables that have absolute value of factor loading ≥ 0.3.

The dominant variables that make up this factor are shown:

X_8: Passenger safety is the possibility of road safety, which can lead to human security. It has a factor loading of 0.0841 (Table 1).

X_{10}: Security from possible criminal offenses against passengers, such as theft. It has a factor loading of -0.0448.

X_5: Daily traffic frequency is the level of routing frequencies performed by the daily transport modes involved. It has a factor loading of -0.0100.

X_9 : Baggage damage caused by carelessness or tremors during the trip. It has a factor loading of -0.0227.

X_{11} : Safety equipment refers to the facilities that are available for personal safety in an emergency. It has a factor loading of 0.0103.

This means that the above five variables are the last factor that can influence the respondents' decision regarding the trip from Medan to Pematang Siantar . The values indicate that these five variables have a high degree of mutual dependence on each other. Four of these five variables are derived from the safety factor, relating to the level of security of passengers and baggage throughout the trip, including while waiting at the departure point. Only one variable is derived from the time factor.

Safety factor has a variance of 6.1619%, which is derived from responses of respondents influenced by safety factors. The overall average value of the safety factor shown by the initial variables is $\frac{X_8 + X_0 + X_5 + X_9 + X_{11}}{5} = 3.8560$ and indicates that this factor is considered to be very important for travellers. Therefore, entrepreneurs should consider and pay attention to the safety factor of their passengers.

4 Conclusion

This study uses factor and cluster analyses. Analysis of factors was performed to determine the most dominant out of five factors. The cluster analysis was used to determine advantages and disadvantages of five modes of transport, namely taxi, trade rail, economy bus, mini bus, and executive bus.

This study aimed to find out the perceptions of users of Medan-Pematang Siantar route. The results of the study show that there are five dominant factors that are considered before service users decide on the mode of transport to use, namely comfort factor, which is the most important consideration, followed by time factor, cost factor, accessibility factor, and safety factor.

The average advantages of the five modes of transport along the Medan-Pematang Siantar route is seen from the five factors of comfort, time, cost, accessibility and safety based on the market segments that each one possesses. So, generally, the most favored are taxis, executive buses, mini buses, trade trains and economic buses.

References

[1] AZIS, I. J. *Regional economics and some of its applications in Indonesia* (in Bahasa Indonesia). Jakarta: LP-FEUI, 1994. ISBN 979-814-035-4.

[2] The Ministry of Transportation of Indonesia. Profile of Medan, Bertari City. Development Planning Agency at Sub-National Level. Medan: Pemko Medan. 2003.

[3] SCHIFFMAN, L. G. *Consumer behaviour.* Prentice Hall, 1997. ISBN 072-480-220-7.

[4] MOWEN J. C., MINOR, M. *Consumer Behavior* (in Bahasa Indonesia). Vol. 1, 5th ed., Jakarta: Erlangga, 2002. ISBN 979-688-318-x.

[5] MOWEN J. C., MINOR, M. *Consumer behavior* (in Bahasa Indonesia). Vol. 2, 5th ed. Jakarta: Erlangga, 2002. ISBN 79-688-319-8.

[6] KOTLER, P. *Marketing management: analysis, planning, implementation, and control.* 9. ed. Upper Saddle River, NJ: Prentice Hall International, 1997. ISBN 013-261-363-8.

[7] DRUCKER, P. *The practice of management.* Allied Publishers, 1975. ISBN 817-023-030-6.

[8] LOUDON, D. L., DELLA BITTA, A. J. *Consumer behvior: Concepts and applications.* 4. ed. New York: Singapore: McGraw-Hill, 1993. ISBN 007-112-511-6.

[9] SUMARWAN, U. *Consumer behavior: Theory and its application in marketing* (in Bahasa Indonesia). Jakarta Selatan: Penerbit Ghalia Indonesia, 2009. ISBN 979-450-451-3.

[10] *PETER, J. P., OLSON, J. C. Consumer behaviour and marketing strategy* (in Bahasa Indonesia). Jakarta: Erlangga, 2000. ISBN 979-411-736-6.

[11] MURRAY, K. B. A Test of services marketing theory: Consumer information acquisition activities. *Journal of Marketing* [online]. 1991, **55**(1), p. 10-25. ISSN 0022-2429. Available from: https://doi.org/10.2307/1252200

[12] MIRO, F. *Transportation Planning.* Jakarta: Erlangga, 2004. ISBN 9789790993112.

[13] MANHEIM, L. M. *Fundamentals of transportations systems analysis. Vol. 1: Basic conseps.* London: MIT Press, 1979. ISBN 978-0262131292.

[14] KUSBIANTORO, X. *A Study of urban mass transit performance: consep measurement and explanation.* Ph.D. dissertation. University of Pensylvania, Philadelphia, 1985.

[15] BEN-AKIVA, M. E., LERMAN, S. R. *Discrete choice analysis: Theory and application to travel demand.* Cambridge, MA: MIT Press, 1985. ISBN 978-0262022170.

[16] BEN-AKIVA, M. E., LERMAN, S. R. *Discrete choice analysis: Theory and application to travel demand.* Cambridge, MA: MIT Press, 1985. ISBN 978-0262022170.

Martin Vlkovsky

IMPACT OF VEHICLE TYPE AND ROAD QUALITY ON CARGO SECURING

The article is concerned with comparison of the three transportation experiments using the two vehicle types (Tatra 810 and Tatra 815 MK IV) on two road types (higher and lower quality). From the transportation experiments, three datasets were obtained to be compared mutually and to the normatively determined values of acceleration coefficients, as well. In the article, the calculation of the probability of excess and double excess of the normatively determined limits is also included. For the purpose of the comparison, statistical tests of equality and three different parameters are employed. Statistically significant differences between the datasets are the outcome of the article, i.e. there are statistically significant differences between the vehicles and roads tested with regard to generated shocks. The results are primarily usable in the cargo securing system optimisation in road transportation and transport safety.

Keywords: *transportation, cargo securing, acceleration coefficient, comparison, statistical test*

1 Introduction

Since 2013, the amount of cargo transported via roads within the European Union (EU) has been slowly growing. The situation is similar in the Czech Republic. The year 2018 will not be an exception; in spite of the fact that there is no available data from Belgium yet, the amount of cargo transported via roads within the EU (15,114,072 thousand tons) is higher than in the previous year (14,668,624 thousand tons) [1]. Provided that the amount of road-transported cargo in Belgium is analogical to the previous 5 years, i.e. approx. 300,000 tons, the increase in the amount of road-transported cargo in 2018, if compared to 2017, will be more than 5 %. When comparing the estimation for 2018 (15,414,072 thousand tons of transported cargo), the increase, as against 2013 (13,772,040 thousand tons), is almost 12 % [1]. The number of people killed in road accidents within the EU has been rather stagnating and the data is only available for 2017 (25,257 casualties). The difference against 2013 is slightly positive; the number of casualties has decreased by more than 2.6 % from the total of 25,942 [2].

The growing amount of cargo transported within the EU makes higher demands on transport infrastructure, which often cannot be maintained and fixed as required by individual EU countries. In general, the lower road quality results in greater shocks during the transport, and if the cargo securing system was not adapted, the probability of cargo loosening grows, which may, in consequence, lead to a road accident. According to European Commission Directorate-General for Energy and Transport (currently European Commission Diractorate-General - Mobility and Transport) estimations, as much as 25 % of truck road accidents are caused by inappropriate or insufficient cargo securing [3]. Should the estimation (25 %) be applied to the Czech Republic in 2018, out of the total of 21,889 road accidents, 52.7 % are caused by truck drivers (11,542 accidents) [4-5]. Hence, it follows from the European Commission estimation that in 2018 inappropriate cargo securing resulted in 2,886 truck road accidents, which makes for 13.2 % of the total number of road accidents in the Czech Republic. For the sake of comparison, a highly discussed problem - drink driving - was the cause of 4,626 accidents in 2018, which makes for 21.1 % out of the total number of road accidents, and drugs were detected in 260 road accidents, which makes for "only" 1.2 % [4].

2 Literature review

The issue of cargo securing is dealt with in a number of reference texts. A crucial source of cargo securing principles for selected transportation types (road, railway and sea) within the EU (Czech Republic) is EN 12195-1:2010 standard that describes several methods of cargo securing, including the formulas for the calculation of securing forces [6]. Cargo securing by means of textile lashing straps is described in linking standard EN 12195-2:2003 [7]. Cargo fixation in road vehicles is also covered in two more standards EN 12640:2019 and EN 12642:2016 [8], concentrating on fixing points and car body construction [9-10]. The above-mentioned standards have been detailed in a comprehensive document "European Best Practice Guidelines on Cargo Securing for Road Transport" [3]. The best practice examples within the EU are also based on "IMO/ILO/UNECE Code of Practice for Packing of Cargo Transport Units (CTU Code)" [11]. In monographs, the issue of cargo securing is discussed rather marginally. The issue

Martin Vlkovsky
Department of Logistics, Faculty of Military Leadership, University of Defence in Brno, Czech Republic
E-mail of corresponding author: martin.vlkovsky@unob.cz

of securing by means of the top-over lashing method is dealt with in T. Lerher's book "Cargo Securing in Road Transport Using Restraining Method with Top-over Lashing" that is complemented with case studies from the cargo securing sphere [12]. A detailed description of respective models can be found in a monograph by G. Grossmann and M. Kassmannova "Transport Safe Packaging and Cargo Securing" [13]. In reference articles, the issue of cargo securing is covered less often, as well. Cargo securing using EN 12195-1:2010, or EN 12195-2:2003 is described in articles [14-15]. The same problem is solved in other papers and focused mostly on cargo securing by fastening straps, e.g. [16-17]. An experimental approach to analyse the acceleration of vehicle was chosen in paper [18]. The issue of cargo securing a transport safety in a selected region (country) is dealt with in [19-21].

3 Transportation experiment

In order to obtain the data, three measurements (transportation experiments) were taken using respective vehicles on respective types of roads without cargo. For the first two transportation experiments, from which datasets formally designated as d_1 and d_2 were obtained, an off-road truck Tatra 810-V-1R0R26 13 177 6×6.1R (further in the text only "Tatra 810") [22] was used. Tatra 810 has gross weight of 13,000 kg and curb weight 8,500 kg. The front axle of the vehicle is suspended by coil springs and the rear axle by leaf springs in a rocker arm arrangement. In the third transportation experiment, from which the dataset d_3 was obtained, container carrier Tatra 815-260R81 36 255 8×8.2 Multilift MK IV (further in the text only "Tatra 815 MK IV") [23] was used. Tatra 815 MK IV has gross weight 32,000 kg and curb weight 15,500 kg. The front axle is suspended by leaf springs and the rear axle by combination of leaf springs with compressed air bellows. The first (d_1) and third (d_3) experiments were carried out on a high-quality road - highway [24], while the second (d_2) experiment was carried out on a low-quality road - Class III road:

d_1 - in total measured values n_1 = 4,059 (1,353 per axis), highway transportation between Vyskov and Brno, average speed v_1 = 71.84 km·h^{-1}, distance s_1 = 27.0 km, Tatra 810;

d_2 - in total measured values n_2 = 1,182 (394 per axis), Class III road transportation between Vyskov and Dedice, average speed v_2 = 39.29 km·h^{-1}, distance s_2 = 4.3 km, Tatra 810;

d_3 - in total measured values n_3 = 4,059 (1,353 per axis), highway transportation between Vyskov and Brno, average speed v_3 = 71.84 km·h^{-1}, distance s_3 = 27.0 km, Tatra 815 MK IV.

The transport conditions of the experiments were optimal - excellent visibility, dry road, no rainfall and temperatures between 7 °C and 11 °C.

For the measurement of required data (acceleration coefficient values) in three axes (x - longitudinal, y - transversal, and z - perpendicular to the direction of the vehicle movement), a measuring device - OM-CP-ULTRASHOCK-5 three-axes accelerometer with a calibration certificate and a measuring range ± 5g was used. The measuring device was placed on the cargo space steel frame in case of Tatra 810 and on the steel frame of an ISO 1C container in case of Tatra 815 MK IV, which forms part of a vehicle. During the transportation experiments, no data outside the measuring range were recorded. In the z-axis, the measuring device only records values over 1g (acceleration of gravity) and the coordinate axis is shifted by this value (1g), which reflects even in the normatively determined limits as per EN 12195-1:2010. The normatively determined limits are formally designated with index s for individual axes:

c_{xs} - acceleration coefficient in the longitudinal direction (x-axis) for forward/backward movements is 0.8/0.5;

c_{ys} - acceleration coefficient in the transverse direction (y-axis), displacement/tilting is 0.5/0.6;

c_{zs} - vertical acceleration coefficient (z-axis) is 1.0 [6].

For the purpose of the article, the "worst values" were used that can be formally written in the form of a basal vector of acceleration coefficients (c_s), including the shift of z-axis by 1g:

$$c_s = (0.8, 0.6, 2.0), \quad (1)$$

for the purpose of double excess of the normatively determined limits another basal vector (b_s) was also determined:

$$b_s = (1.6, 1.2, 3.0). \quad (2)$$

For the mutual comparison of the datasets measured and the normatively determined limits (c_s, b_s), the following parameters were used: distribution (σ_i), mean value - arithmetic mean of absolute values (μ_i), probability of excess (ϖ_i) or the double excess of normatively determined limits (ρ_i). Index i refers to the respective dataset and its value is 1, 2 or 3. For the purpose of parametric tests, the normality of experimentally obtained data (d_1, d_2, d_3) was verified graphically using the Q-Q plots [25]. Although minor deviations from normality were detected, the respective quantiles lay approximately in one line [26]. For the mutual comparison of the datasets taking the differences between the road types and vehicle types into consideration, statistical tests of equality were employed at the level of significance α = 0.05. For each parameter, a hypothesis of equality ($H_1 = H_2$, or possibly $H_1 = H_3$, or $H_2 = H_3$) was tested, and then two-tailed tests were conducted in order to find out whether the respective parameter in a dataset is, in statistical terms, significantly smaller or bigger if compared to another dataset. The comparison of the datasets was made for all the pairs (d_1 - d_2, d_1 - d_3, d_2 - d_3).

4 Results and discussion

For the data analysis, the above-mentioned parameters were calculated that were further used in the statistical

Table 1 *The probabilities of excess or the double excess of normatively determined limits*

d_i	d_1			d_2			d_3		
Axis	x	y	z	x	y	z	x	y	z
n	1.353	1.353	1.353	394	394	394	1.353	1.353	1.353
c_s	0.8	0.6	2.0	0.8	0.6	2.0	0.8	0.6	2.0
f_c	293	942	68	202	303	181	3	7	1
ϖ	0.2166	0.6962	0.0503	0.5127	0.7690	0.4594	0.0022	0.0052	0.0007
b_s	1.6	1.2	3.0	1.6	1.2	3.0	1.6	1.2	3.0
f_b	1	20	0	9	86	8	0	0	0
ρ	0.0007	0.0148	0.0000	0.0228	0.2183	0.0203	0.0000	0.0000	0.0000

c_s normatively determined limit as per EN 12195-1:2010

b_s double limit arising from c_s

f_c, f_b number of measured values excessing limit c_s, or possibly b_s

Table 2 *Statistical tests of equality*

Confidence intervals for	Acceleration coefficients values in individual axes								
	x			y			z		
$d_1<d_2$	σ_1/σ_2	$\mu_1 - \mu_2$	$\varpi_1 - \varpi_2$	σ_1/σ_2	$\mu_1 - \mu_2$	$\varpi_1 - \varpi_2$	σ_1/σ_2	$\mu_1 - \mu_2$	$\varpi_1 - \varpi_2$
LB	0.419	-0.190	-0.350	0.483	-0.238	-0.121	0.372	-0.328	-0.460
UB	0.491	-0.120	-0.242	0.567	-0.156	-0.024	0.436	-0.242	-0.359
PE	0.454	-0.155	-0.296	0.524	-0.197	-0.073	0.403	-0.285	-0.409
$d_1>d_3$	σ_1/σ_3	$\mu_1 - \mu_3$	$\varpi_1 - \varpi_3$	σ_1/σ_3	$\mu_1 - \mu_3$	$\varpi_1 - \varpi_3$	σ_1/σ_3	$\mu_1 - \mu_3$	$\varpi_1 - \varpi_3$
LB	1.765	0.492	0.192	2.676	0.540	0.666	1.181	0.468	0.038
UB	1.963	0.511	0.236	2.977	0.563	0.716	1.313	0.492	0.061
PE	1.861	0.502	0.214	2.822	0.552	0.691	1.245	0.480	0.050
$d_2>d_3$	σ_2/σ_3	$\mu_2 - \mu_3$	$\varpi_2 - \varpi_3$	σ_2/σ_3	$\mu_2 - \mu_3$	$\varpi_2 - \varpi_3$	σ_2/σ_3	$\mu_2 - \mu_3$	$\varpi_2 - \varpi_3$
LB	3.789	0.623	0.461	4.981	0.709	0.722	2.856	0.722	0.409
UB	4.442	0.692	0.560	5.839	0.788	0.806	3.348	0.807	0.508
PE	4.095	0.657	0.510	5.384	0.749	0.764	3.087	0.765	0.459

PE Parameter estimation

LB Lower boundary of the 95 % confidence interval

UB Upper boundary of the 95 % confidence interval

tests of equality. In Table 1, the probabilities of excess, or the double excess of the normatively determined values of acceleration coefficients, specified in EN 12195-1:2010, are presented, taking the shift of coordinate axis in the measuring device in *z*-axis by 1*g* into consideration.

The probabilities of excess of the normatively determined limits reach high values especially with Tatra 810 off-road vehicle, or possibly Class III road. The highest values were recorded in d_1 and d_2 in the *y*-axis, which is also due to the magnitude of the normatively determined limit (c_{ys} = 0.6) as per EN 12195-1:2010. For the Tatra 815 MK IV vehicle the probability values are negligible, in all the three axes they were lower than 1 %. As far as e probabilities of the double excess of normatively determined limits are concerned, the values (refer to the experiment conducted) for Tatra the 815 MK IV and for d_1 in the *z*-axis were not available. The highest value was recorded in d_2 in the *y*-axis again.

If the extreme results of d_2 are taken as a basis, i.e. 86 double excesses of normatively determined values in the *y*-axis out of the total number of 394 measured values, the greatest risk of the cargo loosening during the transportation by Tatra 810 vehicle on Class III road is in the transversal axis. The hypothesis also works for considerably lower average transportation speed on Class III road, which was almost half the highway transportation speed.

Furthermore, statistical tests of equality at the level of significance α = 0.05 (refer to Table 2) were conducted proving statistically significant differences in monitored parameters for each pair of datasets.

From the results it clearly follows that the biggest differences are between d_2 and d_3, i.e. despite the transport speed on a lower-quality road being half the highway speed, Class III road still generates greater shocks than a highway. The magnitude of the difference is also underlined by

Table 3 Mean values (arithmetic means) of acceleration coefficients - absolute values

	d_1			d_2		
	x	y	z	x	y	z
Arith. mean (ABS)	0.6873	0.7226	1.7075	0.8425	0.9196	1.9924
Median (ABS)	0.6700	0.7100	1.6900	0.8150	0.8500	1.9500

differences between the test vehicles as it is evident that Tatra 810 generates greater shocks than Tatra 815 MK IV under comparable transport conditions.

The results complement statistically significant differences in probabilities (ϖ_i) of excess of the normatively determined values of acceleration coefficients in individual axes as per EN 12195-1:2010, although in the two cases the statistical difference at the level of significance α = 0.05 was close to the threshold value (refer to $d_1<d_2$ in y-axis and $d_1>d_3$ in z-axis).

It follows from the analyses conducted that in general, the Tatra 810 off-road vehicle generates greater shocks than the Tatra 815 MK IV vehicle on a high-quality road - highway. The shock values are even higher in case of Tatra 810 being operated on a low-quality road - Class III road. The mean values in d_1 and d_2 - arithmetic means of absolute values, or possibly medians of absolute values (refer to Table 3) - differ to a relatively great extent. If more precise arithmetic mean of acceleration coefficient absolute values is calculated, its value in d_2 is for 22.6 % higher in the x-axis than in d_1, or for 27.3 % in the y-axis, or for 16.7 % in the z-axis. Furthermore, the results suggest that while the acceleration coefficient values can be used to determine a securing method for Tatra 815 MK IV vehicle, they are not, or to a very limited extent, applicable to Tatra 810 operation under normal conditions (see above). On a lower-quality road, the normatively determined values of acceleration coefficients are completely inapplicable for the determination of a securing method for Tatra 810 and potentially dangerous, especially in the context of possible accident occurrence (not only road-related) in consequence of the cargo shifting in the vehicle cargo space.

5 Conclusions

The cargo securing in road transportation is still a topical issue and a cargo is often inappropriately or insufficiently secured, which supports the above-mentioned European Committee estimations. Those insufficiencies often result from negligence, i.e. when the method of proper cargo securing is known to a responsible person (a driver, a logistics employee), but the responsible person opts for another method, usually less laborious, cheaper or less time-demanding. In the road transportation, cargo is sometimes not secured at all, as a responsible person does not expect to encounter any problems during the transport. This article, as well as author's further scientific work, mainly concentrate on another reason of inappropriate or insufficient cargo securing, which is unintentional unawareness of the cargo securing system, despite a responsible person using all the available information sources (e.g. the above-mentioned standards, or manuals, handbooks, etc.). Under normal conditions - especially on the high-quality roads - the difference between the expected magnitude of shocks and their real magnitude is usually small or there is no difference at all, i.e. it is irrelevant in relation to transport safety. The problem is encountered mainly when transporting cargos on the lower-quality roads - lower classes roads, or possibly under specific conditions, e.g. off the road or generally outside common roads, or by special vehicles (e.g. military, agricultural, Integrated Rescue System). The negative consequence may not only be a road accident as such, but an accident in general, e.g. during handling operations (in particular loading/unloading) or other activities in reloading areas, warehouses, etc. The above-mentioned flaws lead to great social losses, that can be (e.g. based on the Transport Research Centre methodology) expressed financially [27]. Hence, the results are mainly usable in the field of cargo securing optimisation and reduction of negative impacts of incorrect securing system selection.

The follow-up research shall concentrate on inclusion of further measurements, the generalisation of the results, taking into account the selected cargo transport specifics, including the transportation of hazardous materials or objects [28-29] and identification of further risks associated with the effect of shocks on cargos transported via roads [30]. In addition, more sophisticated statistical methods [31], or possibly further mathematical tools shall be employed, such as Wavelet analysis allowing the transition of data from time to frequency domain [32].

Acknowledgement

This work was supported by the Ministry of Defence of the Czech Republic under Grant ROZVOLOG: Development of Capabilities and Sustainability of Logistics Support (ROZVOLOG 2016-2020).

References

[1] European commision - Eurostat. Goods transport by road [online]. [Viewed 2019-07-25]. Available from: https://ec.europa.eu/eurostat/databrowser/view/ttr00005/default/table?lang=en

[2] European commision - Eurostat. People killed in road accidents [online]. [Viewed 2019-07-28]. Available from: https://ec.europa.eu/eurostat/databrowser/view/sdg_11_40/default/table?lang=en

[3] European commision - Directorate-general for energy and transport. European best practice guidelines on cargo securing for road transport [online]. [Viewed 2019-07-30]. Available from: www.uirr.com/fr/component/downloads/downloads/302.html

[4] Police of the Czech Republic - Accident statistics 2018 [online]. [Viewed 2019-07-30]. Available from: https://www.policie.cz/clanek/statistika-nehodovosti-900835.aspx?q=Y2hudW09Mg%3d%3d

[5] Ministry of Transport of the Czech Republic - Transport yearbook 2018 [online]. [Viewed 2019-07-22]. Available from: https://www.sydos.cz/cs/rocenka-2018/rocenka/htm_cz/cz18_621000.html

[6] EN 12195-1. *Load restraining on road vehicles - safety - part 1: calculation of securing forces. Prague:* Czech Office for Standards, Metrology and Testing, 2010.

[7] EN 12195-2. *Load restraint assemblies on road vehicles - safety - part 2: web lashing made from man-made fibres. Prague:* Czech Office for Standards, Metrology and Testing, 2003.

[8] JAGELCAK, J., VRABEL, J., NIEUWESTEEG, M. Draft for revision of the standards EN 12640 and EN 12641 regarding the securing of cargo on road means of transport. *LOGI - Scientific Journal on Transport and Logistics* [online]. 2017, 8(2), p. 41-46. ISSN 2336-3037. Available from: https://doi.org/10.1515/logi-2017-0015

[9] EN 12640 *(F draft). Securing of cargo on road vehicles - lashing points on commercial vehicles for goods transportation - minimum requirements and testing. Prague:* Czech Office for Standards, Metrology and Testing, 2019.

[10] EN 12642. *Securing of cargo on road vehicles - body structure of comercial vehicles - minimum requirements. Prague:* Czech Office for Standards, Metrology and Testing, 2016.

[11] United nations economic commission for Europe. IMO/ILO/UNECE code of practice for packing of cargo transport units (CTU Code) [online]. [Viewed 2019-07-25]. Available from: https://www.unece.org/fileadmin/DAM/trans/doc/2014/wp24/CTU_Code_January_2014.pdf

[12] LERHER, T. *Cargo securing in road transport using restraining method with top-over lashing.* New York: Nova, 2015. ISBN 978-1-61122-002-5.

[13] GROSSMANN, G., KASSMAN, M. *Transport safe packaging and cargo securing.* 3. ed. Renningen: Expert Verlag, 2018. ISBN 978-3-8169-3334-2.

[14] JAGELCAK, J. Equation of the standard EN 12195-1 stipulates unreasonable demands for cargo securing. *Communications - Scientific Letters of the University of Zilina* [online]. 2007, 9(4), p. 30-33. ISSN 1335-4205, eISSN 2585-7878. Available from: http://komunikacie.uniza.sk/index.php/communications/article/view/1151

[15] JAGELCAK, J., GNAP, J. Different measures for load securing create barriers in international road freight transport. *Archives of Transport Systems Telematics*. 2011, 4(2), p. 10-17. ISSN 1899-8208.

[16] JAGELCAK, J., SANIGA, J. Analysis of elongation of lashing straps on movements of cargo secured by a top-over lashing at sliding in longitudinal direction. *Perner´s Contacts*. 2013, 8(2), p. 53-62. ISSN 1801-674X.

[17] LININS, A., BERJOZA, D. Experimental investigation in acceleration of vehicle. 9th International Scientific Conference on Engineering for Rural Development Location : proceedings. 2010. ISSN 1691-5976, p. 149-153.

[18] ZAMECNIK, J., JAGELCAK, J., SOKJER-PETERSSEN, S., HVOJNIK, T., LIPKA, M. Influence of a lashing strap winding in tensioning ratchet on the results of the strength tests and cyclic loading tests according to the standard EN 12195-2. *Communications - Scientific Letters of the University of Zilina* [online]. 2017, 19(2), p. 10-17. ISSN 1335-4205, eISSN 2585-7878. Available from: http://komunikacie.uniza.sk/index.php/communications/article/view/175

[19] ZONG, C.-Q., ZHANG, H.-W., HUANG, CH.-Z., DONG, J.-S. Research on the influence of cargo securing force with typical road alignments and vehicle working conditions. 4th International Conference on Transportation Information and Safety (ICTIS): proceedings [online]. IEEE, 2017. ISBN 9781538604380, p. 27-32. Available from: https://doi.org/ 10.1109/ICTIS.2017.8047737

[20] BANNER, S. Restraining order. *Commercial Motor*. 2005, 201(5133), p. 54-59. ISSN 0010-3063.

[21] CIESLA, M., HAT-GARNCARZ, G. The problem of proper cargo securing in road transport - case study. *Transport Problems*. 2013, 8(4), p. 27-33. ISSN 1896-0596, eISSN 2300-861X.

[22] VLKOVSKY, M., VESELIK, P. Cargo securing - comparison of different quality roads. *Acta Universitatis Agriculturae et Silviculturae Mendelianae Brunensis* [online]. 2019, 67(4), p. 1015-1023. ISSN 1211-8516, eISSN 2464-8310. Available from: https://doi.org/10.11118/actaun201967041015

[23] KOLMAS, V., KOHOUTEK, J., VYMETAL, J. Catalog of automotive and tracked vehicles used in the ACR. Prague: Ministry of Defence of the Czech Republic - AVIS, 2007. ISBN 978-80-7278-382-3.

[24] VLKOVSKY, M., BINAR, T., SVARC, J., NEMEC, P., BUCSUHAZY, K. Impact of shocks on cargo securing during the road transport. 4th World Multidisciplinary Civil Engineering, Architecture, Urban Planning Symposium: proceedings. Vol. 471. Prague: IOP Conference Series - Materials Science and Engineering. 2019. ISSN 1757-8981.

[25] JOHNSON, R. A., WICHERN, D. W. *Applied multivariate statistical analysis*. Englewood Cliffs: Prentice-Hall International, 1992. ISBN 0130418072.

[26] VLKOVSKY, M., VLACHOVA, H. Securing cargo during transport on roads of different quality. 5th International Conference on Vehicle Technology and Intelligent Transport Systems 2019: proceedings. Heraklion: SCITEPRESS, 2019. ISBN 978-989758374-2, p. 25-32.

[27] VLKOVSKY, M., VESELIK, P., GRZESICA, D. Cargo securing and its economic consequences. 22nd International Scientific Conference Part I - Transport Means 2018 : proceedings. Kaunas: Kaunas University of Technology, 2018. ISSN 1822-296X, p. 129-135.

[28] VLKOVSKY, M., RAK, L. Cargo securing in selected vehicles and transport of explosives. *Perner's Contacts* [online]. 2017, 12(3), p. 101-110. ISSN 1801-674X. Available from: http://pernerscontacts.upce.cz/PC_482017.pdf

[29] DVORAK, Z., FUCHS, P., NOVAK, J., SOUSEK, R. Individual and social risk during transportation of dangerous substances. *Communications - Scientific Letters of the University of Zilina* [online]. 2011, 13(2), 92-98. ISSN 1335-4205, eISSN 2585-7878. Available from: http://komunikacie.uniza.sk/index.php/communications/article/view/828

[30] DVORAK, Z., RAZDIK, J., SOUSEK, R., SVENTEKOVA, E. Multi-agent system for decreasing of risk in road transport. 14th International Scientific Conference - Transport Means 2010: proceedings. Kaunas: Kaunas University of Technology, 2010. ISSN 1822-296X, p. 100-103.

[31] VESELIK, P., DVORSKA, A., MICHALEK, J. Half a year of co-located gaseous elemental mercury measurements: investigation of temporal changes in measurement differences. *Fresenius Environmental Bulletin*. 2017, 26(5), p. 3128-3137. ISSN 1018-4619.

[32] VLKOVSKY, M., KOZIOL, P., GRZESICA, D. Wavelet based analysis of truck vibrations during off-road transportation. 14th International Conference on Vibration Engineering and Technology of Machinery : proceedings. Lisabon: MATEC Web of Conferences, 2018. ISSN 2261-236X.

Damian Wierzbicki - Kamil Krasuski

DETERMINING THE ELEMENTS OF EXTERIOR ORIENTATION IN AERIAL TRIANGULATION PROCESSING USING UAV TECHNOLOGY

Unmanned Aerial Vehicles (UAVs) are still an interesting and current research topic in photogrammetry. An important issue in this area is determining the elements of exterior orientation of image data acquired at low altitudes. The article presents selected mathematical methods (TGC, TIC, TAD) of estimating elements of exterior orientation for image data obtained at low altitudes. The measurement data for the experimental test were recorded by the Unmanned Aerial Vehicle platform Trimble UX-5. In the framework of the test photogrammetric flight, the authors obtained 506 images and navigation data specifying the position and orientation of the Unmanned Aerial Vehicle. As a result of the research, it is proven possible to show the usefulness of the mathematical models (TGC, TIC, TAD) in estimation of elements of exterior orientation.

Keywords: *GNSS, INS, UAV, digital aerial triangulation, elements of exterior orientation, aerial photogrammetry*

1 Introduction

Development of the UAV technology made it possible to acquire image data o at low altitudes, as well. Georeferencing of image data taken by the Unmanned Aerial Vehicle (UAV) is performed in the process of digital aerial triangulation [1-2]. Within the classical process of digital aerial triangulation, the elements of exterior orientation and also coordinates of the measured ground control points, are taken. In the case of elements of exterior orientation, the coordinates of the centre of projection are determined for each image, referenced to the ground layout and the deflection angles of the camera referenced to the photogrammetric camera system. The typical accuracy of determining the elements of exterior orientation in the process of digital aerial triangulation for linear elements is approximately at a level of 0.1 m, and for angle elements, is respectively higher than 0.1^0. The approximate values of exterior orientation may be determined based on measurements of the GNSS/INS sensors, mounted on an UAV platform [3-4]. The basic navigation equipment of an UAV should contain at least a GNSS single-frequency code receiver and additionally a measurement system of gyroscopes and accelerometers for the needs of the INS system operation. The GNSS satellite receiver primarily facilitates determining the position of an Unmanned Aerial Aircraft in the three dimensional Cartesian coordinate XYZ. It also allows determining the heading and airspeed of an Unmanned Aerial Vehicle [5-7]. The above-mentioned navigation parameters of the GNSS receiver are determined in near real-time by an UAV control system and stored in the device's memory at a specified time interval. The measurement system of the INS sensor recovers the YPR (Yaw, Pitch and Roll) values of rotation angles on the basis of the movement of the gyroscopes and specifying the acceleration value from the accelerometer sensors. The readings of the YPR angles indicate an UAV position in airspace, whereas the acceleration values make it possible to designate the aircraft relative position [8-11].

The navigation parameters from the GNSS receiver are usually referenced to the GPS system time and the INS measurement system may have a separate built-in time pattern to register the observed data. It must be stressed that the GNSS receiver determines the UAV position with the absolute positioning accuracy of up to 10 m, whereas the INS relative accuracy becomes considerably deteriorated during the measurements. Furthermore, the accuracy of recording the YPR rotation angles equals 5^0 for an UAV. In order to correct the designated navigation parameters for an UAV, it is necessary to use exterior mathematical models so as to smooth the obtained findings. One of the examples of the integration of GNSS/INS data is the implementation, in computing, the recursive Kalman filter, reducing and eliminating measurements that stand out from a set of recorded navigational data. In addition, Kalman filtering ensures increasing accuracy in determining the UAV accuracy during the experimental test [12-14].

For aerial photogrammetry, determining the coordinate values and rotation angles for an UAV is a key element in the process of determining the elements of exterior orientation. The designated position of an UAV using a GNSS sensor forms the basis for reconstructing the camera position at the moment of exposure. Besides, the YPR rotation angles are exploited in the process of transformation to determine the angle OPK (Omega, Phi, Kappa) elements

Damian Wierzbicki[1,*], Kamil Krasuski[2]
[1]Institute of Geodesy, Faculty of Civil Engineering and Geodesy, Military University of Technology, Warszawa, Poland
[2]Institute of Navigation, Military University of Aviation, Deblin, Poland
*E-mail of corresponding author: damian.wierzbicki@wat.edu.pl

in the photogrammetric camera layout. The approximate values of exterior orientation are a valuable research and information material for conducting the process of digital aerial triangulation, using the coordinates of ground control points (GCPs).

The aim of this paper is to present mathematical methods for establishing the approximate values of elements of exterior orientation and to verify the obtained results with regard to the final products of digital aerial triangulation. The measurement data for the experimental test come from a photogrammetric flight performed by the Trimble UX-5 rover in Tylicz.

2 Mathematical models for designation of the exterior orientation elements

The chapter describes the mathematical models for the determination of elements of exterior orientation with the on-board GNSS/INS data registered by an UAV and on the basis of the method of digital aerial triangulation.

2.1 Mathematical models for designation of the projection centre coordinates

A single-frequency GNSS receiver, mounted on a UAV platform, can be used to determine approximate coordinate values of the centre of projection. Coordinates of the centre of projection are determined in a two-step process, i.e. in the first stage a UAV position is determined and in the second stage the coordinates of the projection center of each image are designated, taking into account the correction of eccentricity between the position of the GNSS receiver antenna and the camera. The basic observation equation to determine a UAV position for the GNSS sensor can be expressed in the following manner [4]:

$$l = \rho + c \cdot (dtr - dts) + Trop + rel + ion + \\ + bias + M_l, \quad (1)$$

where:
l - measurement code C/A at L1 frequency,
r - geometric distance between the satellites GNSS and the receiver,
$\rho = \sqrt{(X_r - X_s)^2 + (Y_r - Y_s)^2 + (Z_r - Z_s)^2}$,
(X_r, Y_r, Z_r) - position of an unmanned aerial platform in the geocentric frame,
(X_s, Y_s, Z_s) - position of GNSS satellite in orbit,
c - speed of light,
dtr - receiver clock bias for GNSS observations,
dts - satellite clock bias for GNSS observations,
$Trop$ - tropospheric delay for GNSS observations,
Ion - ionospheric delay for GNSS observations,
R*el*- relativistic effects for GNSS observations,
$bias$ - summary expression for hardware delay in the GNSS system,
M_l - multipath effect and measurement noise.

In Equation (1) the determined parameters are the aircraft coordinates, (X_r, Y_r, Z_r) referenced to the phase centre of the antenna receiver mounted on the UAV platform and the receiver clock bias dtr. The unknown parameters from Equation (1) are determined using the Kalman filtering in accordance with interval recording of an observation. The UAV coordinates are used to determine the coordinates of the projection center for each image, see below [13-14]:

$$\begin{bmatrix} X_{kr} \\ Y_{kr} \\ Z_{kr} \end{bmatrix} = \begin{bmatrix} X_r \\ Y_r \\ Z_r \end{bmatrix} + \begin{bmatrix} e_x \\ e_y \\ e_z \end{bmatrix}, \quad (2)$$

where:
(X_{kr}, Y_{kr}, Z_{kr}) - coordinate of the camera projection centre,
(e_x, e_y, e_z) - parameters of the camera eccentricity.

2.2 Mathematical models for designation of the exterior orientation angle elements

The INS sensor installed on a UAV platform ensures reconstruction of a UAV orientation in airspace by means of the YPR rotation angles. The values of YPR angles allow designating approximate angular elements of OPK exterior orientation based on the transformation between the INS sensor layout and the camera layout, as below [15]:

$$C_E^B = T_b^B \cdot \left(C_{n0}^{n'} \cdot C_e^{n0} \cdot (C_e^{ni})^T \cdot C_b^{ni} \right)^T \cdot (T_n^E)^T, \quad (3)$$

where:
C_E^B - orthogonal matrix, containing angular OPK elements,

$$C_E^B = \begin{bmatrix} \cos\varphi\cos\kappa & -\cos\varphi\sin\kappa & \sin\varphi \\ \cos\varpi\sin\kappa + \sin\varpi\sin\varphi\cos\kappa & \cos\varpi\cos\kappa - \sin\varpi\sin\varphi\sin\kappa & -\sin\varpi\cos\varphi \\ \sin\varpi\sin\kappa - \cos\varpi\sin\varphi\cos\kappa & \sin\varpi\cos\kappa + \cos\varpi\sin\varphi\cos\kappa & \cos\varpi\cos\varphi \end{bmatrix}$$

φ - Phi angle,
$\varphi = \arcsin C_E^B(1,3)$,
ϖ - Omega angle,

$$\varpi = -arctg\left(\frac{C_E^B(2,3)}{C_E^B(3,3)} \right),$$

κ - Kappa angle,

$$\kappa = -arctg\left(\frac{C_E^B(1,2)}{C_E^B(1,1)} \right),$$

$$T_b^B = \begin{bmatrix} -1 & 0 & 0 \\ 0 & 1 & 0 \\ 0 & 0 & -1 \end{bmatrix},$$

T_b^B - the determinant of the matrix is equal to 1,

$$C_{n0}^{n'} = \begin{bmatrix} 1 & 0 & 0 \\ 0 & 1 & 0 \\ 0 & 0 & 1 \end{bmatrix},$$

$C_{n0}^{n'}$ - unit matrix,

$$C_e^{n0} = \begin{bmatrix} -\sin B_0 \cdot \cos L_0 & -\sin B_0 \cdot \sin L_0 & \cos B_0 \\ -\sin L_0 & \cos L_0 & 0 \\ -\cos B_0 & -\cos B_0 \cdot \sin L_0 & -\sin B_0 \end{bmatrix},$$

$C_e^{n0} = f(B_0, L_0)$,

C_e^{n0} - matrix that contains UAV coordinates in the ellipsoidal system;

(B_0, L_0) - the UAV coordinates refer to the central point of the flight trajectory,

$$C_e^{ni} = \begin{bmatrix} -\sin B_i \cdot \cos L_i & -\sin B_i \cdot \sin L_i & \cos B_i \\ -\sin L_i & \cos L_i & 0 \\ -\cos B_i & -\cos B_i \cdot \sin L_i & -\sin B_i \end{bmatrix},$$

$C_e^{ni} = f(B_i, L_i)$,

C_e^{ni} - matrix that contains UAV coordinates in the ellipsoidal system;

(B_i, L_i) - UAV coordinates for each measurement epoch,

C_b^{ni} - orthogonal matrix, containing angular YPR elements,

$$C_b^{ni} = \begin{bmatrix} \cos\psi \cdot \cos\theta & \cos\psi \cdot \sin\theta \cdot \sin\phi - \sin\psi \cdot \cos\phi & \cos\psi \cdot \sin\theta \cdot \cos\phi + \sin\psi \cdot \sin\phi \\ \sin\psi \cdot \cos\theta & \sin\psi \cdot \sin\theta \cdot \sin\phi + \cos\psi \cdot \cos\phi & \sin\psi \cdot \sin\theta \cdot \cos\phi - \cos\psi \cdot \sin\phi \\ -\sin\theta & \cos\theta \cdot \sin\phi & \cos\theta \cdot \cos\phi \end{bmatrix}$$

ϕ - Roll angle,

θ - Pitch angle,

ψ - Yaw angle,

$$T_n^E = \begin{bmatrix} 0 & 1 & 0 \\ 1 & 0 & 0 \\ 0 & 0 & -1 \end{bmatrix},$$

T_n^E - the determinant of the matrix is equal to 1.

2.3 Mathematical models for designation of the exterior orientation elements using the digital aerial triangulation method

The method of digital aerial triangulation allows determining exterior orientation of elements with high accuracy: for linear elements of exterior orientation above 0.1 m and for elements of the angular exterior orientation above 0.1^0, respectively. The basic equation of digital aerial triangulation in the classic approach assumes the following form [16-17]:

$$\begin{cases} x_k - x_0 = \\ -f_k \left[\dfrac{r_{11}(X_T - X_{kr}) + r_{21}(Y_T - Y_{kr}) + r_{31}(Z_{T-Z_{kr}})}{r_{13}(X_T - X_{kr}) + r_{23}(Y_T - Y_{kr}) + r_{33}(Z_{T-Z_{kr}})} \right] \\ y_k - y_0 = \\ -f_k \left[\dfrac{r_{12}(X_T - X_{kr}) + r_{22}(Y_T - Y_{kr}) + r_{32}(Z_{T-Z_{kr}})}{r_{13}(X_T - X_{kr}) + r_{23}(Y_T - Y_{kr}) + r_{33}(Z_{T-Z_{kr}})} \right] \end{cases}, \quad (4)$$

where:

(x_k, y_k) - image coordinates,

(x_0, y_0) - centre point of image coordinates,

f_k - focal length,

(X_T, Y_T, Z_T) - coordinates of ground control points in terrain frame,

(X_{kr}, Y_{kr}, Z_{kr}) - coordinates of the projection centre, expressed in terrain frame,

$$R = \begin{bmatrix} r_{11} & r_{21} & r_{31} \\ r_{12} & r_{22} & r_{32} \\ r_{13} & r_{23} & r_{33} \end{bmatrix},$$

- orthogonal matrix; matrix contains angle elements of exterior orientation,

$R = R(\varpi, \varphi, \kappa)$,

$(\varpi, \varphi, \kappa)$ - angle elements of exterior orientation.

3 Experimental test

In the framework of the experimental test, the exterior orientation elements were determined based on equations [2, 5-6, 18]. The navigation data to determine the elements of the exterior orientation from Equations (2) and (3) were recorded during the flight by the Trimble UX-5 unmanned aircraft system. The coordinate values of the platform Trimble UX-5 and YPR orientation angles are recorded by measurement instruments mounted on the platform and stored in the universal text format “log”. The typical accuracy of the obtained coordinates of the Trimble UX-5 platform ranges from 5 m to 10 m and for the YPR orientation angles it is between 1^0 and 5^0, respectively [19]. The photogrammetric flight took place in Tylicz, in the south of Poland, in 2016. During the flight, 506 aerial images were taken, using a Sony NEX5R camera. All the aerial images were arranged in 22 rows (see Figure 1). The photogrammetric flight was executed at an altitude of 150 m, with an assumption that the average height of the terrain is approximately equal to 650 m.

Over the tested area, 10 ground control points and 5 independent check points were also measured for the needs of conducting digital aerial triangulation. The mutual orientation was performed based on an automatic measurement of tie points [16]. All of the measured points were signalled and their coordinates were designated by means of the GNSS RTK technique, with an accuracy no worse than 0.05 m. The process of digital aerial triangulation was carried out in the commercial UASMaster software. After conducting the process of digital aerial triangulation, the value of the mean error of typical observations equalled 5.4 µm (1.1 pixel). Moreover, the determined standard deviations for angle elements of the exterior orientation were over 0.043^0, whereas for the linear elements of exterior orientation they were higher than 0.1 m, accordingly. In addition, the RMS error at the control points equalled 0.21 m for the X coordinate, 0.04 m for the Y coordinate, and 0.11 m for the Z coordinate.

4 Results and discussion

For the sake of the executed experimental test, the elements of exterior orientation were determined based on the following research methods, which were defined by the authors as follows:

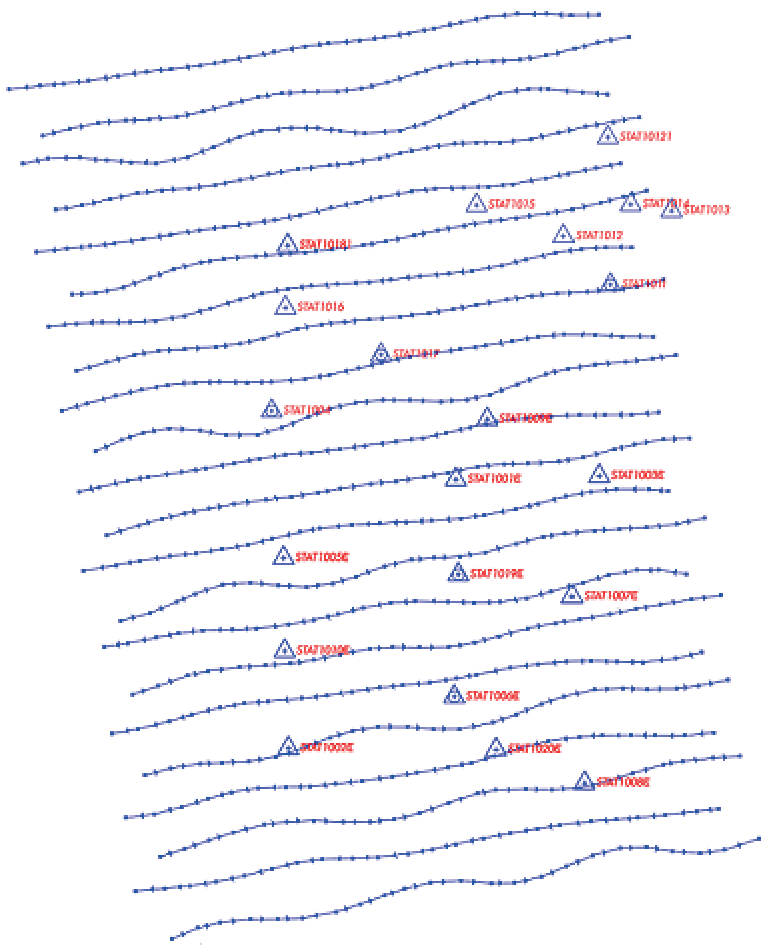

__Figure 1__ Visualization of the test photogrammetric block - altitude 150 m

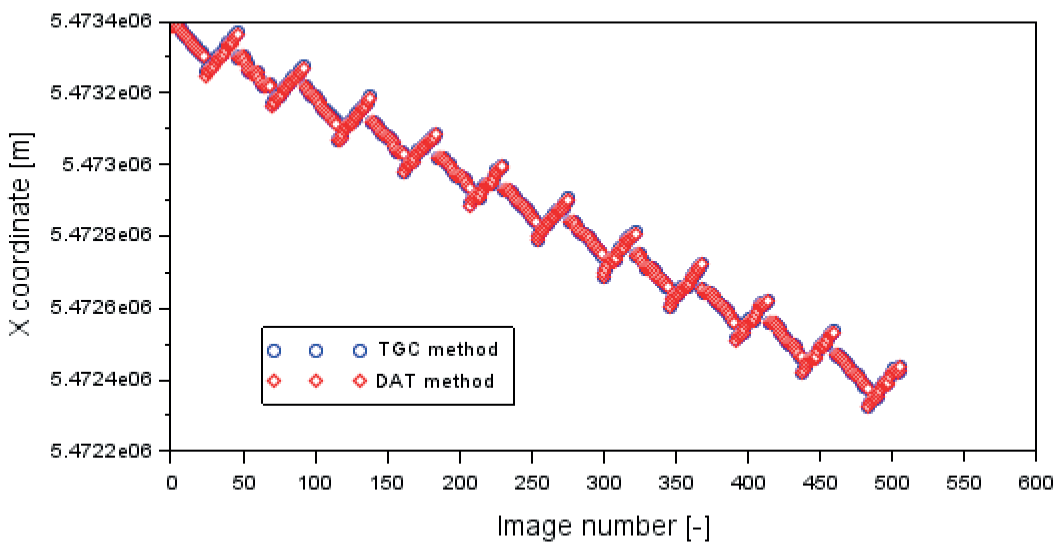

__Figure 2__ Values of the projection centre X coordinate based on TGC and DAT methods

- TGC method (**T**ranslation between **G**PS sensor and **C**amera sensor), the method relies on applying mathematical Equations (1) and (2),
- TGC method (**T**ranslation between **G**PS sensor and **C**amera sensor), the method relies on applying the mathematical model (3),
- DAT method (**D**igital **A**erial **T**riangulation processing), the method relies on applying the mathematical model (4).

Figures 2, 3 and 4 show values of the projection centre coordinates n along the X, Y and Z axes for the research methods TGC and DAT. The coordinates' values of the projection centre are referenced to the coordinate

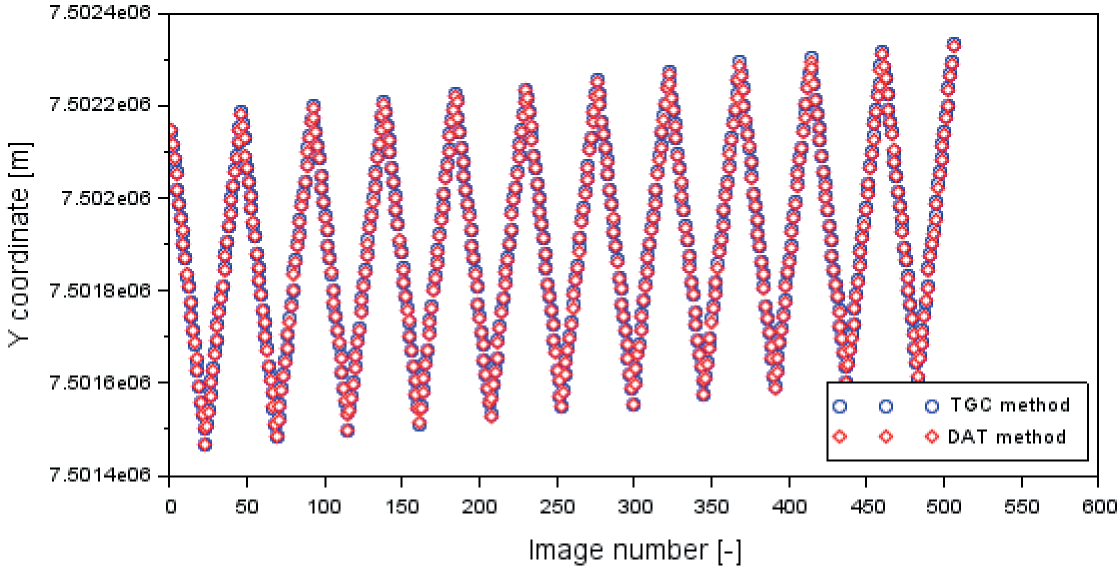

Figure 3 *Values of the projection centre Y coordinate based on TGC and DAT methods*

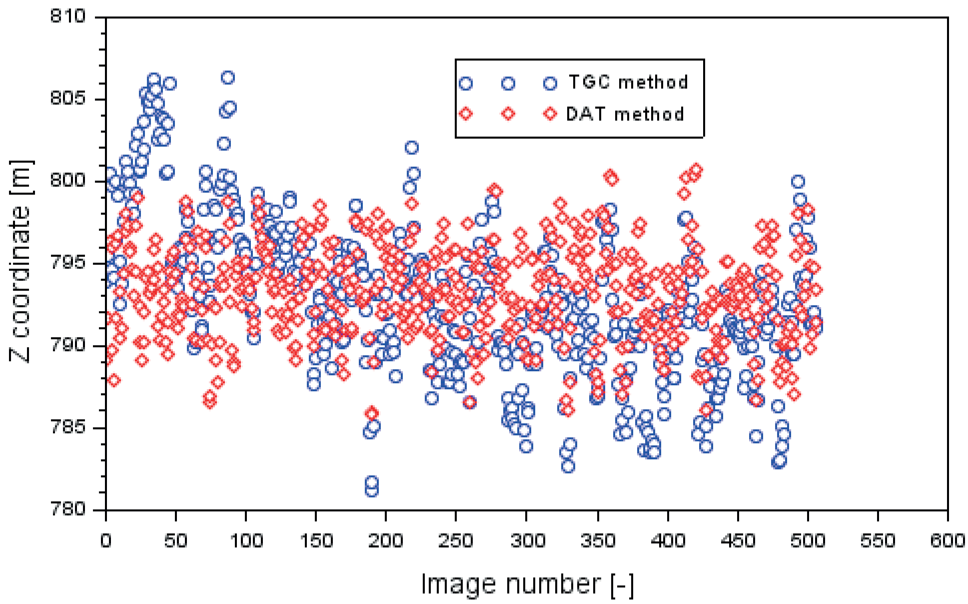

Figure 4 *Values of the projection centre Z coordinate of projection centre based on TGC and DAT methods*

system PUWG2000, zone 7. The X coordinate values in the TGC solution vary from 5472323.01 m to 5473391.36 m. In the DAT method, they change from 5472322.25 m to 5473389.66 m, accordingly. It should be stressed that the trajectory central point coordinates for the X axis are equal 5472869.82 m in the TGD method and 5472868.34 m in the TAD method, accordingly. The Y coordinate values in the TGC solution vary from 7501465.72 m to 7502332.94 m. In the DAT method, they change from 7501466.84 m to 7502331.47 m, respectively. The trajectory central point coordinates for the Y axis equal 7501900.01 m in the TGD method and 7501898.01 m in the TAD method, accordingly. The Z coordinate values in the TGC solution vary from 781.14 m to 806.26 m. In the DAT method, they change from 785.85 m to 800.67 m, respectively. The trajectory central point coordinates for the Z axis are equal 792.84 m in the TGD method and 793.21 m in the TAD method, accordingly.

Figures 5, 6 and 7 show the rotation element values of exterior orientation for the research methods TIC and DAT. Values of the Omega angle for the TIC solution change from -19.14^0 to 18.25^0, whereas in the DAT method they vary from -26.13^0 to 26.59^0, respectively. The average value of the Omega angle in the TIC method equals -0.060, and in the DAT method, it is 0.01^0, respectively. Values of the Phi angle for the TIC solution change from -15.64^0 to 14.32^0, whereas in the DAT method they vary from -9.80^0 to 13.17^0, respectively. The average value of the Phi angle in the TIC method equals 0.17^0, and in the DAT method, it is 0.50^0, respectively. Values of the Kappa angle in the TIC solution change from -179.88^0 to 25.91^0, whereas in the DAT method

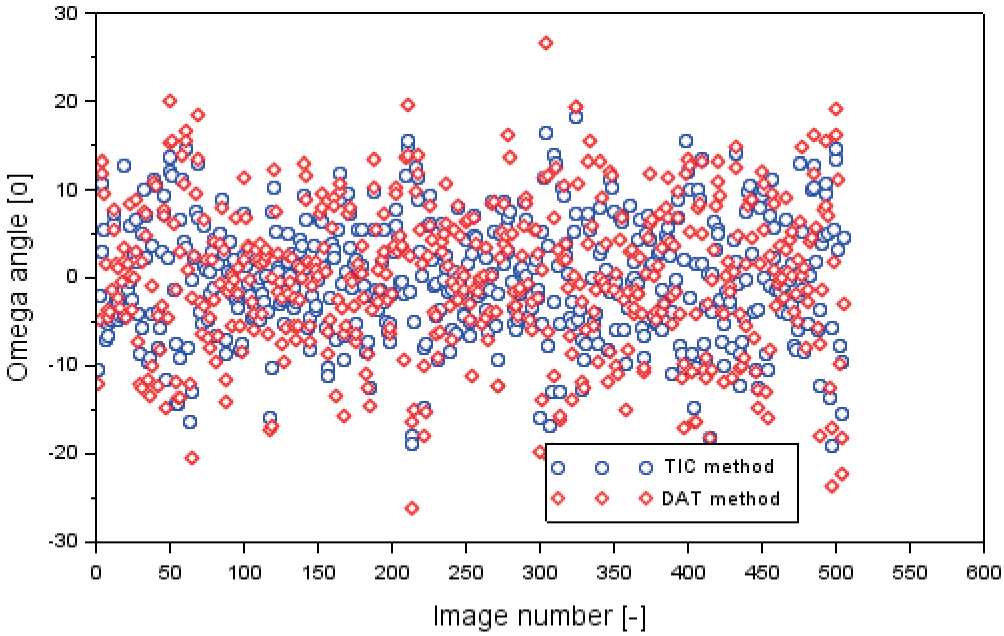

Figure 5 *Values of the Omega angle based on TIC and DAT methods*

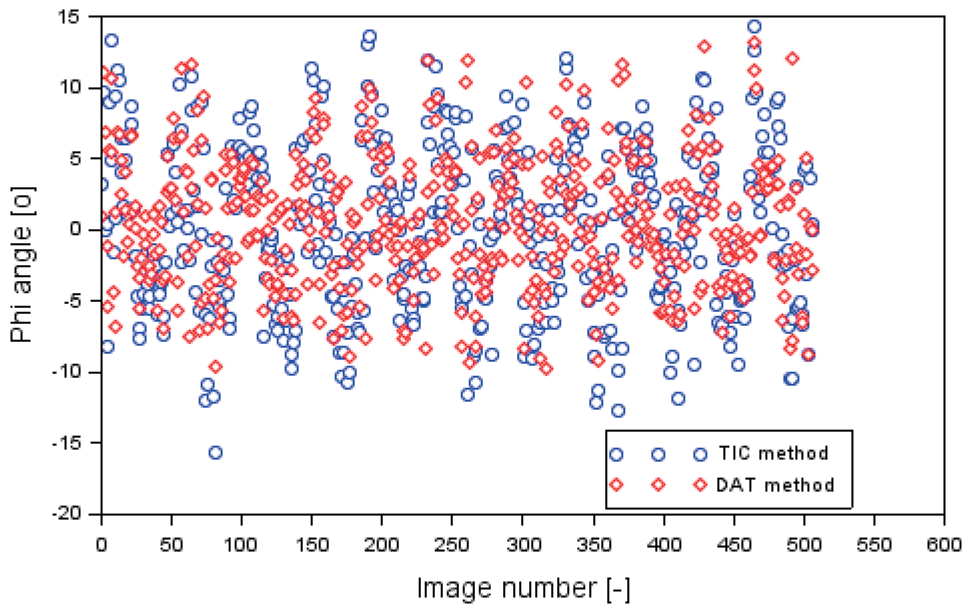

Figure 6 *Values of the Phi angle based on TIC and DAT methods*

they vary from -178.75^0 to 17.82^0, respectively. It should be noted that a large amplitude of results of the Kappa angle is caused by a change in direction of the flight of the Trimble UX-5 aircraft system from the west to the east or vice versa.

Figure 8 shows a difference in coordinate values of the centre of projection along the XYZ axis on the basis of the research methods TGC and DAT. The difference in coordinates of the centre of projection along the X, Y and Z axes were determined based on dependency [11]:

$$\begin{cases} dX = X_{kr}^{TGC} - X_{kr}^{DAT} \\ dY = Y_{kr}^{TGC} - Y_{kr}^{DAT} \\ dZ = Z_{kr}^{TGC} - Z_{kr}^{DAT} \end{cases}, \quad (5)$$

where:

$(X_{kr}^{TGC}, Y_{kr}^{TGC}, Z_{kr}^{TGC})$ - coordinates of the centre of projection in the TGC solution,

$(X_{kr}^{TAD}, Y_{kr}^{TAD}, Z_{kr}^{TAD})$ - coordinates of the centre of projection in the TAD solution.

The average value of the dX parameter equals 1.48 m with the scatter of results ranging from -2.72 m to 8.12 m. In addition, the standard deviation for parameter dX is 1.99 m, with the median being equal to 1.60 m. The average value of the dY parameter equals 1.99 m with the scatter of results between -2.89 m and 7.61. Furthermore, the standard deviation for parameter dY is 2.43 m, with the median being equal to 1.85 m. The average value of parameter dZ equals -0.38 m, with the scatter of results ranging from -8.51 m to

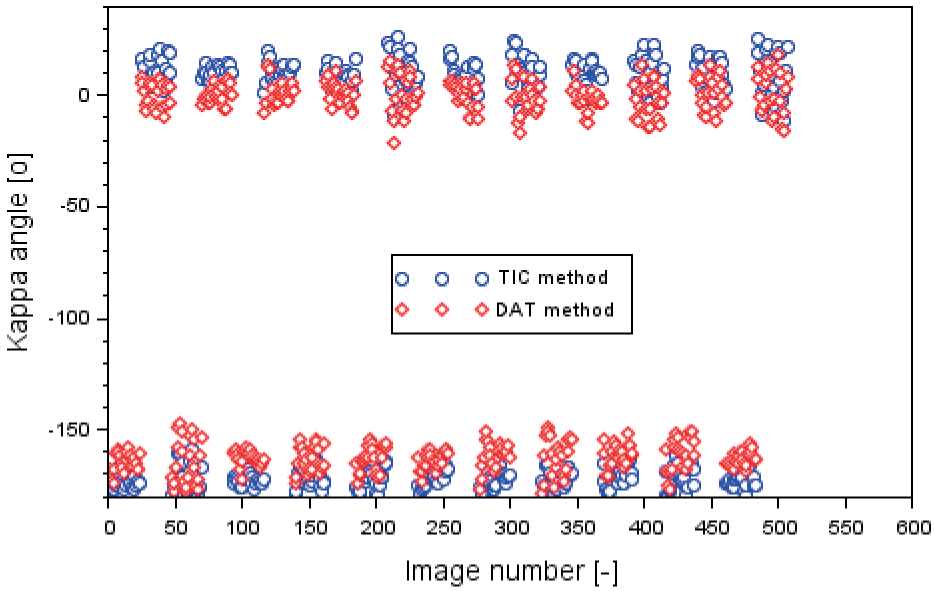

Figure 7 *Values of the Kappa angle based on TIC and DAT methods*

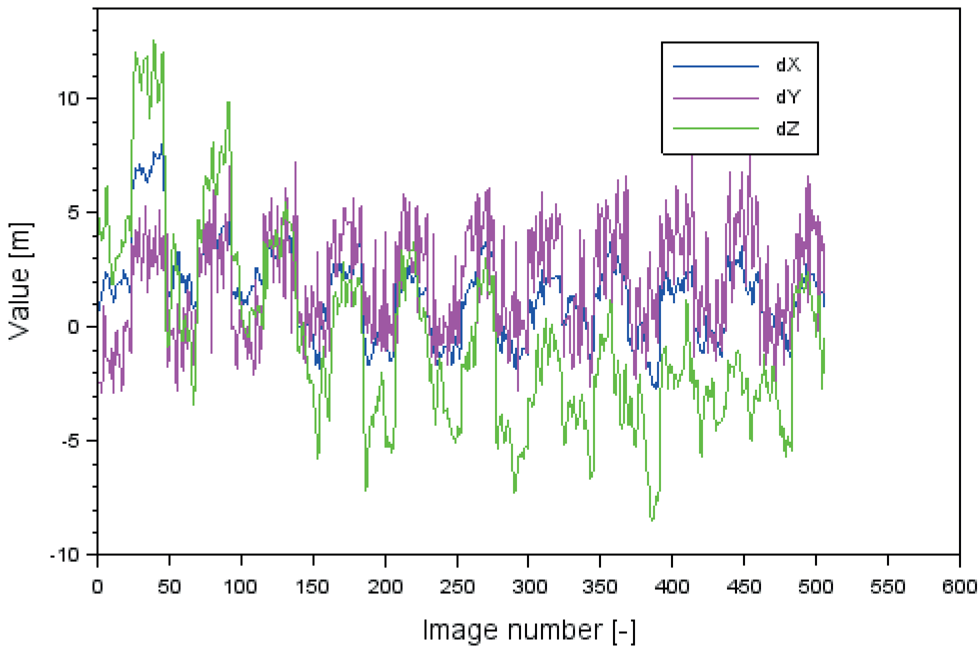

Figure 8 *Difference of projection centre coordinates based on TGC and DAT methods*

12.58 m. The standard deviation for parameter dZ equals 4.20 m, with the median being equal to -1.23 m. Among the calculated parameters dX, dY and dZ, the smallest dispersion (scatter) of results is noticeable for parameter dX. In addition, the dY parameter has the smallest standard values of deviation and of the median. Then, the largest scatter of results and standard deviation are visible for the value of the dZ parameter.

Figure 9 shows a difference in the exterior rotation angle elements on the example of the research methods TIC and DAT. The difference in the values of angle elements of exterior orientation was determined based on dependency [15]:

$$\begin{cases} d\varpi = \varpi^{TIC} - \varpi^{DAT} \\ d\varphi = \varphi^{TIC} - \varphi^{DAT} \\ d\kappa = \kappa^{TIC} - \kappa^{DAT} \end{cases}, \tag{6}$$

where:

$(\varpi^{TIC}, \varphi^{TIC}, \kappa^{TIC})$ - angular elements of the exterior orientation in the TIC solution,

$(\varpi^{TAD}, \varphi^{TAD}, \kappa^{TAD})$ - angular elements of the exterior orientation in the TAD solution.

The average value of parameter dω is equal to -0.07^0 with the scatter of results ranging from -15.40^0 to 14.05^0. Moreover, the standard value for parameter dω is 4.41^0 and the median is equal to -0.20^0. The average value of parameter dφ is equal to -0.33^0 with the scatter of results

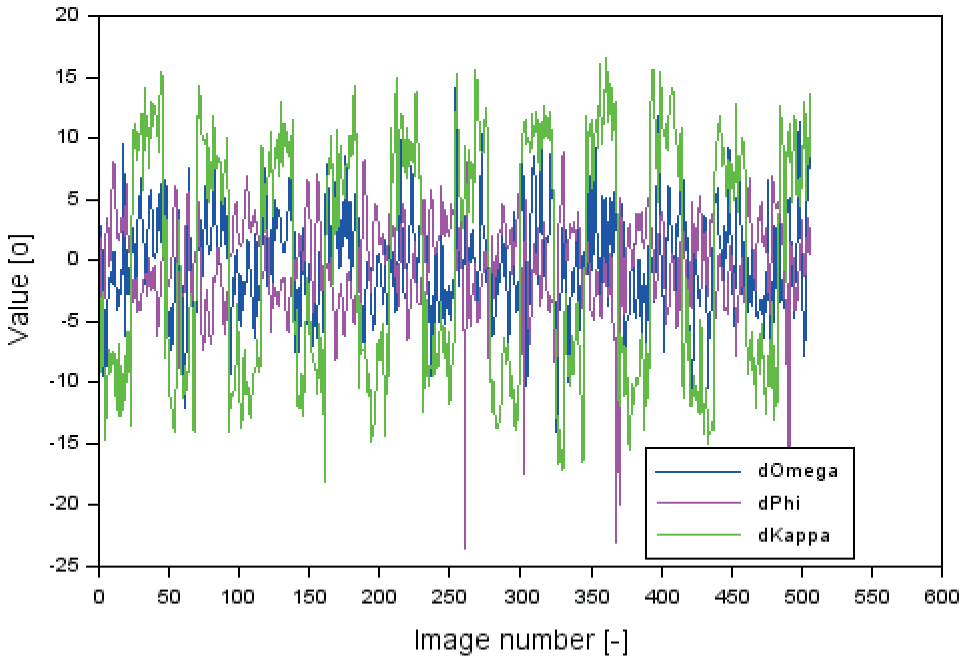

Figure 9 *Difference of the exterior orientation angle elements based on TIC and DAT methods*

ranging from -23.57^0 to 8.98^0. Moreover, the standard value for parameter dφ is 4.00^0 and of the median it is equal to -0.08^0. The average value of parameter dκ is equal to 0.06^0 with the scatter of results ranging from -18.23^0 to 16.64^0. Moreover, the standard value for parameter dκ is 9.86^0, and the median is equal to 2.15^0. The dω parameter has the smallest values of dispersion of the obtained findings, while the standard deviation and the median are the smallest for parameter dφ. The largest value of standard deviation and of the median are visible for parameter dκ.

5 Conclusions

The article describes and presents the results of exploiting three test methods for determining the elements of exterior orientation in photogrammetry for the needs of photogrammetry for aerospace applications. The paper used:

- the TGC method, which allows determining the linear elements of exterior orientation based on navigation data from the GNSS receiver, mounted on an unmanned aircraft system,
- the TIC method, which allows determining the angular elements of exterior orientation based on YPR parameters recorded by the INS sensor,
- the TAD method, which allows designating the linear and angular elements of exterior orientation in the model of digital aerial triangulation.

The research experiment was carried out for navigational data derived from the Trimble UX-5 rover. The photogrammetric flight was executed over Tylicz in 2016. During the flight, 506 images were taken at an altitude of 150 m. They were used in the process of digital aerial triangulation. For the needs of digital aerial triangulation, more than ten ground control points and five independent check points were measured. Based on the conducted investigations, it was found that:

- the calculated dY parameter has the smallest values of the median (e.g. 1.99 m) and of the standard deviation (e.g. 2.43 m),
- the calculated dZ parameter has the smallest values of the median (e.g. -0.38 m) and highest of the standard deviation (e.g. 4.30 m),
- the calculated dX parameter has the smallest value of the median (e.g. 1.48 m),
- the calculated dφ parameter has the smallest values of the median (e.g. -0.33^0) and of the standard deviation (e.g. 4.00^0),
- the calculated dκ parameter has the smallest values of the median (e.g. 0.06^0) and highest of the standard deviation (e.g. 9.86^0),
- the calculated dω parameter has the smallest dispersion of results with range between -15.40^0 to 14.05^0.

Acknowledgements

This paper was supported by Polish Air Force University and by the Military University of Technology, the Faculty of Civil Engineering and Geodesy, Institute of Geodesy.

References

[1] GINI, R., PAGLIARI, D., PASSONI, D., PINTO, L., SONA, G., DOSSO, P., BILL, R. UAV photogrammetry: block triangulation comparisons. *The International Archives of the Photogrammetry, Remote Sensing and Spatial Information Sciences* [online]. 2013, **XLI**(W2), p. 157-162. ISSN 1682-1750, eISSN 2194-9034. Available from: https://doi.org/10.5194/isprsarchives-XL-1-W2-157-2013

[2] COLOMINA, I., MOLINA, P. Unmanned aerial systems for photogrammetry and remote sensing: a review. *ISPRS Journal of Photogrammetry and Remote Sensing* [online]. 2014, **92**, p. 79-97. ISSN 0924-2716, eISSN 1872-8235. Available from: https://doi.org/10.1016/j.isprsjprs.2014.02.013

[3] RIEKE, M., FOERSTER, T., GEIPEL, J., PRINZ, T. High-precision positioning and real-time data processing of UAV systems. *International Archives of the Photogrammetry, Remote Sensing and Spatial Information Sciences* [online]. 2011, **38**(1/C22), p. 119-124. ISSN 1682-1750, eISSN 2194-9034. Available from: https://doi.org/10.5194/isprsarchives-XXXVIII-1-C22-119-2011

[4] GASPAROVIC, M. JURJEVIC, L. Gimbal influence on the stability of exterior orientation parameters of UAV acquired images. *Sensors* [online]. 2017, **17**(2), p. 401. eISSN 1424-8220. Available from: https://doi.org/10.3390/s17020401

[5] JIANG, S., JIANG, W., On-board GNSS/IMU assisted feature extraction and matching for oblique UAV images. *Remote Sensing* [online]. 2017, **9**, p. 813. eISSN 2072-4292. Available from: https://doi.org/10.3390/rs9080813

[6] IZOLTOVA, J., PISCA, P., CERNOTA, P., MANCOVIC, M., Adjustment of code ranging of GNSS observations. *Communications - Scientific Letters of the University of Zilina* [online]. 2016, **18**(4), p. 15-18. ISSN 1335-4205, eISSN 2585-7878. Available from: http://komunikacie.uniza.sk/index.php/communications/article/view/283

[7] SUN, Y., SUN, H., YAN, L., FAN, S., CHEN, R., RBA: Reduced bundle adjustment for oblique aerial photogrammetry. *ISPRS Journal of Photogrammetry and Remote Sensing* [online]. 2016, **121**, p. 128-142. ISSN 0924-2716, eISSN 1872-8235. Available from: https://doi.org/10.1016/j.isprsjprs.2016.09.005

[8] SCHNEIDER, J., LABE, T., FORSTNER, W. Incremental real-time bundle adjustment for multi-camera systems with points at infinity. *The International Archives of the Photogrammetry, Remote Sensing and Spatial Information Sciences* [online]. 2013, **XLI(**W2), p. 355-360. ISSN 1682-1750, eISSN 2194-9034. Available from: https://doi.org/10.5194/isprsarchives-XL-1-W2-355-2013

[9] BLAZQUEZ, M., COLOMINA, I. Relative INS/GNSS aerial control in integrated sensor orientation: models and performance. *ISPRS Journal of Photogrammetry and Remote Sensing* [online]. 2012, **67**, p. 120-133. ISSN 0924-2716, eISSN 1872-8235. Available from: https://doi.org/10.1016/j.isprsjprs.2011.11.003

[10] WIERZBICKI, D. Determine the position and attitude of UAV in air navigation based on GNSS data. 22nd International Conference Scientific Transport Means: proceedings. 2018. ISSN 1822-296X, eISSN 2351- 7034, p. 278-285.

[11] FORLANI, G., DIOTRI, F., MORRA DI CELLA, U., RONCELLA, R. Indirect UAV strip georeferencing by on-board GNSS data under poor satellite coverage. *Remote Sensing* [online]. 2019, **11**(15), p. 1765. eISSN 2072-4292. Available from: https://doi.org/10.3390/rs11151765

[12] WIERZBICKI, D. Determination of Shift/Bias in digital aerial triangulation of UAV imagery sequences. *IOP Conference Series: Earth and Environmental Science* [online]. 2017, **95**, 032033. ISSN 1755-1307, eISSN 1755-1315. Available from: https://doi.org/10.1088/1755-1315/95/3/032033

[13] WIERZBICKI, D. The prediction of position and orientation parameters of UAV for video imaging. *The International Archives of the Photogrammetry, Remote Sensing and Spatial Information Sciences* [online]. 2017, **XLII-2**(W6). ISSN 1682-1750, eISSN 2194-9034. Available from: https://doi.org/10.5194/isprs-archives-XLII-2-W6-407-2017

[14] WIERZBICKI, D., KRASUSKI, K. Determination the coordinates of the projection center in the digital aerial triangulation using data from unmanned aerial vehicle (in Polish). *Aparatura Badawcza i Dydaktyczna*. 2016, **21**, p. 127-134. ISSN 1426-9600.

[15] BURKER, M., HEIMES, F. J. *New* calibration and computing method for direct georeferencing of image and scanner data using the position and angular data of a hybrid inertial navigation system. OEEPE-Workshop Integrated Sensor Orientation: proceedings. 2001.

[16] YI Z., JIANG, G., YANAN D. Speed-up matching method with navigation data for UAV remote sensing images of coastal region. Remote Sensing of the Environment: 19th National Symposium on Remote Sensing of China: proceedings. 2015.

[17] RABAH, M., BASIOUNY, M., GHANEM, E., ELHADARY, A. Using RTK and VRS in direct geo-referencing of the UAV imagery. *NRIAG Journal of Astronomy and Geophysics* [online]. 2018, **7**(2), p. 220-226. eISSN 2090-9977. Available from: https://doi.org/10.1016/j.nrjag.2018.05.003

[18] GRUEN, A. Adaptive least squares correlation: a powerful image matching technique. *South African Journal of Photogrammetry Remote Sensing and Cartography*. 1985, **14**(3), p. 175-187. ISSN 0085-6398.

[19] WIERZBICKI, D. Estimation of angle elements of exterior orientation for UAV images based on ins data and aerial triangulation processing. 17th International Scientific Conference Engineering for Rural Development: proceedings [online]. 2018. ISSN 1691-5976, p. 1990-1996. Available from: https://doi.org/10.22616/ERDev2018.17.N054

Annex - Nomenclature of used abbreviations

Abbreviation	Full name
GNSS	Global Navigation Satellite System
UAVs	Unmanned Aerial Vehicles
INS	Inertial Navigation System
YPR	Yaw, Pitch and Roll
XYZ	Geocentric coordinates
GPS	Global Positioning System
OPK	Omega, Phi, Kappa
GCPs	ground control points
RTK	Real Time Kinematic
TGC	Translation between GPS sensor and Camera sensor
DAT	Digital Aerial Triangulation processing
PUWG2000	Local frame of Cartesian coordinates in Poland
RMS	Root Mean Square

https://doi.org/10.26552/com.C.2020.1.25-34

Geza Katona - Janos Juhasz

THE HISTORY OF THE TRANSPORT SYSTEM DEVELOPMENT AND FUTURE WITH SHARING AND AUTONOMOUS SYSTEMS

The world today is rapidly changing with the spread of automation. Moreover, urban life is more and more common and the number of inhabitants is rapidly growing. This time is the renaissance of bicycle-based vehicles, especially of electric power assisted bicycles. Vehicle sharing is also getting more popular. These progresses will have a crucial effect on traditional transportation networks. Moreover, the traffic volume, parking facilities and public space usage can be drastically modified. A research data is introduced from Paris and Lisbon, which helps to forecast the effect of the autonomous and sharing systems. This evolution can be advantageous, but it can also bring some disadvantages. In this article, these changes are summarized in the mirror of history, especially the Futurama concept and the transport system changes in Los Angeles. This overview will be a good basis for further research and for the development of a routing algorithm.

Keywords: *smart city, multimodal, autonomous, sharing*

1 Introduction

Autonomous development is more and more in the focus of all the developers in the transportation industry. Tesla [1] and Google [2] are the biggest from the IT sector, but conventional car builders also invested a lot in this research area. Not just the automotive sector, but train [3] and aircraft [4] manufacturing companies also take part in this improvement, and their aim is to achieve the biggest available cost savings. This can be realized by cutting down operational costs and by reducing the probability of accidents. Moreover, in the case of the rail industry the infrastructure optimization is also a key factor [5]. Furthermore, the smart city concept can also be effective and be a part of these developments. The evolution of the smart city concept was in the highlight of a study, with the intent to summarize and determine the content of the concept [6]. The outcome was that the definition is still forming, the content is expanding and 'smart city' trends cover the environmental, the digital and the social part of the life, as well. This also has an effect on Urban planning which was examined by Koryagin [7]. Moreover, the smart city conception can affect the transportation performance. These characteristics and the possible changes are also determinative [8].

In the case of a passenger transport in a multimodal transport chain, the level of comfort and available parking spots are the most important factors. This was researched and three scenarios were modeled in [9]. The three alternatives are the following: the first is traveling only with a private car; the second is that the decision can be made between using a private car or using the public transport with a P+R facility and the third alternative considered the personal comfort additionally. This area was also examined by Kirchler [10]. The effect on the environment was also examined from the viewpoint of parking [11].

The environmental impact must be taken into account, as well, regarding the level of pollution and the resources used by the transportation. This, especially the CO_2 emission was in the main focus of a study made at Altao University [12]. The effect on environment was also examined from the viewpoint of parking [13]. One should not forget the economic aspects [14]. Furthermore, the special case of logistics has to be taken in account, as well [15].

Regarding autonomous operation, the acceptance by the society is also a key factor. A wide range survey was made in 2014, which focused on opinion of the common people [16]. Moreover, ethical questions cannot be neglected, either [17]. Furthermore, the testing procedure is also a key factor in this case [18]. In other studies, some predictions were made to sum up the possible advantages and disadvantages of the role of autonomous transportation [19-20]. In addition, the traffic distribution need to be considered, as well [21]. With the usage of the autonomous systems, the door-to-door transport can be made easier. A review was made to summarize the accessibility of the public transport [22].

This article is an extension of a conference paper [23]. That paper focused only on the role of autonomous cars. In this article, their effect on the public transport and the possible function of autonomous vehicles in public transport is presented. One of the inspirations to widen our study was a presentation about the trends and opportunities in the future cities [24].

Geza Katona*, Janos Juhasz
Department of Automotive Technologies, Faculty of Transportation Engineering and Vehicle Engineering, Budapest University of Technology and Economics, Hungary
*E-mail of corresponding author: geza.katona@gjt.bme.hu

Figure 1 *Safe (in the arm of Jesus) [27]*

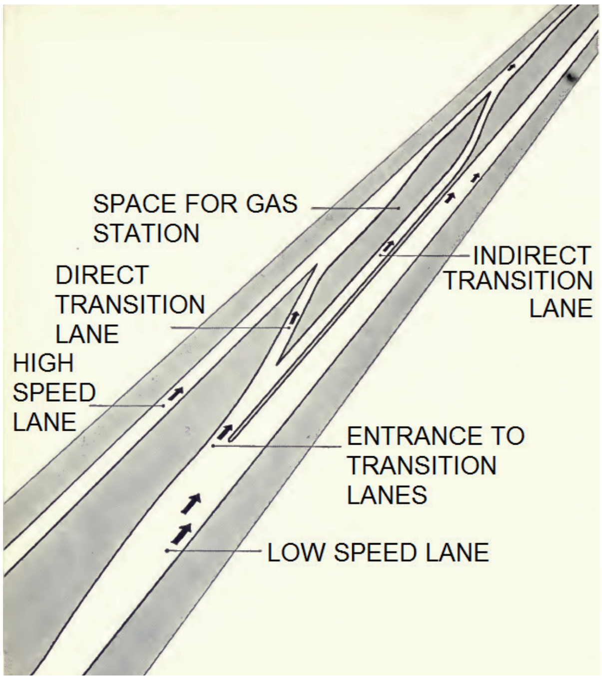

Figure 2 *Transit from one speed to another [27]*

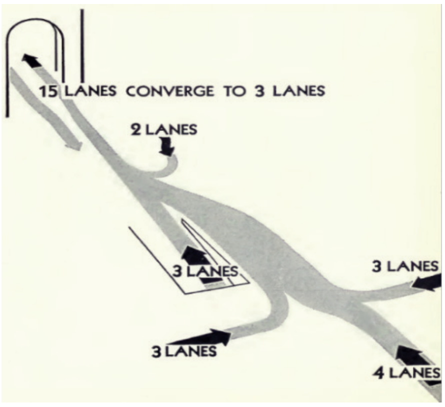

Figure 3 *George Washington bridge approach problem [27]*

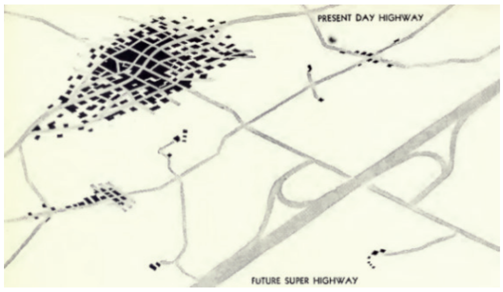

Figure 4 *Motorway feeders from farm and village [27]*

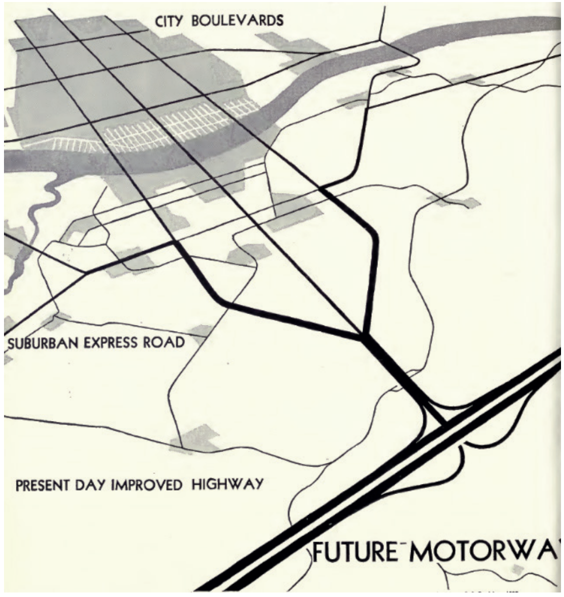

Figure 5 *Motorway feeder to city [27]*

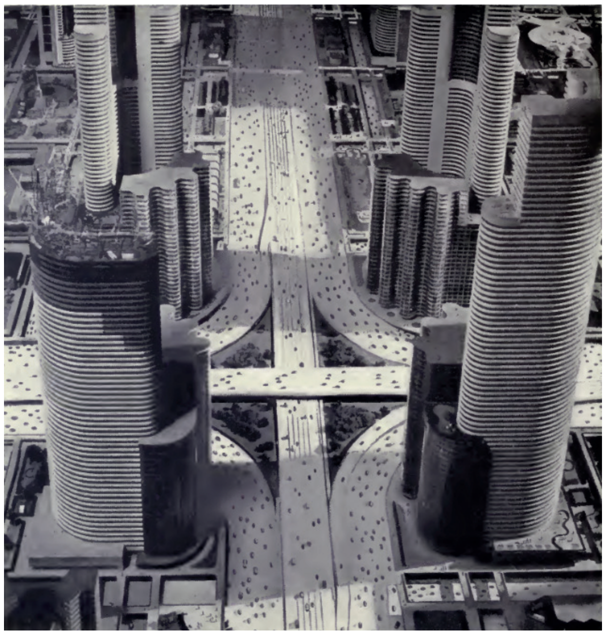

Figure 6 *Express boulevards are the main arteries for the through city traffic [27]*

Regarding the research listed above, there is an active discussion to find some solutions for the problems caused by urbanization. There are several possible answers, such as the smart city concept, the autonomous driving and the Futurama concept - even though it is quite old. The hypothesis is that autonomous vehicles alone cannot solve the traffic congestion problems.

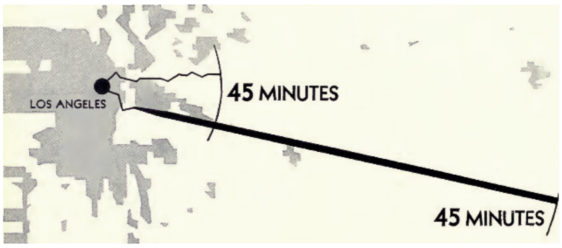

Figure 7 *Commuting radius extension*

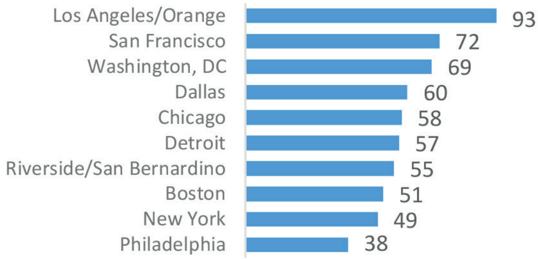

Figure 9 *Annual hours of delay per Traveler by Metropolitan Area, 2003 [30]*

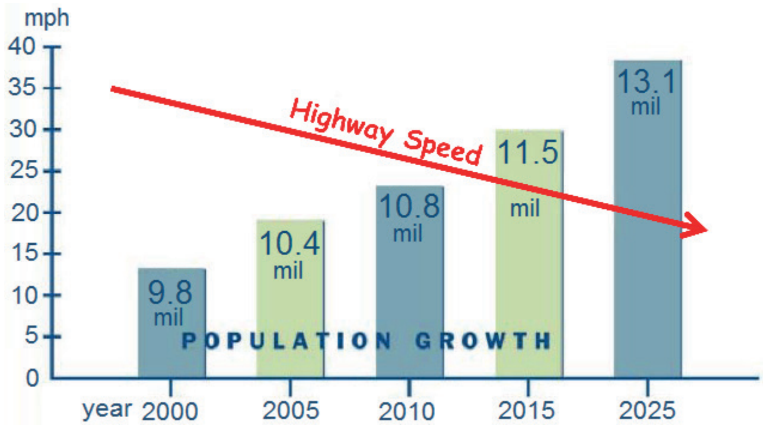

Figure 8 *Comparison of population growth and highway speed [28]*

2 The Futurama concept

In 1939, a new approach was presented in connection with transportation at the New York World's Fair [25-27]. The expo's aim was to predict the trends of the next 20 years. One of the main sponsors of the event was General Motors Corporation. Norman Bel Geddes collected his thoughts about this future in a book [27]. He saw the future in automation. One of the main reasons was to avoid accidents (Figure 1). This is still the core basis of autonomous development.

In this book, the answer for the safety, comfort, speed and economy questions was the concept of highways in and out of cities. The concept of changing between different travel speeds is depicted in Figure 2.

The identified core problem was the change (decrease) of number of lanes, which caused a bottleneck effect (Figure 3).

The connection concept of the smaller cities was the following (Figure 4).

In the case of bigger cities, the following model was proposed (Figure 5).

Image of the city center is presented in Figure 6.

A prediction for the commuter traffic was that the commuting radius can extend 6 times with this concept (Figure 7).

3 The effect of the Futurama

This concept had the most impact on the city of Los Angeles (LA). Therefore, the transportation changes are summarized according to the Futurama with the history of LA.

The Transportation Research Library & Archive made a great collection of the milestones of the developments of transportation in LA [28].

The milestones, according to Barrett, were the following: in 1870s, a horse-drawn system was installed in the city. In the next decade, cable cars replaced the horse power, which was needed due to the rapid growth of the population and transit. This system was highly unreliable because of the dirt in the cable tubes, which caused freezing during operation. Therefore, this system was changed in the 1890s to electrically powered cars. This caused a rapid expand in the network.

Some decades later, a slow degradation was starting. The principles of business started to change before and after the Second World War. The maintenance costs of the network - such as the replacement of old vehicles, the renewal of the stations and tracks - became a priority problem to the local and federal governments. The fares were artificially kept low due to political interests. Additionally, the car became a status symbol. Moreover, General Motors began to sell air-conditioned and air-suspensioned buses with 45 seats. Operators predicted that the freeway system would accommodate and speed up the buses. As a result of these processes, the last rail line was closed in 1963.

In the following decades, the bus was the core of public transport although a public discussion focused on a monorail and metro system. Those times were also characterized by innovative and special solutions that were intended to sustain public transport without a high capacity

***Table 1** Modal-split in 2005 in Los Angeles [30]*

Subject	Total	Male	Female
Workers 16 years and over	1,662,238	954,410	707,828
MEANS OF TRANSPORTATION TO WORK			
Car, truck or van	79.50%	81.00%	77.50%
Drove alone	67.80%	68.90%	66.40%
Carpooled	11.70%	12.10%	11.10%
In 2-person carpool	9.00%	9.20%	8.70%
In 3-person carpool	1.70%	1.90%	1.50%
In 4-or-more person carpool	0.90%	1.00%	0.90%
Workers per car, truck or van	1.37	1.34	1.4
Public transportation (excluding taxicab)	10.30%	9.30%	11.70%
Walked	3.20%	2.90%	3.50%
Bicycle	0.60%	0.90%	0.20%
Taxicab, motorcycle, or other means	1.70%	1.80%	1.50%
Worked at home	4.70%	4.00%	5.70%

***Table 2** Fleet size for different TaxiBot and AutoVot scenarios (% of current Lisbon car fleet, 24-hour weekday average) [33]*

			Fleet size	% of baseline
		Baseline	203 000	
100% shared self-driving fleet	Ride sharing (TaxiBot)	No high-capacity public transport	25 917	12.8
		With high-capacity public transport	21 120	10.4
	Car sharing (AutoVot)	No high-capacity public transport	46 249	22.8
		With high-capacity public transport	34 082	16.8
50% private car use for motorized trips	Ride sharing (TaxiBot)	No high-capacity public transport	13 265+194 537*	102.4
		With high-capacity public transport	10 900+147 767*	78.2
	Car sharing (AutoVot)	No high-capacity public transport	22 887+194 275*	107.0
		With high-capacity public transport	18 358+148 050*	82.0

* = shared + private cars

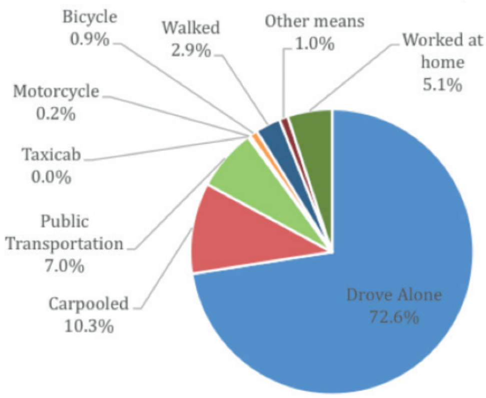

***Figure 10** Modal-split in 2015 in Los Angeles [31]*

core network. After several public vote fails, the first high capacity light rail line was opened in 1990 [29] and since then the network has been rapidly expanding.

Due to the high mobility and motorization, the highway speed was constantly decreasing along with the population growth (Figure 8) and the time spent in traffic jams was also increasing (Figure 9).

In 2005, a Census was made and data was also evaluated in connection with transportation (Table 1). Ten

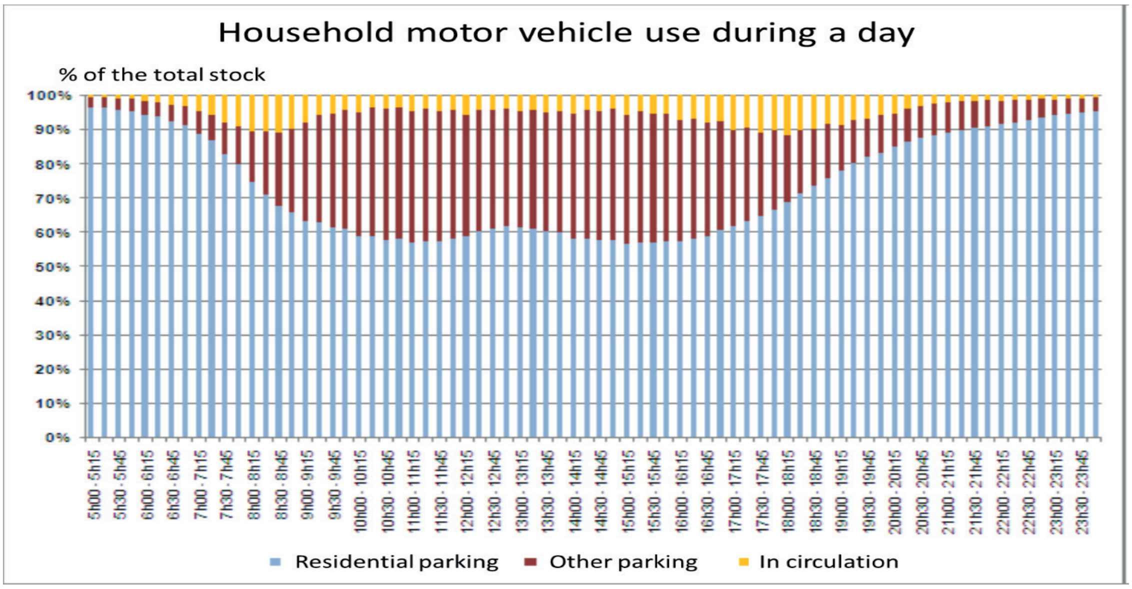

***Figure 11** An average car is parked approximately 23 hours a day [32]*

***Table 3** The Automated levels for driving (SAE 2014) [19]*

	SAE level	Name	Execution of steering and acceleration / deceleration	Monitoring of driving environment	Fallback performance of dynamic driving task	System capability (driving modes)
Human driver monitors the driving environment	0	No automation	Human driver	Human driver	Human driver	n/a
	1	Driver assistant	Human driver and system	Human driver	Human driver	Some driving modes
	2	Partial automation	System	Human driver	Human driver	Some driving modes
Automated driving system monitors the driving environment	3	Conditional automation	System	System	Human driver	Some driving modes
	4	High automation	System	System	System	Some driving modes
	5	Full automation	System	System	System	All driving modes

***Table 4** Possible autonomous vehicle usage [19]*

	Advantages	Disadvantages	Potential group of users
Personal autonomous vehicles - self-driving vehicles in private ownership.	Continuous availability. The private property can be stored in the vehicle.	A vehicle that meets the travel aim cannot be chosen for each trip. High costs.	Frequent travelers on a daily base, and/or the car is used as a storage for private property.
Shared autonomous vehicles - Self-driving taxis, door-to-door service for the users.	A vehicle for the actual need can be chosen. Door-to-door service.	Waiting for a car is possible. No personal staff (driver). The car can be dirty after the previous user.	Not so frequent travelers.
Shared autonomous rides - Self-driving vans (micro-transit) take passengers to or near destinations. Supplementary service for public transport systems.	The cost will probably be the lowest.	The comfort level will be the lowest, the travel time probably will be higher.	Occasional trips.

years later, driving alone was getting more common (Figure 10).

The Futurama concept had the highest impact on the transportation methods of the USA, but the rest of the word was also concerned. A survey was made about the daily car usage in Paris (Figure 11).

Figure 12 In Seattle, parking spaces were designated for dockless bikes [34]

Figure 13 Singapore is still improving its dockless bike-sharing regulation [35]

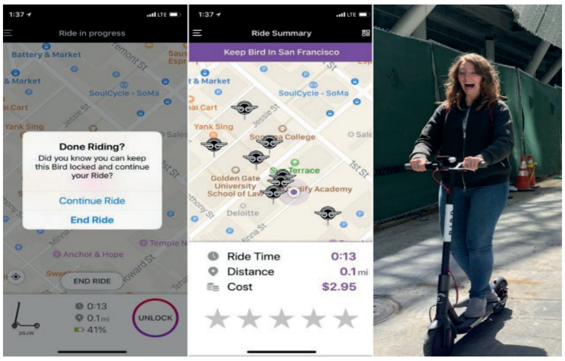

Figure 14 Bird electric scooters are taking over San Francisco [36]

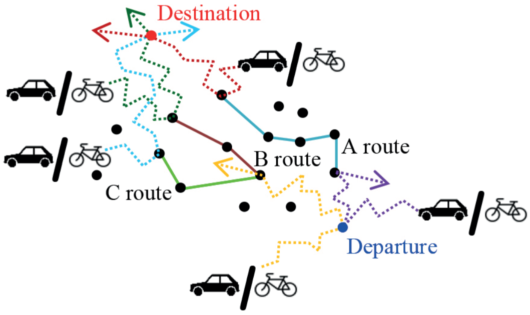

Figure 15 Traditional public transport with the new age solution

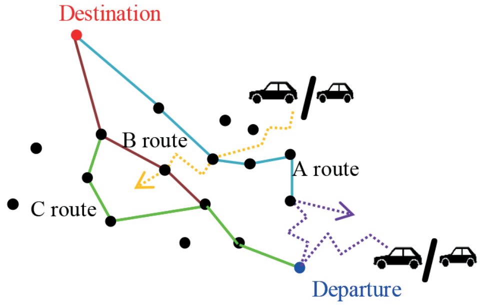

Figure 16 Traditional public transport with the new age solution during the trip

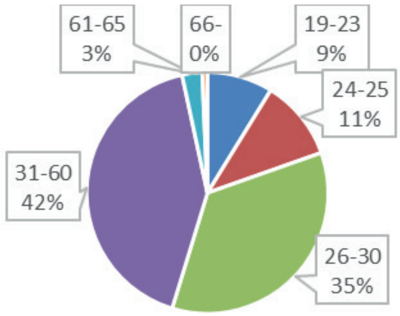

Figure 17 Age distribution

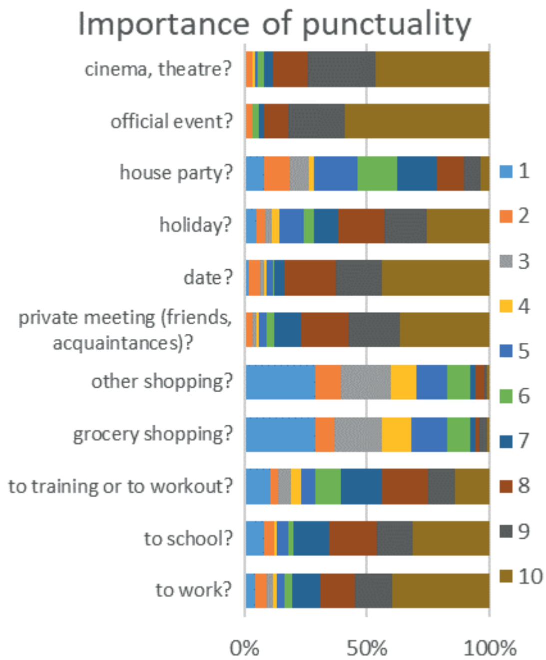

Figure 18 Importance of punctuality

Based on this survey, only 10% of the vehicles are in the traffic flow in peak hours and 90% are parking mainly at home or other locations, especially at the working place.

According to this, only 10% of the cars are causing the traffic jams. In 2015, the International Transportation Forum published a report about the shared self-driving cars [33]. This study was based on experiences of the Autonomous taxi system for New Jersey and the taxi pooling for New York City. The subject of the research was the city of Lisbon.

Based on Table 2, in the case of the 100% shared self-driving fleet with a high-capacity public transport, the actual car fleet size can be reduced by 90%. In the light of the car usage survey [32], this - in general - can cause elimination of the actually not used (parking) cars, but there will be no significant effect on traffic jams and road capacity. Based on

***Table 5** Employment status*

Status	Percent
Employee	70.55%
Entrepreneur	0.68%
Middle manager	13.01%
Pensioner	0.68%
Volunteer	0.68%
Student and part time employee	1.36%
Student	13.01%

this, autonomous cars cannot replace, but only supplement the high-capacity public transport.

4 Supplement transportation

4.1 Autonomous vehicles

Definition of autonomous transport was created based on the Society of Automotive Engineers (SAE) classification [19], this is presented in Table 3 and the possible role of the car is summarized in Table 4.

According to data presented in Table 3, only level 5 is suitable for use of autonomous service.

The most effective solution for society is the shared autonomous ride that requires much less parking facilities, but the economic effect, especially for car producers, can be negative due to decrease in the number of sold cars.

4.2 Bike, scooter share

Traditional bike sharing systems are used worldwide nowadays. They are usually based on a fix docking network. This type of system is working properly, but it usually serves only the high density areas in the cities, if the operation costs and effectiveness are taken into consideration. Moreover, the docking stations mean a restriction for users. Therefore, some operators started to develop dockless solutions.

The greatest advantage of the dockless system is that the user can leave the bicycle anywhere. On the other hand, this can cause a mess in the cityscape. Therefore, parking places for bikes were created as a solution in Seattle (Figure 12) and in Singapore (Figure 13).

In addition to electric bikes, a new solution is underway. This is the electric scooter, which reduces the required space and gives more flexibility to the user. A service was started in San Francisco (Figure 14).

5 Public transport and the new age transport solutions

Considering the possible cooperation between traditional public transport, different sharing solutions and the autonomous vehicles based on the Futurama experiences and the research outcomes, it can be concluded that the public transport can only be supplemented with these solutions and cannot be fully replaced by them. Therefore, the low density areas can be served by the autonomous solution, but bike and scooter sharing systems are the best solutions for the high density city center. A schematic model is created to demonstrate this (Figure 15).

Those solutions cannot be used only to take the so-called last mile, but also to change between the high capacity transportation lines (Figure 16).

In this case, the autonomous vehicle operates as a taxi and the bike/scooter sharing system as a dockless solution.

6 Survey data

In 2017, a preliminary survey was made to examine the people's relationship with travelling. This survey distinguished between commuters and those going on leisure trips. A part of the results is published in another article [37]. The aim of this survey was to measure the effect of different factors on the user decisions according to the travel mode and the route planning. Due to the preliminary nature of the survey, the outcome was not representative. In order to complete the survey, one required internet connection and the questionnaires were shared via e-mail and Facebook. Even so, 146 participants submitted their answers. Those were basically submitted from Budapest and respondents were mainly people with higher education. Regarding the research of Smith [38] and the Pew Research Center [39], the spread of smartphones and internet usage are higher where the population density and the per capita income are higher. Based on this, the probability of the new techniques (e.g.: autonomous car, shared economy, …) usage is higher. Moreover, the commuting and traffic problems appearance is presumably higher, as well. Based on this, result of this survey can be used as good preliminary data for further research. The age distribution of the respondents is presented in Figure 17.

The participants' employment status is given in Table 5.

Regarding the data presented in Figure 9, the importance of punctuality could have a significant role, which helps to understand the effect of delay on travelers. The following diagram summarizes the results regarding punctuality (Figure 18).

In this diagram, “1” represents the least important and “10” represents the most important factor. It clearly demonstrates that punctuality is a key factor if the event’s starting time is fixed, and it is not as important in the case of categories concerning leisure time. In the light of the traffic distribution (Figure 11) and delays (Figure 9) caused by traffic jams, the predictability of commuting is of great importance.

7 Summary

In this article, the Futurama concept and its effect to the world (with the example of Los Angeles) were summarized. The history of LA’s public transport is presented in more detail.

Two important researches were presented in connection with autonomous cars. The outcome of a survey made in Paris on distribution of car usage showed that only 10% of the cars are causing the traffic jams. Another research on autonomous car usage was based on a simulation of Lisbon’s traffic change in the case of presence of autonomous taxis; this study predicted that the number of cars can be reduced to approximately 10%, only if there is a well-functioning, high-capacity public transport. Based on this finding, autonomous transportation cannot replace the traditional public transport systems, it can only supplement them.

Classification of the autonomous systems was also done. Furthermore, the new age bike sharing systems were introduced. These also might have a significant effect on public transport systems and autonomous transportation.

Based on the presented survey data, punctuality is a key factor for travelers. Regarding the delays, caused by the traffic jams and the research data, the autonomous car cannot be the only solution for traffic problems. Based on this, the hypothesis of the article is considered to be supported.

This overview can be a good starting point for future research. As a next step, the routing algorithm needs to be implemented as described in Section 5.

References

[1] Tesla, Inc. [online]. [Viewed 2018-03-18]. Available from: https://www.tesla.com

[2] Alphabet Inc. Waymo - Google - Waymo [online]. [Viewed 2018-03-18]. Available from: https://www.google.com/selfdrivingcar/

[3] VAN LEIJEN, M. First fully autonomous train ride in Australia. *RailFreight.com* [online]. 2017. Available from: https://www.railfreight.com/business/2017/10/05/first-fully-autonomous-train-ride-in-australia/

[4] PARK, K. *Airbus looking forward to a pilotless future* [online]. New York: Bloomberg - Technology L.P., 2017. Available from: https://www.bloomberg.com/news/articles/2017-11-21/airbus-exploring-single-pilot-autonomous-aircraft-in-tech-race

[5] LEITNER, B., REHAK, D., KERSYS, R. The new procedure for identification of infrastructure elements significance in sub-sector railway transport. *Communications - Scientific Letters of the University of Zilina* [online]. 2018, **20**(2), p. 41-48. ISSN 2585-7878, eISSN 2585-7878. Available from: http://komunikacie.uniza.sk/index.php/communications/article/view/86

[6] COCCHIA, A. Smart and digital city: a systematic literature review [online]. In: *Smart city: how to create public and economic value with high technology in urban space*. DAMERI, R. P., ROSENTHAL-SABROUX, C. (eds.). Cham: Springer, 2014, p. 13-43. Available from: https://doi.org/10.1007/978-3-319-06160-3_2

[7] KORYAGIN, M. Urban planning: a game theory application for the travel demand management. *Periodica Polytechnica Transportation Engineering* [online]. 2018, **46**(4), p. 171-178. ISSN 0303-7800, eISSN 1587-3811. Available from: https://doi.org/10.3311/PPtr.9410

[8] CZIMMERMANN, P., KOHANI, M. Characteristics of changes of transportation performance for pairs of critical edges. *Communications - Scientific Letters of the University of Zilina* [online]. 2018, **20**(3), p. 84-87. ISSN 2585-7878, eISSN 2585-7878. Available from: http://komunikacie.uniza.sk/index.php/communications/article/view/258

[9] LI, Z.-CH., LAM, W. H. K., WONG, S. C., ZHU, D.-L., HUANG, H.-J. Modeling park-and-ride services in a multimodal transport network with elastic demand. *Transportation Research Record Journal* [online]. 2007, **1994**(1994), p. 101-109. ISSN 0361-1981, eISSN 2169-4052. Available from: https://doi.org/10.3141/1994-14

[10] KIRCHLER, D. *Efficient routing on multi-modal transportation networks. Data Structures and Algorithms [cs.DS]* [online]. Paris: Ecole Polytechnique X, 2013. Available from: https://pastel.archives-ouvertes.fr/pastel-00877450

[11] RUDOLPH, F., MATRAI, T. Congestion from a multimodal perspective. *Periodica Polytechnica Transportation Engineering* [online]. 2018, **46**(4), p. 215-221. ISSN 0303-7800, eISSN 1587-3811. Available from: https://doi.org/10.3311/PPtr.12048

[12] NOREIKIS, M., BUTKUS, P., NURMINEN, J. K. *In-vehicle application for multimodal route planning and analysis*. Aalto, Finland: Aalto University, 2014.

[13] MORFOULAKI, M., KOTOULA, K. M., MYROVALI, G., AIFADOPOULOU, G. Calculating the impacts of alternative parking pricing and enforcement policies in urban areas with traffic problems. *Periodica Polytechnica Transportation Engineering* [online]. 2017, **45**(1), p. 35-41. ISSN 0303-7800, eISSN 1587-3811. Available from: https://doi.org/10.3311/PPtr.9099

[14] HYKS, O., NEUBERGOVA, K., PRIBYL, P. Influence of driving fluency on economic and ecological aspects of transport. *Communications - Scientific Letters of the University of Zilina* [online]. 2018, 20(3), p. 9-14. ISSN 2585-7878, eISSN 2585-7878. Available from: http://komunikacie.uniza.sk/index.php/communications/article/view/245

[15] PAWESKA, M., RISTVEJ, J. Logistics during population and animals evacuation in case of extraordinary incidents and crisis events. *Communications - Scientific Letters of the University of Zilina* [online]. 2018, **20**(2), p. 88-95. ISSN 2585-7878, eISSN 2585-7878. Available from: http://komunikacie.uniza.sk/index.php/communications/article/view/93

[16] SCHOETTLE, B., SIVAK, M. *A survey of public opinion about autonomous and self-driving vehicles in the U.S., the U.K., and Australia*. Ann Arbor, Michigan, USA: University of Michigan, Transportation Research Institute, 2014.

[17] LIN, P. Why Ethics matters for autonomous cars [online]. In: *Autonomous driving*. MAURER, M., GERDES J., LENZ B., WINNER H. (eds.). Berlin, Heidelberg: Springer, 2016, p. 69-85. ISBN 978-3-662-48845-4, eISBN 978-3-662-48847-8. Available from: https://doi.org/ 10.1007/978-3-662-48847-8_4

[18] SZALAY, Z., NYERGES, A., HAMAR, Z., HESZ, M. Technical specification methodology for an automotive proving ground dedicated to connected and automated vehicles. *Periodica Polytechnica Transportation Engineering* [online]. 2017, **45**(3), p. 168-174. ISSN 0303-7800, eISSN 1587-3811. Available from: https://doi.org/10.3311/PPtr.10708

[19] LITMAN, T. *Autonomous vehicle implementation predictions - implications for transport planning*. Victoria, Canada: Victoria Transport Policy Institute, 2018.

[20] KPMG. *Impact of autonomous vehicles on public transport sector*. Swiss: KPMG International Cooperative, 2017.

[21] PAUER, G., TOROK, A. Static system optimum of linear traffic distribution problem assuming an intelligent and autonomous transportation system. *Periodica Polytechnica Transportation Engineering* [online]. 2018, **47**(1), p. 64-67. ISSN 0303-7800, eISSN 1587-3811. Available from: https://doi.org/10.3311/PPtr.11548

[22] SAIF, M. A., ZEFREH, M. M., TOROK, A. Public transport accessibility: a literature review. *Periodica Polytechnica Transportation Engineering* [online]. 2018, **47**(1), p. 36-43. ISSN 0303-7800, eISSN 1587-3811. Available from: https://doi.org/10.3311/PPtr.12072

[23] KATONA, G., JUHASZ, J. *Autonomous cars in a multimodal transport plan*. Zielona Gora: University of Zielona Gora, 2018. ISBN 978-83-945647-1-1.

[24] VITEZY, D. *A jovo varosanak kozlekedese: veszelyek es lehetosegek / Transport for the city of the future: dangers and opportunities* (in Hungarian). 2018.

[25] FOX, R. W., LEARS, T. J. J. The power of culture: critical essays in American history. Chicago: The University of Chicago Press Ltd., 1993. ISBN 0-226-25955-2.

[26] Handy (Jam) Organization - To new horizons [online]. Available from: https://archive.org/details/ToNewHor1940

[27] GEDDES, N. B. *Magic motorways*. New York: Random House, 1940.

[28] BARRETT, M. *Los Angeles transportation transit history - South LA*. Los Angeles: 2014.

[29] Metro (the Los Angeles County Metropolitan Transportation Authority) - 20 years of metro rail [online]. [Viewed 2018-08-29]. Available from: https://www.metro.net/about/about-metro/

[30] The Public Information Office of the Department of Transportation. *The city of Los Angeles transportation profile 2009* [online]. Los Angeles: City of Los Angeles Department of Transportation, 2009. Available from: https://handels.gu.se/digitalAssets/1344/1344071_city-of-la-transportation-profile.pdf

[31] Shared-Use Mobility Center (SUMC). *Los Angeles county - shared mobility action plan*. Chicago: Shared-Use Mobility Center (SUMC), 2016.

[32] SCHMITT, D. *Motorisation et usage de la voiture en Ile-de-France. Enquete globale transport / Motorization and car usage in the Ile-de-France. Global transport survey* (in French). Paris: Direction regionale et interdepartementale de l'Equipement et de l'Amenagement (DRIEA) d'ile-de-France Service de la Connaissance des Etudes el de la Prospective, 2013.

[33] International Transportation Forum - Corporate Partnership Board. *Urban mobility system upgrade - how shared self-driving cars could change city traffic*. Paris: International Transport Forum at the OECD, 2015.

[34] COX, S. *Seattle tries designated parking for dockless bikes* [online]. Better Bike Share Partnership, 2018. Available from: http://betterbikeshare.org/2018/04/25/seattle-tries-designated-parking-dockless-bikes/

[35] GAUQUELIN, A. *Singapore is still improving its dockless bike-share regulation* [online]. Bikeshare News, 2018. Available from: http://www.bikeshare-news.com/2018/03/05/singapore-is-still-improving-its-dockless-bike-share-regulation/

[36] Robinson, M. *A startup in the West Coast scooter sharing craze is already worth $1 billion - here's what it's like to ride a Bird scooter* [online]. Business Insider Inc., 2018. Available from: https://www.businessinsider.com/bird-electric-scooter-review-2018-4

[37] KATONA, G., JUHASZ, J. User habits and multimodal route planning. *Production Engineering Archives / Archiwum Inzynierii Produkcji*. 2017, **16**, p. 22-27. ISSN 2353-5156, eISSN 2353-7779.
[38] SMITH, A. *Smartphone ownership - 2013 update* [online]. Washington, D. C: Pew Research Center's Internet & American Life Project, 2013. Available from: https://www.pewinternet.org/2013/06/05/smartphone-ownership-2013/
[39] POUSHTER, J. *Smartphone ownership and internet usage continues to climb in emerging economies* [online]. Pew Research Centre, 2016. Available from: https://www.pewresearch.org/global/2016/02/22/smartphone-ownership-and-internet-usage-continues-to-climb-in-emerging-economies/
[40] Futurama (New York World's Fair) - Wikipedia [online]. [Viewed 2018-08-26]. Available from: https://en.wikipedia.org/wiki/Futurama_(New_York_World%27s_Fair)

Beata Zagozdzon

CONDITIONS FOR THE DEVELOPMENT OF PUBLIC-PRIVATE PARTNERSHIP PPP - ANALYSIS BASED ON AN EXAMPLE OF TRANSPORT INFRASTRUCTURE IN POLAND

Transport infrastructure is not currently the domain of activity of solely the public sector. Governments entrust the provision of services or realization of investment tasks to private entities and the form of involvement of private investors may be the public-private partnership PPP. Successful implementation of the PPP projects requires appropriate economic, legal, institutional and social conditions.

The article identifies these determinants based on the literature on the subject and then their analysis in relation to conditions of operation and market development of the PPP projects in the area of transport infrastructure in Poland. The analysis covered the years 2009-2018 and was conducted against the background of development of the PPP market in selected EU countries.

Keywords: *determinants of public-private partnership PPP, transport, PPP in Poland*

1 Introduction

Transport infrastructure has specific characteristics such as: service and social service character, capital intensity, long period of payback of incurred financial expenses, technical and economic indivisibility [1]. These characteristics caused that infrastructure was generally considered to be the domain of activity and financing by public authorities. However, in recent decades, economists dealing with this issue have presented a view that infrastructure is no longer perceived as public goods and should not be provided by the state only, [2-3]. Currently, it is believed that there are no goods and services that can only be provided by the private or public sector [4]. Governments entrust implementation of public services or investment tasks to private entities and the form of involvement of private investors is often a public-private partnership PPP.

However, the practice of the PPP implementation and conducted studies show that the success of a partnership requires appropriate economic, legal, institutional and social conditions [5], [6]. In addition, the latest reports of the EU institution, which has been supporting the development of the PPP for several years, have shown that the implementation of successful projects is possible with appropriate legal, institutional framework and administrative efficiency. These instruments are currently available only in a limited number of countries with many years of implementation experience [7].

The aim of the research is to analyze the determinants of implementation and level of development of the PPP projects in the area of transport infrastructure in Poland. The subject and purpose of the research imply an analysis of the subject literature, statistical data, evaluation reports, as well as legal acts. The method of comparative analysis and analysis of cause and effect relationships have been applied, which increases the accuracy of the obtained results and conclusions formulated on this basis.

2 Determinants of the PPP development – a literature review

Since the subject matter of the PPP is quite well known and it has been the subject of many publications, the article omits wider considerations on the nature and forms of that partnership. Only a general definition of the PPP, based on literature studies, is provided, [8, 9]. A public-private partnership is a type of contract between a public partner and a private partner who work together to implement a project, while retaining their own goals and interests at the same time. The result of this cooperation should be lower costs of the project and a higher quality of services than in the case of their traditional financing from public funds [10]. The form of private entities' involvement in the PPP projects depends on its specificity and the individual needs of the project participants. The detailed classification of PPP forms was presented, among others, by R. Mu, M. de Jong and E. ten Heuvelhof [11]. Here one can only list the basic forms of participation of private entities in infrastructure projects: BOT - construction, exploitation, transfer, DBFO - design, construction, financing, exploitation and BOO - construction, exploitation, ownership (ownership remains permanently in the private sector).

Beata Zagozdzon
Faculty of Transport and Electrical Engineering, Kazimierz Pulaski University of Technology and Humanities in Radom, Poland
E-mail of corresponding author: b.zagozdzon@uthrad.pl

The literature also shows that the success of a partnership requires the provision of appropriate economic, legal, institutional and social conditions (success means a PPP project that has been carried out according to budget, schedule and quality of service standards) [5], [6]. Conditions favorable for the PPP implementation are defined as critical success factors - CSF. Their identification was the subject of extensive research conducted by Harcasttle et al. [12], which identified five main groups of factors: effective purchase process, feasibility of the project, government guarantee, favourable economic conditions and available financial market. The CSF classification, which is based on various aspects of risk associated with the PPP projects, was developed by Ozdogann and Birgonul [13]. Technical, financial and economic, social, environmental, political and legal risks are important determinants considered by decision-makers. An extensive review of the CSF was also presented by Ng et al. [14], who studied the importance of these factors, taking into account the objectives of the public sector, private sector and society. They proposed to divide the factors into four groups: political and legal, economic and financial, technical, social.

Based on literature research, it can be assumed that the classification of the determinants of the PPP success includes the following groups of factors: economic and financial, political and legal, technical and social. In addition, they can be divided according to the level of analysis. Determinants that are shaped by the government and its institutions can be described as factors at the macro level. However, those that affect the practical implementation at the stage of project preparation and feasibility assessment concern the micro-level.

These determinants have a differentiated impact on the success of the PPP. The research conducted by Chou et al. [15] shows that at the macro level, the following have the strongest impact: stable macroeconomic conditions, economic and political support of the government, availability of financing, legal system, competent public advisory agencies, social support, clear procurement process, competition in the procurement process. For transport infrastructure projects, an important factor, emphasised by Hammami et al. [5] and Chou et al. [15], is the stable macroeconomic condition of the country, and in particular such indicators as the GDP growth, purchasing power of customers, market size. Good macroeconomic conditions, according to Mansoor and Klein [16], are able to attract investors and increase the level of financial resources. Well-organised public advisory agencies are also a key factor. Their activity is particularly important in countries that have no experience with the PPP [5].

The element of experience in implementation of projects is worth noting here. It is about the experience of the government, private investors and multilateral lenders in the field of this kind of projects. A trustworthy and experienced private consortium provides the opportunity for agreement at the stage of project preparation and its subsequent technical feasibility. The experience of financial institutions is equally important because the private sector bases its financing structure primarily on external sources. Efficient financial intermediation, free access to capital and financial services are the key factors in the success of the PPPs. Research conducted by Butkiewicz and Yanikkay [17] show that the involvement of multilateral lenders and credit agencies in the project reinforces the positive outcome of this investment.

On the other hand, micro-level factors of significant importance, according to Ng et al. [14], are: socially acceptable level of fees/tariffs, reliable and experienced private consortium, long-term demand for services, stability of service provision, financial attractiveness of the project for private investors and cost effectiveness of the project in comparison with traditional forms of its implementation.

3 Analysis of the PPP functioning conditions in Poland

Implementation of the PPP projects requires that the predefined determinants were realized, especially those at the macro level. They create a fundamental framework for the functioning of partnership, without their fulfilment the PPP formula will not exist at all, not to mention the success of investment implementation. Further, due to the synthetic character of the article, the most important conclusions from the conducted research will be presented. These conclusions were formulated in relation to the basic key factors, which are: the legal system, government support, in particular the activity of public advisory agencies and availability of financing.

Stable law and certainty of its interpretation is a key and necessary condition for implementation of the PPP. In Poland, the first act, which enabled implementation of road investments by the private sector, was drafted in 1994. The practice of implementation showed problems and as a consequence the Act was amended - in 2000 and 2005. However, those legal actions were not enough and in 2008 a new, more flexible act was passed, which initiated the actual process of implementing public tasks in the PPP formula. In 2018, the government decided to increase the scale and effectiveness of the PPP and amended the Act of 2008 [18]. The new regulations simplify the procedure of selecting a partner and the process of concluding contracts. Moreover, they provide comprehensive advisory services for public entities and optional certification (evaluation) of projects by the minister of regional development. Legislative activities of the government have eliminated many legal obstacles. The current regulations are so flexible that even political changes will not be a barrier to the PPP implementation.

The government also plans to establish a guarantee and warranty system for the public and private sectors. It concerns the creation of a special fund for the PPP, preferential rules and interest rates [15]. The latter is very important as it will facilitate access to bank loans for investors. In previous years, external financing was provided mainly to projects that met one of two criteria:

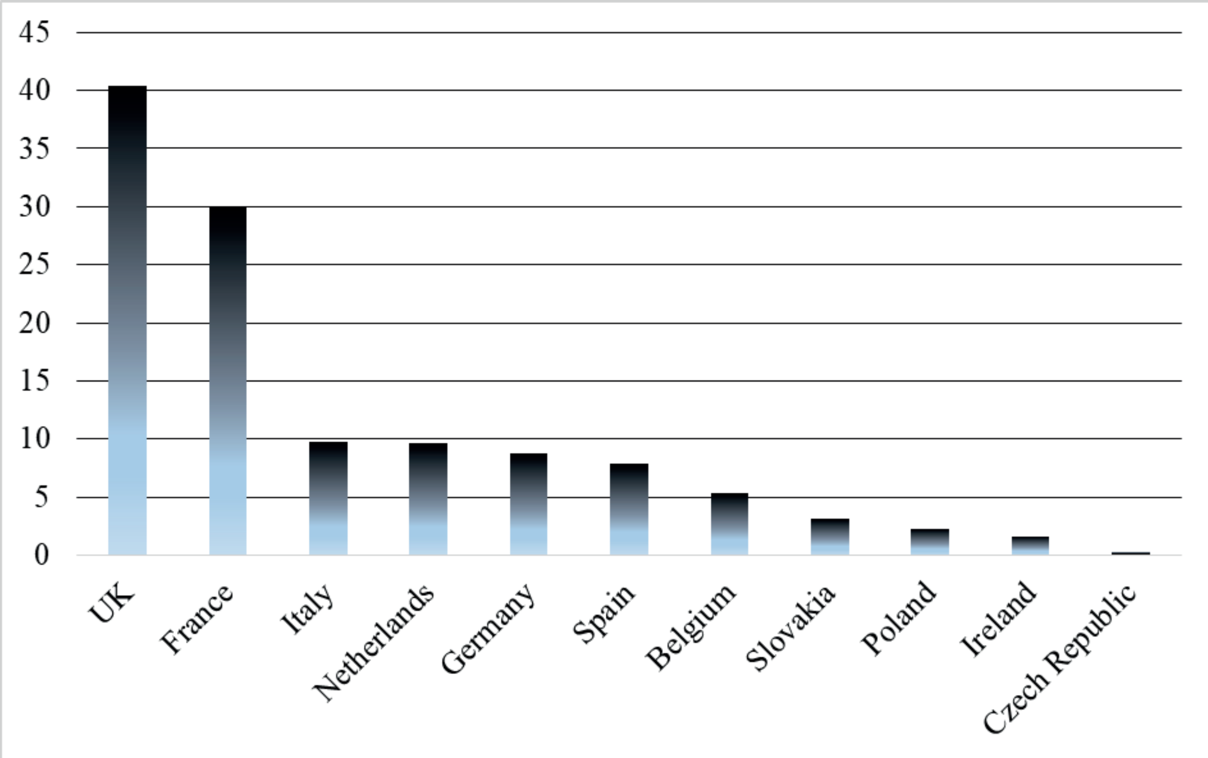

Figure 1 *Total value of the PPP projects in 2009-2018, in selected EU countries (billion euro)*

limited financial involvement of the public partner or a small scale of the enterprise, allowing the private partner to finance with its own contribution. The position of the banks was quite restrictive and a large part of projects did not receive financing.

Another determinant of the PPP success is availability of the public advisory institutions. In 2011, a governmental PPP Platform was established to assist in the preparation and implementation of projects. However, this initiative was not sufficient. Therefore, starting from 2017, the government intensified its activities in this area: a three-year training project was launched, in which the government and local government administration employees participate, the minister for regional development offers free legal, financial and technical advice and agreements were also signed with consortia of consulting companies to provide comprehensive advice to public entities. Moreover, the government plans to initiate 10 pilot projects by the end of 2020.

The government expects that the effect of the above actions will be, among others, the conclusion of at least 100 new agreements by the end of 2020 and an increase in the number of signed agreements in relation to the number of announcements of choosing a private partner to 40% [18].

4 Analysis of development of the PPP market in Poland

While studying the level of the PPP development in Poland, it is worth considering this issue against the background of the EU project market. Figure 1 presents development of the PPP market in selected countries in the years 2009-2018, developed on the basis of research conducted by the European PPP Expertise Centre EPEC [19]. The data include large investment projects - until 2010 these were projects worth more than 5m euro and since 2011 more than 10m euro (the value of the so-called "financial closure" projects).

The leader of the European PPP market was and still is the United Kingdom, which since the beginning of the 1990s has used various forms of cooperation between the public and private sectors to implement investments and provide services. The partnership also has a significant place in countries such as: France, Germany, Italy, the Netherlands and Spain.

It is worth mentioning here that the most important area of the PPP implementation is transport infrastructure. Financial resources earmarked for these enterprises constituted, in the years 1995-2009, an average of 75-90% of the total value of projects. In 2018, their share decreased and amounted to 48% due to the growing value and number of projects in the area of telecommunications and environmental protection for several years [19].

Compared to other EU countries, the value of the market for the large PPP projects in Poland is very small and represents only 2% of the total value. This relatively low level of development of the PPP market will be the subject of further research. These included reports and statistics available on the government's PPP Platform [20].

Figure 2 shows the value and number of the PPP projects in individual years 2009-2018. Figure 3 shows the total value and number of projects by economic sectors in the entire period. These data include all the projects that have been implemented or are being currently implemented

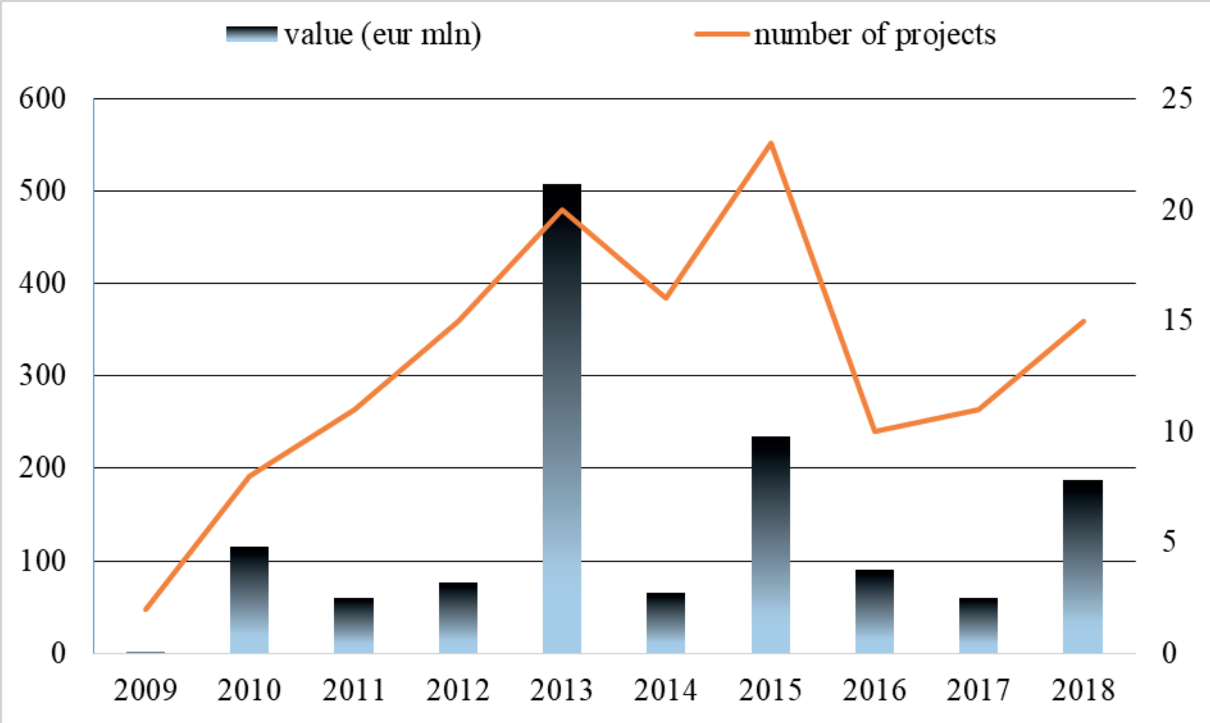

Figure 2 *The PPP project market in Poland by value and number of projects (2009-2018)*

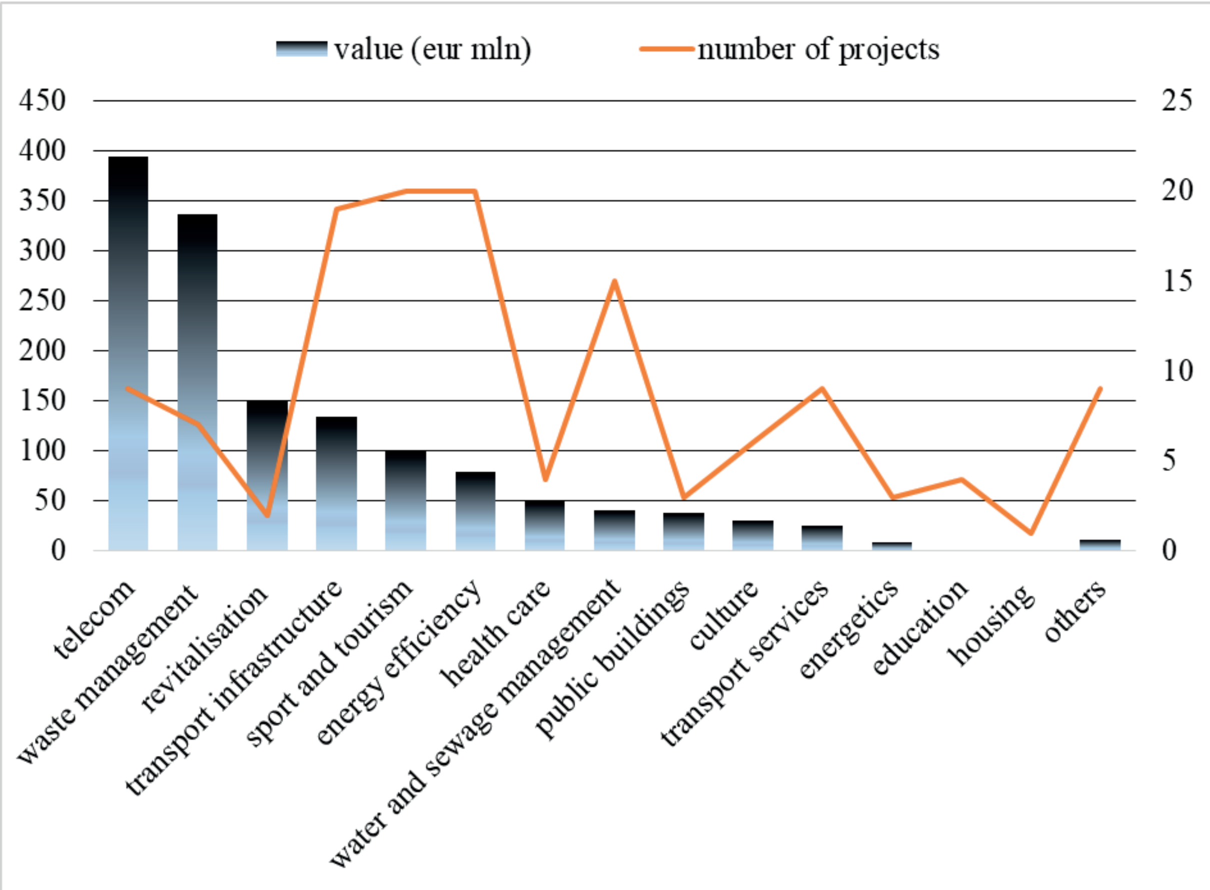

Figure 3 *Total value and number of the PPP projects in Poland, by sector of economy (2009-2018)*

and their value is the sum of the value of investment outlays or services, regardless of the amount of these expenditures.

The PPP project market actually started to develop in 2009, after the change of legal regulations to more flexible ones, corresponding to the specificity of these enterprises.

Between 2009 and 2018, 131 projects were completed and their value amounted to 1.4 bn euro. Both the value and the number of projects vary greatly from year to year. In 2013, the highest value PPP agreements were concluded, as the subject of the agreements were large investment projects, including: construction of waste incineration plant in Poznan (185 m euro) or broadband network in the Mazowieckie and Podkarpackie voivodships (183 m euro). However, in 2016-2017, the number of contracts and the value of projects decreased. This is a consequence of poor activity of local self-governments as entities initiating projects. This activity is a function of, among others, the level of absorption of the EU funds. An increase in use of the EU funds could have been an important factor limiting the interest of the public sector in the PPP projects. This issue will be discussed in the article.

Further analysis of the PPP market allowed to identify its features and changes that took place in the analysed period [20]:

- 131 contracts were signed and executed, and the effectiveness of the PPP proceedings, i.e. the ratio of the number of contracts signed to the number of announcements of choosing a private partner, was in 2009 - 5%, whereas in 2018 - 32%,
- the largest number of contracts concluded concerned projects with a value of up to 10 m euro - 72%, while contracts with a value of more than 60 m euro accounted for only 6%,
- projects are implemented mainly in the following sectors (taking into account their value): telecommunications - 27%, waste management - 24%, revitalisation - 10%, transport infrastructure - 10% (Figure 3),
- investment projects dominate - 58%, however, there is also a large share of service projects - 42%,
- 14 hybrid projects were implemented (co-financed from EU funds), which constituted only 10% of all the PPP undertakings,
- the agreements are concluded mainly by local self-governments - 90% of all the contracts, whereas the central government administration signed only 6 out of 131 contracts,
- among self-government authorities, the largest number of contracts were implemented by large, economically active urban agglomerations (Warsaw, Silesian agglomeration, Krakow, Wroclaw, Gdansk),
- the contribution of the public side to the project consisted in providing the property on which the private partner was to construct the infrastructure in accordance with the “land for infrastructure” principle; more than half of the projects is financed exclusively by the private partner,
- the average contract period is 21-23 years,
- the average time from the date of the project announcement to the conclusion of the contract was in 2009 - 264 days, and in 2018 - 257 days,
- among local authorities that initiate projects, some use external advisory services - in 2016 it concerned 37% of projects, while in 2018 - 54% of projects.

The PPP market in Poland can be described as a “market under construction”, dominated by the low-value projects that are not included in EPEC reports. Projects are initiated by local authorities, mainly in large urban agglomerations. It is worth emphasizing that the effectiveness of the PPP proceedings has improved, the period of negotiations and preparation of contracts has been decreasing and the scope of using the services of external consulting companies has increased. Public entities, operating within the legal framework, adapted to the specificity of the PPP, gain experience in the implementation of projects. These determinants are essential for the success of projects and are an impulse for development of partnership.

When studying the value of the PPP market projects, it can be compared with local government expenditure investments. In 2009-2011, these expenditures amounted to 30.4 bn euro and the value of the PPP projects amounted to 0.18 bn euro, which was 0.06%. However, in 2016-2018 the value of projects was 1.3% in relation to investment outlays (25.3 bn euro - outlays, 0.33 bn euro - PPP projects) [21]. The government plans that the value of the PPP investments should amount to at least 5% of the public sector outlays. A comparable level - 4% of all investments in the public sector, the PPP projects constituted in 2007 in the “old” EU countries.

Turning to the analysis of the PPP projects in the area of transport infrastructure in Poland, one can distinguish the market of relatively small enterprises that initiate local governments and the market of large government projects. The first one includes mainly the construction of parking lots and bus shelters. These investments are not the basic elements of transport infrastructure, but they are the so-called point infrastructure, complementary. Their share in the total value of the PPP projects in 2009-2018 was about 10% (Figure 3). Local authorities therefore carry out transport infrastructure projects with very limited material and financial resources. This is because local authorities have at their disposal EU funds, which they can use to finance up to 85% of the investment costs and they are non-refundable. This system is more advantageous in procedural and financial terms than the PPP.

However, large projects include a programme for the construction and operation of toll motorways, launched by the government in 1996-1997. In 2000-2011, private consortia carried out the following investments in the concession system: section of the A2 motorway Swiecko-Konin (255 km), section of the A1 motorway Gdansk-Torun (152 km), section of the A4 motorway Katowice-Krakow (61 km). Consortia have built and operate about 30% of the current motorway network in Poland [22].

Another government action was a pilot project initiated in 2013, consisting in the reconstruction and maintenance of 187 km of lower category roads in the Lower Silesian Voivodship. The project assumed a thorough reconstruction of 113 km of roads within the first four years of signing the agreement and then their maintenance. The remaining 74 km were planned to be covered by renovation works and current maintenance during 22 years of the agreement’s validity. The procedure of selecting a private partner started in 2014 and the final selection of the company was to take place in July 2018. However, the offers received from two companies were so high that they exceeded the level of availability fees estimated by the self-government authorities of the voivodship several times. Therefore, a private partner was not chosen.

Currently, the government is planning to build some sections of express roads in the form of partnerships. The programme is to cover the following roads: S6 - Gdansk bypass (31 km), S6 - Szczecin bypass (50 km), S6 - Koszalin - DK 6 Bozepole Wielkie (117 km) and S10 - Bydgoszcz - Torun (50 km). The private partner is to design and build roads, maintain them for 30 years and then hand them over to the public party. In return, the public side is obliged to pay a cyclical fee for accessibility [18].

5 Conclusions

Successful implementation of the PPP projects, especially in the area of transport infrastructure, requires specific legal and institutional conditions (activity of public advisory agencies) and availability of financing. Polish legal regulations, after 25 years of experience in the practical implementation of the PPP and legislative changes, are now flexible and adapted to the specificity of projects. In recent years, the government has clearly supported the development of partnership, what is indicated by the activity of government institutions in the area of advisory services. The first effects of these activities and accumulated experience of local authorities are already visible - more and more local authorities use advisory services and the effectiveness of announced projects is increasing. The implementation of 10 pilot projects, planned by the government, as well as creation of a guarantees and warrantees system for the public sector and private PPP partners, is also of great importance for development of partnership. Certainly, this system will facilitate access to external financing of projects.

In the area of transport infrastructure, over the last ten years, projects have been implemented mainly by local public authorities. Those were small, procedurally and financially easy investments, such as the construction of bus shelters or parking lots. On the other hand, large government projects were completed in 2011, when private consortia commissioned about 470 km of motorways (30% of the total length). Therefore, the basic system of transport infrastructure implementation is traditional public financing and the PPP formula remains an alternative and complementary model. Its practical implementation is difficult and procedurally time-consuming, which makes it unattractive for public authorities, especially when they can easily obtain the EU funds. An impulse for the PPP development may be the government's programme of construction and operation of express roads. This project will increase the experience of public authorities and institutions, which is an important success factor in the capital-intensive, multilateral transport projects.

The conducted research is a diagnostics of current macro-conditions and the level of development of the PPP market. Conclusions formulated based on the analysis may be helpful for decision-makers at various levels in the context of identifying problems in implementation of projects and striving to eliminate them and in the context of shaping the directions of the target structure of the PPP market in Poland. An important issue that may be the subject of future research is an analysis of the impact of individual determinants on the success of the PPP implementation, using statistical methods and econometric models.

References

[1] GNAP, J., KONECNY, V. Transport policy related to road transport and sustainable development. *Communications - Scientific Letters of the University of Zilina* [online]. 2003, **5**(1), p. 52-61. ISSN 1335-4205, eISSN 2585-7878. Available from: http://komunikacie.uniza.sk/index.php/communications/article/view/1339

[2] ABERLE, G. Private Verkehrswegefinanzierung: Aus Fehlern lernen - Die Ursachen der Krisen bei Betreibermodellen sind bekannt / Private financing of transport routes: learning from mistakes - the causes of the crises in operator models are known (in German). *Internationales Verkehrswesen*. 2005, **57**. ISSN 0020-9511.

[3] QUINET, E., VICKERMAN, R. *Principles of transport economics*. Cheltenham UK/Northampton: Edward Elgar, MA, USA, 2004. ISBN 978-1-84064-865-2.

[4] STIGLITZ, J. E. *Ekonomika sektora publicznego / Economics of public sector* (in Polish). Warszawa: Wydawnictwo Naukowe PWN, 2004. ISBN 978-8-30115-187-4.

[5] HAMMAMI, M., RUHASHYANKIKO, J.F., YEHOUE, E. *Determinants of public-private partnerships in infrastructure. Working Paper WP/06/99*. IMF Institute, 2006.

[6] GALILEA, P., MEDDA, F. Does the political and economic context influence the success of a transport project? An analysis of transport public-private partnerships. *Research in Transportation Economics* [online]. 2010, **30**(1), p. 102-109. ISSN 0739-8859. Available from: https://doi.org/10.1016/j.retrec.2010.10.011

[7] European Court of Auditors. *Public Private Partnerships in the EU: Widespread shortcomings and limited benefits. Special report* [online]. 2018. Available from: https://www.eca.europa.eu

[8] FLYVBJERG, B., BRUZELIUS, N., ROTHENGATTER, W. *Megaprojects and risk: an anatomy of ambition* [online]. UK: Cambridge University Press, 2003. eISBN 9781107050891. Available from: http://dx.doi.org/10.1017/CBO9781107050891

[9] DEVAPRIYA, K. A. K. Governance issues in financing public-private partnership organisations in network infrastructure industries. *International Journal of Project Management* [online]. 2006, **7**(24), p. 557-565. ISSN 0263-7863. Available from: https://doi.org/10.1016/j.ijproman.2006.07.003

[10] OSBORNE, D., GAEBLER, T. *Reinventing government - how the entrepreneurial spirit is transforming the public sector*. New York: Plume, 1993. ISBN 978-0452269422.

[11] MU, R., DE JONG, M., TEN HEUVELHOF, E. A typology of strategic behaviour in PPPs for expressways: lessons from China and implications for Europe. *European Journal of Transport and Infrastructure Research* [online]. 2010, **10**(1). ISSN 1567-7141. Available from: http://resolver.tudelft.nl/uuid:acb97116-a524-43fc-88ae-8065d25f589b

[12] HARDCASTLE, C., EDWARDS, P. J., AKINTOYE, A., LI., B. Critical success factors for PPP/PFI projects in the UK construction industry: a factory analysis approach. Public Private Partnerships e Opportunities and Challenges : proceedings. 2005, p. 75-83.

[13] OZDOGANM, I. D., BIRGONUL, M. T. A decision support framework for project sponsors in the planning stage of build-operate-transfer (BOT) projects. *Construction Management and Economics* [online]. 2000, **18**(3), p. 343-353. ISSN 0144-6193, eISSN 1466-433X. Available from: https://doi.org/10.1080/014461900370708

[14] NG, S. T., WONG, Y. M. W., WONG, J. M. W. Factors influencing the success of PPP at feasibility stage - a tripartite comparison study in Hong Kong. *Habitat International* [online]. 2012, **36**, p. 423-432. ISSN 0197-3975. Available from: http://dx.doi.org/10.1016/j.habitatint.2012.02.002

[15] CHOU, J.-S., TSERNG, H. P., LIN, CH., YEH, CH.-P. Critical factors and risk allocation for PPP policy: comparison between HSR and general infrastructure projects. *Transport Policy* [online]. 2012, **22**, p. 36-48. ISSN 0967-070X, eISSN 1879-310X. Available from: http://dx.doi.org/10.1016/j.tranpol.2012.05.009

[16] MANSOOR, D., KLEIN, M. *Government support to private infrastructure projects in emerging markets* [online]. Washington: World Bank, 1999. Available from: https://doi.org/10.1596/1813-9450-1868

[17] BUTKIEWICZ, J., YANIKKAYA, H. The effects of IMF and World Bank lending on long-run economic growth: an empirical analysis. *World Development* [online]. 2005, **33**(3), p. 371-391. ISSN 0305-750X. Available from: https://doi.org/10.1016/j.worlddev.2004.09.006

[18] *Polityka rzadu w zakresie rozwoju partnerstwa publiczno-prywatnego. Zalacznik do uchwaly Nr 116/2017 Rady Ministrow / Government policy for the development of public-private partnerships. Annex to Resolution No. 116/2017 of the Council Ministers* (in Polish). 2017.

[19] Market Update. Review of the European PPP Market in 2018 [online]. EPEC, EIB, 2019. Available from: https://data.eib.org

[20] PPP Platform [online]. Available from: https://www.ppp.gov.pl

[21] Statistical Yearbook of the Republic of Poland, 2010-2018 [online]. Warsaw: Central Statistical Office, 2010-2018. Available from: https://stat.gov.pl

[22] ZAGOZDZON, B. Determinants of implementation of public-private partnership in Poland: the case of transport infrastructure. *Advances in Economics and Business* [online]. 2013, **1**(2), p. 57-71. ISSN 2331-5059, eISSN 2331-5075. Available from: https://doi.org/10.13189/aeb.2013.010203

Petr Hruby - Tomas Nahlik - Dana Smetanova

EFFECTS OF BOUNDARY CONDITIONS ON THE MODAL AND SPECTRAL PROPERTIES OF THE SHAFT

Influence of boundary conditions (i.e. mounting type of shafts ends) on spectral and modal properties is studied in this paper. Cases with joints at both ends and with joint at one end and fixed end are described in detail. The vibration problem of rotating shaft is generalized to problem of vibration of the shaft in the rotating plane. The problem is illustrated on testing models. The real mounting type of shafts is presented.

Keywords: *shaft, boundary conditions, critical velocity, deflection, vibration*

1 Introduction

The calculation of modal and spectral properties of the shaft is among the basic calculations that are required to support propulsion projects for various vehicles, ships and construction machines.

The mathematical model of the rotating shaft is influenced by many factors, such as vibration noise [1], flexibility of shaft [2], increasing rotation velocity [3], workspace of universal joints [4] and others [5]. A number of powerful software packages for calculation of torsional vibration already exists [6].

This paper is devoted to study deflection, critical velocity and eigenvalues of frequencies in the rotating shaft. Influence of boundary conditions in mathematical model is illustrated on testing examples.

2 Theoretical background

The mathematical model of the rotating shaft is described by the 4th order differential equation. An unknown function in the given differential equation is the shaft deflection depending on the distance from the shaft end.

By solving the equation, a general solution that includes all the solutions to the problem is calculated. The number of solutions is infinite.

The particular solution is obtained by applying the boundary conditions (i.e. mounting types of ends of the shaft - Figures 5 and 6, [7]).

This means that boundary conditions play significant role in the calculation of model (Table 2 and Table 4).

2.1 Shaft with continuously distributed mass

Consider a prismatic shaft, which rotates at constant angular velocity ω. The shaft bends at critical velocity and it rotates in a bent state (see Figure 1). Centrifugal force dC acts on the shaft element dx (see Figure 1)

$$\mathrm{d}C = \mu y(x)\omega^2 \mathrm{d}x \tag{1}$$

where $y(x)$ is deflection depending on distance from shaft end $(0 \le x \le l)$, μ is a specific mass per unit length of the shaft; $\mu = S\rho$ and S is the cross-section of the shaft, ρ is a density of the shaft material.

Continuous strain $q(x)$ of the length element is

$$q(x) = \frac{\mathrm{d}C}{\mathrm{d}x} = \mu y(x)\omega^2\,. \tag{2}$$

as is well known that deflection curve satisfies

$$E\,J\,y''(x) = -M_0(x)\,, \tag{3}$$

By differentiating the above equations twice, with $EJ = constant$, one obtains

$$E\,J\,y^{IV}(x) = -M_0''(x) = q(x) = \mu y(x)\omega^2\,, \tag{4}$$

i.e.

$$E\,J\,y^{IV}(x) - {}_0\mu y(x)\omega^2 = 0\,. \tag{5}$$

The above equation is rewritten to form

$$y^{IV}(x) - a^4 y(x) = 0,\ a^4 = \frac{\mu\omega^2}{E\,J}. \tag{6}$$

Meanings of symbols in equations above are precisely described in Table 3.

Petr Hruby[1], Tomas Nahlik[2], Dana Smetanova[2,*]
[1]Department of Mechanical Engineering, Institute of Technology and Business, Ceske Budejovice, Czech Republic
[2]Department of Informatics and Natural Sciences, Institute of Technology and Business, Ceske Budejovice, Czech Republic
*E-mail of corresponding author: smetanova@vstecb.cz

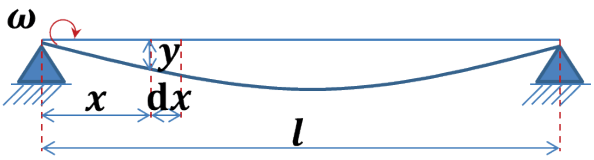

***Figure 1** Shaft with joint ends*

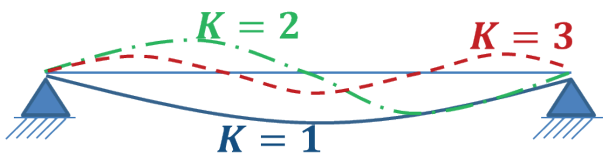

***Figure 2** Deflections of a shaft*

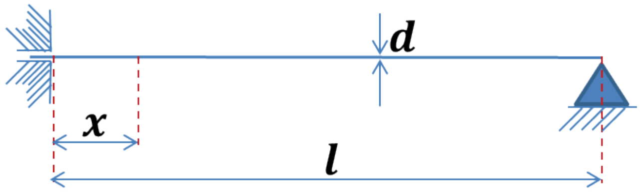

***Figure 3** Shaft with joint and fixed end*

***Table 1** Boundary conditions at the ends of a shaft*

	Mounting type		
	Joint	Fixed end	Free end
Boundary conditions in x = 0 or x = l	$y(x) = 0$, $y''(x) = 0$	$y(x) = 0$, $y'(x) = 0$	$y''(x) = 0$, $y'''(x) = 0$

The general solution of Equation (5), respectively Equation (6), is

$$y(x) = A\cosh ax + B\sinh ax + C\cos ax + D\sin ax. \quad (7)$$

The integration constants can be determined from the boundary conditions that correspond to the shaft's ends' mounting type. The particular solution is obtained by the straightforward calculation of the constants.

2.2 Critical angular velocities of shaft with joints

The shaft shown in Figure 1 (c.f. Table 1, mounting type A in Table 2) satisfies the boundary conditions

$$y(0) = 0, y(l) = 0, y''(0) = 0, y''(l) = 0. \quad (8)$$

Those boundary conditions (by straightforward calculation of Equation (7)) are equivalent to equations for integration constants

$$A = 0,\ C = 0,\ B\sinh al = 0,\ D\sin al = 0. \quad (9)$$

Note that $\sinh al \neq 0$ for $\omega \neq 0$, than $B = 0$. The last equation is satisfied if $D = 0$ or are valid.$\sin al = 0$ Equality $D = 0$ means that there is no deflection of shaft and D plays the role of the maximal deflection (amplitude). The solution of equation $\sin al = 0$ is $al = K\pi$, where $K = 1, 2, \ldots,$ $\left(i.e.\, a = \frac{K\pi}{l}, a^4 = \left(\frac{K\pi}{l}\right)^4\right)$ and $\left(\frac{K\pi}{t}\right)^4 = \frac{\mu}{EJ}\omega^2$.

The infinite number of critical angular velocities was obtained. The K-th critical velocity is expressed by equation

$$\omega_{crK} = \left(K\frac{\pi}{l}\right)^2 \sqrt{\frac{EJ}{\mu}} = K^2\,\omega_{cr1}, \qquad \omega_{cr1} = \left(\frac{\pi}{r}\right)^2 \sqrt{\frac{EJ}{\mu}}, \quad (10)$$

where ω_{cr1} is the first critical velocity $(K = 1)$.

A shape of deflection curve depends on critical velocity. Expression for the deflection curve y_K (see Figure 2) for the K-th critical velocity ω_{crK} is

$$y_K = D\sin\frac{K\pi x}{l} \quad (11)$$

2.3 Critical angular velocities of shafts with one fixed end

The critical velocity of the shaft with fixed end is now determined by analytical method (see Figure 3 and Table 1, mounting type E in Table 2).

The parameter d in Figure 3 indicates the shaft diameter (i.e. the characteristics of the cross-section).

Analytical solution (without damping and shifting forces and friction) is solution of differential Equation (5) (resp. Equation (6)). The general solution is of the form

$$y(x) = A\cosh ax + B\sinh ax + C\cos ax + D\sin ax, \quad (12)$$

where $a = \sqrt[4]{\frac{\mu\omega^2}{EJ}}$, with boundary conditions

$$y(0) = 0, y(l) = 0, y'(0) = 0, y''(l) = 0. \quad (13)$$

Table 2 *Role of mounting types (i.e. boundary conditions) in solutions of the frequency equation*

	Mounting type	Frequency equation	Solutions
A	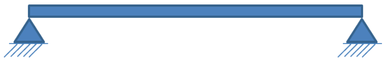	sin al = 0	$(a)_k = \frac{K\pi}{l}$
B		cos al cosh al = 1	$(a)_1 l = 0,$ $(a)_2 l = 4.730,$ $(a)_3 l = 7.853,$ $(a)_4 l = 10.996,$ $\dots$
C		cos al cos al = 1	$(a)_1 l = 4.730,$ $(a)_2 l = 7.853,$ $(a)_3 l = 10.996,$ $(a)_4 l = 14.134,$ $\dots$
D		cos al cosh al = - 1	$(a)_1 l = 1.875,$ $(a)_2 l = 4.694,$ $(a)_3 l = 7.855,$ $(a)_4 l = 10.996,$ $\dots$
E		tan al = tanh al	$(a)_1 l = 3.927,$ $(a)_2 l = 7.069,$ $(a)_3 l = 10.210,$ $(a)_4 l = 13.352,$ $\dots$

By straightforward calculation of the above conditions one obtain transcendental equation

$$\tan al = \tanh al$$

with solutions

$$(al)_K = \frac{4K+1}{4}\pi, K = 1,2,\dots \quad (14)$$

Therefore the K-th critical velocity is expressed by equation

$$\omega_{crK} = \left(\frac{4K+1}{4}\frac{\pi}{l}\right)^2 \sqrt{\frac{EJ}{\mu}} \quad (15)$$

and the first critical velocity is

$$\omega_{cr1} = \left(\frac{5}{4}\frac{\pi}{l}\right)^2 \sqrt{\frac{EJ}{\mu}} \doteq 15,4\frac{1}{l^2}\sqrt{\frac{EJ}{\mu}}. \quad (16)$$

In Table 2 one can see role of the mounting type of shafts and beams in the frequency equation (c.f. [8]). The most obvious mounting types A and E of shafts are more precisely discussed above.

Technical realization of the most common mounting types A and E is presented in the Conclusion (see technical design in Figures 5 and 6).

See [8] and [9] for more details on theoretical background in mechanical properties and [10-12] for more details of the computational methods.

3 Analytical solution of generalized problem

The problem mentioned above is the vibration of a shaft in a plane. Generalization of the above problem is vibration of one-dimensional continuum in the rotating plane with angular velocity ω. By analytical method it is possible to obtain the following description of the problem, c.f. [13].

$$\frac{\partial^4 y}{\partial x^4} - \frac{\rho S r^2}{4EJ}\cdot\frac{\partial^4 y}{\partial t^2 \partial x^2} + \frac{\rho S}{EJ}\cdot\frac{\partial^2 y}{\partial t^2} - \\ - \frac{\rho S r^2 \omega^2}{4EJ}\cdot\frac{\partial^2 y}{\partial x^2} - \frac{\rho S \omega}{EJ}\cdot y = 0 \quad , \quad (17)$$

Contrary to ordinary differential Equation (6), the above Equation (17) is partial differential equation.

Assume that each shaft cross-section performs an oscillating motion with the amplitude depending on location, with a time course identical along the entire shaft, i.e.

$$y(x,t) = Y(x)e^{i\Omega t}, \quad (18)$$

where $Y(x)$ is amplitude of deflection depending on coordinate x and $\Omega\,[rad \cdot s^{-1}]$ is the natural frequency of relative oscillations.

Substituting Equation (18) to Equation (17), with undamping condition identical all the time, one obtains ordinary differential equation for amplitude as

***Table 3** Parameters of testing examples*

Parameter	Value		Description
	Simple shaft	Skoda 781	
E	$2 \cdot 10^{11}$	$2 \cdot 10^{11}$	Modulus of elasticity $[Pa]$
ρ	7800	7800	Density $[kg \cdot m^{-3}]$
l	1	0.65	Length $[m]$
r	0.0564	0.0105	Radius $[m]$
S	0.01	0.0003	Cross-section $[m^2]$
J	$7.9578 \cdot 10^{-1}$	$9.5466 \cdot 10^{-9}$	$J = \frac{\pi}{4} \cdot r^4 [m^4]$
μ	78	2.7016	$\mu = S \cdot \rho [kg \cdot m^{-1}]$

***Table 4** Critical velocities of testing examples based on different mounting types*

		$\omega_K [rad \cdot s^{-1}]$			
		1	2	3	4
Simple Shaft	2 joints	1409.82	5639.26	12688.35	22557.06
	1 joint 1 fixed	2202.84	7137.19	14891.18	25464.81
Skoda 781	2 joints	621.01	2484.05	5589.11	9936.19
	1 joint 1 fixed	970.33	3143.87	6559.44	11217.03

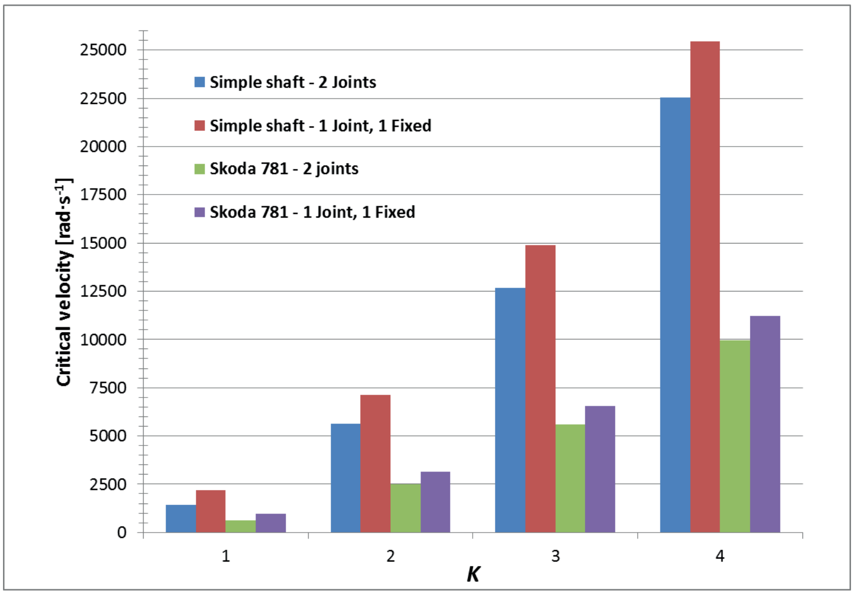

***Figure 4** Critical velocities*

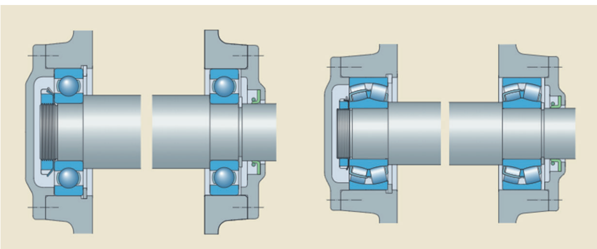

***Figure 5** Shaft with joints in technical practice [7]*

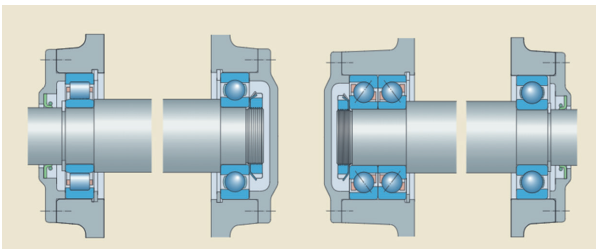

***Figure 6** Shaft with joint and fixed end in technical practice [7]*

$$Y^{IV}(x) + bY''(x) - cY(x) = 0, \tag{19}$$

where

$$b = \frac{\rho S r^2}{4EJ}(\Omega^2 - \omega^2),\ c = (\Omega^2 + \omega^2).$$

Applying the boundary conditions for ends with joints (see Table 1) the particular solution of Equations (19) has assumed the form:

$$Y(x) = Y_{const}\sin p_K x, \tag{20}$$

where l is length of shaft, $p_K = \frac{K\pi}{l}$, and $K = 1, 2, \ldots$.

Substituting Equation (20) to Equation (18) one obtains the frequency equation

$$(p_K^4 - bp_K^2 - c)Y_{const}\sin p_K x = 0. \tag{21}$$

Calculating the above equation, the eigenvalues of frequencies of the vibration have the form:

$$\Omega_n = \left(\frac{EJ}{qS}\right)^{\frac{1}{2}}\left(\frac{\left(\frac{K\pi}{l}\right)^4 - \frac{\rho S\omega^2}{EJ}\left[1 - \left(\frac{K\pi r}{2l}\right)^2\right]}{1 + \left(\frac{K\pi r}{2l}\right)^2}\right)^{\frac{1}{2}}. \tag{22}$$

4 The testing model

Derived equations were tested on two different examples (mounting type A and E in Table 2). The first one was simple shaft with circular cross-section and the second was shaft from the Skoda 781. Parameters of both examples are shown in Table 3.

Results of calculations are shown inn Figure 4.

Meaning of K in Figure 4 and Table 4 is shown in Figure 2.

It is clear from the Equations (10) and (15) that the shaft parameters also influence the critical velocity (see Figure 4 and Table 4). The critical speed is proportional to the parameter $\sqrt{EJ}$ and inversely proportional to parameters l^2 and $\sqrt{\mu}$.

There can be seen how different mounting types can change values critical velocities. The exact values are shown in Table 4.

5 Conclusions

In Table 2 are presented all the possibilities of mounting types of shafts and beams. The usual technical designs of the shaft's ends are presented in Figure 5 (shaft with joint) and Figure 6 (shaft with join and fixed end).

As shown in Figure 4 and Table 4, the critical velocity depends significantly on the mounting type of shaft's ends and parameters E, J, l, μ of the shaft. It is clear from results that the mounting types of shaft's ends need to be taken into account when calculating the modal and spectral properties of shafts.

Acknowledgement

The work presented in this paper was supported by grant IGS: 2019 - UTT 8210-010 of the Institute of Technology and Business in Ceske Budejovice.

References

[1] ERTURK, A. T., KARABAY, S., BAYNAL, K., KORKUT, T. Vibration noise harshness of a light truck driveshaft, analysis and improvement with six sigma approach. *Acta Physica Polonica A* [online]. 2017, **131**(3), p. 477-481. ISSN 0587-4246, eISSN 1898-794X. Available from: https://doi.org/10.12693/APhysPolA.131.477

[2] RODRIGUEZ-CIANCA, D., RODRIGUEZ-GUERRERO, C., VERSTRATEN, T., JIMENEZ-FABIAN, R., VANDERBORGHT, B., LEFEBER, D. A Flexible shaft-driven remote and torsionally compliant actuator (RTCA) for wearable robots. *Mechatronics* [online]. 2019, **59**, p. 178-188. Available from: https://doi.org/10.1016/j.mechatronics.2019.04.004

[3] XU, H.-B., TANG, S., XI, H.-F., GAO, P.-Y., LI, M.-Y. Joint interface during arc milling brazing of aluminium alloy to low carbon steel with cutter milling at various rotation speeds. *Rare Metals*. 2017, **36**(11), p. 872-877. ISSN 1001-0521, eISSN 1867-7185.

[4] ZHANG, G., DU, J., TO, S. Study of the workspace of a class of universal joints. *Mechanism and Machine Theory* [online]. 2014, **73**, p. 244-258. ISSN 0094-114X, eISSN 1873-3999. Available from: https://doi.org/10.1016/j.mechmachtheory.2013.11.004

[5] HRUBY, P., NAHLIK, T., SMETANOVA, D. Mathematical modelling of shafts in drives. *Communications-Scientific letters of the University of Zilina* [online]. 2018, **20**(4), p. 36-40. ISSN 1335-4205, eISSN 2585-7878. Available from: http://komunikacie.uniza.sk/index.php/communications/article/view/637

[6] ZOUL, V., KOVAC, P. A brief overview about the development of torsional vibration calculation and education of methods for their calculation. *Scientific Journal of Silesian University of Technology. Series Transport* [online]. 2018, **99**, p. 205-211. ISSN 0209-3324. Available from: https://doi.org/10.20858/sjsutst.2018.99.19

[7] Rolling bearings – SKF group [online]. 2018. [Viewed 04-06-2019]. Available from: https://www.skf.com/binary/21-121486/Rolling-bearings---17000-EN.pdf

[8] JULIS, K., BREPTA, R. *Mechanics / Mechanika* (in Czech). Prague: SNTL, 1987. REKTORYS, K. *Variational methods in mathematics, science and engineering*. Springer Science & Business Media, 2012. ISBN 9789401164504.
[9] Group of Authors. *Flexibility and strength II / Pruznost a Pevnost II* (in Czech). Prague: Czech Technical University in Prague (CVUT), 1979.
[10] RALSTON, A., RABINOWITZ, P. *A first course in numerical analysis*. 2. ed. Dover Publications, 2001. ISBN 978-0486414546.
[11] REKTORYS, K. *Solving ordinary and partial boundary value problems in science and engineering*. 1. ed. CRC Press, 1998. ISBN 9780849325526.
[12] REKTORYS, K. *Variational methods in mathematics, science and engineering*. Springer Science & Business Media, 2012. ISBN 9789401164504.
[13] HRUBY, P. *Cardan coupling shaft vibrations in the rotating plane*. PhD. Thesis. Plzen: University of Mechanical and Electrical Engineering (VSSE), 1979.

Guyk A. Manuylov - Sergey B. Kosytsyn - Maksim M. Begichev

CLASSICAL SOLUTION AND EDGE EFFECT IN THE PROBLEM OF STABILITY OF AN AXIALLY COMPRESSED CYLINDRICAL SHELL

The classical solution for critical stresses in the problem of stability of a circular longitudinally compressed cylindrical shell consists of two terms, reflecting the ability of the shell to resist buckling due to bending and membrane deformations. However, with usual boundary conditions the classical solution appears only with the absence of the Poisson expansion of a shell. With a non-zero Poisson's ratio, an axisymmetric edge effect presents. It reduces the critical load and causes the initial arrangement of its own forms to change as the load increases.

Keywords: *cylindrical shell, spherical shell, edge effect, loss of stability, competition of eigen forms*

1 Introduction

It is known that the solution of the linear stability problem of an axially compressed circular elastic cylindrical shell without initial imperfections gives the classical value of the critical stresses

$$\sigma_{cr.cl} = E\delta/R\sqrt{3(1-\upsilon^2)}\,. \quad (1)$$

Buckling of the shell occurs either in an axisymmetric form or in a form that is a linear combination of axisymmetric $(n = 0)$ and skew-symmetric $(n = 1)$ eigen forms. Here n is the number of total circumferential waves in critical equilibrium.

Equation (1) was obtained by Lorenz (1908, non-axisymmetric buckling [1]) and Timoshenko (1910, symmetrical buckling [2]). However, in subsequent years it was established that if the shell material has a nonzero Poisson's ratio $(\upsilon \neq 0)$, then in many cases of boundary conditions the classical critical load is not achieved even in calculations. The reason is a development of a non-linear axisymmetric edge effect, caused by the constraint with the boundary conditions of free Poisson expansion. In the book [3] Panovko wrote that the axisymmetric boundary effect makes the linear eigen value problem inhomogeneous, and to obtain the solution of the stability problem one should perform a geometrically nonlinear calculation. This remark is true in relation to axisymmetric eigen forms. But with respect to non-axisymmetric forms of loss of stability (forms of "wave formation"), the eigen value problem remains homogeneous. These forms of stability loss of an axially compressed cylindrical shell are unstable (watershed), since they separate the stable subcritical equilibrium from another stable but strongly deformed distant equilibrium, meaning the destruction of the shell [4-5].

Another important point is a significant decrease of the critical load with certain boundary conditions (for example, under the condition of a free edge and some others).

In general, this is due to the fact that the total resistance of the shell to buckling is created from the bending energy and the energy of the circumferential membrane deformations.

In this paper, the above-mentioned expansion of the critical load expression is considered into two terms, the solution is being analyzed, as well as results of the study of the influence of the edge effect by Almros [6-7]. It is shown that the edge effect leads to disappearance of the axisymmetric form of loss of stability. Some features of development of the edge effect and its role in the wave formation at the time of loss of stability were also studied. In addition, some variants of boundary conditions of the shell were considered that lead to reduction of the critical load by half in comparison with the classical one. In the paper, the periodic buckling modes of an axially compressed cylindrical shell are being examined. Matters of localized buckling modes are being considered in other works of the authors [4, 8].

2 On the classical critical load

The bifurcation problem of the stability of an axially compressed circular cylindrical shell is known [9] to be described by a linear partial differential equation with respect to the deflection *W (x, y)* for zero boundary conditions

$$\frac{D}{\delta}\nabla\nabla\nabla\nabla W + \frac{E}{R^2}\frac{\partial^2 W}{\partial x^4} + \sigma\nabla\nabla\left(\frac{\partial^2 W}{\partial x^4}\right) = 0\,. \quad (2)$$

For the case of pinned edge

Guyk A. Manuylov[1], Sergey B. Kosytsyn[2], Maksim M. Begichev[2,*]
[1]Department of Structural Mechanics, Russian University of Transport (MIIT), Moscow, Russia
[2]Department of Theoretical Mechanics, Russian University of Transport (MIIT), Moscow, Russia
*E-mail of corresponding author: noxonius@mail.ru

$$W = \frac{\partial^2 W}{\partial x^4} = \sigma_x = V = 0 \quad \text{for} \quad x = 0.1\,, \tag{3}$$

where:
V - transverse displacement,
∇ - Laplace operator,
D - cylindrical rigidity,
σ - axial compressive stress.

As a solution (non-axisymmetric form of loss of stability), one can take

$$W = A_{\min} \sin\frac{\pi m x}{1} \sin\frac{ny}{R}\,, \tag{4}$$

where n and m are integers that determine the number of circumferential waves and axial half-waves. Substitution of the expression for the deflection in the form of a product of sinusoids makes it possible to express the critical stress in the following form:

$$\sigma_{cr} = \frac{E\partial}{R}\left[\frac{\partial l^2 R}{12(1-v^2)\pi^2 m^2}\left(\frac{\pi^2 m^2}{l^2} + \frac{n^2}{R^2}\right) + \right. \\ \left. + \frac{\pi^2 m^2}{\partial l^2 R\left(\frac{\pi^2 m^2}{l^2} + \frac{n^2}{R^2}\right)^2}\right] \tag{5}$$

If the dimensionless quantities are introduced

$$\eta = n^2\delta/R\,; \quad \xi = b/a = \pi R m/nl\,, \tag{6}$$

where a and b are the dimensions of the rectangular wave formation cells along the generator and the cylinder guide. If one denotes

$$\frac{\pi^2 m^2 R^4}{\delta l^2 R n^4} = \frac{\pi^2 m^2 R^2}{l^2 n^2} \cdot \frac{R}{\delta n^2} = \xi^2/\eta\,, \tag{7}$$

then one can write

$$\sigma_{cr} = \frac{E\delta}{R}\overline{\sigma}_{cr} = \frac{E\delta}{R}\left[\frac{(1+\xi^2)\eta^2}{12(1-v^2)\xi^2} + \frac{\xi}{(1+\xi)^2\eta}\right], \tag{8}$$

or

$$\sigma_{cr} = \frac{E\delta}{R}[\overline{\sigma}_b + \overline{\sigma}_m] = \frac{E\delta}{R}\overline{\sigma}_{cr}\,. \tag{9}$$

Here the first term in parentheses determines the energy contribution of the flexural deformations of the shell to the total buckling resistance; the second term is the contribution of the energy of circumferential membrane deformations. The expression in square brackets consists of two actually reciprocal quantities. Therefore, the smallest value of the critical stress is achieved when these terms are equal. Then, each of them is equal to half of the minimum critical load

$$\sigma_{cr}^{\min} \to \sigma_{cr}^{b} = \sigma_{cr}^{b} = \frac{1}{2}\sigma_{cr}^{\min}\,. \tag{10}$$

To determine $\sigma_{cr}^{\min}$ it is convenient to introduce the notation

$$\Psi = (1+\xi^2)^2\eta/\xi^2\,. \tag{11}$$

Then, according to what has been said, follows:

$$\overrightarrow{\sigma}_{cr}^{\min} = \left[\frac{\Psi}{12(1-v^2)} + \frac{1}{\Psi}\right] \to \Psi^2 = 12(1-v^2); \\ \Psi = 2\sqrt{3(1-v^2)}. \tag{12}$$

Finally, one obtains an expression for the classical critical stress

$$\sigma_{cr}^{\min} = \frac{E\delta}{R}\left(\frac{1}{2\sqrt{3(1-v^2)}} + \frac{1}{2\sqrt{3(1-v^2)}}\right) = \\ = \frac{E\delta}{2\sqrt{3(1-v^2)}}. \tag{13}$$

The number of circumferential waves n depends on the ratio of the sides of the rectangular wave formation cells $\xi = a/b$

$$n = \frac{\xi}{1+\xi^2}\sqrt[4]{\frac{R^2}{\delta^2}12(1-v^2)}\,. \tag{14}$$

For $\xi = 1$ (square cells) the well-known equation is obtained $n \cong 0.909\sqrt{\frac{R}{\delta}}$.

The energy justification of Equation (9) will be shown in deriving a critical force $(P = \sigma_{cr}\delta)$, as Timoshenko did [10].It used the sinusoidal form of deflections $\left(w = A\sin\frac{\pi m x}{R}\right)$ as an axisymmetric form of loss of stability.

The condition for achieving the critical equilibrium can be represented as the vanishing of the second variation of the total potential energy

$$\delta^2 E = I_\sigma + I_b + I_m = 0\,, \tag{15}$$

where I_σ is the work of the external load,
I_b and I_m is the potential energy of bending and membrane deformations,

$$I_\sigma = -2\pi RP\int_0^1 \frac{1}{2}\left(\frac{dW}{dx}\right)^2 dx = -PA^2\pi^3 m^2 R/21\,, \tag{16}$$

$$I_b = 2\pi RD\int_0^1 \frac{1}{2}\left(\frac{d^2W}{dx^2}\right)^2 dx = A^2 D\pi^4 m^4 R/21^3\,, \tag{17}$$

$$I_m = \frac{2\pi RE\delta}{2(1-v^2)}\int_0^1\left[\left(\frac{du}{dx} - \frac{w}{R}\right)^2 + 2(1-v)\frac{wdu}{Rdx}\right]\cdot \\ \cdot dx = A^2\pi E\delta 1/R. \tag{18}$$

The critical load is obtained in the form of two components in accordance with the representation of the energy of elastic deformation as the sum of the energy of the bending deformation and the energy of the membrane deformation.

$$P_{cr} = \frac{E\delta^3 2m^2\pi^2}{24|(1-v^2)l^2} + \frac{E\delta l^2}{\pi^2 m^2 R^2} = \frac{E\delta^2}{R}\overline{P}_{cr}\,, \tag{19}$$

or

$$P_{cr} = \frac{E\delta^2}{R}\left(\frac{\delta R\pi^2 m^2}{12(1-v^2)l^2} + \frac{l^2}{\delta R\pi^2 m^2}\right) = \\ = \frac{E\delta^2}{R}(\overline{P}_b + \overline{P}_m). \quad (20)$$

In the above derivation of the equation of the classical critical stress, it corresponds to the equality of the terms in parentheses

$$\min P_{cr} \Rightarrow \overline{P}_b = \overline{P}_m = \frac{1}{2}\overline{P}_{cr\cdot cl}. \quad (21)$$

If one denotes

$$1/\psi = \delta R\pi^2 m^2/l^2; \; 1/\psi = \overline{P}_m, \quad (22)$$

then

$$\overline{P}_m = \overline{P}_b = \frac{1}{2\sqrt{3(1-v^2)}} = \frac{1}{2}\overline{P}_{cr\cdot cl}. \quad (23)$$

Finally, one gets

$$P_{cr} = \frac{E\delta^2}{R}\left(\frac{1}{2\sqrt{3(1-v^2)}} + \frac{1}{2\sqrt{3(1-v^2)}}\right) = \\ = \frac{E\delta^2}{R\sqrt{3(1-v^2)}}. \quad (24)$$

The number of axial half-waves m is defined as follows:

$$m = \sqrt{2\sqrt{3(1-v^2)}}\,1/\pi\sqrt{R\delta}. \quad (25)$$

It should be noted that the decomposition of the critical force into a bending and equal membrane component is valid only for the classical solution of the linearized stability problem considered above. In the case of the development of the edge effect, the ratio between $\overline{P}_b$ and $\overline{P}_m$ can change. At the same time, under certain boundary conditions, it can turn out that $\overline{P}_m$ is much smaller $\overline{P}_b$, and then the critical force $\overline{P}_{cr}$ will be much lower than the classical value.

3 Influence of the edge effect

Studies of the edge effect on the axially compressed cylindrical shells were carried out by Geckeler [11], Fisher [12], Ohira [13], Almros [6], Hoff and Reifeld [14]. Especially important are the results obtained by Almros. He presented the general solution for deflection W and stress function f at the moment of loss of stability in the form of two terms

$$W = W_0 + W_1; \; f = f_0 + f_1. \quad (26)$$

The first terms are solutions of the differential equation of the boundary effect (for details see [6])

$$Dw_0xxxx + Pw_0xx + E\delta w_0/R^2 - \frac{vP}{R} = 0. \quad (27)$$

The second summand are zero eigen modes $(W_1 = \xi W^0_{c\varphi})$, which are found by numerically solving the homogeneous equilibrium and deformation compatibility equations, after substituting in them the solutions for the edge effect in them W_0 and f_0

$$D\nabla^4 W_1 + f_{1,xx/R} + PW_{1,xx} - W_{0,xx}f_{1,yy} + \\ + \left(vP - \frac{E\delta W_0}{R}\right)W_{1,yy} = 0, \quad (28)$$

$$\frac{1}{E\delta}\nabla^4 f_1 - W_{1,xx/R} + W_{0,xx}W_{1,yy} = 0. \quad (29)$$

Here, the subscripts xx and yy after the comma mean differentiation with respect to the corresponding coordinate. Using

$$f_1 = F(x)\sin\frac{ny}{R}; \; W_1 = W(x)\sin\frac{ny}{R}. \quad (30)$$

Almros moved to a system of ordinary equations with variable coefficients with respect to $F(x)$ and $W(x)$

$$D\left[W'''' - 2\left(\frac{n}{R}\right)^2 W'' + \left(\frac{n}{R}\right)^4 W\right] + \frac{F}{R} + \\ + PW'' + \left(\frac{n}{R}\right)^2 W_0''F - \left(\frac{n}{R}\right)^2 \cdot \\ \cdot\left(vP - \frac{E\delta W_0}{R}\right)W = 0, \quad (31)$$

$$\frac{1}{E\delta}\left[F'''' - 2\left(\frac{n}{R}\right)^2 F'' + \left(\frac{n}{R}\right)^4 F\right] - \frac{W''}{R} - \\ - \left(\frac{n}{R}\right)^2 W_0'' W = 0. \quad (32)$$

Boundary conditions were expressed through W and F in the usual way in the case when they include W, f, P, N_{xy}. The conditions for displacements were written as follows:

$$U = 0 \to F'' + vF\left(\frac{n}{R}\right)^2 = 0, \quad (33)$$

$$V = 0 \to F''' - (2+v)F\left(\frac{n}{R}\right)^2 - E\delta W' = 0. \quad (34)$$

A classical solution is obtained if one assumes that

$$W_0 = vPR/E\delta. \quad (35)$$

The solution of equations and determination of the critical load were carried out numerically by the method of finite differences (MFD).

The homogeneous problem of determining the bifurcation load corresponding to a non-axisymmetric form of loss of stability was solved from the condition that the determinant of the corresponding matrix be zero.

Studies of the convergence of MFD showed that to obtain two valid signs of the critical load, it is sufficient to have 50-100 sampling points. Refinement of the critical load (3-4 valid marks) required a substantial grinding of the grid (up to 400-600 points) and, correspondingly, an increase in the labor intensity of problem solving.

In problems with pinned boundary condition, convergence from below was observed, whereas in the

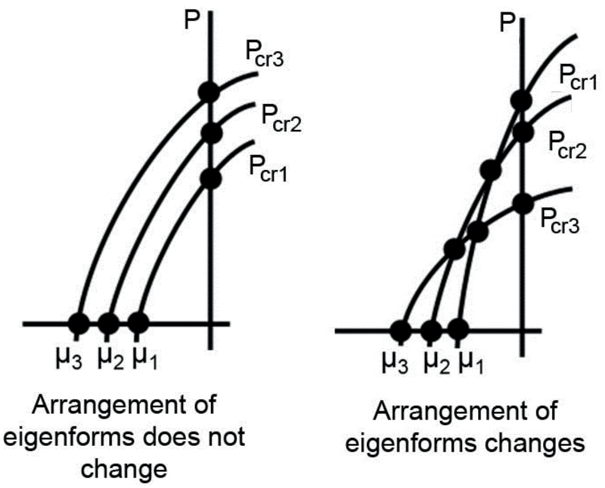

Figure 1 *Competition of eigen modes*

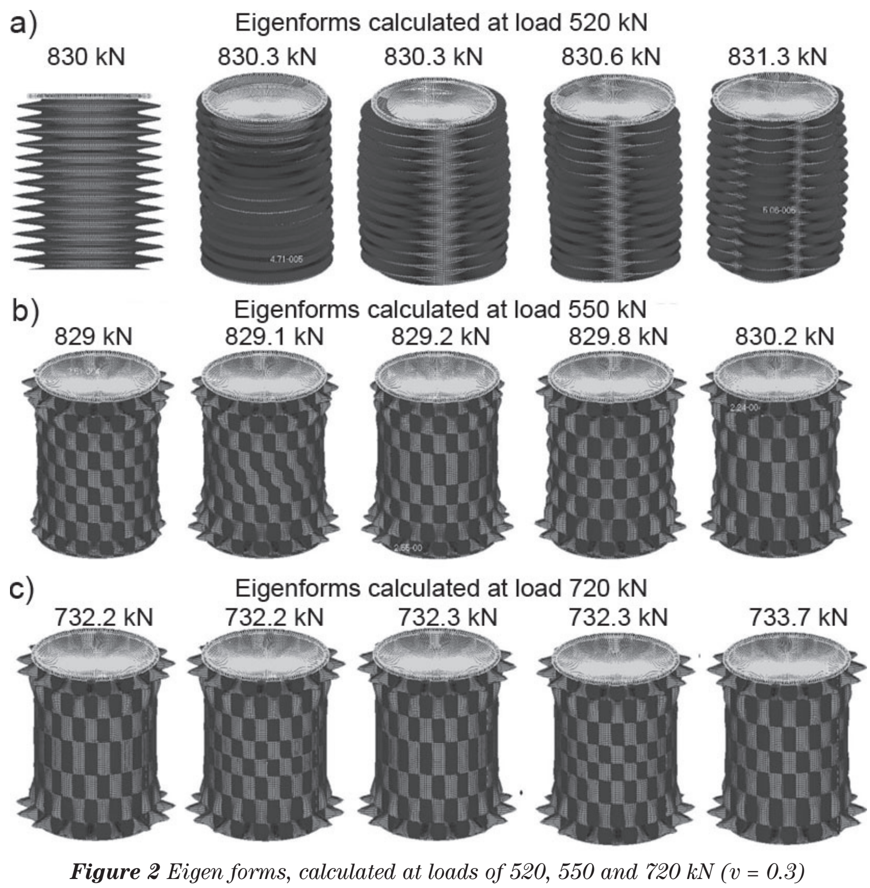

Figure 2 *Eigen forms, calculated at loads of 520, 550 and 720 kN (v = 0.3)*

case of fixed edges of the shell, the convergence of the approximate values of the critical load was from above.

The results of this investigation with respect to $\eta = \frac{\sigma_{cr}^{cr\cdot eff}}{\sigma_{cr\cdot cl}}$ with eight different combinations of boundary conditions are given in the article`s table [6]. Note that Almros used not all combinations of R/δ and R/δ.

As follows from results in that table, influence of those shell parameters on the critical load is much less than the influence of the boundary conditions. Thus, for standard hinge support conditions

$$S_1(W|_\Gamma = W''|_\Gamma = N_x|_\Gamma = V|_\Gamma = 0) \text{ at } 4R > \frac{1}{2}, \quad (36)$$

$$\eta = \sigma_{cr}^{cr\cdot eff} \big/ \sigma_{cr\cdot cl} \approx 0.8 - 0.87, \quad (37)$$

under the boundary condition

$$S_2(w|_\Gamma = w''|_\Gamma = u|_\Gamma = V|_\Gamma = 0)\eta \cong 0.84, \quad (38)$$

for $S_3(w|_\Gamma = w''|_\Gamma = N_x|_\Gamma = N_{xy}|_\Gamma = 0)$
value η smaller $(\eta \approx 0.5 \div 0.51)$. (39)

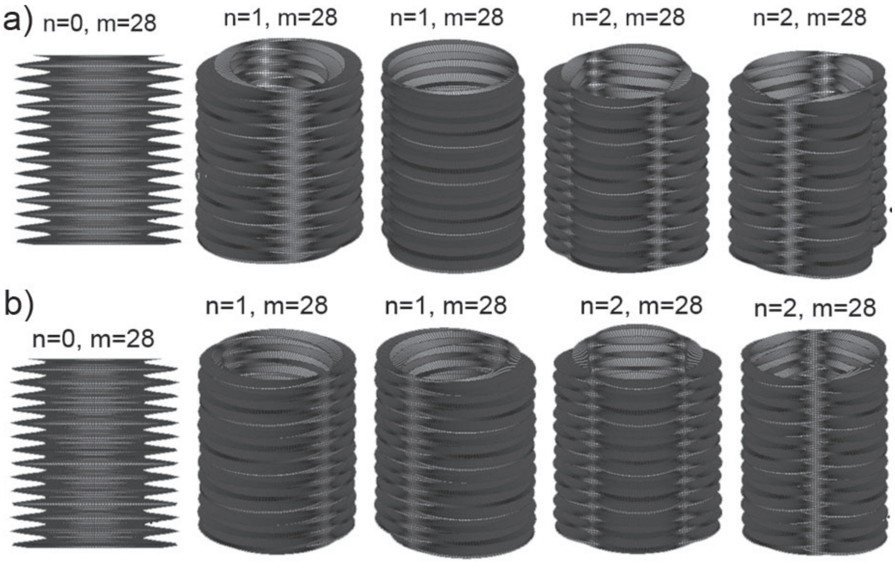

Figure 3 *The eigen forms of a shell with zero Poisson's ratio*

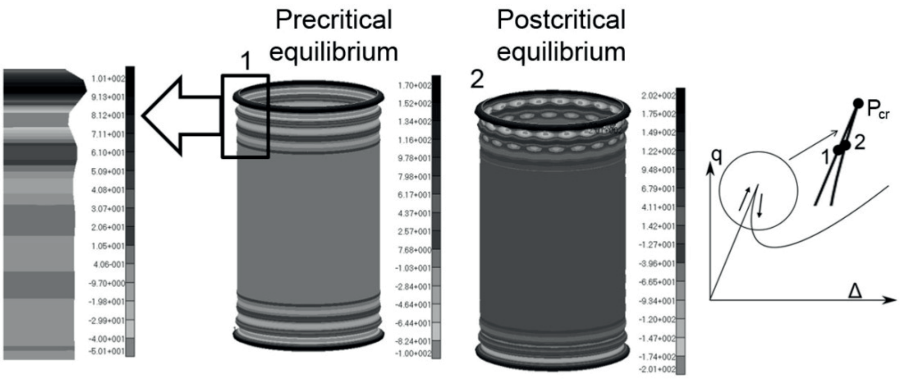

Figure 4 *Distribution of stresses in the circumferential direction in pre critical and post critical equilibrium*

Practically the same values $\eta\,(\eta \cong 0.5 \div 0.51)$ were obtained for the case

$$S_4(w|_\Gamma = w''|_\Gamma = N_x|_\Gamma = N_{xy}|_\Gamma = 0)\ . \quad (40)$$

It was noted that in the case of S_3 and S_4, the reduction in the critical load is the same as without taking into account the edge effect. These last two results (S_3 and S_4) indicate an important inhibiting role of circumferential membrane stresses. In the absence of these stresses, the critical load is almost halved compared to the classical one.

In the case of a standard fixed edge (the condition $C_3(w|_\Gamma = W'|_\Gamma = N_x|_\Gamma = N_{xy} = 0))$, as in the case of the condition $C_1(w|_\Gamma = W'|_\Gamma = u|_\Gamma = V|_\Gamma = 0)$, reduction of the load somewhat less $\eta = 0.91 \div 0.93$.

A slightly smaller value η for the case $C_2(C_2(W|_\Gamma = W'|_\Gamma = N_x|_\Gamma = v|_\Gamma = 0))$. Here $\eta \backsimeq 0.86 \div 0.91$. Approximately the same values η are for the combination C_4 $(C_4(W|_\Gamma = W'|_\Gamma = N_x|_\Gamma = N_{xy}|_\Gamma = 0))$, $\eta \backsimeq 0.86 \div 0.91$.

It was found that the form of a non-axisymmetric loss of stability has 8-9 circumferential waves for all the cases except for S_3 and S_4, for which the number of circumferential waves decreased to two ($n_{cr} = 2$).

The finite element calculations of the authors (NASTRAN, MARC) showed a critical pressure $P_{cr} = 713$ *kN* for the hinged shell of Croll [15] (*R/δ = 300*, *R = 300 mm*, *L/R = 2.88*, $E = 2.1{\cdot}10^4$ *kg/mm*^{2}, *v = 0.3*). For a close-sized shell (*R/δ = 100*, *L/R = 3.2*) with the same pinned edge Almros obtained *P ~ 693 kN*. The classical critical load for this shell is:

$$P_{cr\cdot cl} = 1.21\pi E\delta^2 = 798.28\,kN\ . \quad (41)$$

The Almros's result is $\eta = 0.868$. Here the result is slightly larger $(\eta = 0.893)$. The number of circumferential waves is *n = 15*, and not *9* as in Almros, which is explained by a much larger value of *R/δ = 250> 100*. It is noted that the development of a nonlinear axisymmetric edge effect due to the constraint of the Poisson expansion of the shell's edge leads to a competition of eigen modes as the compressive load increases. This means that the curves of changes in the corresponding eigenvalues, with respect to the load of the derivative of the nonlinear operator, intersect each other.

Thus, the mutual arrangement of the eigen forms of loss of stability changes (Figure 1).

Calculations in this paper for a number of hinged and fixed shells showed that the axisymmetric and skew-symmetric forms of loss of stability remain first up to a load of *(0.65-0.7)* P_{cr}. However, further, these forms “yield” the first place (corresponding to the least rigidity of the shell) to skew-symmetric forms. A particularity of these forms is the development of waves of the greatest amplitude near the edge of the shell. When from the edges, the wave amplitude decreases sharply [16]. This change in forms of loss of stability occurs with simultaneous more intensive development of the edge effect (as the compressive load approaches the critical value). When the load reaches the pre-critical value of the axisymmetric and skew-symmetric forms of loss of stability, there are no among the first ten eigen forms of the shell (Figure 2). At this point, the first two “zero” eigen forms W_1^0 and W_2^0 are the same. These are cyclically symmetrical double waveforms, rotated relative to each other by 6°. Therefore, the initial form of loss of stability is formed as a linear combination of these forms, which is summed with an axisymmetric pre-critical equilibrium

$$\vec{W}_{f.post/cr.} = \vec{W}_{precr.} + \xi_1 \overrightarrow{W_1^0} + \xi_2 \overrightarrow{W_2^0}. \quad (42)$$

When can a classical solution be actually used? The answer is simple - when the edge effect will not develop (the standard conditions for hinging and fixing are meant). However, with such boundary conditions, one can avoid constraining Poisson expansion if the Poisson’s ratio is zero ($v = 0$). In this case, the linearized classical solution of the stability problem can be used

$$\sigma_{cr} = \frac{E\delta}{\sqrt{3}R}. \quad (43)$$

In this case, the first eigen form of loss of stability is axisymmetric. But it can be a multiple.

Figure 3 shows eigen forms for the Kroll’s shell at zero load (*a*) and for pre-critical equilibrium (*b*), ($P = 760\ kN$, $P_{cr.p} = 761.8\ kN$). It can be seen that the initial order of the arrangement of the first 5 eigen forms is preserved up to the critical equilibrium. Consequently, among these eigen forms there is no competition in the absence of an edge effect. In this paper it is established that even a very small nonzero Poisson’s ratio ($v = 0.05$) causes development of the edge effect.

It is noted that, due to the edge effect, a powerful belt of large tensile circumferential membrane stresses is created in the edge zone of the hinged shell. Such a belt (as a hoop) substantially increases the stability margin of a longitudinally compressed shell (Figure 4). Simultaneously with this belt a belt of significant compressive circumferential membrane stresses is formed. Here, the shell experiences a biaxial contraction - this is the most provocative zone from the point of view of the onset of wave formation. Indeed, upon transition to the initial post critical equilibrium, it is precisely along the zone of this compression belt that the first “wave formation elements” develop (Figure 4), which then expands to the entire shell surface.

4 Conclusion

Calculations performed on model shells showed that the development of a nonlinear edge effect leads to a change in the order of the eigen forms of loss of stability of the cylindrical shell. For model shells with a pivotally fixed edge, the axisymmetric form of buckling remained the first up to a load equal to (0.65-0.7) P_{cl}. Upon exceeding the indicated load values, the cyclically symmetric forms of buckling were becoming the first. The axisymmetric form of buckling remained the first until the critical load was reached on shell models where a nonlinear edge effect does not develop. This can be achieved with a zero Poisson’s ratio, as well as when fixing the shell at its edges only with tangent supports (they prevent movement along the circumferential coordinate). However, the last fixing option (absence of radial support) leads to a significant reduction in the critical load.

References

[1] LORENZ, R. Achsensymmetrische Verzerrungen in dunnwandigen Hohlzylinder / Axisymmetric distortions in thin-walled hollow cylinders (in German). *Zeitschrift des Vereines Deutscher Ingenieure*. 1908, **52,** p. 1766-1793. ISSN 0341-7255.

[2] TIMOSHENKO, S. P. Einige Stabilitatsprobleme der Elastizitatstheorie / Several stability problems of elasticity theory (in Russian). *Zeitschrift fur angewandte Mathematik und Physik /Journal of Applied Mathematics and Physics*. 1910,**58**, p. 337-385. ISSN 0044-2275, eISSN 1420-9039.

[3] PANOVKO, Y. G., GUBANOVA, I. I. *Ustoychivost i kolebaniya uprugikh sistem: Sovremennyye kontseptsii*, *paradoksy i oshibki / Stability and oscillations of elastic systems: Paradoxes*, *fallacies*, *and new concepts* (in Russian). 6 ed. Moscow: KomKniga, 2007. ISBN 978-5-484-00857-5.

[4] MANUYLOV, G. A., KOSITSYN, S. B., BEGICHEV, M. M. O yavlenii poteri ustoychivosti prodolno szhatoy krugovoy tsilindricheskoy obolochki. Chast 1: O poslekriticheskom ravnovesii obolochki / On the phenomenon of buckling of an axially compressed circular cylindrical shell, Part one: On the post-critical equilibrium of the shell (in Russian). *International Journal for Computational Civil and Structural Engineering* [online]. 2016, **12**(3), p. 58-72. ISSN 2587-9618, eISSN 2588-0195. Available from: https://doi.org/10.22337/1524-5845-2016-12-3-58-72

[5] GROH, R. M. J., PIRRERA, A. Localized post-buckling states of axially compressed cylinders and their energy barriers. American Institute of Aeronautics and Astronautics SciTech Forum : proceedings [online]. 2019. eISBN 978-1-62410-578-4. Available from: https://doi.org/10.2514/6.2019-0231

[6] ALMROTH, B. O. Influence of Edge Conditions on the Stability of Axially Compressed Cylindrical Shells*AIAA Journal*[online]. 1966, **4**(1), p. 134-140. ISSN 0001-1452, eISSN 1533-385X. Available from: https://doi.org/10.2514/3.3396

[7] EVKIN, A., KRASOVSKY, V., LYKHACHOVA, O., MARCHENKO, V. Local buckling of axially compressed cylindrical shells with different boundary conditions. *Thin-Walled Structures* [online]. 2019, **141**, p. 374-388. ISSN 0263-8231. Available from: https://doi.org/10.1016/j.tws.2019.04.039

[8] MANUYLOV, G. A., BEGICHEV, M. M. O nachalnom poslekriticheskom ravnovesii prodolno szhatoy krugovoy tsilindricheskoy obolochki i minimalnom energeticheskom baryere / On the initial postcritical equilibrium of an axially compressed circular cylindrical shell and the minimum energy barrier (in Russian). *Stroitelnaya Mekhanika Inzhenernykh Konstruktsiy i Sooruzheniy / Structural Mechanics of Engineering Constructions and Buildings*[online]. 2017, **1**, p. 58-69. ISSN 1815-5235, eISSN 2587-8700. Available from: http://journals.rudn.ru/structural-mechanics/article/view/15206

[9] VOLMIR, A. . *Gibkiye plastinki i obolochki/ Flexible plates and shells* (in Russian). Moscow: Izdatelstvo Tekhniko-Teoreticheskoi Literatury. 1956.

[10] TIMOSHENKO, S. P. *Kurs teorii uprugosti / Elasticity theory course* (in Russian). Kiev: Naukova Dumka. 1972.

[11] GEKKELER, I. *Statika uprugogo tela / Statics elastic body* (in Russian). Moscow: Gosudarstvennoye Tekhniko-Teoreticheskoye Izdatelstvo. 1934.

[12] FISHER, G. N. Uber den Einfluss der gelenkigen Lagerung auf die Stabilitat diinnwandiger Kreiszylinderschalen unter Axial- und Innendruck /On the influence of the hinge support on the stability of thin-walled circular cylindrical shells under axial and internal pressure (in German). *Zeitschrift fur Flugwissenschaften und Weltraumforschung*. 1963, **11**(3), p. 111-116. ISSN 0342-068X.

[13] OHIRA, H. Local buckling theory of axially compressed cylinders. 11th Japan National Congress of Applied Mechanics : proceedings. 1961, p. 37-40.

[14] HOFF, N.J., REHFIELD, L.W. Buckling of axially compressed circular cylindrical shells at stresses smaller than the classical critical value. *Journal of Applied Mechanics*. 1965, **32**, p. 533-538. ISSN 0021-8936, eISSN1528-9036.

[15] CROLL, J. G. A., BATISTA, R. A. Explicit lower bounds for the buckling of axially loaded cylinders. *International Journal of Mechanical Sciences*[online]. 1981, **23**(6), p. 331-343. ISSN 0020-7403. Available from: https://doi.org/10.1016/0020-7403(81)90063-1

[16] KRIEGESMANN, B., JANSEN, L. E., ROLFES, R. Design of cylindrical shells using the Single Perturbation Load Approach - potentials and application limits. *Thin-Walled Structures*[online].2016, **108**, p. 369-380. ISSN 0263-8231. Available from: https://doi.org/10.1016/j.tws.2016.09.005

Jana Pastorkova - Martina Jackova - Filip Pastorek - Zuzana Florkova - Juliana Drabikova

EFFECT OF PHOSPHATING TEMPERATURE ON SURFACE PROPERTIES OF MANGANESE PHOSPHATE COATING ON HSLA STEEL

A phosphating process modified for a high-strength low-alloy (HSLA) steel was performed at various temperatures and influence on the surface properties of the Domex steel covered by manganese phosphate (MnP) was investigated by electrochemical corrosion tests supported by a photo documentation performed by the SEM. Corrosion measurements were performed in 0.1M NaCl solution at 22±2 °C using electrochemical impedance spectroscopy and potentio-dynamic polarisation in order to obtain thermodynamic and kinetic corrosion characteristics and individual elements of equivalent circuits. It is that a temperature of the phosphating process has a very significant effect on protection properties of the created manganese phosphate coating on the Domex steel and needs to be strictly monitored. According to results of corrosion testing and surface morphology observations, the optimal temperature for the phosphating process on the tested Domex steel was chosen.

Keywords: *HSLA steel, corrosion properties, manganese phosphate, surface treatment*

1 Introduction

At present, the trend is to replace conventional structural steels with high-strength low-alloy steels. The HSLA steels have been developed to replace carbon steels in order to reduce the weight of structures. Their biggest advantage is a weight to strength ratio. Using the HSLA steels instead of conventional carbon steels can save up to 20% of weight while maintaining the high strength, stiffness and toughness of a structure [1-3]. However the HSLA steels are also attacked by common types of corrosion like standard steels [1], hence their surface needs to be protected by the application of surface treatments. Phosphating is one of the simple, affordable and inexpensive processes for formation of the surface conversion layers. Individual types of phosphating are a preferred surface treatment for the majority of metallic materials. The phosphate coatings improve corrosion resistance and abrasion resistance, increase adhesion at a metal-paint interface, serve as carriers for lubricants, and at the same time exhibit relatively low costs compared to other paint systems and coatings. The main types of phosphating include manganese, ferrous and zinc phosphating. The manganese phosphate has high mechanical resistance and good sliding properties. Good adhesion, distribution and uniform crystal size of this phosphate type result in increased corrosion resistance [4-8]. As listed by Narayanan [9], phosphating may be performed at temperatures ranging from 30-99 °C and processing time can be varied from a few seconds to several minutes depending on the nature of the metal to be coated, thickness and weight of a coating required and a bath composition. The effect of phosphating bath temperature on various surface characteristics of standard carbon and CrMoV steels was studied by some authors [10-11]. However, the research on corrosion resistance evolution of the MnP coating, prepared by the manganese phosphating on the HSLA steel at various temperatures, was not revealed yet. Hence, the aim of this paper is to optimize the phosphating temperature in order to reach the MnP coating on the Domex steel with the most protective character.

2 Experimental material and methods

The high-strength low-alloy Domex 700 steel without additional heat treatment was used as the experimental material. The chemical composition of the Domex 700 is shown in Table 1.

The samples of the experimental material for phosphating and electrochemical tests were prepared with dimensions of 80 ± 0.1 x 20 ± 0.1 x 5 ± 0.1 mm (Figure 1). A 3 mm diameter hole was subsequently drilled into samples to allow suspension of samples during the phosphating.

Two different electrochemical measurement techniques were used to compare and determine the corrosion resistance of the Domex 700 steel after phosphating at different temperatures: the potentio-dynamic polarization measurements (PD) and the electrochemical impedance spectroscopy (EIS) measurements. A solution of 0.1M NaCl (simulating an environment containing aggressive chloride ions) was chosen

Jana Pastorkova, Martina Jackova, Filip Pastorek*, Zuzana Florkova, Juliana Drabikova
University of Zilina, Slovakia
*E-mail of corresponding author: filip.pastorek@rc.uniza.sk

Table 1 Chemical composition of the Domex 700 steel (wt. %)

C	Si	Mn	S	P	Al	Nb	V	Ti	Fe
0.110	0.090	0.720	0.009	0.007	0.015	0.094	0.210	0.130	balance

Table 2 Parameters of the phosphating process

Demi. H_2O	H_3PO_4 (85.8 wt. %)	MnO_2 (99.9 wt. %)	Ultrafine steel wool (grade 0000)	Temperature range	Time
500 ml	7.5 g / 1 l	7.5 g / 1 l	2.5 g / 1 l	50 - 90 °C	75 min

Table 3 Chemical composition of the MnP layers formed on a ground surface of the Domex 700 steel at various phosphating temperatures (wt. %)

Phosp. temperature	O	Mn	P	Fe
50 °C	5.3	2.9	0.9	91.0
60 °C	23.2	10.5	7.9	57.2
70 °C	28.9	12.7	10.7	47.7
80 °C	35.0	15.8	13.4	35.8
90 °C	45.6	33.6	16.1	5.0

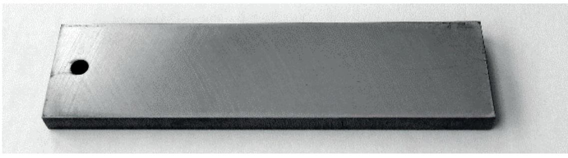

***Figure 1** Sample of Domex 700 steel designed both for phosphating and electrochemical tests*

as the test medium for all the electrochemical tests. All the electrochemical measurements were performed at 22 ± 2 ° C.

A technique with a constant potential change per time unit was used for the PD measurements. The PD tests were performed over the potential range from -250 mV to +300 mV vs. an open circuit potential (E_{OC}) value, after 5 minutes of stabilization in the 0.1M NaCl test environment. The constant change of applied potential during the measurements was 1 $mV.s^{-1}$. The measured area of the samples was 1 cm^2. The Tafel analysis of the measured curves was performed using the EC-Lab V11.10 software.

The EIS measurements were realized after 5 minutes of stabilization, too. The measurements were performed in the frequency range from 100 kHz to 10 mHz with the frequency 10 times per decade. The amplitude of the applied AC voltage was 10 mV around the open circuit potential value (E_{OC}). The output of the EIS measurements were represented by the Nyquist diagrams, which were analysed by the equivalent circuits with the EC-Lab V11.10 software.

The samples were pre-treated by grinding with a p500 grit SiC paper to provide a uniform and homogeneous substrate prior to MnP phosphating. The grain size of the abrasive paper used was chosen based on the previous experimental works and the experience of the authors with the manganese phosphating process [7, 12]. Prior to the phosphating process, the samples were thoroughly degreased and cleaned in an ultrasonic cleaner for 15 minutes before being dried with a stream of air. The phosphating process was performed by immersing the samples in the phosphating bath. The samples were placed vertically. After the phosphating process, the samples were washed with demineralised water and dried with a stream of air. The individual parameters of the phosphating process are shown in Table 2.

3 Results and discussion

Created MnP layer is composed of Mn from the solution and Fe from the steel wool/matrix. Depending on the Mn/Fe ratio the chemical composition of the layer is $(Mn, Fe)_3(PO_4)_2{-}2(Mn, Fe)HPO_4{-}4H2O$, where Fe and Mn are interchangeable. The total Mn and Fe content in the well prepared MnP structure is 39-40 wt% [7, 13-14]. However, as proved in our previous study, higher Mn content helps to reach better corrosion properties of the layer [15]. Therefore, it is important to know the chemical composition of the MnP layers for the deeper evaluation of the surface properties. The morphology and chemical composition of the MnP layers formed at the different temperatures are documented in Figure 2 and in Table 3. As can be seen, the change in the phosphating temperature significantly affects the formation of the MnP layer. As the temperature increase, a more compact and homogeneous MnP layer is formed, a direct effect of which on the surface layer composition was as detected by the EDX analysis. Figure 2a reveals that MnP phosphating of the tested HSLA steel in the chosen phosphating solution

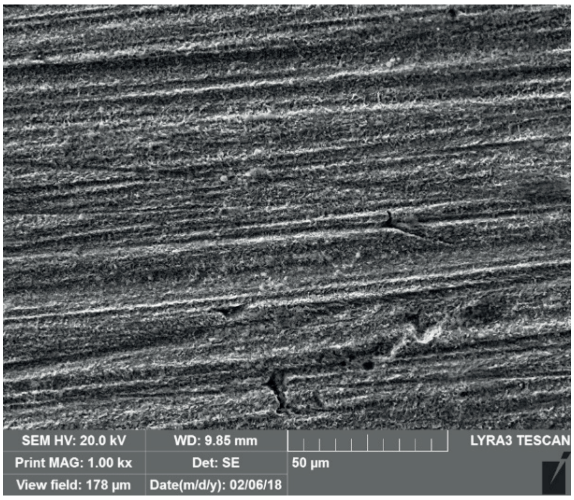

50 °C

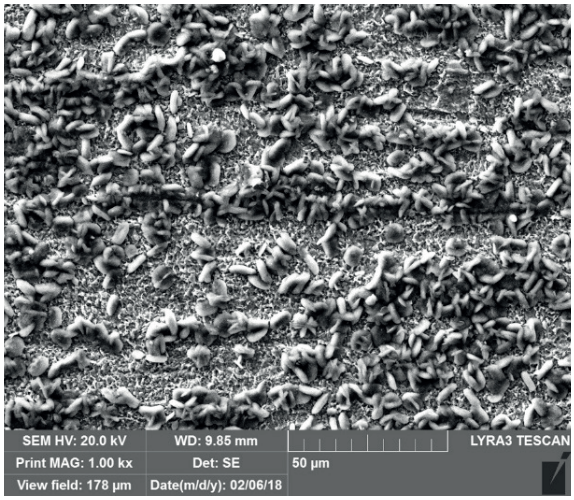

60°C

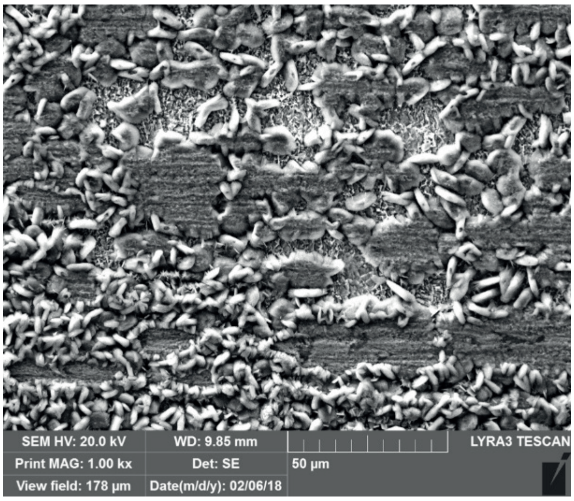

70 °C

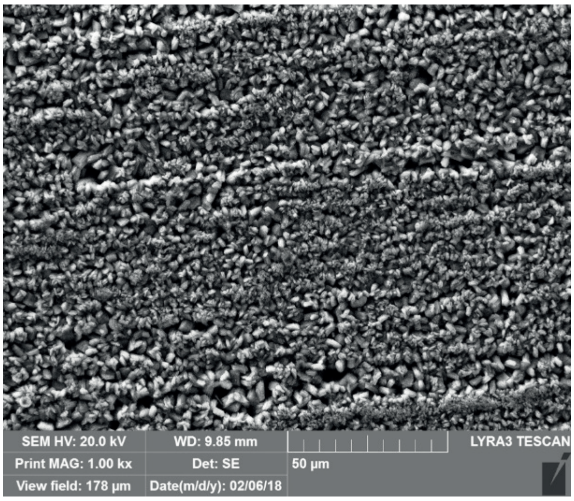

80 °C

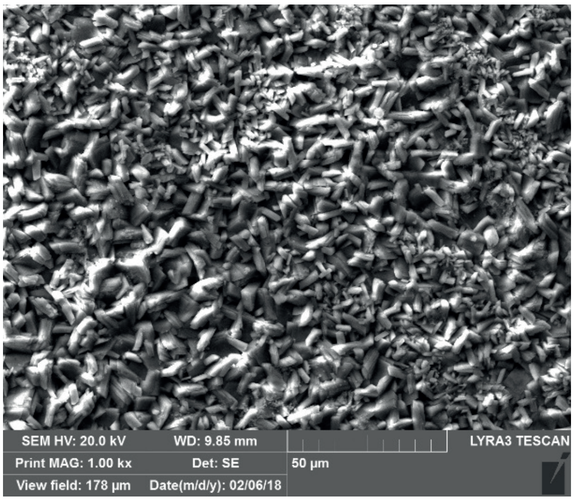

90 °C

Figure 2 *Morphology of the MnP layers formed on a ground surface of the Domex 700 steel at various phosphating temperatures*

is very unsatisfactory at temperatures up to 60 °C as almost no MnP layer is visually detectable on the steel surface. Even the surface morphology after the final grinding operation is still clearly visible on the phosphate surface. The formation of just a fine MnP film is proved by the small percentage of Mn and P in the surface layer (Table 3). The 91% Fe content in the surface layer demonstrates that the performed EDX analysis detected the matrix. Thus, there is no thermodynamic

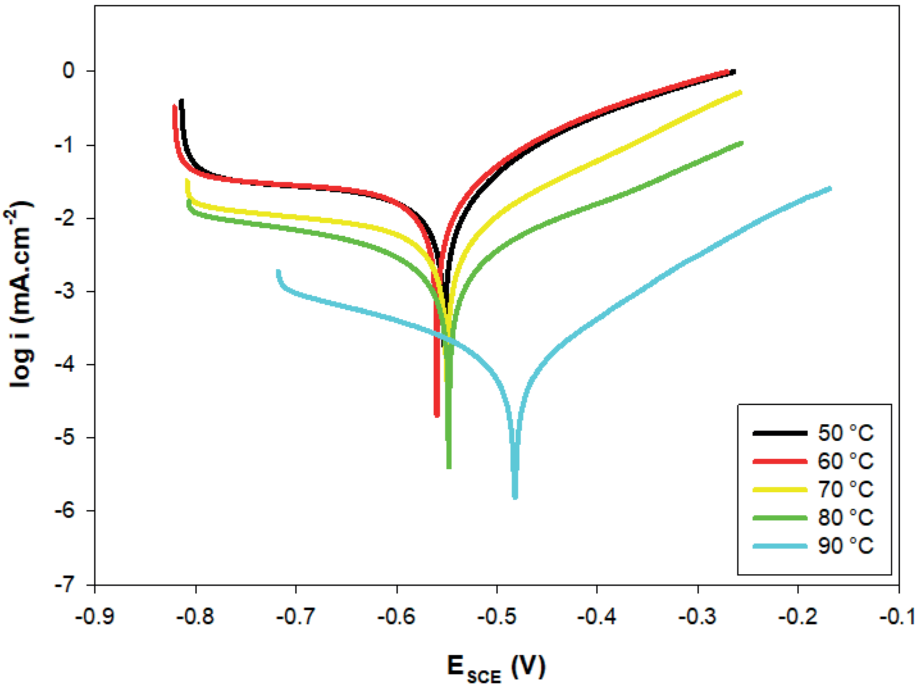

***Figure 3** PD curves of the MnP layers formed on a ground surface of the Domex 700 steel at various phosphating temperatures*

assumption for a serious nucleation of the MnP layer crystals at the low temperatures (below 50 °C). At 60 °C, the conditions for the MnP layer formation are slightly better, as demonstrated by the nucleation and distinct local formation of the MnP facets. Although the layer is non-compact, the significant increase in Mn and P content measured by the EDX analysis presents superior thermodynamic conditions for the MnP layer formation to the phosphating at 50 °C. The trend of the MnP growth at 70 °C is very similar to the one at 60 °C apart from the slight increase in Mn and P content. The morphological change is negligible. Similar results with the local smooth facets formation at 70 °C were also obtained by Wang et al. [10]. However, the very high Fe content in the surface layer still confirms the fact that a significant part of the surface is still not covered by the MnP layer. When the phosphating temperature reaches 80 °C the relatively homogeneous layer of the fine MnP crystals is formed that copies the surface morphology after grinding. Thus, the temperature of 80 °C is the limit for reaching the thermodynamic conditions allowing a visually continuous MnP layer formation after 75 minutes of phosphating. However, the Fe content is still very significant meaning that the layer is very thin and porous allowing the EDX to detect the matrix. Only phosphating at the temperature close to the boiling point (90 °C) allowed the increase of the diffusion kinetics of the nucleation process and the growth of the MnP crystals to such an extent that the formation of a thick and homogenous MnP layer was possible. Although there is only a 10 °C difference to the previous phosphating temperature (80 °C), this temperature change has a critical effect on the phosphating process efficiency. The MnP crystals formed at 90 °C were considerably thicker and the layer was more compact, as proven also by results of EDX analysis, where a significant decrease in the Fe content and an increase in the Mn content were detected. In addition, the Mn content (33.6 wt.%) markedly exceeded the recorded Fe content (5.0 wt.%). This fact does not only indicate the reduction of pores and layer defects, but also the thermodynamic state of the phosphating system where the phosphate $Mn_3(PO_4)_2$-$2MnHPO_4$- $4H_2O$ is preferably formed in the MnP structure.

The results from the morphological and chemical analysis of the tested layers were also supported by the electrochemical tests to provide a more comprehensive assessment of the quality of the formed layers. The measured PD curves and EIS curves of the created MnP layers at different phosphating temperatures are shown in Figures 3 and 4. The individual electrochemical characteristics obtained by the analysis of these curves are shown in Table 4. It was proven, that the higher temperatures of phosphating lead to lower values of the corrosion current density i_{Corr} and the corrosion rate v_{Corr}. This confirms the formation of a protective layer on the surface of the base material and a gradual increase in the corrosion resistance in the aggressive chloride-containing solution. The decrease of the i_{Corr} values is gradual and fluent up to 80 °C. However, the layer formed at 90 °C reached the i_{Corr} value of 2 orders of magnitude lower compared to one formed at 80 °C. This radical difference between two phosphating temperatures supports the similar differences reached by the EDX and morphology observations. The corrosion potential values did not show significant change in either direction in the range of phosphating temperatures from 50 °C to 80 °C. Hence, it can be stated that from the thermodynamic point of view neither the character of the formed layer nor the thermodynamic stability of the

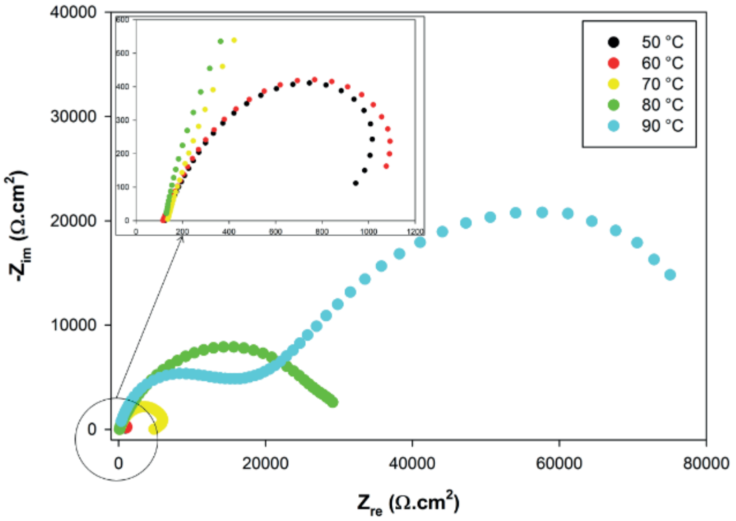

Figure 4 *Nyquist diagrams of the MnP layers formed on a ground surface of Domex 700 steel at various phosphating temperatures*

Table 4 *Electrochemical corrosion characteristics of the MnP layers formed on a ground surface of the Domex 700 steel at various phosphating temperatures*

Phosp. temp.	E_{Corr} (mV)	i_{Corr} (μA.cm^{-2})	v_{Corr} (μm.year^{-1})	R_{P1} (Ω.cm^2)	R_{P2} (Ω.cm^2)	R_P (Ω.cm^2)	CPE_1 (10^{-6}.F.s^{n-1})	CPE_2 (10^{-6}.F.s^{n-1})
50 °C	-552 ± 9	11.78 ± 1.13	273 ± 21	1 250 ± 51	-	1 250 ± 51	477 ± 21	-
60 °C	-561 ± 11	10.97 ± 1.21	255 ± 18	1 295 ± 61	-	1 295 ± 61	457 ± 23	-
70 °C	-551 ± 8	4.57 ± 0.87	106 ± 9	5 972 ± 195	-	5 972 ± 195	23 ± 5	-
80 °C	-548 ± 13	2.31 ± 0.51	54 ± 4	27 788 ± 347		27 788 ± 347	3.3 ± 0.6	-
90 °C	-482 ± 7	0.07 ± 0.01	1.7 ± 0.2	66 140 ± 1 234	16 214 ± 201	82 354 ± 1 435	0.06 ± 0.01	7.4 ± 0.5

whole system changes markedly. However, by increasing the phosphating temperature up to 90 °C, a step change (66 mV) is achieved, similarly to the case of the current density. In this case, a significant decrease in the Fe content of the surface layer and an increase in the Mn content are responsible for the potential shift to more positive values. This results in the better thermodynamic stability of the surface layer in the corrosion test medium.

The EIS measurements and Nyquist diagram analysis provide a comprehensive view of the corrosion resistance of the formed MnP coating on the tested HSLA steel. The most relevant electrochemical parameter in this area is the polarization resistance R_p, which expresses the resistance of the surface layer to the corrosion process [16-17]. In a more complex systems, this polarization resistance is given by the sum of the partial resistances R_{p1} and R_{p2}. This situation appears when the measured Nyquist diagram is composed of two capacitive loops. Only one capacitive loop was recorded in the Nyquist diagrams measured up to 80 °C on the samples. This fact expresses a situation where the formed layer does not reach the level of compactness necessary to form its own impedance loop. However, the gradual increasing of the MnP layer quality, reached by increasing the phosphating temperature, caused the reduction in charge transfer between the corrosive medium and the base material, which is documented by the gradual increase of the R_p values (Table 4). The considerably higher R_p value of the MnP layer reached after phosphating at 90 °C compared to 80 °C, is caused due to both a significant reduction in the charge transfer through the base material / environment interface and an additive effect of the MnP layer resistance itself. The layer formed at this temperature reveals a high level of compactness that allows formation of the second capacitive loop in the Nyquist diagram. The decreasing values of the constant phase element CPE_1 also documents e reduction of the active surface area of the base material and the increasing thickness of the formed layer. The quality of the MnP layer, formed at 90 °C, is evident very well from this parameter as it reached the CPE_1 value of 4 orders of magnitude lower compared to those prepared at 50 or 60 °C. As the only one MnP layer (formed at 90 °C) revealed 2 capacitive loops, the value of the constant phase element CPE_2, related to the electrolyte penetration ability of the formed layer, could not be compared to the other ones. The phosphating temperature of 90 °C was also found to be optimal by Wang et al. [10], who observed the effect of higher temperatures (70 - 90 °C) of phosphating on morphology and electrochemical characteristics of a different steel type. Thus, it can be concluded that despite the certain specifics and differences in the phosphating process, it is necessary to maintain the phosphating bath temperature of at least 90 °C throughout the phosphating, regardless of the fact that the phosphated material is a standard or HSLA steel.

4 Conclusions

Based on the measured data and analyses the following was concluded:

A. There are several step changes during the manganese phosphating of the Domex 700 HSLA steel depending on the process temperature resulting in the quality and surface properties differences of the formed MnP layers.
B. The threshold for forming a visually compact MnP layer is to maintain the phosphating temperature of at least 80 °C.
C. The chemical composition of the MnP layer with the higher Mn content than Fe is ensured by phosphating at the temperature of 90 °C
D. The most compact MnP layer with the highest corrosion resistance and electrochemical stability in the aqueous medium containing chloride ions is achieved at the highest tested phosphating temperature (90 °C).

Acknowledgements

Authors are grateful for the support in experimental works to Slovak Research and Development Agency by the projects No. APVV-15-0120, APVV-16-0300, APVV-16-0276 and APVV-14-0772.

References

[1] GARCIA, C. I. Chapter 6 - High strength low alloyed (HSLA) steels. In: Automotive steels. Design, metallurgy, processing and applications. University of Pittsburgh:Woodhead Publishing , 2016, p. 145-167. ISBN 0081006535
[2] LI, J., WU, J., WANG, Z., ZHANG, S., WU, X., HUANG, Y., LI, X. The effect of nanosized NbC precipitates on electrochemical corrosion behavior of high-strength low-alloy steel in 3.5% NaCl solution. *International Journal of Hydrogen Energy* [online]. 2017, **42**(34), p. 22175-22184 [accessed 2019-10-09]. ISSN 0360-3199. Available from: https://doi.org/10.1016/j.ijhydene.2017.03.087
[3] KIM, W.K., KOH, S. U., YANG, B. Y., KIM, K. Y. Effect of environmental and metallurgical factors on hydrogen induced cracking of HSLA steels. *Corrosion Science* [online]. 2008, **50**, p. 3336-3342 [accessed 2019-10-09]. ISSN 0010-938X. Available from: https://doi.org/10.1016/j.corsci.2008.09.030
[4] PASTOREK, F., BORKO, K., DUNDEKOVA, S., FINTOVA, S., HADZIMA, B. Elektrochemicke korozne charakteristiky fosfatovanej ocele S355J2 v prostredi siranov / Electrochemical corrosion characteristics of phosphated S355J2 steel in sulfate environment (in Slovak). *Koroze a ochrana materialu*[online]. 2016, **60**(4), p. 107-113. [accessed 2019-10-09]. ISSN 1804-1213. Available from: https://www.degruyter.com/downloadpdf/j/kom.2016.60.issue-4/kom-2016-0017/kom-2016-0017.pdf
[5] PASTOREK, F., BORKO, K., FINTOVA, S., KAJANEK, D., HADZIMA, B. Effect of surface pre-treatment on quality and electrochemical corrosion properties of manganese phosphate on S355J2 HSLA steel. *Coatings* [online]. 2016, **6**(4), p. 46. [accessed 2019-10-09]. ISSN 2079-6412. Available from: https://doi.org/10.3390/coatings6040046
[6] OLSOVSKY, M. *Zaklady povrchovej upravy kovov / Basics of surface treatment of metals* (in Slovak). Novaky: MSM Martin, 2015. ISBN 978-80-971929-9-0.
[7] GALVAN-REYES, C. SALINAS-RODRIGUEZ, A. FUENTES-ACEITUNO, J. C. Degradation and crystalline reorganization of hureaulite crystals during the manganese phosphating of a high strength steel. *Surface and Coatings Technology* [online]. 2015, **275**, p. 10-20. [accessed 2019-10-09]. ISSN 0257-8972. Available from: https://doi.org/10.1016/j.surfcoat.2015.05.030
[8] KELLY, R. G., SCULLY, J. R., SHOESMITH, D., BUCHHEIT, R. G. *Electrochemical techniques in corrosion science and engineering*. Boca Raton, USA: CRC Press, 2003. ISBN 978-0-8247-9917-5.
[9] NARAYANAN, T. S. N. Surface pretreatment by phosphate conversion coatings - a review. *Reviews on Advanced Materials Science* [online]. 2005, **9**(2), p. 130-177. [accessed 2019-10-09]. ISSN 1605-8127. Available from: http://www.ipme.ru/e-journals/RAMS/no_2905/narayanan.pdf
[10] WANG, C. M., LIAU, H. C., TSAI, W. T. Effects of temperature and applied potential on the microstructure and electrochemical behavior of manganese phosphate coating. *Surface and coatings Technology* [online]. 2006, **201**(6), p. 2994-3001. [accessed 2019-10-09]. ISSN 0257-8972. Available from: https://doi.org/10.1016/j.surfcoat.2006.06.010

[11] HIVART, P., HAUW, B., BRICOUT, J. P., OUDIN, J. Seizure behaviour of manganese phosphate coatings according to the process conditions. *Tribology International* [online]. 1997, **30**(8), p. 561-570. [accessed 2019-10-09]. ISSN 0301-679X. Available from: https://doi.org/10.1016/S0301-679X(97)00019-4

[12] GALVAN-REYES, C. FUENTES-ACEITUNO, J. C. SALINAS-RODRIGUEZ, A. The role of alkalizing agent on the manganese phosphating of a high strength steel part 2: The combined effect of NaOH and the amino group (NH_4OH, mono-ethanolamine and NH4NO3) on the degradation stage of the phosphating mechanism. *Surface and Coatings Technology* [online]. 2016, **299**, p. 113-122. [accessed 2019-10-09]. ISSN 0257-8972. Available from: https://doi.org/10.1016/j.surfcoat.2016.04.059

[13] BOGI, J., MACMILLAN, R. Phosphate conversion coatings on steel. *Journal of Materials Science* [online]. 1997, **12**(11), p. 2235-2240. [accessed 2019-10-09]. ISSN 1573-4803. Available from: https://link.springer.com/article/10.1007/BF00552245

[14] KOZLOWSKI, A. Dry friction of manganese phosphate coatings on steel and cast iron. *Electrodeposition and Surface Treatment* [online]. 1974, **2**(2), p. 109-122. [accessed 2019-10-09]. ISSN 0300-9416. Available from: https://doi.org/10.1016/0300-9416(74)90009-1

[15] HADZIMA, B., PASTOREK, F., BORKO, K., FINTOVA, S., KAJANEK, D., BAGHERIFARD, S., GHOLAMI-KERMANSHAHI, M., TRSKO, L., PASTORKOVA, J., BREZINA, J. Effect of phosphating time on protection properties of hurealite coating: differences between ground and shot peened HSLA steel surface. *Surface and Coatings Technology* [online]. 2019, **375**, p. 608-620. [accessed 2019-10-09]. ISSN 0257-8972. Available from: https://doi.org/10.1016/j.surfcoat.2019.07.056

[16] MINARIK, P., KRAL, R., HADZIMA, B. Substantially higher corrosion resistance in AE42 magnesium alloy through corrosion layer stabilization by ECAP treatment. *Acta Physica Polonica-Series A General Physics* [online]. 2012, **122**(3), p. 614. [accessed 2019-10-09]. ISSN 1898-794X. Available from: http://psjd.icm.edu.pl/psjd/element/bwmeta1.element.bwnjournal-article-appv122z3p46kz

[17] BUKOVINOVA, L., HADZIMA, B. Electrochemical characteristics of magnesium alloy AZ31 in Hank's solution. *Corrosion Engineering, Science and Technology* [online]. 2012, **47**(5), p. 352-357. [accessed 2019-10-09]. ISSN 1478-422X. Available from: https://doi.org/10.1179/1743278212Y.0000000033

Ruzica Nikolic - Dusan Arsic - Aleksandra Arsic - Zivce Sarkocevic - Dragan Cvetkovic - Branislav Hadzima

THE FAULT TREE ANALYSIS OF CAUSES OF THE WELDED PIPES FAILURES IN EXPLOITATION

Premature failure or damage of parts and components of the oil and gas well piping, as well as pipelines for transport of oil and gas, are generally caused by the simultaneous influence of a large number of technological, metallurgical, structural and exploitation factors. Therefore, the convenient structural solutions, which provide the mechanical safety of parts and integrity of structures, can be realized only through total comprehension of their behavior in various operation regimes.

Importance of technical diagnostics for monitoring and state analysis of welded pipes/pipelines in oil industry is considered in this paper. An analysis of causes of the welded pipes failures in exploitation has been performed through use of the fault tree analysis. Based on the suggested structure of a database, regarding the causes of failure, possibilities are presented to set measures for prevention of damage and failure of welded pipes/pipelines and for extension of their service life. A suggestion for improvement of the organizational scheme for monitoring the state and maintenance of welded pipes/pipelines during the exploitation has been made, as well.

Keywords: *welded pipes, damage, failure, the fault tree, database, preventive measures*

1 Introduction

Due to the fact that oil and gas well piping and pipelines for transport of oil and gas are considered as highly responsible structures, quite susceptible to corrosion and occurrence of cracks, Figures 1 and 2, it is very important to know the pipe's residual strength, in the case that any of the mentioned types of damages would appear on them [1].

The API 5CT standard prescribes regulations for production of protective seam welded pipes, which are used in wells, [2-4]. Automatic or semi-automatic production of welded pipes enables the continuous production of longitudinal-seam welded pipes where the basic intention is to reach the welding speed equal to speed of the pipe-forming. Machines aimed for the continuous production of longitudinal-seam welded pipes are mainly designed for the automatic high-frequency contact welding [5].

Based on the precise examination, regarding the defect type and size, as well as on calculation of operating ability of the welded joint, the decision, referring to possibility of reintegrating the pipe into the system, can be made [6-9].

Steel pipes in oil industry are continuously exposed to corrosive effects, which are enhanced by high pressures and temperatures existing within the well. Corrosion can cause a decrease of steel's mechanical properties, which in turn, in combination with unfavorable operating conditions, may lead to appearance of an initial crack and a subsequent fracture. Failure of protective pipes can be caused and accelerated by various corrosion mechanisms [10-15], or some other factors [16-18].

2 Technical diagnostics

During the exploitation of oil well piping and transport pipelines, useful properties of assemblies and their constitutive parts get gradually degraded. Degradation of the material properties and/or deformation of elements, can get accelerated due to exploitation and assembling errors, therefore, the periodic or permanent diagnostic measurements and periodic inspections are necessary in order to keep under control the processes that may create conditions leading to a system failure.

If the technical diagnostics was carried out correctly, it would prevent sudden failures of well piping and transport pipelines, ensure safe working conditions for the employees, rational techno-economic exploitation and protection of the environment.

Procedures for the pipe column inspection mostly consist of the following actions [1]:

- coupon testing through use of the steel plates, located within the pipeline, to monitor the corrosion layers,
- determination of hydrogen content through application of an analyzer,
- determination of the CO_2 and H_2S contents, as well as the iron content (if the Fe content is less than 0.02%,

Ruzica Nikolic[1,*], Dusan Arsic[2], Aleksandra Arsic[3], Zivce Sarkocevic[4], Dragan Cvetkovic[2], Branislav Hadzima[1]
[1]Research Center, University of Zilina, Slovakia
[2]Faculty of Engineering, University of Kragujevac, Serbia
[3]Faculty of Mechanical Engineering, University of Belgrade, Serbia
[4]Faculty of Technical Sciences, University of Kosovska Mitrovica, Serbia
*E-mail of corresponding author: ruzicarnikolic@yahoo.com

Figure 1 *General corrosion of well pipes*

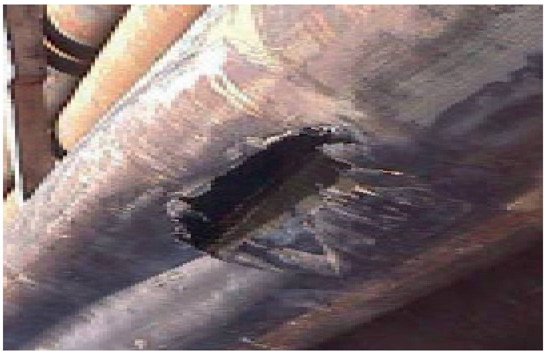

Figure 2 *Pipeline failure*

FeS_2, which actually causes the corrosion, cannot be created),

- determination of the Benfield solution content (content of Fe less than 0.02%, V < 0.7% and H_2S),
- determination of inhibitor content in the condensate (for protection of the pipe surfaces),
- ultrasonic wall thickness measurement,
- corrosion inspection of the pipes' inner surfaces through use of a calibrator,
- inspection performed through use of the corrosion measuring probes,
- ultrasonic inspection of the gas pipeline inner surface during the operation.

Procedures for inspection of the oil and gas transport pipelines include:

- inspection of the gas pipelines' inner surfaces during the operation through use of the magnetic flux leakage (MFL) inspection method using the MFL inspection tools (magnetic flux expands longitudinally with respect to the pipeline axis),
- inspection of the gas pipelines' inner surfaces during the operation through use of the combined MFL inspection tool,
- ultrasonic wall thickness measurement,
- ultrasonic inspection of the gas pipelines' inner surfaces during the operation.

3 Failure analysis of welded pipes in oil industry

The production systems, such as oil wells, are very hard to analyze due to their complex structure, operating conditions and inaccessibility of pipes. In such cases, the fault tree analysis can be very successfully applied, with several minor simplifications. The fault tree is suitable for analyses of the complex systems, consisting of functionally related or dependable subsystems with different performances. The fault tree analysis is regularly used for the nuclear power plants, aircrafts and communication systems, chemical and other industrial processes. However, that does not apply to processes in the oil industry. Through analysis of singular influences, the fault tree provides the conclusion, which refers to causes of and singular contributions to failure [19-21].

Main advantages of the fault tree method are:

- the simple graphic depiction of the logic of failure,
- the logic of failure can be followed gradually,
- the possibility of making the quality and quantity analysis, through use of the Boolean algebra,
- the quantity analysis can be carried out when the quantity input data is available. When there is no reliable input data available, only the quality analysis is carried out,
- the fault tree analysis can envelop various influences, unlike other methods,
- no special training and knowledge are necessary for application of the fault tree method.

Results of the fault tree analysis are used for failure prevention, failure analysis, or in other words for influence of various factors on reliability, as well as for clearer definition and quantifying of individual influences that affect the reliability, ensuring conditions that would provide for the good reliability.

During the process of oil/gas exploitation, the well piping and transport pipelines are subjected to varying loads (pressure, temperature) and to occurrence of corrosion in all the parts of the system, starting from the well, until the master pipeline entry and through the pipeline to the consumer. Failures of welded pipes during exploitation or transport of oil/gas, which occur due to damaging, influence the operation reliability and safety. Failures generally occur due to corrosion fatigue, Figure 3. Procedures concerning the material degradation of pipes/pipelines during the exploitation are presented in Figure 4. However, it is not uncommon that defects pass undetected during the NDI (non-destructive inspection) methods, Figure 5. Conditions for the crack propagation until it reaches the critical size (case A – Figure 3) are presented in Figure 6. Legends of symbols and notation presented in Figures 3 to 6 are shown in Tables 1 and 2, respectively.

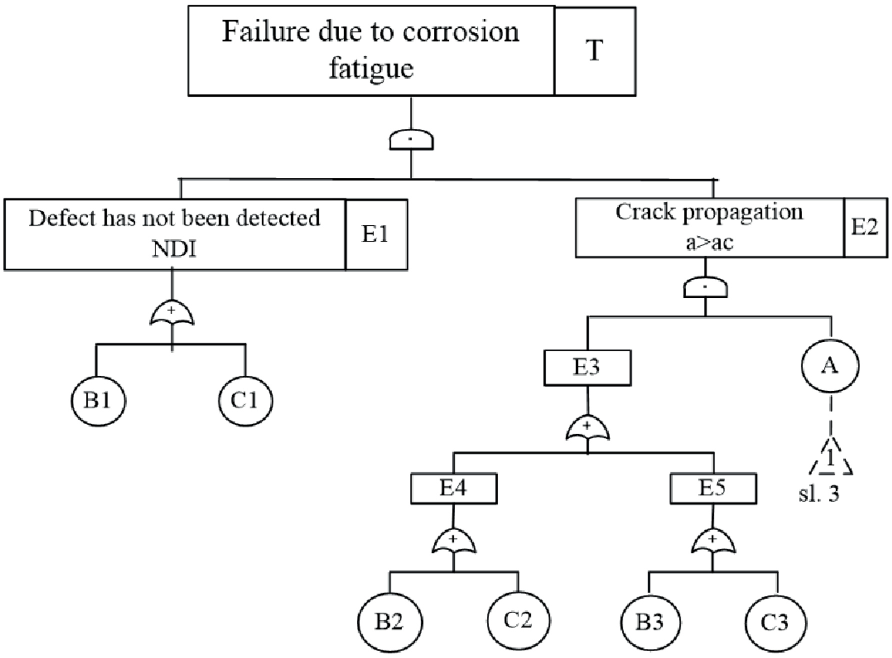

Figure 3 *Schematic presentation of failure due to corrosion fatigue*

Table 1 *Legend of symbols used in Figures 3 to 6*

Symbol	Meaning
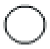	Elementary event, initial defect
	Intermediate event or on top (I)
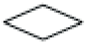	Undeveloped event due to a lack of information
	AND gate: a defect on the output side occurs if all defects on the input side occur
	OR gate: a defect on the output side occurs if one defect on the input side exists
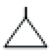	Further development of the fault tree on the other figure
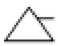	Entrance of the part of the fault tree from the other figure

Table 2 *Notation presented in Figures 3 to 6*

Notation	Meaning
T	Failure due to corrosion fatigue
E1	Fatigue defect has not been detected
E2	Crack propagation, $a > a_c$
E3	Defect has not been detected by the NDI methods
E4	Defect has not been detected by the NDI methods immediately after the occurrence
E5	Defect has not been detected by the NDI methods in the later stages of inspection
A	Conditions for the crack propagation
B	Device does not detect the defect
C	Operator does not detect the defect despite the fact that the device is capable of detecting it

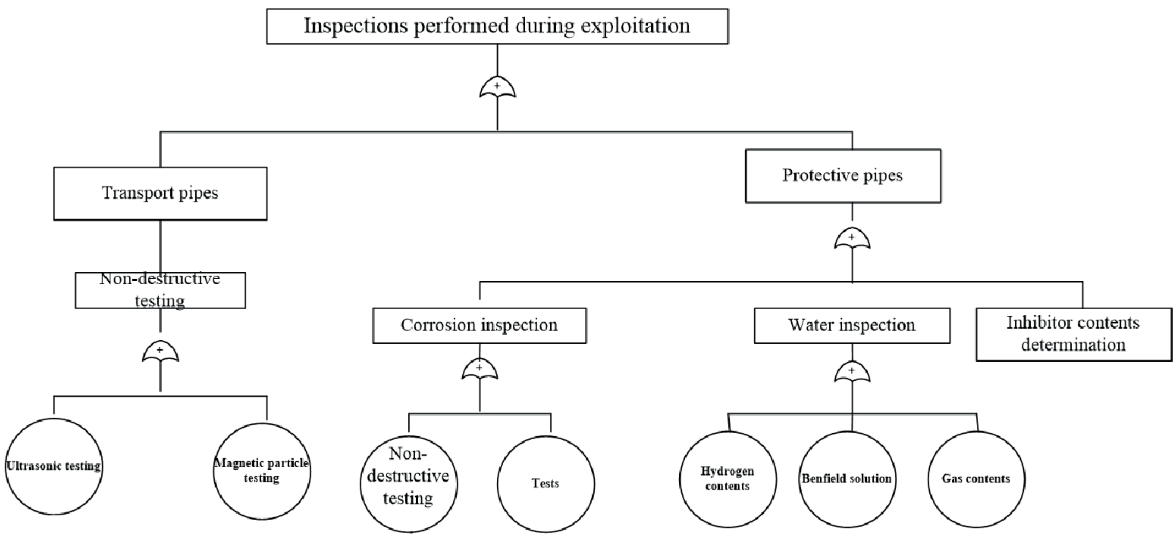

***Figure 4** Scheme of the pipeline material degradation inspection during exploitation*

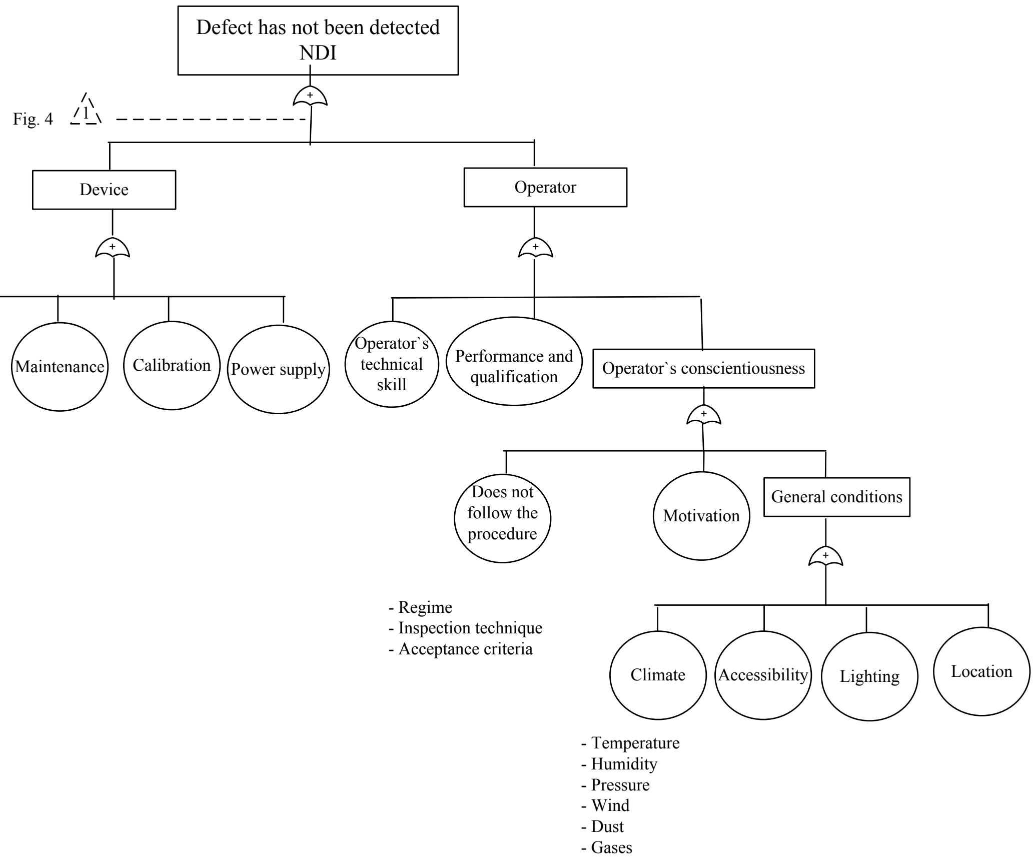

***Figure 5** Scheme of the event elaboration - defect has not been detected*

Derivative of the reduced fault tree is:

T = E1*E2

= E2(B1 + C1) - A*E3(B1 + C1)

= A(E4 + E5)(B1 + C1) - A(B2 + C2 + B3 + C3)(B1 + C1)

By applying the law of absorption one gets T ≈ A(B1 + C1).

4 Database

An adequate database is required if one wants to obtain the reliable evaluation of integrity and suitability for operation of the structure elements of welded pipes/pipelines in the oil industry. Additional software packages enable the more efficient use of databases, analysis of certain influential factors, possibilities of failure prevention

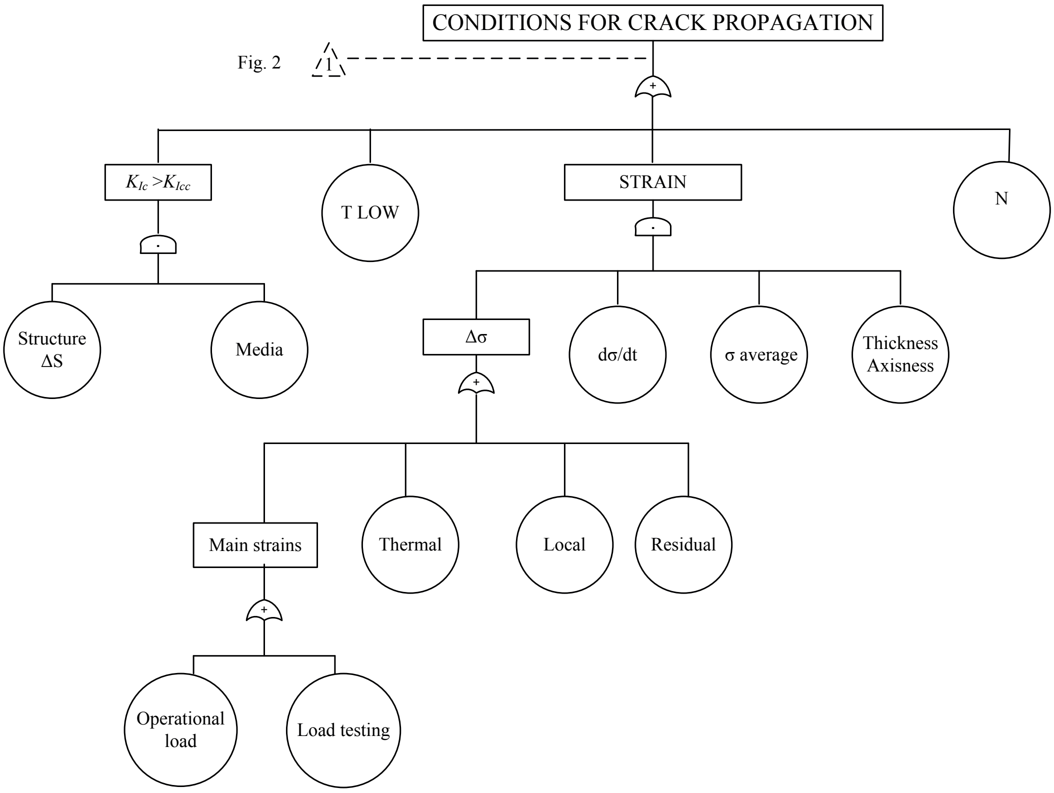

Figure 6 *Scheme of elaboration of possibility for the crack propagation until it reaches* $a > a_c$ *(event A in Figure 3)*

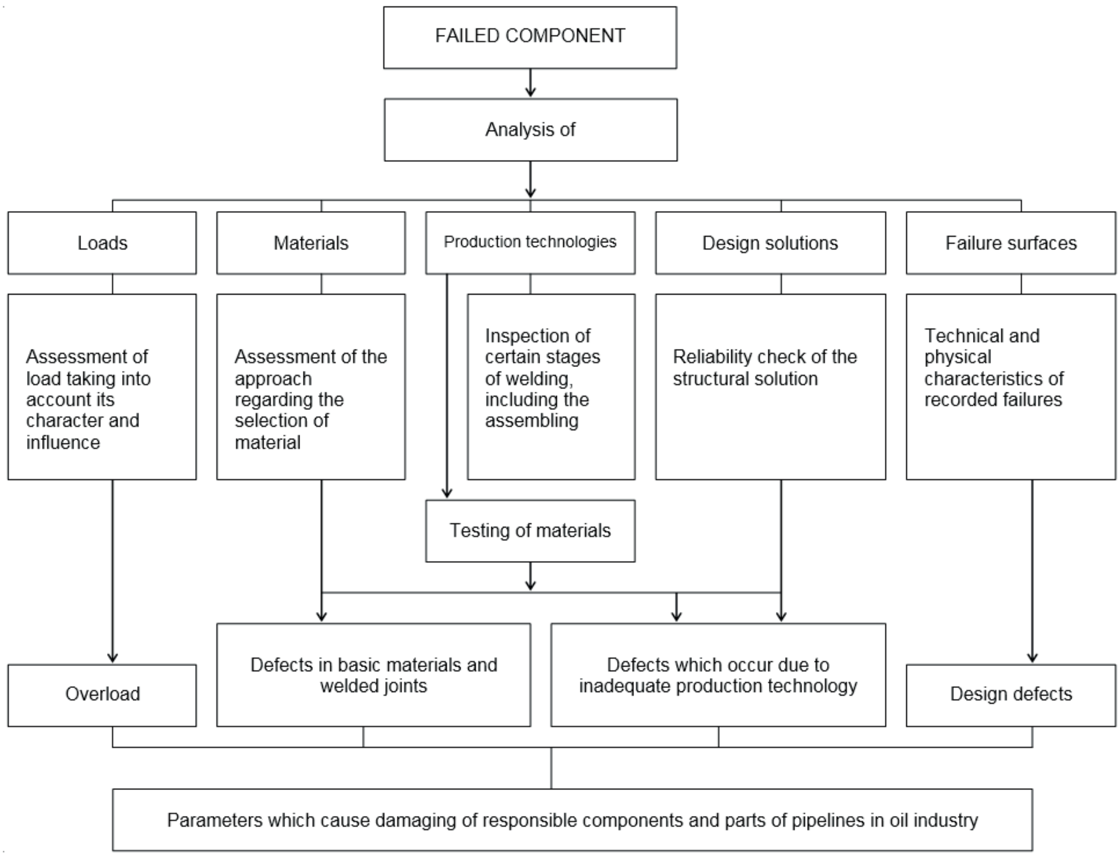

Figure 7 *Process analysis of damage and failure of welded pipes and pipelines in oil industry*

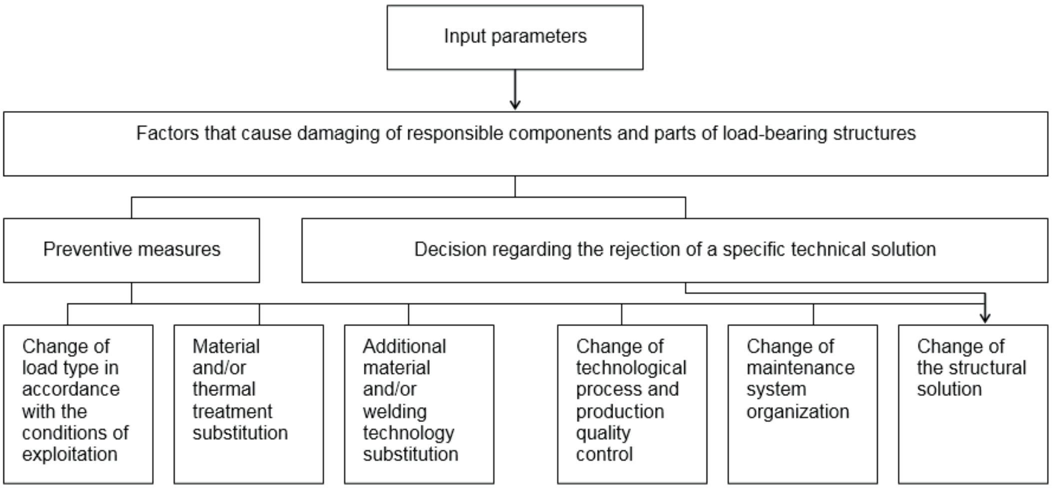

Figure 8 *Preventive measures*

and creation of alternative solutions in all the phases of design and structure development.

Creation of the damage and failure analyses of parts and elements of bearing structures is enabled by information on improvement of the design methods for bearing parts and elements of bearing structures, as well as on improvement of properties of the existing materials and technologies for their processing and development of new materials. The damage and failure analyses can enable development of new technical solutions and testing methods already in the prototype phase. A systematic approach is required if one wants to determine and prevent causes of damage and failure, Figure 7.

Databases, which refer to realized inspections and failure analyses, regarding adequate oil and gas well piping, as well as transport pipelines, offer big possibilities when it comes to determining changes of the mechanical properties of materials and welded joints. This is due to the fact that a large number of influential factors are varying and some undesirable effects should be reduced to bearable values, or, in other words, the satisfying structural solution should be created.

5 Measures for damage and failure prevention

Causes that can lead to failure could be determined through analysis of damage and failure of responsible parts and pipeline elements in oil industry, thus enabling the decision making, referring to rejection of the specific technical solution or preventive measures, Figure 8.

The preventive measures, shown in Figure 8, are primarily related to execution of processes that can, in a certain way, influence the integrity and service life of a pipeline, which can be determined according to experience or based on conducted analyses.

Variation of the load type can significantly affect the integrity of a structure, since the pipeline can in some phase of exploitation be exposed to tensile stresses, which belong into a group of the most unfavorable ones. Therefore, changing the load, e.g. from tensile to compression, can have multiple effects on extending the service life.

Material replacement, as one of the preventive measures, implies the substitution of material at critical places for the sake of extending the pipeline service life. For instance, there are frequent examples that the used material is inadequate from the aspect of corrosion [21-22], thus it *per se* represents the critical point of a structure, what preventively can be solved by replacing the critical material.

The same applies for the places of joints in construction, where the referral is to the welded joints and vicinity of the weld and not to the material as a whole [8, 16, 23].

Sometimes, the preventive measures can be related to the process of manufacturing the construction. During the design, it is recommended to select the technological process of the construction execution in such a way that it corresponds to the type of construction, as well as to its exploitation conditions. If, during the construction operation, was found out that the cause of failure could be in the way the construction was made, it could be possible, in some of the following phases, to change the construction production process in order to eliminate the cause of possible failures.

In this phase, it is very important that the maintenance personnel defines the critical spots in a proper manner and determines the real cause of failures, based on which they can propose certain measures for the purpose of extending the construction's service life [10, 24].

Finally, if some of the mentioned measures did not produce the desired effect, the solution should be sought in the design phase. Namely, different examples from practice have shown that poorly designed construction can cause serious problems, which cannot be eliminated by any other measure, but by correcting the error made in the design or manufacturing phases.

A decision to reject a specific technical solution can initialize making of a new, optimal structural solution, in

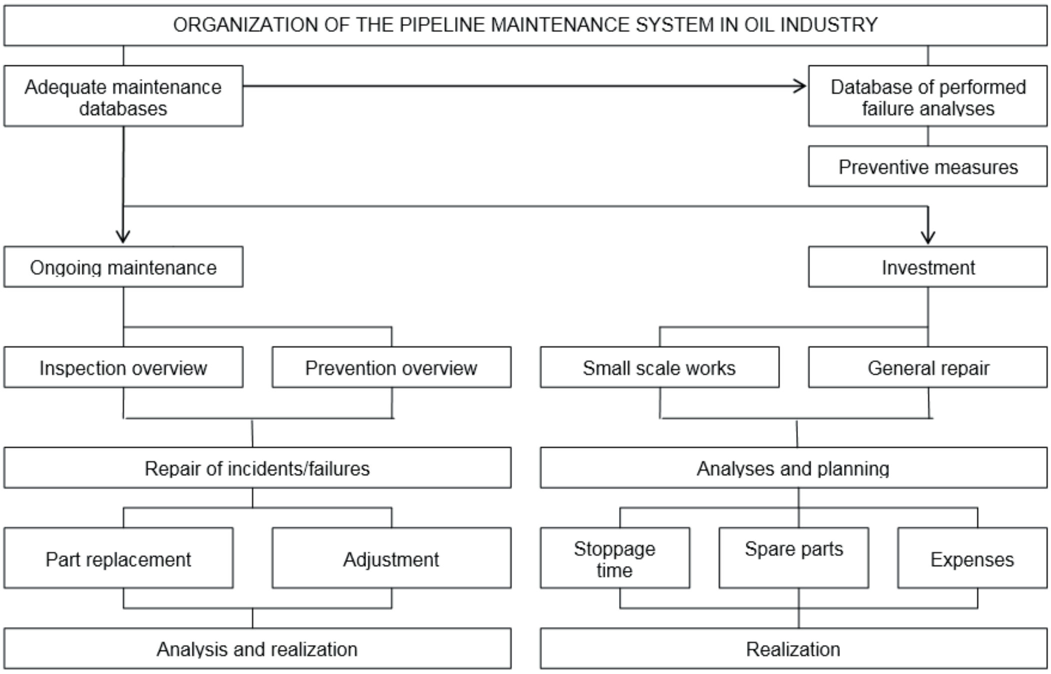

Figure 9 *Organizational model of the pipeline maintenance system in oil industry*

varying load conditions, for various operation regimes, dimensions of parts and bearing structure elements, shapes of welded joints, materials, processes and quality of production.

When the responsible parts and pipeline elements are concerned, a change of the load type, according to the exploitation conditions can lead to experimental determination of operational loads, as well as to change of the structural solution and determination of operating conditions and load regimes, which would secure the reliable operation for the specific technical solution.

Change of technology of the production process refers to alteration of shapes and dimensions of parts and elements of bearing structures, welding procedures, basic material and regimes of the heat treatment.

Alteration of inspection of the production quality refers to the more strict inspection and testing before and during the production, as well as after assembling.

Since all those measures for prevention of damage and failure represent the group of complex and expensive solutions, which are assumed to be able to enhance the security of responsible parts and pipeline elements, many eminent institutions all over the world have undertaken the comprehensive experimental research in order to develop techniques for simpler and cheaper improvement of the static and fatigue properties of parts and pipeline elements in the oil industry.

Improved techniques that were thus achieved are not equally successful with various structural solutions, because their effects depends on the load type and regime, material properties and type of a structure that consists of welded elements. Therefore, recommendations referring to application of certain methods primarily depend on possibility of a structure building and designer`s experience.

Organization of a maintenance system, regarding piping and transport pipelines, depends mostly on the shape and structure of tubing, exploitation conditions, number of employees, experience of experts and adequate databases regarding maintenance and inspection of pipelines in oil industry.

Based on realized researches and experience based data regarding the pipeline maintenance system in oil industry, an organizational model of the pipeline maintenance system in oil industry is proposed, shown in Figure 9.

6 Conclusions

Presented results and realized research offer big possibilities regarding behavior analyses of welded pipes and pipelines in oil industry. That was done to determine changes in mechanical properties of materials and welded joints of oil and gas well piping and transport pipelines, in conditions when many of the influential parameters are varying. This presents an attempt to design safer structures and/or to reduce certain undesirable effects to bearable values, i.e. in other words to design a satisfying solution regarding the well structures and transport pipelines as a whole.

Quick and reliable solution of problems, regarding responsible parts and structure elements, is achievable only with help of adequate databases. Additional software packages can enable the more efficient use of those databases, as well as analyses of certain influential factors, improvement techniques, possibilities for failure prevention and alternative solutions in all the phases of designing and development of the well structures and transport pipelines in the oil industry.

Note: *The shorter version of this research was presented at 24th International Seminar "SEMDOK 2019", reference [25].*

Acknowledgement

This research was partially financially supported by project of Operational Program Research and Innovation: "Research and development activities of the University of Zilina in the Industry of 21st century in the field of materials and nanotechnologies", No. 313011T426, co-funded by the European Regional Development Fund and by the Ministry of Education, Science and Technological Development of Republic of Serbia through grant TR35002.

References

[1] SARKOCEVIC, Z. *Resistance to damage and failure of protective welded pipes in oil wells*. PhD Dissertation. Belgrade: University of Belgrade, 2008.

[2] API 5CT American Petroleum Institute. *Specification for Casing and Tubing.*

[3] JONSTA, P., JONSTA, Z., VLCKOVA, I., SOJKA, J. Influence of physical-metallurgical factors on resistance of API carbon steels to sulphide stress cracking. *Communications - Scientific letters of University of Zilina* [online]. 2018, **20**(4), p. 41-46. ISSN 1335-4205, eISSN 2585-7878. Available from: http://komunikacie.uniza.sk/index.php/communications/article/view/638

[4] ZHU, X., LIU, B. The reliability-based evaluation of casing collapsing strength and its application in marine gas reservoirs. *Engineering Failure Analysis* [online]. 2018, **85**, p. 1-13. ISSN 1350-6307. Available from: https://doi.org/10.1016/j.engfailanal.2017.12.005

[5] SARKOCEVIC, Z., ARSIC, M., RAKIN, M., SEDMAK, A. Fabrication of high strength seam welded steel pipes and quality indicator testing. *Structural Integrity and Life* [online]. 2008, **8**(2), p. 81-98. ISSN 1451-3749, eISSN 1820-7863. Available from: http://divk.inovacionicentar.rs/ivk/ivk08/ivk0802-1.html

[6] SARKOCEVIC, Z., ARSIC, M., MLADENOVIC, M., RAKIN. M., RADAKOVIC, Z. Influence of production defects and pipe damage on oil well reliability and the environment. The 3rd International Scientific Expert Meeting GNP 2010: Civil Engineering - Science and Practice: proceedings. 2010. p. 1337-1342.

[7] MEDJO, B., RAKIN, M., GUBELJAK, N., MATVIENKO, Y., ARSIC, M., SARKOCEVIC, Z., SEDMAK, A. Failure resistance of drilling rig casing pipes with an axial crack. *Engineering Failure Analysis* [online]. 2015, **58**, p. 429-440. ISSN 1350-6307. Available from: https://doi.org/10.1016/j.engfailanal.2015.05.015

[8] AMARA, M., BOULEDROUA, O., MELIANI, M. H., MUTHANNA, B. G. N., ABBES, M. T., PLUVINAGE, G. Assessment of pipe for CO_2 transportation using a constraint modified CTOD failure assessment diagram. *Structural Integrity and Life* [online]. 2018, **18**(2), p. 149-153. ISSN 1451-3749, eISSN 1820-7863. Available from: http://divk.inovacionicentar.rs/ivk/ivk18/ivk1802-9.html

[9] MILOVANOVIC, A., SEDMAK, A. Integrity assessment of turbine flat cover pipe. *Structural Integrity and Life* [online]. 2018, **18**(3), p. 181-183. ISSN 1451-3749, eISSN 1820-7863. Available from: http://divk.inovacionicentar.rs/ivk/ivk18/ivk1803-4.html

[10] SHABANI, H., GOUDARZI, N., SHABANI, M. Failure analysis of a natural gas pipeline. *Engineering Failure Analysis* [online]. 2018, **84**, p. 167-184. ISSN 1350-6307. Available from: https://doi.org/10.1016/j.engfailanal.2017.11.003

[11] RYAKHOVSKIKH, V., BOGDANOV, R. I., IGNATENKO, V. E. Intergranular stress corrosion cracking of steel gas pipelines in weak alkaline soil electrolytes. *Engineering Failure Analysis* [online]. 2018, **94**, p. 87-95. ISSN 1350-6307. Available from: https://doi.org/10.1016/j.engfailanal.2018.07.036

[12] ASME B31G, American Society of Mechanical Engineers. *Manual for determining the remaining strength of corroded pipelines*. New York, 1991.

[13] SARKOCEVIC, Z., ARSIC, M., MEDJO, B., KOZAK, D., RAKIN, M,, BURZIC, Z., SEDMAK, A. Damage level estimate of API J55 steel for welded seam casing pipes. *Strojarstvo*. 2009, **51**(4), p. 303-311. ISSN 0562-1887.

[14] JONSTA, P., VLCKOVA, I., JONSTA, Z., TOMASEK, V., FENCLOVA T. Resistance of high strength steel to stress corrosion cracking depending on external environment pH factor. *Communications - Scientific letters of University of Zilina* [online]. 2018, **20**(3), p. 19-23. ISSN 1335-4205, eISSN 2585-7878. Available from: http://komunikacie.uniza.sk/index.php/communications/article/view/247

[15] MILOVANOVIC, N., DJORDJEVIC, B., TATIC, U., SEDMAK, S., STRBACKI, S. Low-temperature corrosion damage and repair of boiler bottom panel tubes. *Structural Integrity and Life* [online]. 2017, **17**(2), p. 125-131. ISSN 1451-3749, eISSN 1820-7863. Available from: http://divk.inovacionicentar.rs/ivk/ivk17/ivk1702-6.html

[16] LAZIC, V., ARSIC, D., NIKOLIC, R., RAKIC, D., ALEKSANDROVIC, S., DJORDJEVIC, M., HADZIMA, B. Selection and analysis of material for boiler pipes in a steam plant. *Procedia Engineering* [online]. 2016, **149**, p. 216-223. eISSN 1877-7058. Available from: https://doi.org/10.1016/j.proeng.2016.06.659

[17] BEKETOV, S. B., KUNINA, P. S., BUNYAKIN, A. V., DUBOV V. V. Failure of industrial pipelines due to low-frequency vibrations. *Russian Journal of Nondestructive Testing* [online]. 2017, **53**(9), p. 669-676. ISSN 1061-8309, eISSN 1608-3385. Available from: https://doi.org/10.1134/S1061830917090030

[18] MANESKI, T., BAJIC, D., MOMCILOVIC, N., MILOSEVIC-MITIC, V., BALAC, M. Determination of internal pressure value causing pipe branch model to plastically deform. *FME Transactions* [online]. 2018, **46**(2), p. 218-223. ISSN 1451-2092, eISSN 2406-128X. Available from: https://doi.org/10.5937/fmet1802218M

[19] ARSIC. M., SARKOCEVIC, Z., RAKIN, M., MLADENOVIC, M., VELJOVIC, A., ANDJELKOVIC, Z. Failure analysis of welded pipes in oil industry. *Energy, Economy, Ecology*. 2010, **12**(3), p. 121-130. ISSN 2363-7692, eISSN 2363-8338.

[20] XIE, M., TIAN, Z. A review on pipeline integrity management utilizing in-line inspection data. *Engineering Failure Analysis* [online]. 2018, **92**, p. 222-239. ISSN 1350-6307. Available from: https://doi.org/10.1016/j.engfailanal.2018.05.010

[21] SEVERIANO, J. A., SILVA, A. S., SUSSUSHI, E. M., SANT'ANNA, M. V. S., CUNHA, M. A., BERGMANN, C. P., GRIZA, S. Corrosion damages of flow regulation valves for water injection in oil fields. *Engineering Failure Analysis* [online]. 2019, **96**, p. 362-373. ISSN 1350-6307. Available from: https://doi.org/10.1016/j.engfailanal.2018.11.002

[22] BOULEDROUA, O., ZELMATI, D., HASSANI, M. Inspections, statistical and reliability assessment study of corroded pipeline. *Engineering Failure Analysis* [online]. 2019, **100**, p. 1-10. ISSN 1350-6307. Available from: https://doi.org/10.1016/j.engfailanal.2019.02.012

[23] PILIC, V., MIHAJLOVIC, V., STANOJEVIC, P., ANDJELKOVIC, A, BALOS, D. Application of innovative risk assessment methodology for damage mechanisms identification on part of amine regeneration unit. *Structural Integrity and Life* [online]. 2019, **19**(1), p. 29-35. ISSN 1451-3749, eISSN 1820-7863. Available from: http://divk.inovacionicentar.rs/ivk/ivk19/ivk1901-6.html

[24] PLUVINAGE, G., CAPELLE, J., HADJ MELIANI, M., Pipe networks transporting hydrogen pure or blended with natural gas, design and maintenance. *Engineering Failure Analysis* [online]. 2019, **106**, in press. ISSN 1350-6307. Available from: https://doi.org/10.1016/j.engfailanal.2019.104164

[25] ARSIC, D., NIKOLIC, R., ARSIC, A., SARKOCEVIC, Z., CVETKOVIC, D. Failure prevention and service life extension of welded pipes in oil industry. Invited paper. 24th International Seminar SEMDOK 2019: proceedings. 2019. ISBN 978-80-554-1214-6, p. 7-12.

https://doi.org/10.26552/com.C.2020.1.71-76

Miroslav Kohan - Miroslava Spronglova - Nadezda Visnovcova - Jakub Misek - Gabriela Spanikova
Viera Jakusova - Jan Jakus

MONITORING OF DATA TRANSMISSION AND CHANGES IN VALUES OF ELECTROMAGNETIC FIELD IN LIVING ENVIRONMENT

A crucial aspect concerning the intelligent transport systems is data transmission between vehicle and central control and information systems. Transportation needs a reliable system of data transfer based on GSM or WiFi networks. However, these networks employ a wide range of different frequencies which can be harmful to the health of drivers. The detrimental effect of electromagnetic radiation can negatively affect the process of transportation. This study determines the intensity of electric field levels (E) of the radiofrequency electromagnetic field (RF EMF) during the data transmission through the 3G, 4G and local WiFi networks, comparing them with the limit values. Conclusions: Our results showed a significantly higher level of the E-field intensity during 4G transmission in all places. The limit values were not exceeded. The lowest E-field values were found in local WiFi network.

Keywords: *intelligent transport systems, data transfer, exposure to electromagnetic field, electric intensity, mobile phone, transmission networks*

1 Introduction

Intelligent transportation needs reliable data transfer between vehicle and control headquarters. Data transfer is based on GSM or WiFi networks. However, these communication networks employ a variety of different frequencies which can have an adverse effect on biological systems including humans. The detrimental effect of electromagnetic radiation can negatively affect driver and persons inside the vehicle, and thus may result in serious problems of transporation.

The history of wireless communication started with the 1st generation (1G) of the mobile network system. The principle was based on analogue transmission of information. 1G network had used frequencies of 450 MHz and 900 MHz. The successor of 1G network, also called the Global System for Mobile Communication (GSM), was the 2nd generation (2G) mobile system. The system had used a cellular principle for signal transmission, which divided the geographic territory into the same large parts (cells). Another system was the 3rd generation (3G) mobile network also called Universal Mobile Telecommunication System (UMTS). The 3G system has enhanced the data transmission. The UMTS system used a frequency range of 2100 MHz. The 4th generation (4G) was designed for broadband internet access, in the Europe known as the Long Term Evolution system (LTE). It operated at 800, 900, 1800 and 2600 MHz. However, Wireless Local Area Network (WLAN, known as WiFi) operating at 2400 MHz is also very common for data transfer and local internet coverage. It allows users to have a wireless connection within the local area (among buildings, business center, etc.) [1-4].

During the last 20 years the exposure by mobile phones and WiFi routers has rapidly increased. People are exposed to EMF mainly by microwave operating devices and other electronic devices that emit the pulse modulated, high or low frequency EMF [5-6], what seems to be similar problem both at home (a living environment) and work (a working environment). Hence, the exposure of humans to radiofrequency (RF) EMF has always been one of the major topics at the Meetings of the World Health Organization (WHO) [7] and the International Commission on Non-Ionizing Radiation Protection (ICNIRP) [8]. Over the past two decades, worldwide sale of mobile phones has extremely raised up reaching now more than 7.3 billion. In many countries (such as Belgium, Great Britain, Russia, Japan etc.) the number of mobile phones is even higher than the total number of population [9-10]. Thus, the potential detrimental effects of RF EMF are in the interest of both the professionals and also general public. There are many studies referring to the adverse effects of the RF EMF generated by mobile phones on human health [11-16]. WHO has stated that the exposure to RF fields transmitted by mobile phones seems to be now generally higher than from BTSs [17]. Also “urbanicity” seems to be an important determinant of total exposure. Thus, people living in the urban environments have higher RF EMF exposure comparing to those living in the rural environment [18].

Miroslav Kohan[1,*], Miroslava Spronglova[2], Nadezda Visnovcova[1], Jakub Misek[1], Gabriela Spanikova[3], Viera Jakusova[4], Jan Jakus[1]
[1]Department of Medical Biophysics, Jessenius Faculty of Medicine in Martin, Comenius University in Bratislava, Slovakia
[2]Department of Biomedical Engineering, Faculty of Electrical Engineering, University of Zilina, Slovakia
[3]Clinic of Pediatric Surgery, Jessenius Faculty of Medicine in Martin, Comenius University in Bratislava, Slovakia
[4]Department of Public Health, Jessenius Faculty of Medicine in Martin, Comenius University in Bratislava, Slovakia
*E-mail of corresponding author: miroslav.kohan@gmail.com

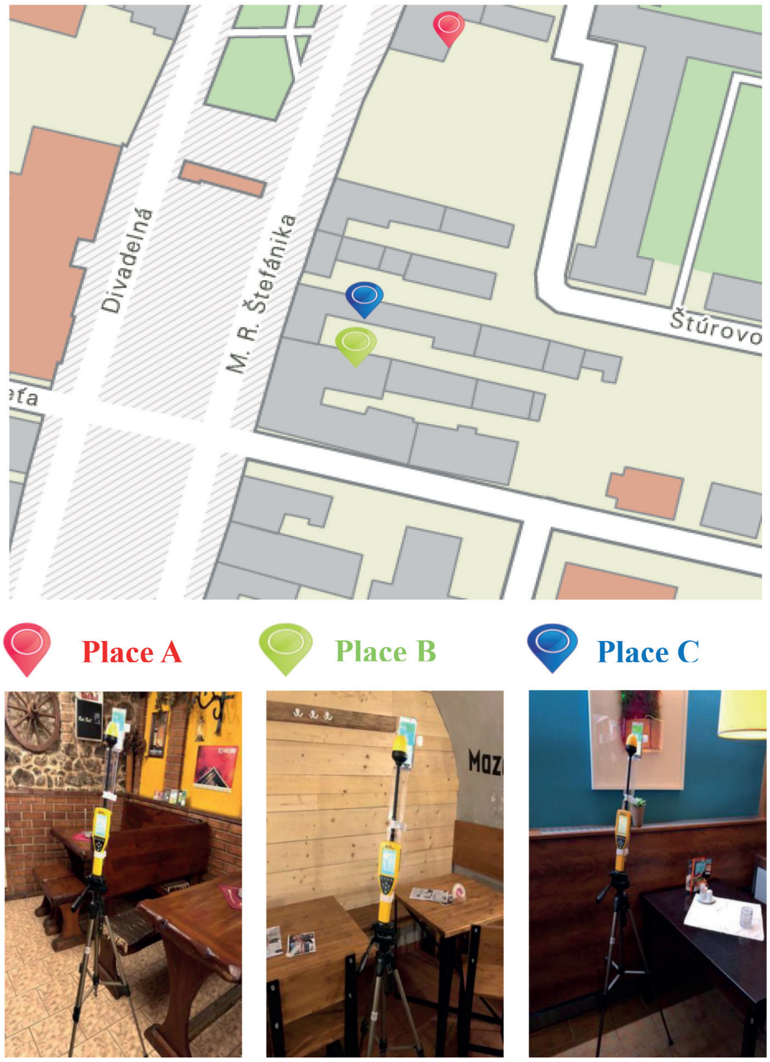

Figure 1 *Arrangement of measurement at three places (A, B, C) in city of Martin (see text for detail)*

The aim of this study is to determine the changes in E of RF EMF during data transmission through 3G, 4G and local WiFi networks at different areas of the living environment.

2 Methods

The E intensity of EMF emitted by mobile phones was monitored during the data transfer at three different areas in the city of Martin, Slovakia. All measured places were situated at the basement of the buildings near the city center (either in the restaurant or bar; Figure 1). However, each place was covered by the 3G and 4G signal at least for 75%, measured by the mobile phone itself. The local WiFi was also available at each place. The measurements were conducted always during the afternoon between 3:00-6:00 PM, from Monday to Friday. The E of EMF was measured by the broadband EMF meter Narda NBM 550 which enabled to measure E-field within the frequency range from 100 kHz to 3 GHz. Two mobile phones were utilized for the measurements, the Samsung Galaxy 5 as a measured phone and the iPhone 6 as a calling (broadcasting) phone. Both enabled selection between 3G, 4G or WiFi networks for data transmission. The Narda 550 was fixed on a tripod together with the measuring Galaxy 5 phone (Figure 1) by the custom made plastic holder. The distance between the measuring mobile phone and EMF meter was 0.2 cm. This mobile phone was attached at the height of 140 cm, what corresponds to a person sitting on a chair. In addition, the background E of EMF was measured at each of the measured place. The arrangement of the trial and measured places are shown in Figure 1.

Before the measurement, the broadband EMF meter Narda NBM 550 was self-calibrated. The measured mobile phone (Samsung Galaxy 5) was set up before each measurement, as follows:

- WCDMA (Wide Band Code Division Multiple Accers) - the standard for the 3G network
- LTE (Long Term Evolution) - the standard for the 4G network
- WiFi - connected to a local Wifi network

Table 1 *Mean values (x±SD) for E of EMP (in V/m) for data transfer through 3G, 4G and WiFi networks at three places (A, B, C). *** = p<0.001, ** = p<0.01, * = p<0.05 (comparison between WiFi and data 3G, 4G is given above numbers, between data 3G and 4G below numbers at all places the background E was significantly (p<0.001) lower compared to data 3G, 4G and WiFi)*

	Place A x ± SD [V/m]	Place B x ± SD [V/m]	Place C x ± SD [V/m]
Data 3G	8.84 ± 0.79 ** (n=10)	11.21 ± 1.16 * (n=10)	5.69 ± 0.72 (n=10)
Data 4G	21.06 ± 1.59 *** *** (n=10)	20.96 ± 3.05 *** ** (n=10)	11.85 ± 2.07 * ** (n=10)
WiFi	4.03 ± 0.29 (n=10)	4.23 ± 0.41 (n=10)	3.7 ± 0.57 (n=10)
Backg.	0.35 ± 0.24 (n=5) ***	0.93 ± 0.47 (n=5)***	0.26 ± 0.17 (n=5)***

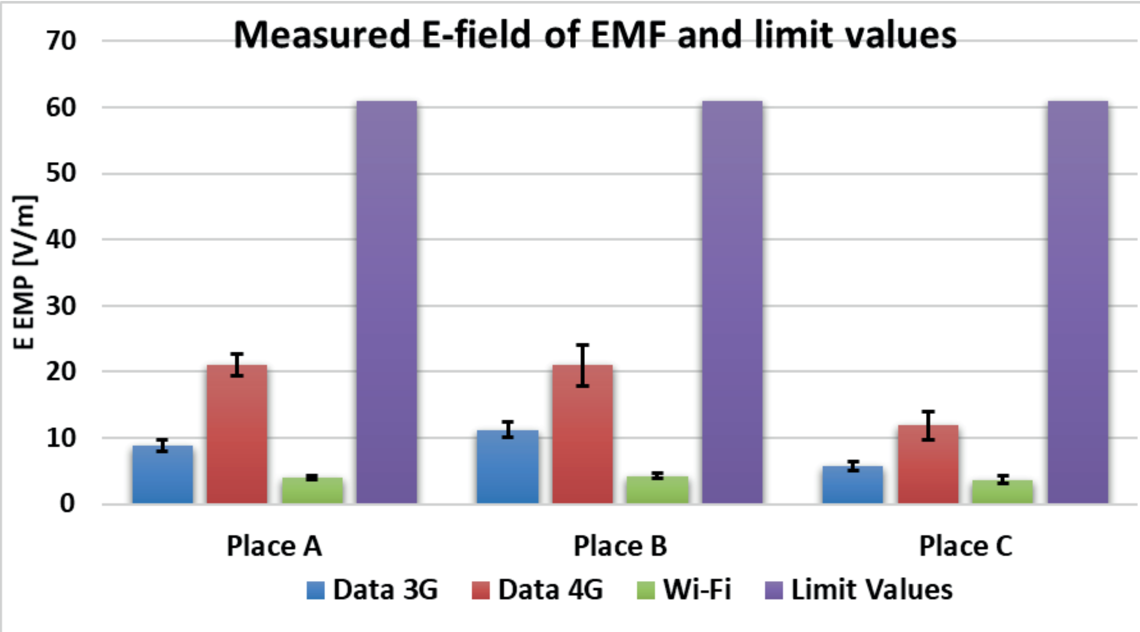

Figure 2 *Graphical representation of the mean values of E EMF for tested networks (Data 3G, Data 4G, WiFi) taken at places A, B, C, and the limit values (Limit Values) given by the Decree of Ministry of Health No. 534/2007 C*

The application *Messenger* was utilized for data transmission. It is a software application for cell phones widely used for calling or a video chat. In our study, this application was used to make a call between the cell phones. During the data transmission, the calling phone was distant enoughfrom the measuring phone not to disturb the transmission. The measurement started after the call was answered. The total number of the measurements was 105 of which ten measurements were performed for each place and standard and 5 for background. One measurement lasted 6 minutes and the limit value according to the ICNIRP recommendations was set to 61V/m.

For statistical evaluation Microsoft Office Excel and GraphPad InStat 3 was used. These programs allowed to compare the values obtained under three different tested conditions. Data are expressed as mean and standard deviation (x±SD). T-test and ANOVA were used to compare the data between the measured networks.

3 Results

The results showed the significant differences between the local WiFi network and the 3G network at the place A (p<0.01) and B (p<0.05), but not at the place C (Table 1). The significant differences were also found between the local WiFi network and the 4G network at places A (p<0.001), B (p<0.001), and C (p<0.05). Significant differences between the 3G and the 4G were identified at place A (p<0.001), B (p<0.01) and C (p<0.01). The background values of E EMF were significantly ($p<0.001$) lower at all measured places compared to the values of active data.

As stated before, the limit value for each measured frequency range was 61 V/m. According to the results, the limit values have not been exceeded at any place (Figure 2).

4 Discussion

In this study we evaluated E-field intensity of the EMF during the data transmission through the 3G, 4G and local WiFi networks at selected places of the living environment in the city of Martin. Our results showed that the highest values of E EMF were revealed during the data transmission using the 4G network at all measured places. The 4G values were approximately twice as much compared to the 3G and 4 to 5 times higher compared to WiFi. The lowest values were measured during the local WiFi network transmission at the same places. It is interesting, that at the place with minimal background (Place C), the 3G, 4G and WiFi values were also the lowest.

For voice and data transmissions the 3G uses frequency range 2100 MHz and the 4G mobile network 2600 MHz or 800 MHz [19-20]. The upcoming network of the fifth-generation (5G), nowadays intended solely for the data transmission, employs the frequency range around 26 GHz (in Europe) [20]. At this frequency, the wavelength of the EMF wave is approx.1mm representing extremely short waves. The ability of such short waves to cause different types of the resonance effects (frequency windows [21]) is higher for inhomogeneous biological tissues as the human body is. Belyaev [21] proposed that 2G users during the talk are exposed to microwave radiation at several frequency bands. The base transceiver station (BTS) can change the transmission frequency even during the talk by frequency hopping. The 2G uses Gaussian Minimum Shift Keying modulation but the 3G employs Quadrature Phase Shift Keying modulation what may explain its higher biological effect. [22] Parameters such as frequency and signal modulation can also significantly affect biological effects caused by mobile phones. It is most likely that an excessive exposure to mobile devices working at 4G or 5G networks becomes more dangerous for the biological system.

Study group Misek et al. [23] described the measurement of RF EMF in the living environment. They found that, the distribution of E EMF in the city center was 0.16±0.02 V/m for 3G, 0.048±0.005 V/m for 4G and $9.81 \pm 3.66 * 10^{-3}$ V/m for WiFi. Similar results were revealed by the Hardell group [24], where six places in Stockholm Old Town were investigated for the distribution of 3G, 4G and WiFi networks. However, our results of the background E EMF in the city center was higher in all measured environments even measured in the basements of the buildings. The difference could be given by a different distance from BTS and WiFi transmitters as well as their number resulting in different signal coverage.

In the earlier study of our experimental group [25], the E of EMF produced by mobile phones was measured at the working environment in the grammar school. These results are in line with the data presented in this study in active mode of the phone (calling, data transmission, messages) and also for the background measurements. However, comparing to our results, we utilized one cell phone only where Spiguthova et al. used several phones in a time with higher distance from the meter.

Paljanos et al. [26] assessed the exposure of mobile phone using 3G and 4G networks. In this study, they compare near-field radiated power levels from mobile phone for various data and voice application services. General observations have shown that the higher 3G values barely reached the 4G highest measured values. The mobile application “Messenger” did not show higher EMF exposure comparing to the “WhatApp” mobile application. They revealed approximately 2.5 fold higher levels for 4G network rather than 3G network. These results are consistent with our results since we observed 2.38 fold higher E-field for the 4G compared to the 3G network.

The study presented by Khalid et al. [27] investigated WiFi exposure at schools. They surveyed EMF exposure in the form of WiFi signal from WiFi devices at 0.5m distance. They found, that the E EMF from the WiFi device is influenced by the WiFi signal. This study showed lower measured values than our study. However, they placed measuring device 0.5m away from the WiFi source, comparing to our study where the broadband meter was placed 0.2cm from the WiFi source represented by the mobile phone.

It appears that the limit values for EMF radiation are currently insufficient and outdated, hence they were defined in 1998. For the frequency range from 2GHz to 300 GHz, the constant limit of 61 V/m applies, which is no longer an adequate value. Based on the results of the studies, consideration should be given to reassessing and possibly changing of the existing limit values in relation to a current EMF sources, as well as in relation to proposal of the 5G networks.

The E of RF EMF emitted from the mobile devices is influenced by several parameters such as its frequency, character of an environment (shielded or unshielded), SAR value of mobile phone, a distance from the source, modulation, polarization, etc. Nowadays the most of the mobile providers do not admit the possible hazard and serious side effects of the RF EMF on the human and the animal bodies from the cellular phones and the BTSs. Providers are trying to speed up the data transfer selecting between the 3G, 4G and 5G networks trying to increase the frequency and decrease the E of EMF and the SAR. Thus, the emitted spectrum contains additional frequencies which may oscillate DNA in living cells and thus affect the genetic material of the cells [28].

Therefore, we consider as important to continue with studies of the RF EMF transmissions through the 3G, 4G, the local Wifi networks and the future 5G in the living and the working environments. Proper analyses of detrimental effects of the mobile networks on the human body are necessary.

5 Conclusion

Our measurements showed a higher level of the E of EMF generated by a mobile phone during data transmission at the 4G and 3G networks compared to a local WiFi network at the underground places. Results proved that safer way of the data transmission is to use the WiFi network. However, the limit values listed in the Decree of the Ministry of Health of the Slovak Republic were not exceeded during the transmission for any of the measured standards.

Acknowledgment

This study was supported by the Slovak Research and Development Agency under the project APVV-0189- 11 (prof. Jakus).

Reference

[1] Electromagnetic fields report, Special Eurobarometer 347/Wave 73.3 - ZNS Opinion and Social - European Commission [online]. [Viewed 2019-01-18]. Available from: http://ec.europa.eu/commfrontoffice/publicopinion/archives/ebs/ebs_347_en.pdf

[2] AZIRA, E., ZOBIDACH, O. S. An acceptance of 4G (fourth generation) mobile network in Malaysia. *International Journal of Information and Communication Technology Research* [online]. 2013, **3**(8), p. 232-237. ISSN 2223-4985. Available from: https://www.academia.edu/37207597/AN_ACCEPTANCE_OF_4G_FOURTH_GENERATION_MOBILE_NETWORK_IN_MALAYSIA

[3] ANWAR, T. L., LI, L. W. Performance analysis of 3G communication network. *ITB Journal of Information and Communication Technology* [online]. 2008, **2**(2), p. 130-157. ISSN 2338-5499. Available from: http://journals.itb.ac.id/index.php/jictra/article/view/179

[4] SOOD, R., GARD, A. Digital society from 1G to 5G: a comparative study. *International Journal of Application or Innovation in Engineering & Management* [online]. 2014, **3**(2), p. 186-193. ISSN 2319-4847. Available from: https://pdfs.semanticscholar.org/9a4d/f06daea14e6521e24ee1fc3b949f257b7a0f.pdf

[5] BARABAS, J., RADIL, R., MALIKOVA, I. Modification of S. cerevisiae growth dynamics using low frequency electromagnetic fields in the 1-2 khz range. *BioMed Research International* [online]. 2015, 694713, p. 1-5. ISSN 2314-6133 , eISSN 2314-6141. Available from: http://dx.doi.org/10.1155/2015/694713

[6] BARABAS, J., RADIL, R., JANOUSEK, L. Role of magnetic flux density in LF EMF experiments targeting Ca2+, Na+ and K+ ions. 2018 EMF-Med 1st World Conference on Biomedical Applications of Electromagnetic Fields (EMF-Med) : proceedings. 2018. ISBN 978-953-290-078-8, p. 1-2.

[7] Electromagnetic fields and public heath Intermediate Frequencies (IF) - International EMF Project Information Sheet [online]. [Viewed 2018-12-10]. Available from: https://www.who.int/peh-emf/publications/facts/intermediatefrequencies_infosheet.pdf

[8] Statement on the "Guidelines for limiting exposure to time-varying electric, magnetic and electromagetic fields (up to 300 GHz)" - ICNIRP [online]. [Viewed 2018-10-12]. Available from: https://www.icnirp.org/cms/upload/publications/ICNIRPemfgdl.pdf

[9] ROSCH, P. J. *Bioelectromegnetic and subtle energy medicine*. 2 ed. NY: CRC Press, 2015. ISBN 978-1-14822-3319-3.

[10] Global ICT developments 2018 - ITU Statistics [online]. [Viewed 2018-12-12]. Available from: http://www.itu.int/en/ITU-D/Statistics/Pages/stat/default.aspx

[11] KIM, J. H., LEE, J.-K., KIM, H.-G., KIM, K.-B., KIM, H. R. Possible effects of radiofrequency electromagnetic field exposure on central nerve system. *Biomolecules and Therapeutics* [online]. 2019, **27**(3), p. 265-275. ISSN 1225-6110. Available from: https://doi.org/10.4062/biomolther.2018.152

[12] MORGAN, L. L., MILLER, A. B., SASCO, A., LEE DAVIS, D. Mobile phone radiation causes brain tumors and should be classified as a probable human carcinogen (2A). *International Journal of Oncology* [online]. 2015, **46**(5), p. 1865-1871. ISSN 1019-6439. Available from: https://doi.org/10.3892/ijo.2015.2908

[13] MAREGU, N. Long term exposure of mobile phone radiation and human health. *Journal of Information Engineering and Applications* [online]. 2016, **6**(8), p. 22-30. ISSN 2225-0506, eISSN 2225-0506. Available from: *https://iiste.org/Journals/index.php/JIEA/article/download/32277/33166*

[14] ABESHU, M. A., GELETA, B. Physical health hazards of mobile phone use. *Health Care: Current Reviews* [online]. 2015, **3**(2), p. 1-2. ISSN 2375-4273. Available from: http://dx.doi.org/10.4172/2375-4273.1000153

[15] WANG, D., LI, B., LIU, Y., MA, Y. F., CHEN, S. Q., SUN, H. J., DONG, J., MA, X. H., ZHOU, J., WANG, X. H. Impact of mobile phone radiation on the quality and DNA methylation of human sperm in vitro (in Chinese). *National Journal of Andrology* [online]. 2015, **21**(6), p. 515-520 ISSN 1009-3591. Available from: https://www.ncbi.nlm.nih.gov/pubmed/26242041

[16] KUCER, N., PAMUKCU, T., Self-reported symptoms associated with exposure to electromagnetic fields: a questionnaire study. *Electromagnetic Biology and Medicine* [online]. 2013, **33**(1), p. 15-17. ISSN 1236-8386. Available from: https://doi.org/10.3109/15368378.2013.783847

[17] What are the health risks associated with mobile phones and their base stations? - WHO [online]. [Viewed 2018-10-10]. Available from: https://www.who.int/features/qa/30/en/

[18] LINHARES, A., SOARES, A., TERADA, M. Determination of measurement points in urban environments for assessement of maximum exposure to EMF associated with a base station. *International Journal of Antennas and Propagation* [online]. 2014, 297082, p. 1-7. ISSN 1687-5869, eISSN 1687-5877. Available from: http://dx.doi.org/10.1155/2014/297082

[19] WIESER V. Mobilne radiove siete II. Adaptacia technickych a systemovych parametrov / Mobile radio networks II. Adaptation of technical and system parameters (in Slovak). Zilina: EDIS, 2004. ISBN 80-8070-345-0.

[20] Radio spectrum policy group strategic spectrum roadmap towards 5G for Europe, Second Opinion on 5G networks - European Commission [online]. [Viewed 2018-09-12]. Available from: https://circabc.europa.eu/sd/a/fe1a3338-b751-43e3-9ed8-a5632f051d1f/RSPG18-005final-2nd_opinion_on_5G.pdf

[21] BELYAEV I. Non-thermal biological effects of microwaves. *Microwaves Review* [online]. 2005, **11**(2), p. 13-29. ISSN 1450-5835. Available from: https://doi.org/10.1080/15368370500381844

[22] BELYAEV, I., DEAN, A., EGER, H., HUBMANN, G., JANDRISOVITS, R., KERN, M., KUNDI, M., MOSHAMMER, H., LERCHER, P., MULLER, K., OBERFELD, G., OHNSORGE, P., PELZMANN, P., SCHEINGRABER, C., THILL, R. European EMF guideline 2016 for the prevention, diagnosis and treatment of EMF - related health problems and illnesses. *Reviews on Environmental Health* [online]. 2016, **31**(3), p. 363-397. ISSN 2191-0308. Available from: https://doi.org/10.1515/reveh-2016-0011

[23] MISEK, J., LAUKOVA, T., KOHAN, M., VETERNIK, M., JAKUSOVA, V., JAKUS, J. Measurement of low-level radiofrequency electromagnetic fields in the human environment. *Acta Medica Martiniana* [online]. 2018, **18**(2), p. 27-33. ISSN 1335-8421. Available from: https://doi.org/10.2478/acm-2018-0010

[24] HARDELL, L., CARLBERG, M., KOPPEL, T., HEDENDAHL, L. High radiofrequency radiation at Stockholm Old Town: An exposimeter study including the Royal Caste, Supreme Court, three major squares and the Swedish Parliament. *Molecular and Clinical Oncology* [online]. 2017, **6**(4), p. 462-476. ISSN 2049-9469, eISSN 2049-9469. Available from: https://doi.org/10.3892/mco.2017.1180

[25] SPIGUTHOVA, D., HABINAKOVA, H., MISEK, J., JAKUSOVA, V., JAKUS, J. Meranie parametrov elektromagnetickych poli pri pouzivani prostriedkov mobilnej komunikacie v skolskom prostredi / Measurement of electromagnetic fields using mobile communication in school environment (in Slovak). *Lekar a technika* [online]. 2015, **45**(4), p. 122-128. ISSN 2336-5552, eISSN 2336-5552. Available from: https://ojs.cvut.cz/ojs/index.php/CTJ/article/view/4260

[26] PALJANOS, A., MICLAUS, S., BECHET, P., MUNTEANU, C. Assessment of mobile phone user exposure to UMTS and LTE signals: comparative near-field radiated power levels for various data and voice application services. *Journal of Electromagnetic Waves and Applications* [Online]. 2016, **30**(9), p. 1-15. ISSN 1569-3937. Available from: https://doi.org/10.1080/09205071.2016.1167634

[27] KHALID, M., MEE, T., PEYMAN, A., ADDISON, D., CALDERON, C., MASLANYJ, M., MANN, S. Exposure to radio frequency electromagnetic fields from wireless computer networks: duty factors of Wi-Fi devices operating in schools. *Progress in Biophysics and Molecular Biology* [online]. 2011, **107**(3), p. 412-420. ISSN 0079-6107, eISSN 1873-1732. Available from: https://doi.org/10.1016/j.pbiomolbio.2011.08.004

[28] MARKOV, M. *Mobile communications and public health.* NY: CRC Press, 2018. ISBN 978-0-203-70510-0.

Branislav Dobrucky - Slavomir Kascak - Michal Prazenica - Roman Konarik

BASIC COMPARISON AND EVALUATION OF FUNCTIONALITY AC-AC MATRIX CONVERTER CONCEPTS FOR HEV VEHICLE - PART I

The paper deals with the direct AC-AC propulsion system and compares two matrix converter concepts with five-phase traction induction motors (IM) for the hybrid electric vehicle (HEV) including electronic differential. The first one consists of [3x5] matrix converter and [3x1] active PWM rectifier (4Q-converter) for full power performance. The second one comprises one [3x5] matrix converter for full power and auxiliary [0x5] matrix converter for partial output power. Configurations of [3x5] + [0x5] MxC converters with five-phase motor(s) are not analyzed in available literature so far. The advantage of the proposed connection is in supposed higher efficiency of matrix converter then clasiccal VSI one. Part I deals with a theoretical study of converter concepts for hybrid electric vehicle. Based on simulation results the comparison and evaluation of the property and quality of the quantities of different type of the matrix powertrain are discussed in Part II.

Keywords: *AC/AC powertrain, 3x5 matrix converter, 0x5 matrix converter, five-phase induction motor, electric drive, 4QC converter, modeling and simulation, HEV vehicle*

1 Introduction

The mostly series HEV powertrains use front-end converter system with a DC-voltage interlink [1-5]. Since in-vehicle driving tests for evaluating performance and diagnostic functionalities of engine management systems are often time-consuming, expensive and not reproducible, simulation methods with HIL (hardware in the loop) or SIL (software in the loop) simulators allow to validate new hardware and software automotive solutions.

One of the important questions is the number of phases of the generator and/or traction motor, respectively. If the number of phases of the generator are smaller than three, so the power fluctuation in fictitious DC interlink is rather high [6-7]. Similarly, on the opposite, if the number of phases of the motor is just three (no more) then there is not possible to connect both traction motor to on one common direct traction converter [8-13], Figure 1.

Advantages and operation of a five-phase induction motor are described in [14], its operation under loss of one phase of a feeding source in [15].

Such a configuration of the AC/AC powertrain makes it possible both pure electric operating modes and/or pure engine mode, as well as hybrid mode: the vehicle is propelled by ICE engine and accu-battery energy in parallel operation [1].

Note, to provide of full autonomous HEV operation from accu-battery AB (i.e. traction one), the sizing of 4QC converter should be done for nominal traction power of two traction motors TM.

The mostly powertrains with matrix converters use [3x3] MxC with three-phase IM/SM motors [8, 16-17], except for the author works [6, 18-19] and partially [8]. It is assumed that total efficiency will be higher as classical one because of higher efficiency of MxC then VSI [11], and nearly the same efficiency of [3x3] and [3x5] MxCs [8, 19]. The [0x5] MxC (with partially power) is supposed for parallel operation only, so, the total operational efficiency should be higher.

2 Direct AC-AC matrix converter powertrain without 4QC

The configuration of novel simplified AC/AC powertrain shown in Figure 2 can be applied for following possible operation modes [6, 18]:

a. traction drive/brake from/to ICE engine: ICE->>SG->>MxC->>5PIM or, respectively 5PIM->>MxC->>SG->>ICE
b. traction drive/brake/charging from/to accu-battery: AB->>MxC->>5PIM or, respectively 5PIM->>MxC->>AB
c. starting-up of the engine/charging of the accu-battery: AB->>MxC->>SG->>ICE or, respectively ICE->>SG->>MxC->>AB.

In above modes are followed:

- ICE - internal combustion engine
- SG - synchronouos generator
- MxC - direct matrix converter(s)
- 5PIM - five-phase induction motor(s)
- AB - accu-battery(-ies).

Branislav Dobrucky*, Slavomir Kascak, Michal Prazenica, Roman Konarik
Department of Mechatronics and Electronics, Faculty of Electrical Engineering and Information Technology, University of Zilina, Slovakia
*E-mail of corresponding author: branislav.dobrucky@fel.uniza.sk

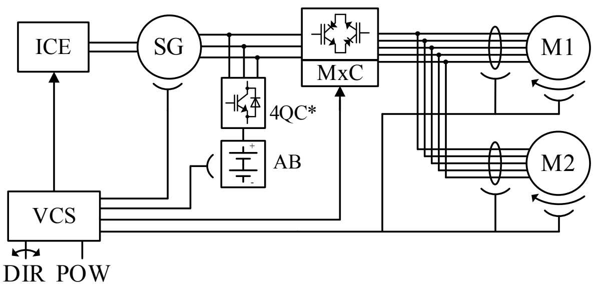

Figure 1 *Direct AC-AC propulsion system with one [3x5] matrix converter and parallel connected two five-phase IM traction motors [6]*

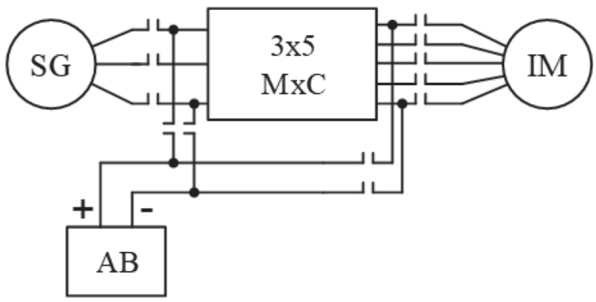

Figure 3 *Connection for autonomous modes of HEV*

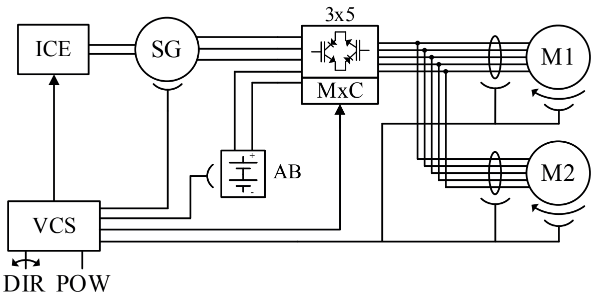

Figure 2 *Novel enhanced AC/AC series/parallel HEV with one MxC converter and two traction motors with independent control*

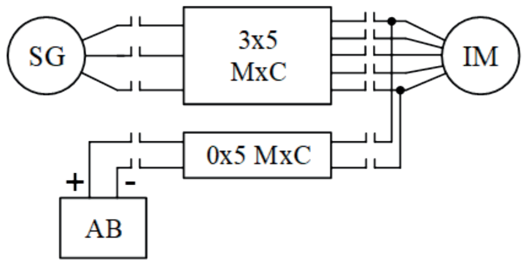

Figure 4 *Hybrid parallel operation of HEV of ICE and AB using 0x5 MxC converter*

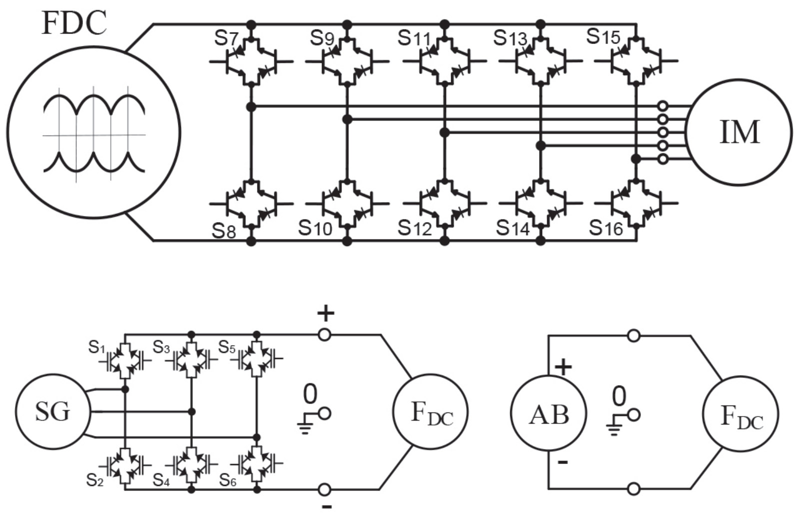

a) *b)*

Figure 5 *Structural schemes of MxC converter with indirect control (FDC - is fictitious DC interlink with a) three-phase rectified voltage or with b) DC voltage) without filter and protection circuitry*

Since the 4QC converter is omitted, the novel scheme of HEV powertrain, Figure 2 makes it possible the parallel operation of ICE and AB using 0x5 MxC converters. It gives a sophisticated solution making possible as parallel as the autonomous operation of ICE and AB.

Since it deals with parallel operation, such an HEV is series and parallel vehicle. The sizing of paralleling converter (4QC or 0x5 MxC) is then done just for the different power of traction motors and ICE, Figure 4. Practically, the parallel mode is using during the accelerating and ICE start-up/AB charging regime only.

Structural schemes of AC/AC matrix converters (3x5 MxC, 0x5 MxC) are classical circuitry with three-phase input and five-phase output (3x5 MxC) or DC input and five-phase output (0x5 MxC), respectively. The structural schemes of MxC converter with indirect control [9, 16-19] used for simulation are shown in Figure 5.

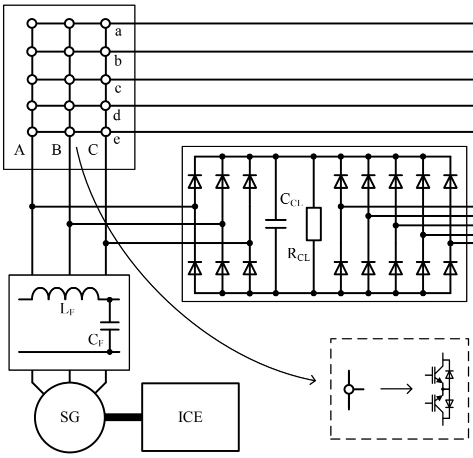

Figure 6 *Schematics of MxC propulsion drive with floating clamping protection and input filter*

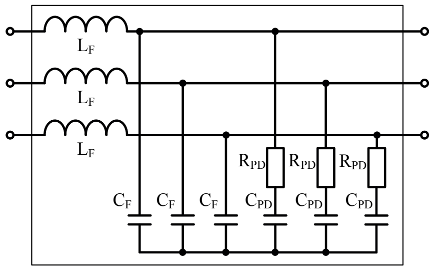

Figure 7 *Schematics of the input filter for MxC converter in detail*

Modeling indirect control we get:

$$[\boldsymbol{u}_{out}] = \boldsymbol{T} * [u_{in}] = \boldsymbol{I} * \boldsymbol{R} * [\boldsymbol{u}_{in}] \tag{1}$$

$$[\boldsymbol{i}_{in}] = \boldsymbol{T}^T * [\boldsymbol{i}_{out}], \tag{2}$$

where $\boldsymbol{T}$, $\boldsymbol{I}$, $\boldsymbol{R}$ are transfer matrix of matrix converter, fictitious inverter and rectifier, respectively

$$\boldsymbol{T} = \begin{bmatrix} S_{RA} & S_{SA} & S_{TA} \\ S_{RB} & S_{SB} & S_{TB} \\ S_{RC} & S_{SC} & S_{TC} \\ S_{RD} & S_{SD} & S_{TD} \\ S_{RE} & S_{SE} & S_{TE} \end{bmatrix} = \begin{bmatrix} S_7 & S_8 \\ S_9 & S_{10} \\ S_{11} & S_{12} \\ S_{13} & S_{14} \\ S_{15} & S_{16} \end{bmatrix} * \begin{bmatrix} S_1 & S_3 & S_5 \\ S_2 & S_4 & S_6 \end{bmatrix} \tag{3}$$

$$\begin{bmatrix} u_A(t) \\ u_B(t) \\ u_C(t) \\ u_D(t) \\ u_E(t) \end{bmatrix} = \begin{bmatrix} m_7(t) & m_8(t) \\ m_9(t) & m_{10}(t) \\ m_{11}(t) & m_{12}(t) \\ m_{13}(t) & m_{14}(t) \\ m_{15}(t) & m_{16}(t) \end{bmatrix} * \\ * \begin{bmatrix} m_1(t) & m_3(t) & m_5(t) \\ m_2(t) & m_4(t) & m_6(t) \end{bmatrix} * \begin{bmatrix} u_R(t) \\ u_S(t) \\ u_T(t) \end{bmatrix} = \\ = \boldsymbol{M}_I(t) * \boldsymbol{M}_R(t) * \begin{bmatrix} u_R(t) \\ u_S(t) \\ u_T(t) \end{bmatrix}, \tag{4}$$

where are modulating matrices with their elements

$$m_{oi}(t) = \frac{t_{oi}}{T_s}, \tag{5}$$

where t_{oi} for output indexes $o \in < A,B,C,D,E >$ and input indexes $i \in < R,S,T >$

$$[\boldsymbol{u}_{out}] = \begin{bmatrix} S_7 & S_8 \\ S_9 & S_{10} \\ S_{11} & S_{12} \\ S_{13} & S_{14} \\ S_{15} & S_{16} \end{bmatrix} * \begin{bmatrix} U_{DC+} \\ U_{DC-} \end{bmatrix} = \begin{bmatrix} U_{DC+} \\ U_{DC-} \end{bmatrix} = \\ = \begin{bmatrix} S_1 & S_3 & S_5 \\ S_2 & S_4 & S_6 \end{bmatrix} * [\boldsymbol{u}_{in}] \tag{6}$$

where U_{DC+} and U_{DC-} is equal $U_{DC}/2$ so, $U_{DC} = U_{DC+} - U_{DC-}$.

Using this approach a space vector PWM can be used for IM control.

3 Clamping protection and filtering circuits

Compulsory parts of the matrix converter mentioned rarely are protection and filtering circuits [5, 20]. Schematics of MxC propulsion drive with floating clamping protection and input filter is shown in Figure 6.

3.1 Designing input LC filter and clamping protection unit

The input filter is very important for MxC especially in the case of the non-harmonic input currents of MxC will be loaded with the synchronous generator by additional distortion power. Design of LC filter should be considered basically from the next points of view [20-21]:

Filter operation at a basic mains frequency of the range 100 - 200 Hz (output frequency of the synchronous generator)

Filter combination behavior in the frequency domain (filter transfer function)

The resonant frequency should be in a range between ten times the line frequency and one-half of the switching frequency, to avoid resonance problems in the lower and upper parts of the harmonic spectrum

Passive damping must be sufficient to avoid oscillation, but losses cannot be so high as to reduce efficiency [5]

Regarding the clamping unit: In generally, energy accumulated in coils is given by their inductances and the appropriate currents flowing through them.

The design procedure for both LC filter (Figure 7) and clamping protection unit has been used by [20].

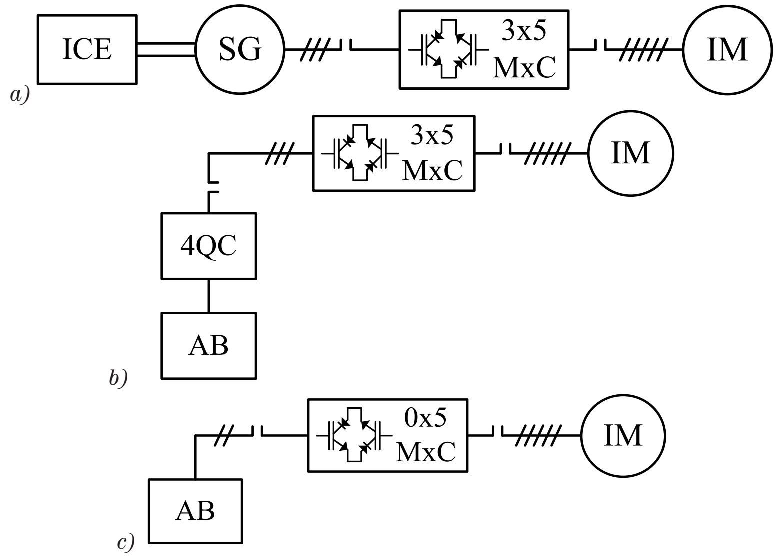

Figure 8 *Possible operational model of novel enhanced AC/AC powertrain*

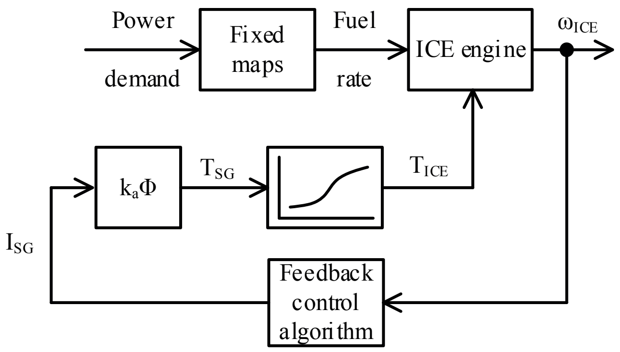

Figure 9 *Principle block diagram for ICE engine - PMSG generator control*

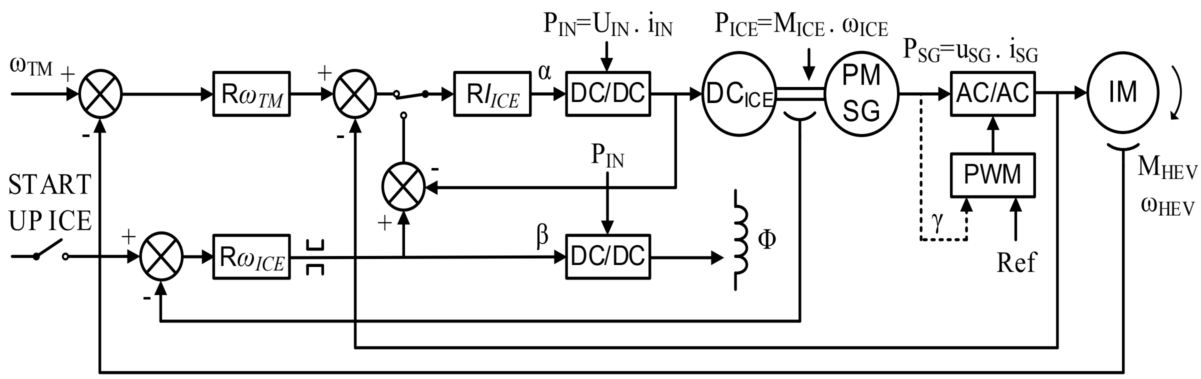

Figure 10 *Principle control diagram for ICE engine, PMSG generator, MxC converter and IMs*

Designing input LCL filter is needed for 4QC autonomous operation as charging of accu-battery by ICE/SG unit or at starting-up the ICE/SG using accu-battery. To design the filter, some limits on the parameter values should be introduced [22-23]

The capacitor value is limited by the decrease of the power factor at rated power (generally less than 5%). The power factor decrease can also be a function of the ac sensor position as discussed in [22].

The total value of inductance should be less than 0.1 p.u. to limit the ac voltage drop during operation. Otherwise, a higher dc-link voltage will be required to guarantee current controllability, which will result in higher switching losses.

To design the LCL input filter the design procedure using [23] can be used.

Table 1 *Parameters of the powertrain*

Item	Quantity	Value (dimension)
ICE engine (DC motor, separate exciting)	Output power	30 hp (22 kW)
	Armature voltage	500 V
	Nominal speed	3 000 rpm
	Field voltage	300 Vdc
3 phase PMSG generator	Power	11.5 hp (8.5 kW)
	Nominal torque	27 N.m
	Nominal speed	3 000 rpm
Fictive DC bus voltage	Nominal value	300 Vdc
5 Phase IM induction motor	Output power	7.5 kW
	Output voltage	150 Vrms
	Nominal torque	23 N.m
	Synchronous speed	3 000 rpm
AB accu-battery	Nominal voltage	300 V

Table 2 *Parameters of the input filter and floating protection*

Input LC filter	Floating protection
L_F=100 μH; C_F=28.2 μF; R_{PD}=0.94 Ω; C_{PD}=112.8 μF	C_{CL}=1 mH; R_{CL}=10 kΩ

4 Modeling and simulation

Possible operational modes of novel advanced AC/AC powertrain suitable for simulation are shown in Figure 8 a, b, c.

(a) traction drive/brake: ICE->>SG->>MxC->>5PIM or, respectively 5PIM->>MxC->>SG->>ICE,
(b) traction drive/brake/charging: AB->>4QC->>MxC->>5PIM or, respectively 5PIM->>MxC->>4QC->>AB,
(c) traction drive/brake/charging: AB->>MxC->>5PIM or, respectively 5PIM->>MxC->>AB

For simulation purpose, the ICE engine has been substituted by DC separately exciting motor. The main block diagram of a control strategy for ICE engine - SG generator assembly is shown in Figures 9 and 10 [18], created by [24-26].

Algorithm for ICE engine - generator assembly control consisting basically of three steps:

- start-up of ICE engine to reach the idle speed, then
- start-up of traction motor to demanded speed and continuously
- setting-up of the ICE engine to adequate speed and power.

Hybrid operational mode of HEV powering. Parallel operation of ICE engine and traction accu-battery AB is possible using the novel scheme of HEV powertrain, Figure 4 makes it using 0x5 MxC converters. It gives a sophisticated solution making possible as parallel as the autonomous operation of ICE and AB. The parameters of the powertrain are as follows given in Tables 1 and 2.

5 Conclusion

Basically, using of [3x5] matrix converter drive with 5-phase motors brings:

- higher efficiency against VSI front-end converter system
- the possibility of independent control of 5-phase motors which is not possible with 3-phase motors.
- battery autonomous traction and a braking regime where 4QC should be completed by [3x5] MxC since auxiliary [0x5] MxC should not be,
- also, charging mode from ICE/SG unit with 4QC needs either control by ICE engine or further DC/DC converter since auxiliary [0x5] MxC not need.

Total comparison and evaluation can be done until when all operation modes of both concepts (with 4QC and with [0x5] MxC) will be simulated and their result known. Both of those concepts make it possible to also combine (parallel) modes of the HEV powertrain.

The article continues in Part II (will be published in Communications - Scientific Letters of the University of Zilina No. 2/2020).

References

[1] EHSANI, M., GAO, Y., EMADI, A. *Modern electric, hybrid-and fuel cell vehicles*. Boca Raton, USA: CRC Press, 2010. ISBN 9781420053982.

[2] LIVINT, G. H., HORGA, V, RATOI, M., ALBU, M. *Control of hybrid electrical vehicles, electric vehicles - modelling and simulations*. InTech, 2011. ISBN 978-953-307-477-1.

[3] PEREZ-PINAL, F. J., CERVANTES, I., EMADI, A. Stability of an electric differential for traction applications. *IEEE Transactions on Vehicular Technology* [online]. 2009, **58**(7), p. 3224-3233. ISSN 0018-9545, eISSN 1939-9359. Available from: https://doi.org/10.1109/TVT.2009.2013473

[4] HARTANI, K., BOURAHLA, M., MILOUD, Y., SEKOUR, M. Electronic differential with direct torque fuzzy control for vehicle propulsion system. *Turkish Journal of Electrical Engineering Computer Sciences*. 2009, **17**(1), p. 21 -38. ISSN 1303-6203.

[5] WHEELER, P. W., CLARE, J.C., EMPRINGHAM, L. A Vector controlled MCT matrix converter induction motor drive with minimized commutation times and enhanced waveform quality. IEEE Industry Applications Conference : proceedings [online]. 2002. ISBN 0-7803-7420-7, ISSN 0197-2618, p. 466-472. Available from: https://doi.org/ 10.1109/IAS.2002.1044127

[6] DOBRUCKY, B., KASCAK, S., PRAZENICA, M., PAVLASEK, P. Direct AC-AC propulsion system using matrix converter and 5φ traction motor for HEV vehicle. *Communications - Scientific Letters of the University of Zilina* [online]. 2018, **20**(1), p. 4-12. ISSN 1335-4205, eISSN 2585-7878. Available from: http://komunikacie.uniza.sk/index.php/communications/article/view/36

[7] BEDNAR, B., DRABEK, P., PITTERMANN, M. Algorithm implementation of traction converter topology based on MFT and single-phase matrix converter. *Electrical Engineering-Archiv fur Elektrotechnik* [online]. 2017, **99**(4), p. 1305-1315. ISSN 0003-9039, eISSN 0948-7921. Available from: https://doi.org/10.1007/s00202-017-0619-y

[8] REZAOUI, M. M., KOUZOU, A., MAHMOUDI, M. O., NEZLI, L. Comparison performances between two matrix converters [3x3] and [3x5] supplying a multi-phases induction machine. *Journal of Electrical Engineering*. 2016, **16**(1), p. 217-227. ISSN 1582-4594.

[9] JONES, M., LEVI, E., VUKOSAVIC, S. N. Independent control of two five-phase induction machines connected in parallel to a single inverter supply. 32nd Annual Conference on IEEE Industrial Electronics IECON 2006 : proceedings [online]. IEEE, 2006. eISBN 978-1-5090-9155-3, ISSN 1553-572X, p. 1257-1262. Available from: https://doi.org/10.1109/IECON.2006.348152

[10] CHOMAT, M., SCHREIER, L., BENDL, L. Effect of stator winding configuration on operation of convertor fed five-phase induction machine. 18th International Conference on Electrical Drives and Power Electronics EDPE : proceedings [online]. IEEE, 2015. eISSN 1339-3944, p. 488-496. Available from: https://doi.org/10.1109/EDPE.2015.7325343

[11] BERNET, S., PONNALURI, S., TEICHMANN, R. Design and loss comparison of matrix converters, and voltage-source converters for modern AC drives. *IEEE Transactions on Industrial Electronics* [online]. 2002, **49**(2), p. 304-314. ISSN 0278-0046, eISSN 1557-9948. Available from: https://doi.org/10.1109/41.993263

[12] KIMURA, Y., HIZUME, M., MATSUSE, K. Independent vector control of two PM motors with five-leg inverter by the expanded two-arm modulation method. 2005 European Conference on Power Electronics and Applications : proceedings [online]. IEEE, 2005. ISBN 90-75815-09-3, p 1-7. Available from: https://doi.org/10.1109/EPE.2005.219400

[13] LIM, C. S., RAHIM, N. A., HEW, W. P., LEVI, E. Model predictive control of a two-motor drive with five-leg-inverter supply. *IEEE Transactions on Industrial Electronics* [online]. 2013, **60**(1), p. 54-65. ISSN 0278-0046, eISSN 1557-9948. Available from: https://doi.org/10.1109/TIE.2012.2186770

[14] ZASKALICKY, P. Mathematical model of a five-phase voltage-source PWM controlled inverter. *Electrical Engineering-Archiv fur Elektrotechnik* [online]. 2017, **99**(4), p. 1179-1184. ISSN 0003-9039, eISSN 0948-7921. Available from: https://doi.org/10.1007/s00202-017-0643-y

[15] SCHREIER, L., BENDL, J., CHOMAT, M. Operation of five-phase induction motor after loss of one phase of feeding source. *Electrical Engineering-Archiv fur Elektrotechnik* [online]. 2017, **99**(1), p. 9-18. ISSN 0003-9039, eISSN 0948-7921. Available from: https://doi.org/10.1007/s00202-016-0370-9

[16] ZHUANG, X. An indirect space-vector modulated three-phase AC-DC matrix converter for hybrid electric vehicles. *Energy Procedia* [online]. 2015, 75(4), p. 1968-1974. eISSN 1876-6102. Available from: https://doi.org/10.1016/j.egypro.2015.07.242

[17] BAK, Y., LEE, E., LEE, K.-B. Indirect matrix converter for hybrid electric vehicle application with three-phase and single-phase outputs. *Energies* [online]. 2015, **8**(5), p. 3849-3866. eISSN 1996-1073. Available from: https://doi.org/10.3390/en8053849

[18] DOBRUCKY, B., KASCAK, S., PRAZENICA, M., DRGONA, P., PAVLASEK, P. AC/AC powertrain control under different HEV supply network. 2018 ELEKTRO : proceedings [online]. IEEE, 2018. p. 2811-2823. Available from: https://doi.org/10.1109/ELEKTRO.2018.8398272

[19] DOBRUCKY, B., KASCAK, S., PRAZENICA, M., JARABICOVA, M. Improving efficiency of hybrid electric vehicle using matrix converters. *Elektronika ir Elektrotechnika* [online]. 2019, **25**(4), p. 29-35. ISSN 1392-1215, eISSN 2029-5731 Available from: https://doi.org/10.5755/j01.eie.25.4.23967
[20] BAUER, J., FLIGL, S., STEIMEL, A. Design and dimensioning of essential passive components for the matrix converter prototype. *Automatika* [online]. 2012, **53**(3), p. 225-235. ISSN 0005-1144, eISSN 1848-3380. Available from: https://doi.org/10.7305/automatika.53-3.134
[21] TRENTIN, A., ZANCHETTA, P., CLARE, J., WHEELER, P. Automated optimal design of input filters for direct AC/AC matrix converters. *IEEE Transactions on Industrial Electronics* [online]. 2012, **59**(7), p. 2811-2823. ISSN 0278-0046, eISSN 1557-9948. Available from: https://doi.org/10.1109/TIE.2011.2163283
[22] LINDGREN, M., SVENSSON, J. Control of a voltage-source converter connected to the grid through an LCL filter - application to active filtering. PESC 98 Record. 29th Annual IEEE Power Electronics Specialists Conference (Cat. No.98CH36196) : proceedings [online]. IEEE, 1998. ISBN 0-7803-4489-8, ISSN 0275-9306, p. 229-235. Available from: https://doi.org/10.1109/PESC.1998.701904
[23] LISERRE, M., BLAABJERG, F., HANSEN, S. Design and control of an LCL-filter-based three-phase active rectifier. *IEEE Transactions on Industry Applications* [online]. 2005, **41**(5), p. 1281-1291. ISSN 0093-9994, eISSN 1939-9367. Available from: https://doi.org/10.1109/TIA.2005.853373
[24] JUSSILA, M., TUUSA, H. Comparison of direct and indirect matrix converters in induction motor drive. 32nd Annual Conference of the IEEE Industrial Electronics Society IECON'06 „ proceedings [online]. IEEE, 2006. eISBN 978-1-5090-9155-3, ISSN 1553-572X, p. 1621-1626. Available from: https://doi.org/10.1109/IECON.2006.347423
[25] NOBILE, G., CACCIATO, M., SCARCELLA, G., SCELBA, G. Multi-criteria experimental comparison of batteries circuital models for automotive applications. *Communications - Scientific Letters of the University of Zilina* [online]. 2018, **20**(1), p. 97-104. ISSN 1335-4205, eISSN 2585-7878. Available from: http://komunikacie.uniza.sk/index.php/communications/article/view/54
[26] HUSAIN, I. *Electric and hybrid vehicles - design fundamentals*. 2. ed. CRC Press, 2011. ISBN 978143981175.

Natalia Davidich - Andrii Galkin - Vladimir Sabadash - Igor Chumachenko - Tatyana Melenchuk - Yurii Davidich

PROJECTING OF URBAN TRANSPORT INFRASTRUCTURE CONSIDERING THE HUMAN FACTOR

Projecting of urban transport infrastructure, which forms a comfortable habitat and development of territories, is impossible without forecasting the parameters of transport and passenger flows. These parameters are formed under the influence of the subjective choice of urban residents on the routes along the road and route network. The study aims to identify factors affecting the distribution of transport and passenger flows through the existing urban transport network. It is revealed that the gravity function of employees of city-forming enterprises, which determines the emergence and absorption of transport and passenger flows of the city districts, can be described by parameters of urban structure, socio-economic factors and parameters that characterize zones of residence and main area of employment. The developed model was tested on real data from Kharkov - the second largest city in Ukraine.

Keywords: *infrastructure, transport and passenger flows, the gravity function, transit, mobility*

1 Introduction

Transport and transport infrastructure have a significant impact on the economic development of cities, the main area of employment, productivity of people, the cost indicators of the transport process. This is largely due to the geographical situation, the structure of the street-road network, the patterns of settlement and various scenarios of economic development. The growth of the level of motorization causes the need to develop a street-road network, increase the throughput and carrying capacity of the urban transport system.

2 Analysis of recent research and publications

The urban transport sector is economically sustainable when resources are efficiently used and allocated to maximize benefits and minimize external mobility costs [1]. Urban residential zones, in which live more than half the world's population, are facing unprecedented challenges in the field of transport and mobility. [2]. In the context of globalization and a significant increase in the level of motorization, one of the tasks in the development of transport infrastructure is forecasting the parameters of transport and passenger flows while improving the transport provision of new residential districts and various urban objects. Moreover, it is often necessary to assess the impact of the designed object on the transport infrastructure. Thus, the solution of problems of the formation and development of transport infrastructure requires consideration of a large number of factors related to the indicators of the technical development of the city [3]. Determining the directions of the development of transport infrastructure, the implementation of which will lead to a sustainable transport system, is a serious problem, as it is associated with a high degree of uncertainty about the future impact of the proposed measures on the transport system and urban environment [4].

Researchers identify four levels of transport planning: object, sectoral, integrated transport, relating to the transport system of the city, and urban, containing the complex of relations between the city and transport [5]. A well-functioning transport infrastructure ensures the sustainability and availability of transport for the population; the possibility of free transit in the zone and increasing mobility; creates the conditions for the development of the system of settlement, employment, recreation [6]. This requires a balance and coordination of land use, building and development of transport infrastructure. Such coordination is necessary and possible not only at the planning stage of new development zones. It should be carried out in the course of any major projects of urban territorial development [7]. The prerequisite for a smart city is that, having the right information at the right time, citizens, service providers and municipal authorities will be able to make more correct decisions that will lead to an improvement in the quality of life of the inhabitants and the overall sustainability of the city [8]. This should be one of the directions of state policy in which planning decisions

Natalia Davidich[1], Andrii Galkin[2,*], Vladimir Sabadash[3], Igor Chumachenko[1], Tatyana Melenchuk[4], Yurii Davidich[2]
[1]Department of Project Management in Municipal Services and Construction, O. M. Beketov National University of Urban Economy in Kharkiv, Ukraine
[2]Department of Transport System and Logistics, O. M. Beketov National University of Urban Economy in Kharkiv, Ukraine
[3]Kharkiv Research Institute of Forensic Examinations Hon. Prof. M. S. Bokarius, Ukraine
[4]Odessa State Academy of Technical Regulation and Quality, Ukraine
*E-mail of corresponding author: galkin.tsl@gmail.com

regarding the development of cities must be coordinated with the development of transport [9].

The constant increase in the number of cars makes it necessary to optimize the road network so as to satisfy most of the needs of the city. To reduce the risk of investment to a minimum, it is necessary to take into account the patterns of development of the system of roads, the distribution of the load on its individual sections. Therefore, modelling and optimal planning of the transport network takes on particular importance [10]. At the same time, the current problem of road congestion for the largest cities is one of the central ones that requires urgent attention [5].

The most important and fundamental feature of the formation of the loading of a transport network is that the choice of means and ways of travel users of the network affects the same choice that is being made by other users. This circumstance creates a feedback in the process of forming the loading of a transport network. The choice is based on a comparison of the parameters of different ways, while the parameters themselves are determined by the load on the transport network. At the same time, there is some uncertainty in predicting the routes by drivers. [11]. The state of flows is generated by the mutual transit of vehicles that implement the well-known OD matrix [12].

According to the researchers, if the flows in the network are in an equilibrium state, then the parameters of all the used ways connecting the two districts are in such a state as well. Formation of transport and passenger flows can be described by the gravity function, which determines the probability of choosing to travel to the zone j by population that leaves the zone i. The gravity function may include parameters characterizing the arrival and departure zones, as well as parameters characterizing the availability of alternative travel options (e.g., public transport). To form a origin-destination matrix, the gravitational modeling approach can be used. [13]. In this case, the formation of the mobility of the population is mainly influenced by the social composition of the population and the target nature of mobility [14]. Existing at present gravity functions are offered for all inhabitants of cities irrespective of social composition of urban population and as a parameter have only transit time [15]. The difference is only the type of function used. Some researchers describe it by hyperbolic dependence [15]. Others use the exponential model [16]. The third, according to the materials of the personal data, conclude that the best approximation of the gravity function is the function of the EVA [17].

In fact, residents belonging to different groups of the population have different priorities when choosing zones of gravity [15]. Researchers identify the following independent groups of population: employees of city-forming enterprises; employees of city service enterprises; students of higher educational institutions, colleges, secondary vocational schools. As a result, the gravity function should be formed separately for each group of active urban populations. In this case, in all processes in which a person is involved, there is an individual and collective behavior of people [18]. The purpose of users of the network may be to minimize travel-related losses, such as travel time, expenses of nervous energy and maximize their safety with the slightest deviation from comfortable conditions when traveling along several routes [19]. An adequate description of human behavior in practice is needed [20]. In this case, a combination of technological efficiency and behavioral changes is advisable [9].

A large role on the parameters of travel have individual qualities of a person [21]. The researchers propose to combine individual characteristics of people with the same properties of the central nervous system. In their opinion, the properties of nervous processes form certain combinations that determine the type of the nervous system or the type of higher nervous activity [22]. Thus, we can conclude that the individual characteristics of urban residents, which are determined by the type of nervous system, significantly affect the choice of mobility parameters and the choice of the route.

3 Research problem and purpose statement

The conducted researches aimed to determine the regularities of changing the gravity function of workers of city-forming enterprises for the projecting of urban transport infrastructure taking into account the human factor.

To achieve this goal, the following tasks were solved:

- identification of factors influencing the patterns of distribution of transport and passenger flows through the transport network;
- analysis of the influence of the parameters of the city structure, socio-economic factors and factors that characterize the zones of residence and employment on the change of the gravity function between the urban districts.

4 Data and results of research

4.1 Mathematical model

The projecting of transport infrastructure should be based on the results of a study of the patterns of influence of urban parameters on the distribution of transport and passenger traffic along the road network. Formation of flows occurs on the basis of the dispersal of urban residents, which determines the gravity function of the city districts. The amount of transport and passenger traffic flows transit is complemented by the visiting population. Adequate gravity functions should take into account not only time of travel, as at present, but also a more complex dependence, which includes other parameters influencing the choice of population of places of gravity.

The gravity function of inter-zone work-related mobility can be formalized as follows:

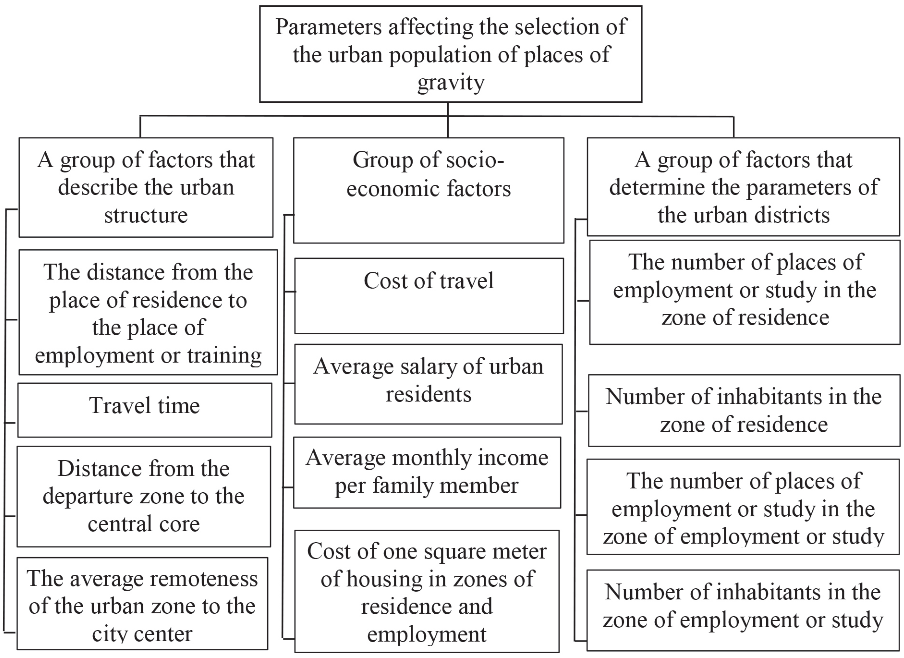

***Figure 1** Parameters affecting the selection of the urban population of places of gravity*

$$d^{mt}_{ij} = f\,(G, S, R), \qquad (1)$$

where:
d^{mt}_{ij} - the gravity function of inter-zone labor transit between (mt) the i - th zone of departure and the j-th zone of arrival,
G - group of factors that describe the urban structure,
S - group of socio-economic factors and data,
R - group of factors determining the urban zones.

It is possible to identify the following factors of each group (Figure 1).

The factors that describe the structure of the city, characterize the features of the organizational structure of the road network and the trip distance around the city.. The distance from the residence to the work and the traveling time directly reflect the difficulty of communication between the transport zones. The distance from the origin zone to the city core and the average distance from the residence to the city core characterize the organizational structure of the urban road network and the distance.

The factors that determine the parameters of the city's zones reflect the essence of the gravity function of the fact that people move from places of residence in which the number of workplaces or places of study is less than the number of workplaces or places of study in other zones.

Socio-economic factors estimate the costs for transit of urban residents and the expediency of changing their place of residence in relation to the place of work or study.

Travel costs indicate the difficulty of travelling in terms of financial loss. The average wage estimates the financial capacity of the population, which has a direct impact on the travel quantity and the choice of the route. The average monthly income per household member reflects the financial security of urban residents. It also depends on the choice of transport and the possibility of changing the place of residence relative to the place of work. The cost of one square meter of housing in the area of residence and the cost of one square meter of housing in the area of employment reflect the ability to change a place of residence relative to the place of work or study, that is, whether an employee can buy housing in the place of work in terms of their financial capacity, and vice versa to change the place of work. All socio-economic factors should be considered in relation to the value of the average wage in the research region.

Using the method of expert assessments, the general type of gravity function for intra-zone travel not connected with work was determined:

$$\begin{aligned} d^{bk}_{jz} &= a1 \cdot \exp\left(1 - \frac{\Theta_z}{\overline{\Theta}}\right) + a2 \cdot \exp\left(\frac{L_{jz}}{\overline{L}}\right) + \\ &+ a3 \cdot \left(\frac{N_j}{\overline{N}}\right) + a4 \cdot \log\left(\frac{\delta_{jz}}{\overline{\delta}}\right) + a5 \cdot \log\left(\frac{R_{jz}}{\overline{R}}\right) + \\ &+ a6 \cdot \log\left(\frac{S_z}{\overline{S}}\right), \end{aligned} \qquad (2)$$

where:
d^{bk}_{jz} - the gravity function between the j-th zones of departure and the z-th store for intra-zone cultural and social mobility (bk),
$\Theta_z, \overline{\Theta}$ - respectively, the value parameters of gravity that characterize the store z, and the average cost parameters of the gravity of stores in all zones, UAH,
$L_{jz}, \overline{L}$ - respectively, the distance from the j-th zone to the z-th trade establishment and the average distance from the zone to stores in the all zones, km,
$N_j, \overline{N}$ - respectively, the number of consumers in the j-th zone and the average number of consumers in all zones, ppl.,

$\delta_{jz}, \overline{\delta}$ - respectively, the slope factor ratio of the locality when moving from the j-th zone to the z-th store and the average slope factor in the all zones,
$R_{jz}, \overline{R}$ - respectively, the non-linearity factor of the connection when moving from the j-th microdistrict to the z-th trade establishment and the average non-linearity factor of the connection in all zones,
$S_z, \overline{S}$ - respectively, the trade service dimension in the z-th store and the average zone of trade service institutions in all zones, m^2,
$a1$, $a2$, $a3$, $a4$, $a5$, $a6$ - calibration coefficients, the value of which depends on the parameters of microdistricts and trading establishments.

The direction of influence of each factor was determined by analyzing its essence in relation to the function of attraction. The use of gravity functions that take into account the above-mentioned factors will allow to receive a matrix of correspondence of the urban population. This matrix can be used to model transport and passenger flows, considering the projected parameters of the urban infrastructure.

4.2 Data of instance

In order to realize the dependence (1), the definition of the gravity function of employees of city-forming enterprises of Kharkiv city was carried out. Kharkiv is the regional center of Ukraine and the second largest after Kiev. Currently, the urban population is about 1.5 million people. The total area of Kharkiv is now 35002.26 ha. The length of the backbone network of the city (citywide streets, streets of the regional significance and highways) is 391.2 km, and the average population density is 47.9 people per ha.

Kharkiv is one of the largest transport hubs of Ukraine (railways and highways, international airport). The city has an extensive network of street public transport: metro, route taxis, buses, trolley buses, trams. The total length of the Kharkiv metro lines is 33 km, the number of stations is 26. There are 18 tram, 29 trolleybus and 48 bus routes organized in the city. The fare in the city electric transport is \$ 0.19, subway \$ 0.27, buses \$ 0.37. The average wage is \$ 285. The total fleet of individual cars is 196.8 thousand cars. The level of automobilization is 134.8 cars per 1000 inhabitants.

In order to obtain the initial data needed to determine the gravity function between the place of employment and residence, field surveys were carried out. The study was conducted by a questionnaire method among workers of city-forming enterprises of the city of Kharkiv (Figure 2). The possibility of using a large sample survey to identify data on the preferences of urban dwellers has previously been substantiated. [23]. Employees of 58 city-forming enterprises located in various urban zones took part in the survey. During the survey, the places of employment and residence of employees were recorded, the type of mobility (transit), its temporary indicators, types of transport, price of transit and average monthly income per family member were determined. The total number of respondents was 874 people. Processing the questionnaires was to identify zones of departure and arrival. These zones were formed in accordance with the places of residence of workers and their place of employment. To solve this problem, a topological map of the city of Kharkiv was developed, consisting of 63 transport hubs and 100 connections. Using this scheme, the average distance of the districts from the geographical center of the city and the distance to the zone of employment was determined. The average travel time was defined as the sum of transport element's time from the place of residence to the place of employment or training: walking to stopping point, waiting for a vehicle, time to transfer from one mode of transport to another, walking time from the final stop to place of employment. The average cost of transit was also determined. For calculations for each zone of the urban housing prices were determined as well as the number of residents and places of employment in the zones of residence and work.

At the next stage the following data were determined: the significance of the gravity function of city-forming enterprises between zones i and j (d^y_{ij}), the distance between zones i and j (l_{ij}, km), the travel time between zones i and j (tn_{ij}, min), the ratio of the travel cost between zones to the average salary in the city of Kharkiv (S_{ij}/Zsr), the ratio of the distance from the departure zone i to the central core to the average distance from the urban zone to the center (Lr_i/Lrs), the ratio of income of a resident to the average wage in the Kharkiv (D_i/Zsr), the ratio of the cost of one square meter of housing in the zone of residence i to the average salary in the city of Kharkiv (Zz_i/Zsr), the ratio of the cost of one square meter of housing in the industrial zone j to the average salary (Zr_j/Zsr), number of places of employment in the zone of residence ($Qr.z_i$, units), the amount of residents in the zone ($Qz.z_i$, ppl.), the amount of places of employment in the zone j ($Qr.r_j$, units), the number of inhabitants in the inhabitans zone j ($Qz.r_j$, ppl.). An example of the results of the calculation of the data is given in Table 1.

Thus, after conducting a field survey and processing its results, all the data needed to determine the gravity function between the employment zones and residence, depending on the factors that affect it, were obtained.

4.3 Computer experiment

The information obtained during the survey, makes it possible to carry out a mathematical description of the dependence of the change in the gravity function of the workers of the city-forming enterprises. For this purpose, the methods of correlation and regression analysis were used. The values of the regression coefficients were calculated using the least squares method. Model parameters were determined using appropriate statistical methods. A multifactor model of change of gravity function between the zones i and j was developed. The results of calculations of the parameters of the model of the change

Questionnaire

Dear residents of Kharkiv, *the Department of Transport Systems and Logistics of the O.M.Beketov National University of Urban Economy in Kharkiv conducts a survey to identify the laws of selecting the places of attraction of workers of city-forming enterprises in Kharkiv with the aim of improving the organization of the transport infrastructure of the city.* ***All information provided by you will be used exclusively in the framework of this scientific study***

1. Place of residence (territorial location)____
2. Place of work, training (territorial location)____________________________________
3. Type of enterprise ____
4. The start time of the trip____
5. Time of the end of the trip ____
6. Trip route ____
7. What kind of transport do you use (please fill and underline your answers)

Type of transport	Time spent traveling to work	Time spent traveling to your place of residence	Number of transfers (specify types of transport and waiting time for transport)
A) personal			
B) public			
- trolleybus (Tr)			
- tram (T)			
- minibus (MB)			
- subway (S)			
- taxi			
Total time			

8. Travel cost (total in one way)______________________________UAH.
9. How much time you spend on the walking to the stop point (SP):
a) from home to SP _________________, b) from work to SP_________________
10. How much time do you spend on waiting for a vehicle at a stopping point when traveling from home ____
11. Your average monthly income per family member, $:

to 50	50-100	100-200	200-300	300-400	400-500	500-600	600-700	800-900	900-1000	1000-1100	1100-1200	1300-1400	1500-1600	1700-1800	1800-1900	more than 2000

12. Your age ________________________ 13. Gender __________________________

Thank you very much. We hope that you were interested in answering our questions and this will give a positive result in the study of this issue.

Figure 2 *Questionnaire for workers of city-forming enterprises*

Table 1 *The results of the survey data calculation*

d^y_{ij}	l_{ij}	t^y_{ij}	$\frac{S_{ij}}{Zsr}$	$\frac{L_{ri}}{L_{rs}}$	$\frac{D_i}{Zsr}$	$\frac{Zz_i}{Zsr}$	$\frac{Zr_j}{Zsr}$	$Qr.z_i$	$Qz.z_i$	$Qr.r_j$	$Qz.r_j$
0.04	6.05	15	0.0012	1.13	0.67	2.79	3.77	8700	10205	30783	23463
0.017	15.4	54	0.0018	1.24	1.72	3.59	3.81	8700	10205	17801	27552
0.023	10.2	46	0.0013	1.07	1.14	4.23	3.13	18737	20992	31786	44432
0.034	12	61	0.0016	1.05	1.33	3.38	2.54	21749	35278	25783	24453
0.029	16	75	0.0019	1.13	1.78	3.38	3.76	13049	48107	34673	43567
…	…	…	…	…	…	…	…	…	…	…	…
0.046	3.2	33	0.0011	1.25	0.35	4.49	2.73	12046	4082	23527	36534
0.006	12.4	70	0.0013	1.08	1.38	3.88	3.78	3747	41547	32587	42566
0.029	14	59	0.003	1.19	1.56	3.6	3.34	4216	44900	29837	41232
0.017	20.1	90	0.0023	1.31	2.233	3.47	3.81	12046	6123	18865	25765
0.003	7.2	17	0.0008	0.66	0.8	3.601	4.1	7027	19680	16532	22687

***Table 2** Limits of measurement of the model of change of the gravity function of employees of city-forming enterprises*

Indicator	Designation, dimension	Measurement boundaries
Travel time between zones i and j	tn_{ij}, min.	9.5-100.1
The ratio of the distance from the departure zone i to the center to the average distance from the zone to the city center	$\frac{L_{ri}}{L_{rs}}$	0.39-2.44
The ratio of the cost of one square meter of housing in the zone of residence i to the cost of one square meter of housing in the work zone j	$\frac{Zz_i}{Zr_j}$	0.726-1.21
The ratio of number of places of application of labor in the zone of work i to the number of places of application of labor in the residence zone j	$\frac{Qr \cdot r_i}{Qr \cdot z_j}$	0.49-23
The ratio of the travel cost between zones i and j to the average income of a resident of zone i	$\frac{S_{ij}}{D_i}$	0.0005-0.0092
Quantity of inhabitants in the zone of residence j	$Qz.z_j$, ppl.	3061-103794

***Table 3** Characteristics of the model of change of the gravity function of employees of city-forming enterprises*

Factor	Coefficient	Standard error	Student's t-test	
			actual	calculated
$\frac{1}{tn_{ij}}$	1.531	0.265	5.77	1.98
$1/\left(\frac{Lr_i}{Lrs}\right)$	0.0212	0.009	2.27	1.98
$\log\left(\frac{Zz_i}{Zsr}\right)$	-0.164	0.016	-10.2	1.98
$\log\left(\frac{Q_{r\cdot rj}}{Q_{r\cdot zi}}\right)$	0.043	0.004	11.45	1.98
$\sqrt{\left(\frac{S_{ij}}{Zsr}\right)}$	-0.743	0.17	-4.36	1.98
${Q_{z\cdot zi}}^{1,2}$	0.000000027	0.000000013	2.06	1.98

***Table 4** Confidence intervals of the coefficients of the model*

Factor	Lower bound	Upper bound
$\frac{1}{tn_{ij}}$	0.849	2.213
$1/\left(\frac{Lr_i}{Lrs}\right)$	0.0028	0.0452
$\log\left(\frac{Zz_i}{Zsr}\right)$	-0.205	-0.123
$\log\left(\frac{Q_{r\cdot rj}}{Q_{r\cdot zi}}\right)$	0.034	0.053
$\sqrt{\left(\frac{S_{ij}}{Zsr}\right)}$	-1.181	-0.304
${Q_{z\cdot zi}}^{1,2}$	0.0000000066	0.000000061

$Qr.z_i$ - number of places of application of labor in the zone of residence I, ppl.
S_{ij} - cost of travel between areas i and j, UAH
D_i - average income of a resident of i zone, km
$Qz.z_j$ - number of residents in the zone of residence I, ppl.
S_{ij} - cost of travel between zones i and j, UAH
D_i - average income of a resident of i district. UAH.

in the gravity function of the workers of the city-forming enterprises are given in Tables 2-4.

The multiple regression model has the following form:

$$d_{ij}^{v} = 1.531\frac{1}{t_{nij}} + 0.0212\left(1/\left(\frac{L_{rj}}{L_{rs}}\right)\right) - \\ - 0.164\left(\log\left(\frac{Z_{zi}}{Z_{rj}}\right)\right) + 0.043\left(\log\left(\frac{Q_{r.rj}}{Q_{r.zi}}\right) - , \\ - 0.743\sqrt{\left(\frac{S_{ij}}{D_i}\right)} + 0.000000027{Q_{z.zi}}^{1,2} \quad (3)$$

__Table 5__ The results of the evaluation of the model of changes of the gravity function of the workers of the city-forming enterprises

Indicator		Value
Student's t-test:	tabular	1.25
	calculated	125.24
Multiple correlation coefficient		0.99
Average approximation error, %		13.4

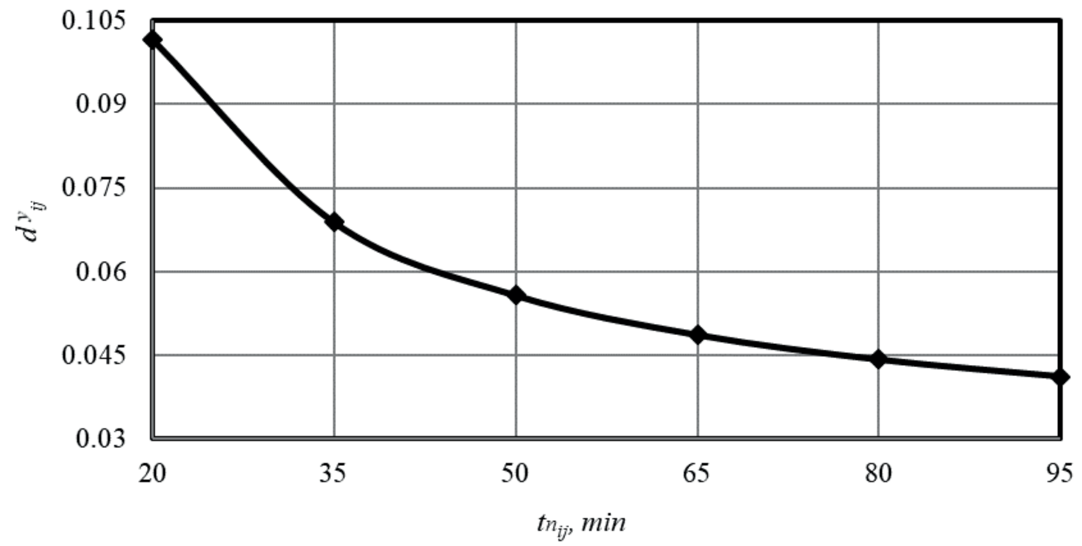

Figure 3 *Graph of changes in the gravity function of employees of city-forming enterprises, depending on the travel time between zones i and j*

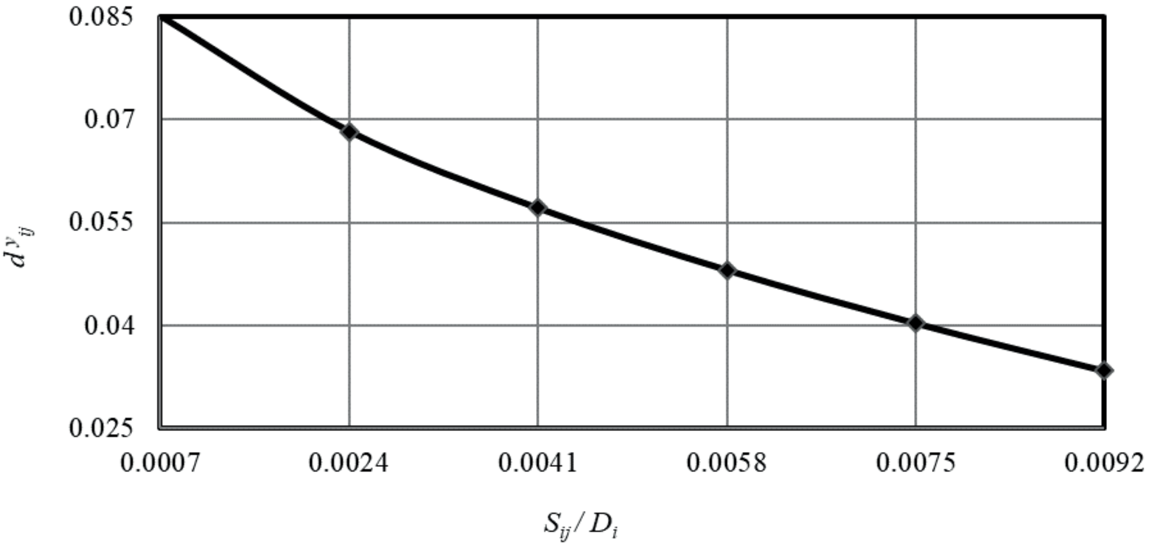

Figure 4 *Graph of changes in the gravity function of employees of city-forming enterprises, depending on the ratio of the travel cost to the average income of residents of the zone of departure i*

where:
d^y_{ij} - the gravity function of the workers of the city-forming enterprises between regions i and j,
tn_{ij} - travel time between zones i and j,
Lr_i - distance from the zone of departure i to the city center,
Lrs - average distance from the zone to the center,
Zz_i - the cost of one square meter of housing in the urban residence I,
Zr_j - the cost of one square meter of housing in the work zone j,
$Qr.r_j$ - the number of places of employment in the work zone j.

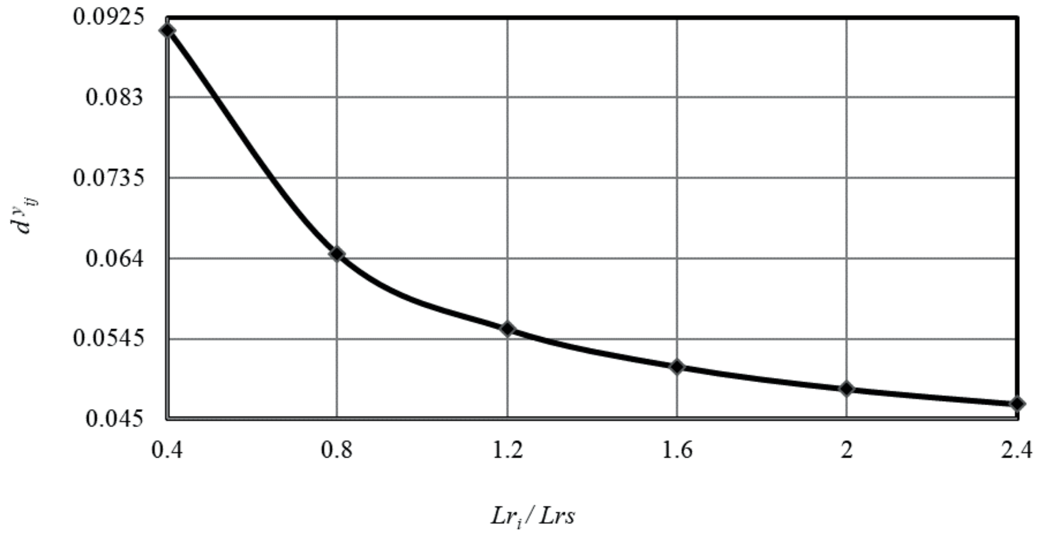

Figure 5 *Graph of changes in the gravity function of employees of city-forming enterprises, depending on the ratio of remoteness of the zone of departure i to the center to the average remoteness of the zones of the city from the center*

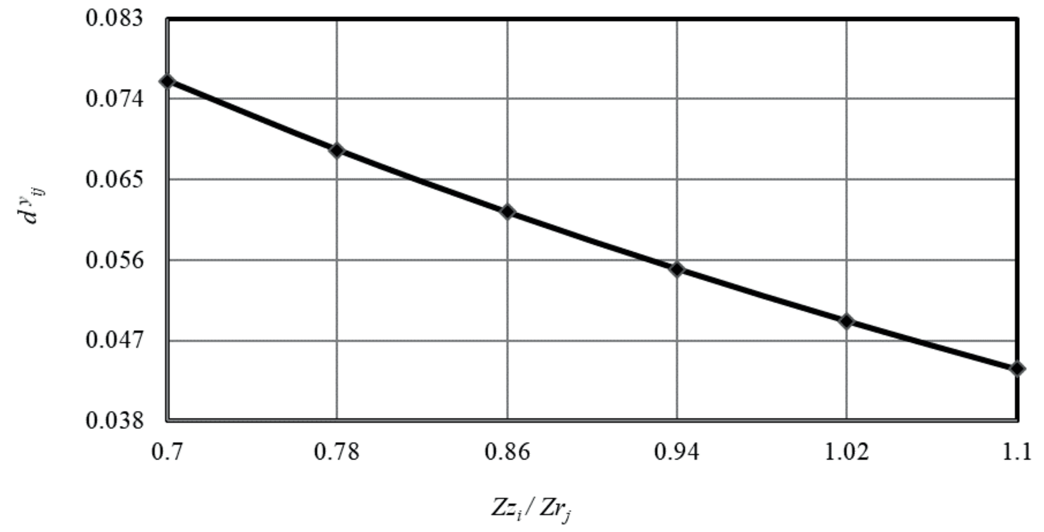

Figure 6 *Graph of changes in the gravity function of workers of city-forming enterprises, depending on the ratio of the cost of one square meter of housing in the zone of residence i to the cost of one square meter of housing in the zone of work j*

After the development of the regression model, its statistical evaluation was carried out. The results of the calculations are given in Table 5.

5 Discussion

The results of the research showed that in determining the patterns of change in the gravity function of the workers of the city-forming enterprises, of all the factors studied, only ten turned out to be significant, they form certain ratios. This is evidenced by the calculated value of Student's t-test, which is bigger than the table value. The closeness of the relationship between the dependent variable and the factors that influence its level was determined by the coefficient of multiple correlation. The value of the coefficient of multiple correlation indicates a high degree of closeness of the connection between the values of the gravity function and the selected factors. The assessment of the adequacy of the developed model was carried out in terms of the average approximation error. Its value corresponds to the permissible limits.

To analyze the changes in the gravity function of the workers of city-forming enterprises, graphs of its changes were constructed depending on the influence of each of the previously determined factors. When plotting the graphs, the value of one of the factors changed with the average values of others. The calculation results are shown in Figures 3-8.

Analysis of the received gravity function shows that the increase of the travel time between the areas of departure

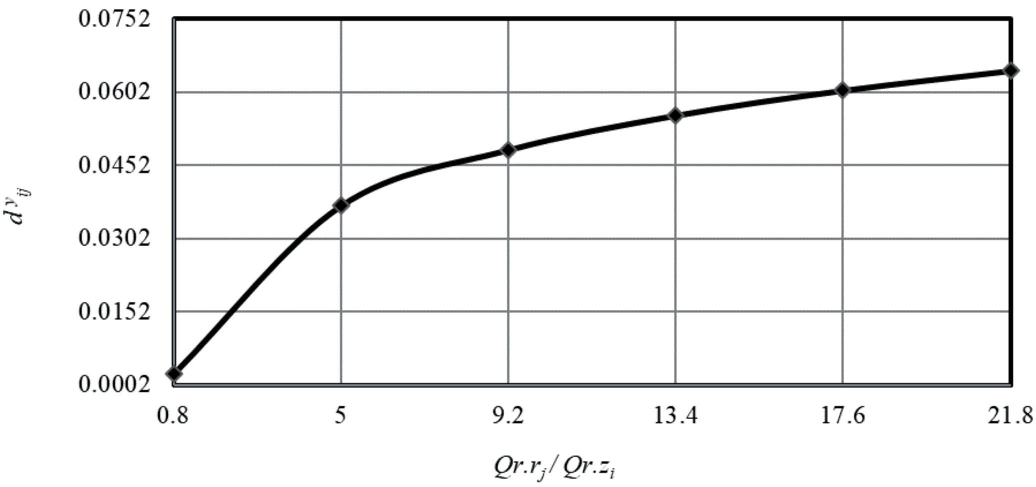

Figure 7 *Graph of changes in the gravity function of workers of city-forming enterprises depending on the ratio of the number of places of application of labor in the industrial zone j to the number of places of application of labor in the zone of residence i*

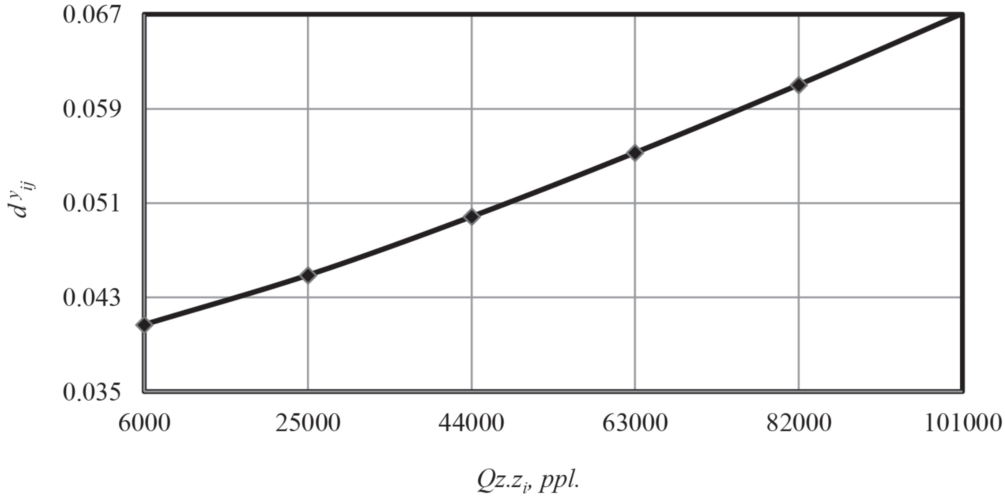

Figure 8 *Graph of changes in the gravity function of employees of city-forming enterprises, depending on the number of residents in the zone of residence i*

and arrival reduces the value of the gravity function. The more time it takes to travel, the fewer people will carry it. This conclusion is consistent with the results of previous studies.

An increase in the ratio of the travel cost to the average income of the residents of the area of departure leads to a decrease in the value of the gravity function. This is due to the fact that the higher is the travel cost in relation to income, the less people will make this trips. In this case, the route with a lower cost will be chosen.

The ratio of the remoteness of the area of departure from the city center to the average remoteness of the zone of the city from the center reduces the value of the gravity function. This is due to the fact that with an increase in the distance, possible transfers from one type of transport to another increase, the trip time and the cost of travel increase. All this causes a decrease in the attractiveness of potential travels from the area.

With the increase in the ratio of the cost of one square meter of housing in areas of residence and employment, the value of the gravity function decreases. This is due to the fact that employees of city-forming enterprises have more opportunities to purchase housing at the industrial zone. In addition, the cost of housing determines the prestige of the zones and residents may prefer to work in them.

With an increase in the ratio of the number of places of place of employment in the industrial area to the number place of employment in the zone of residence, the value of the gravity function increases. This is due to the fact that the likelihood of finding work in the area of gravity is higher than in the area of residence.

With the increase in the number of residents in the area of residence, the gravity function increases. With a large number of residents in the area of residence it is more difficult to find a job and residents will be forced to move to other parts of the city.

Thus, we can conclude that the change in the gravity function of the workers of the city-forming enterprises is described with sufficient accuracy by the regression equation, in which the variables are factors that describe the urban structure, socio-economic factors and factors determining the parameters of zones of residence place of employment. As a result of the calculations, it is possible to conclude that it is acceptable to use the resulting model of the change of the gravity function of employees of the city-forming enterprises when designing the urban transport infrastructure.

6 Conclusion

The design of the urban transport infrastructure should be focused on creating a comfortable living environment and the development of territories. In accordance with this premise, it is necessary that decision makers in the sphere of design of urban transport infrastructure take into account the influence of the human factor on changes in the parameters of transport and passenger flows. The existing methods for determining the parameters of transport and passenger flows did not fully considered the patterns of settlement of urban residents, their subjective choice of method and ways of travel due to the lack of mathematical formalization of the gravity function, the patterns of choice of public and individual transport for the travel, as well as the distribution of the formed transport and passenger correspondence for the existing route and street-road network. The proposed gravity function of the workers of the city-forming enterprises is based on the parameters of the urban structure, socio-economic data and factors that determine the parameters of the zones of residence and place of employment. However, it should be noted that the given ranges for measuring the factors of the obtained model correspond to the input data for which they were obtained. As a result, they cannot be considered typical, since the parameters of cities and their transport systems may differ significantly. There is a need for further broader research of the influence of factors that determine the patterns of change in the gravity function of urban residents. The obtained data on the change in the gravity function of the workers of city-forming enterprises, depending on the parameters of the city, increase knowledge of the degree of influence of town-planning and socio-economic factors on the patterns of settlement of urban residents. The proposed gravity function will help municipal services to assess changes in the parameters of transport and passenger flows in the improvement of the urban transport infrastructure, as well as in the construction of new areas of residential development. This will allow the identification of such measures, which will provide the population with better living conditions to a greater extent. In the future, it is expected to continue research in the design of urban transport infrastructure, taking into account the human factor in determining its parameters. It is planned to determine the probability of choosing different types of travel: hiking, cycling, transport; the probability of choosing individual and public transport for transportation; the proportion of correspondence, which is realized by alternative ways of travel on an individual transport; determination of the proportion of passenger correspondence, which is realized by alternative routes of travel on public transport. The advantage of these researches is to take into account the individual characteristics of the urban inhabitants, namely gender, age and type of the nervous system.

References

[1] CERVERO, R. *Transport infrastructure and the environment: sustainable mobility and urbanism* [online]. Working Paper 2013-03. Berkeley: University of California, 2013 [accessed 2016-11-08]. Available from: http://iurd.berkeley.edu/wp/2013-03.pdf

[2] VICENTE, P., REIS, E. Ex-regular users of public transport: their reasons for leaving and returning. *Journal of Public Transportation* [online]. 2018, **21**(2), p. 101-116. ISSN 1077-291X, eISSN 2375-0901. Available from: https//doi.org/10.5038/2375-0901.21.2.7

[3] BRANIS, M., HODAKOVA, D., CAPAYOVA, S., SCHLOSSER, T., GALKIN, A. Future of evaluating public transport services. 18th International Multidisciplinary Scientific GeoConference SGEM: Surveying Geology & Mining Ecology Management : proceedings. 2018. ISBN: 978-1-5108-7357-5, p. 565-571.

[4] SHIFTAN, Y., KAPLAN, S., HAKKERT, S. Scenario building as a tool for planning a sustainable transportation system. *Transportation Research Part D: Transport and Environment* [online]. 2003, 8(5), p. 323-342. ISSN 1361-9209, eISSN 1879-2340. Available from: https://doi.org/10.1016/S1361-9209(03)00020-8

[5] ALLSTROM, A., BARCELO, J., EKSTROM, J., GRUMERT, E., GUNDLEGARD, D., RYDERGREN, C. Traffic management for smart cities. In: *Designing, developing, and facilitating smart cities*. ANGELAKIS, V., TRAGOS, E., POHLS, H. C., KAPOVITS, A., BASSI, A. (eds.). Cham: Springer, 2017, p. 211-240. ISBN 978-3-319-44924-1.

[6] MUNDA, G. Social multi-criteria evaluation for urban sustainability policies. *Land Use Policy* [online]. 2006, 23(1), p. 86-94. ISSN 0264-8377, eISSN 1873-5754. Available from: https://doi.org/10.1016/j.landusepol.2004.08.012

[7] VUCHIC, V. R. Transportation for livable cities. Center for Urban Policy Research, 1999. ISBN 978-0882851617.

[8] KHANSARI, N., MOSTASHARI, A., MANSOURI, M. Impacting sustainable behavior and planning in smart city. *International Journal of Sustainable Land Use and Urban Planning* [online]. 2014, 1(2), p. 46-61. ISSN 1927-8845. Available from: https://doi.org/10.24102/ijslup.v1i2.365

[9] BANISTER, D. The sustainable mobility paradigm. *Transport Policy* [online]. 2008, 15(2), p. 73-80. ISSN 0967-070X, eISSN 1879-310X. Available from: https://doi.org/10.1016/j.tranpol.2007.10.005

[10] MILAN, L., KIN, B., VERLINDE, S., MACHARIS, C. Multi-actor multi-criteria analysis for sustainable city distribution: a new assessment framework. *International Journal International Journal of Multicriteria Decision Making* [online]. 2015, 5(4), p. 334-354. ISSN 2040-106X, eISSN 2040-1078. Available from: https://doi.org/10.1504/ijmcdm.2015.074088

[11] Great Britain Department for Transport - Design manual for roads and bridges: volume 12 Traffic appraisal of roads schemes, section 1 Traffic appraisal manual, Part 1 The application of traffic appraisal to trunk roads schemes, Section 2 Traffic apprasial advice [online]. 1999. Available from: http://www.standardsforhighways.co.uk/ha/standards/dmrb/vol12/section1.htm

[12] CHUMACHENKO, I. V., DAVIDICH, Y. A., GALKIN, A. S., DAVIDICH, N. V. Quality assessment of passenger transportation by urban transport while using various number of fixed-route transport facilities. *Science & Technique* [online]. 2017, 16(5), p. 415-421. ISSN 2227-1031, eISSN 2414-0392. Available from: https://doi.org/10.21122/2227-1031-2017-16-5-415-421

[13] TOLEUEI, R., PSARRAS, S., PRINC, R. Origin-destination trip matrix development: conventional methods versus mobile phone data. *Transportation Research Procedia* [online]. 2017, 26, p. 39-52. ISSN 2352-1465. Available from: https://doi.org/10.1016/j.trpro.2017.07.007

[14] DRIL, N., GALKIN, A., BIBIK, N. Applying city marketing as a tool to support sustainable development in small cities: case study in Ukraine. *Transportation Research Procedia* [online]. 2016, 16, p. 46-53. ISSN 2352-1465. Available from: https://doi.org/10.1016/j.trpro.2016.11.006

[15] DOLYA, V. K. *Pasazhirski perevezennya / Passenger transportation* (in Ukranian). Harkiv: Fort, 2011. ISBN 978-966-8599-92-7.

[16] FEDOROV, V. P., BULYICHEVA, N. V., LOSIN, L. A., PAHOMOVA, O. M. Transportnaya sistema tsentra krupnogo goroda. Analiz s pomoschyu metodov matematicheskogo modelirovaniya / Transportation system of the center of a large city. Analysis using mathematical modeling methods (in Russian). *Upravlenie Razvitiem Territorii / Territorial Development Management*. 2009, 4, p. 18-25.

[17] SHAROV, M. I. *Sovershenstvovanie metodi otsenki transportnogo sprosa na perevozki gorodskim pasazhirskim transportom / Improvement of methods of estimation of transport demand for transportation by urban passenger transport* (in Russian). Author's abstract dissertation on the degree of Candidate Technical Sciences: 05.22.10. Irkutsk: ITTU, 2008.

[18] FURLETTI, B., GABRIELLI, L., GIANNOTTI, F., MILLI, L., NANNI, M., PEDRESCHI, D., GAROFALO, G. Use of mobile phone data to estimate mobility flows. Measuring urban population and inter-city mobility using big data in an integrated approach. 47th Meeting of the Italian Statistical Society : proceedings. 2014. ISBN 978-88-8467-874-4, p. 1-11.

[19] GAVRILOV, E. V., LINNIK, I. E., SIROTA, V. M. Ergonomicheskoe obespechenie organizatsii dorozhnogo dvizheniya / Ergonomic support of the organization of road traffic (in Ukrainian). *Kommunalnoe hozpodarstvo gorodov / Municipal economy of cities*. 2004, 58, p. 163-169. ISSN 2522-1809.

[20] Novak, R. Management of the transport infrastructure development programme in the Czech Republic. *Communications - Scientific Letters of the University of Zilina* [online]. 2000, 2(4), p. 95-99. ISSN 1335-4205, eISSN 2585-7878. Available from: http://komunikacie.uniza.sk/index.php/communications/article/view/1081

[21] KLEBELSBERG, D. *Verkehrspsychologie / Traffic psychology* (in German) [online]. Berlin, Heidelberg, New York: Springer, 1982. ISBN 978-3-642-47507-8. Available from: https://doi.org/10.1007/978-3-642-47507-8

[22] GHYSEN, A. The origin and evolution of the nervous system. *The International Journal of Developmental Biology. 2003*, **47**(7-8), p. 555-562. ISSN 0214-6282, eISSN 1696-3547.

[23] YAN, X., LEVILE, J., ZHAO, X. Integrating ridesourcing services with public transit: an evaluation of traveler responses combining revealed and stated preference data. *Transportation Research Part C: Emerging Technologies* [online]. 2019, 105, p. 683-696. ISSN 0968-090X, eISSN 1879-2359. Available from: https://doi.org/10.1016/j.trc.2018.07.029

Daniil A. Loktev - Alexey A. Loktev - Alexandra V. Salnikova

THE SYSTEM OF FACIAL RECOGNITION IN THE INFRARED RANGE

In this paper, a new approach is introduced upgrading the complex object recognizing monitoring system up to the image processing system capable of operating both in the visible and the infrared wavelength ranges. For this purpose, both new algorithmic software and user interface are provided that require from the operator neither special knowledge, nor specific competencies in the fields of object detection, tracking and recognition, while allowing determining the thermal imager parameters necessary for constructing a high-quality image of an object. There are formulated the conditions required for obtaining such image that, by its quality, would make the satisfactory detection of the desired object possible. By means of the conducted tests, it is demonstrated that the application of the proposed mathematical and algorithmic support of the complex monitoring and control system provides the solution for the problem of the highly accurate individual recognition.

Keywords: *object image, background image, cascade classifier, thermal imager, object contour, background subtraction*

1 Introduction

The current stage of development of security systems and passenger traffic control is associated with the detection, capture and recognition of images of many people, as well as with the definition of the individual parameters characterizing their condition and behavior. One of the promising areas of development of such systems is the identification of individuals according to their biometric personal data. It is important not only to determine the identity of the person, but also to determine his mental and physical condition, the adequacy of behavior, forecasting and tracking his or her routes within the transport infrastructure and choice of the rolling stock. Since low temperatures prevail in Russia and several European countries for most of the year, passengers widely use various insulating accessories that reduce the surface of the face, suitable for creating an image for recognition.

This paper is devoted to the study of the possibility of recognizing a person based on the image of his face, obtained in the infrared wavelength range. To obtain the primary image of the object under study, a Fluke TIX 580 thermal imager with a sensitivity of 0.05°C is used. As passengers move within the boundaries of the transport infrastructure, in order to solve the complex problem of recognition it is proposed to use a modified method of analogies involving constructing the system of verification comparisons between the models of physical objects and information processes where the main parameters are quantitative characteristics describing the geometric and physical quantities that can be detected in the monitoring system [1-5]. Depending on the distance from the passenger to the photodetector, it is proposed to use the categories “far” and “close” objects and, depending on the speed of movement of the passenger - the categories “fast” and “slow”. For the primary classification of objects by the distance to them, their speed and type, it is proposed to use the method of analyzing the image blur in the optical range [2, 6-8].

2 Problem statement

Since the presented monitoring system examines the images obtained in the infrared range, the considered approaches and algorithms are not suitable for “fast” objects [9-10], because thermoelastic processes in conventional environments are sufficiently inertial and depend on the amount of heat, the surface area through which the heat is distributed, the thermal conductivity of the medium in which the monitoring system operates.

This paper does not study the aspects of the interdependences of the heat flow speed, the speed of passenger movements and the speed of image acquisition by means of the thermal imager in the infrared range. For the classification of the recognizable objects in the context presented above, it is assumed that the speed of movement of both passenger traffic and individual

Daniil A. Loktev[1], Alexey A. Loktev[2], Alexandra V. Salnikova[3,4*]
[1]Department of Information Systems and Telecommunications, Bauman Moscow State Technical University, Russia
[2]Department of Transport Construction, Russian University of Transport (MIIT), Moscow, Russia
[3]International Laboratory of Statistics of Stochastic Processes and Quantitative Finance, National Research Tomsk State University, Russia
[4]Department of Building Engineering and Urban Planning, University of Zilina, Zilina, Slovak Republic
*E-mail of corresponding author: amicus.lat@yandex.ru

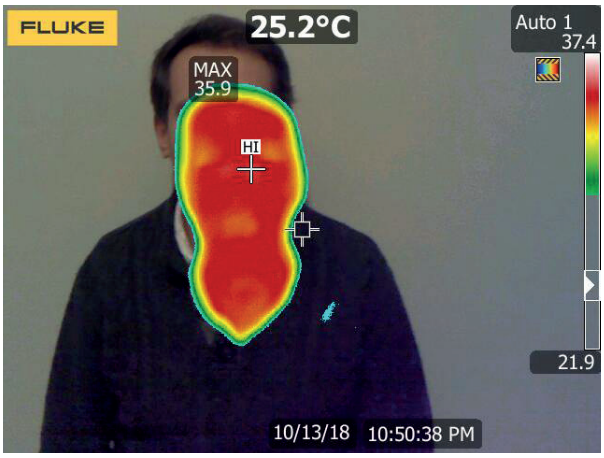

Figure 1 *Combined passenger image in the visible and infrared wavelength range at a distance of 1.5 meters*

Figure 2 *Combined passenger image in the visible and infrared wavelengths at a distance of 0.5 meters*

passengers is quite small, and that the objects of recognition are located near the infrared detector.

It is proposed to perform passenger face recognition by applying the aggregated approach [11] using the cascade classifiers based on Haar primitives and on background subtraction algorithms [2, 3, 6]. Since the resulting images in the infrared range have fewer colors than regular photography, the use of the described approaches is reasonable [12-14].

Cascade classifiers are determined by means of an adaptive boosting algorithm (AdaBoost), well-known from the researches performed by domestic and foreign scientists and the modern software system descriptions [15-16].

3 Object detection using cascade of classifiers

Now let us consider an image obtained in the optical and infrared range using a thermal imager that detects thermal radiation at wavelengths from 3 to 15 μm [17] (such radiation corresponds to the thermal processes on a human body surface) and is set at 1.5 meters from the object of examination. (Figure 1). The average background temperature determined by the thermal imaging system is 25.2°C, and the maximum temperature of the desired object (passenger) is 35.9°C. From Figure 1, it is seen that the image quality is not good enough for the successful construction of a unique cascade classifier based on Haar primitives [2, 3, 6].

Changing the parameters of the monitoring system when receiving the primary image of the object [18] means, first of all, reducing the distance between the object and the detector that can lead to the appearance of distinct elements on the image of the passenger's face (Figure 2) [19]. The maximum detectable temperature of the object is equal to 37.0°C and the average temperature of the background is equal to 36.0°C. The image obtained under such conditions can be used in recognition algorithms based on both the cascade classifiers and the background subtraction procedures [8, 10, 20].

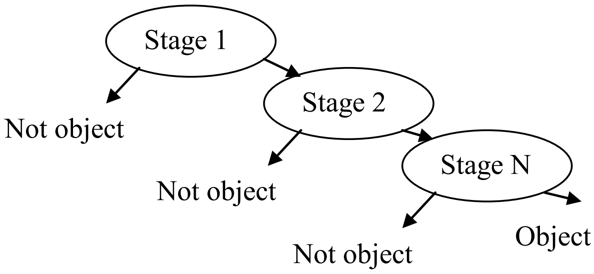

Figure 3 *Cascade of classifiers*

When using the gradual complication of the primitives of the Haar [2, 3, 6], each successive classifier of the cascade meets the more stringent conditions of accuracy and completeness (Figure 3).

The second approach used in this study is the method of background subtraction when, to represent each pixel, one uses not one model (mean and variance), but several Gaussian ones [18, 21]. This paper presupposes that for each pixel there are three Gaussian models. If the pixels do not match the Gaussian background distribution, then they are considered to be in the foreground. The available methods of background subtraction differ significantly from each other, but they all assume that the observed series of images I consists of a static background B and moving objects in front of it [21]. It is also assumed that any moving object has a color distribution different from the background. In general, the methods of subtracting the background can be represented as a ratio:

$$\chi_t(s) = \begin{cases} 1, & \text{if } d(I_{s,t}, B_s) > \tau, \\ 0, & \text{otherwise} \end{cases} \qquad (1)$$

where:
χ_t - motion mask at a time t,
$I_{s,t}$ - the color of the pixel s at a time t,
B_s - pixel background s,
d - distance between $I_{s,t}$,
B_s , τ - threshold value.

4 Background subtraction algorithm

Now there will be considered several ways to detect motion in an image. The easiest way to get background B is to create a single gray or color image that does not contain moving objects. For this, there is done a photo of the object of transport infrastructure without moving objects (people) or a picture with a median filter [22]. To reduce the effects of light and changes, the background can be represented by the following iterative expression [23]:

$$B_{s,t+1} = (1-\alpha)B_{s,t} + \alpha I_{s,t},, \quad (2)$$

where $\alpha = 0.1$ is a certain constant.

The presented background model allows determining pixels belonging to moving objects located in the foreground by finding the threshold of distance functions of different orders:

$$d_0 = |I_{s,t} - B_{s,t}|, \quad (3)$$

$$d_1 = |I^R_{s,t} - B^R_{s,t}| + |I^G_{s,t} - B^G_{s,t}| + |I^B_{s,t} - B^B_{s,t}|, \quad (4)$$

$$d_1 = (I^R_{s,t} - B^R_{s,t})^2 + (I^G_{s,t} - B^G_{s,t})^2 + (I^B_{s,t} - B^B_{s,t})^2, \quad (5)$$

$$d_1 = (|I^R_{s,t} - B^R_{s,t}|,|I^G_{s,t} - B^G_{s,t}|,|I^B_{s,t} - B^B_{s,t}|), \quad (6)$$

where indexes R, G and B indicate the intensity of red, green, and blue in the marked pixel, while d_0 is the initial distance measure, defined in shades of grey.

The proposed scheme allows one to use the previous frame I_{t-1} as a background image B. This approach reduces the resulting computational complexity of the procedure [24]. Also, this approach allows detecting movement by comparing neighboring frames, it is resistant to changes in the illumination of the entire picture, while at the same time it is difficult to select the entire moving object and not its parts.

Pixels belonging to the background can be detected by means of the *MinMax* method, which specifies a condition whose satisfaction is a criterion for assigning a pixel to a static object:

$$|M_s - I_{s,t}| < \tau d_\mu, \quad (7)$$

where:
τ - threshold set by the monitoring system operator,
d_μ - median value of the largest absolute difference between frames across the image,
s - background pixel,
M_s - the maximum difference between frames, which is associated with the minimum value of this difference m_s and the maximum difference of successive frames D_s observed during the examination of the series of images.

Equation (7) takes into account that, in the noisy area of the image, the pixel changes greater than in the area of a stable background [25]. According to this approach, the description of the desired background pixel by the three extremum values m_s, M_s, D_s is more informative than the one using the traditional mean vector and covariance matrix. As this Equation (7) holds for grayscale images, they may carry less information than the color frame sequences [17, 21].

The estimation of the pixel belonging to the background image can also be performed by modeling the multimodal probability distribution function:

$$P(I_{s,t}) = \frac{1}{N}\sum_{i=t-N}^{t-1} K(I_{s,t} - I_{s,i}), \quad (8)$$

where:
K is kernel,
N is a number of previous frames,
$P(I_{s,t})$ is an estimated probability.

If the evaluation is based on a sequence of color frames, then, in expression (8), one-dimensional kernels can be used:

$$P(I_{s,t}) = \frac{1}{N}\sum_{i=t-N}^{t-1} \prod_{j=(R,G,B)} K\left(\frac{I^j_{s,t} - I^j_{s,i}}{\sigma_j}\right), \quad (9)$$

where σ_j can be fixed or pre-evaluated.

If the background image is quite complex in structure and color gamut, then the functions of the multimodal probability distribution can be used. In this case, each pixel is modeled by a set of K Gaussians [21-22], and the probability of occurrence of a certain color in a given pixel s can be represented as:

$$P(I_{s,t}) = \sum_{i=1}^{K} \omega_{i,s,t} N(\mu_{i,s,t}, \Sigma_{i,s,t}), \quad (10)$$

where:
$N(\mu_{i,s,t}, \Sigma_{i,s,t})$ - representation of the i-th model of the Gaussian [18, 21],
$\omega_{i,s,t}$ - weight of i-th model.

In the calculation it can assumed that $\Sigma_{i,s,t} = \sigma^2 Id$, i.e. the covariance matrix is diagonal, and the values included in Equation (10) for the Gaussian the intensity $I_{s,t}$ of which does not exceed the specified deviation from the mean value is determined by the recurrence relations:

$$\omega_{i,s,t} = (1-\alpha)\omega_{i,s,t-1} + \alpha, \quad (11)$$

$$\mu_{i,s,t} = (1-\alpha)\mu_{i,s,t-1} + \rho I_{s,t}, \quad (12)$$

$$\sigma^2_{i,s,t} = (1-\rho)\sigma^2_{i,s,t-1} + \rho d_2(I_{s,t}, \mu_{i,s,t}), \quad (13)$$

where:
α is a set value showing the speed of learning of the algorithm,
$\rho = \alpha N(\mu_{i,s,t}, \Sigma_{i,s,t})$ is a second approximation of the speed of learning,
d_2 is the distance between the pixels.

It is assumed that the values μ and σ for non-coincident distributions do not change, and only their weight is decreasing:

$$\omega_{i,s,t} = (1-\alpha)\omega_{i,s,t-1} + \alpha. \quad (14)$$

If at a certain stage of the iterative process the component under consideration does not correspond to the color $I_{s,t}$ with the lowest weight, it is replaced by the Gaussian having a greater initial dispersion σ_0^2 and a smaller weight coefficient ω_0 [18, 22]. After each Gaussian is redefined, the weights are normalized and added to the sum of a single value. After that, K distributions are ordered according to the ratio $\omega_{i,s,t}/\sigma_{i,s,t}$ and H of the most reliable of them are defined as background:

$$H = \arg\min_{h}\left(\sum_{i=1}^{h}\omega_i > \tau\right). \tag{15}$$

After the described procedure, pixels having a color $I_{s,t}$ that differs by a greater deviation than the specified one from all the obtained distributions H are detected as belonging to a moving object.

In the presence of a significant noise in the original images and the use of the algorithms based on the Gaussian model [18], the noise components may increase. To reduce this effect, it is proposed to use morphological operators that are erosion and dilation.

Binary representation of erosion has the following form:

$$A\Theta B = \bigcap_{b\in B} A_b\,, \tag{16}$$

where A is a main binary image and B is a binary representation of the structural element causing erosion. Image B moves around the entire image A and, if the unit pixel A and B are the same, then there occurs the logical centering of the central pixel B with the corresponding pixel A. As a result, the original image is cleared of the objects smaller than the structural element.

The binary dilation operator is represented as:

$$A \oplus B = \bigcup_{b\in B} A_b\,. \tag{17}$$

If the origin of the structural element B coincides with a single pixel, the entire element B is transferred and then added to the corresponding pixels of the image A.

The operator (15) is mainly used to clear the background, while the operator (16) is used to select foreground objects. In fact, both erosion and dilation affect the boundaries of the objects, primarily changing the graphic elements of the small size, and thus there often arises a separate task of detecting the boundaries of the objects as well as the corner points. One of the methods of allocation of the boundaries of the objects is the Kanye method. Its implementation includes the following main stages:

1. Applying the Gaussian filter in order to smooth the image and remove noise.
2. Defining the gradients of the image intensity; where the maximum gradient value is detected, the boundary is marked.
3. Making use of the non-maximum filtration procedure.
4. Applying the double threshold method in order to determine potential boundaries.
5. Tracing the ambiguity region, simultaneously suppressing all the boundaries that are not associated with the specific edges.

The described operator is most often implemented in a grayscale image - to reduce the cost of computing power.

Defined in the proposed way, the contour is an array of points connected to a curve. Each foreground object (movable) is characterized by its contour. This procedure will help to detect the overlap of the studied objects and to select the objects that have all the points on the contour curve and are to be recognized and classified lately.

The developed facial recognition system consists of the following modules: loading a series of images of passenger traffic, entering the parameters of recognition by the user, the background subtraction algorithm, the mode of matching subsequent frames, the detection of an individual passenger, object recognition and entry into the database.

5 Implementation of image processing algorithms

In this study, when considering the complex monitoring system, more attention is paid to the object detection unit that uses the background subtraction algorithm and is expected to take into account a number of factors, including sudden or gradual change in illumination; repetitive and oscillatory movements of individual elements at the background; long-term changes in the position of the objects in the overall picture.

The procedure of background subtraction is quite well known and it is used in various modifications in many graphic editors and image processing programs to create a foreground mask (a binary image that includes pixels related to moving objects). The foreground mask is determined by means of subtraction of the background image from the current frame, while this very background image is formed taking into account the parameters of the observed picture and the characteristic time of the individual object position changes, as well as the settings of the photo system.

The implementation of the presented algorithm is possible with the help of OpenCV technical vision library also allowing working with the cascade classifiers based on the Haar primitive use [2, 3, 6]. As a subtraction method, the method is used that segments the background and foreground objects using a set of Gaussians [18, 21] for each of the elements; in the library, this method is referred to as MOG2. The specified algorithm selects the most accurate Gaussian distribution for each of the pixels and therefore it can adapt well to changing shooting conditions.

To perform the described procedure, several functions are sequentially used. The function *setShadowValue()* is responsible for the detection and designation of shadows and has one parameter that takes values from 0 to 255.

a)

b) c)

Figure 4 *Representation of the passenger object in the visible optical range: a) the initial image of the object, b) selecting an object without a shadow, c) the contour of the object with the averaged background in the place of an object*

Next, a function *apply()* is performed that finds the foreground mask and has three parameters: *image*, *fgmask*, *learningRate*. The field *Image* defines the next frame of the sequence which is used without scaling. The field *Fgmask* sets the foreground mask as an 8-bit binary image. *LearningRate* is the parameter specifying the rate of change of the background, its equality to zero means that the background remains the same for the entire series of images, and the unit indicates that the background is each time redefined by the last image of the series. This parameter can take negative values. In this case, the speed of background change is selected automatically.

The next step is to use a function *setHistory()* that determines the number of frames that are taken into account when the background model is obtained.

To detect and select the individual moving objects, it is proposed to use a function *findAndDrawContours()* that detects contours in a binary representation. If the contours found have a size larger than the user-defined threshold value denoted by the parameter *areaThreshold*, then using the function *drawBoundingBox()*, the objects to which the corresponding contours belong are indicated by rectangular frames. Figure 4 demonstrates the use of the above functions with some modifications needed to work with multi-color images [16, 21].

In this study, software that implements the above algorithms in the form of a single complex of monitoring and control is developed. For the convenience of its use by an operator without special skills, a graphical user interface (GUI) [26-27] has been developed, which provides developers with an ability to create forms with the necessary placement, related classes and dialogs.

6 Conclusion

Since the interaction of the operator-user with the hardware-software complex of monitoring and control occurs according to a certain scenario, when designing and implementing it, it is necessary to take into account the individual characteristics of the operators and the requirements to them depending on the task to be solved and the individual functions of the software complex. This approach is taken into account in this work when creating the user interface. The system of classes, functions and concepts associated with the scenario of interaction between the user and the software application, as well as the individual modules of the monitoring software and hardware complex between them, determines the set of the possible states of dialogue and actions that allow moving from one state to another. The state of interaction is determined by an event occurring with a separate interface element.

The developed interface of the main modules of the monitoring system has been tested by means of the GOMS (Goals, Operators, Methods, and Selection Rules) method making it possible to determine the time needed to solve a specific task together with the speed of the application operation in various situations. The implementation of the user actions is evaluated by defragmenting the task being performed into typical components and by calculating the time spent by operators for the operation with each of the interface elements.

In general, the proposed mathematical and algorithmic software can be used in complex monitoring and control systems in both optical and infrared wavelengths, and the formulated parameters for obtaining the primary image provide a solution for the problem of detection and recognition of individual passengers.

Acknowledgement

This study was financially supported by the Russian Science Foundation (research project No. 17-11-01049).

References

[1] GRYAZNOV, N., LOPOTA, A. Computer vision for mobile on-ground robotics. *Procedia Engineering* [online]. 2015, **100**, p. 1376-1380. ISSN 1877-7058. Available from: https://doi.org/10.1016/j.proeng.2015.01.506

[2] LOKTEV, D. A. Determination of object parameters by a series of its images in the integrated monitoring system (in Russian). *Path and Track Facilities*. 2015, **2**, p. 31-33. ISSN 0131-5765.

[3] SUN, Z., BEBIS, G., MILLER, R. On-road vehicle detection using optical sensors: a review. 7th International IEEE Conference on Intelligent Transportation Systems : proceedings [online]. 2004. ISBN 0-7803-8500-4. Available from: https://doi.org/10.1109/ITSC.2004.1398966

[4] COLLINS, R., LIPTON, A., KANADE, T. *A system for video surveillance and monitoring*. Technical Report CMU-RI-TR-00-12. Pittsburgh: The Robotics Institute, Carnegie Mellon University, 1999. Available from: https://www.ri.cmu.edu/pub_files/pub2/collins_robert_2000_1/collins_robert_2000_1.pdf

[5] LOKTEV, D. A., LOKTEV, A. A., SALNIKOVA, A. V., SHAFOROSTOVA, A. A. Determination of the dynamic vehicle model parameters by means of computer vision. *Communications - Scientific Letters of the University of Zilina* [online]. 2019, **21**(3), p. 5-11. ISSN 1335-4205, eISSN 2585-7878. Available from: http://komunikacie.uniza.sk/index.php/communications/article/view/93

[6] HAHNE, U. *Real-time depth imaging* [online]. Ph.D. Thesis. Berlin: Technische Universitat Berlin, 2012. Available from: https://d-nb.info/1023762218/34

[7] LINDNER, M., KOLB, A. Calibration of the intensity-related distance error of the PMD TOF-camera. SPIE - The International Society for Optical Engineering : proceedings [online]. 2007. ISBN 978-0-8194-6924-3. Available from: https://doi.org/10.1117/12.752808

[8] GIL, P., POMARES, J., TORRES, F. Analysis and adaptation of integration time in PMD camera for visual serving. 20th International Conference on Pattern Recognition : proceedings [online]. 2010. ISSN 1051-4651. Available from: https://doi.org/10.1109/ICPR.2010.85

[9] MULJOWIDODO, K., RASYID, M. A., SAPTO, A. N., BUDIYONO, A. Vision based distance measurement system using single laser pointer design for underwater vehicle. *Indian Journal of Marine Sciences* [online]. 2019, **38**(3), p. 324-331. ISSN 0379-5136. Available from: http://nopr.niscair.res.in/bitstream/123456789/6209/1/IJMS 38(3) 324-331.pdf

[10] DESCHENES, F., ZIOU, D., FUCHS, P. *Enhanced depth from defocus estimation: tolerance to spatial displacements*. Technical Report No. 256. Quebec: Universite de Sherbrooke, 2000.

[11] ALFIMTSEV, A. N., SAKULIN, S. A., LOKTEV, D. A., KOVALENKO, A. O., DEVYATKOV, V. V. Hostis humani ET mashinae: adversarial camouflage generation. *Journal of Advanced Research in Dynamical and Control Systems* [online]. 2019, **11**(2), p. 382-392. ISSN 1943-023X. Available from: http://jardcs.org/abstract.php?id=320
[12] HU, H., HAAN, G. Low cost robust blur estimator. IEEE International Conference on Image Processing : proceedings [online]. 2006. ISBN 978-1-4244-0481-0. Available from: https://doi.org/10.1109/ICIP.2006.312411
[13] Zaman, T. Depth estimation from blur estimation. Delft: Delft University of Technology, 2012. Available from: https://pdfs.semanticscholar.org/dbf5/e58c54fe68591bf749d22b5ac002ca8cfe38.pdf
[14] LIN, H.-Y., CHANG, C.-H. Depth from motion and defocus blur. *Optical Engineering* [online]. 2006, **45**(12), p. 127201-1-127201-12. ISSN 0091-3286, eISSN 1560-2303. Available from: https://doi.org/10.1117/1.2403851
[15] BORACHI, G., CAGLIOTI, V. Motion blur estimation at corners. 3rd International Conference on Computer Vision Theory and Applications : proceedings. 2008. ISBN 978-989-8111-21-0.
[16] SCHAPIRE, R. E., FREUND, Y. Boosting: foundations and algorithms. Massachusetts: MIT Press, 2012. ISBN 978-0-2620-1718-3.
[17] BOURLAI, T., MAVRIDIS, N., NARANG, N. On designing practical long range near infrared-based face recognition systems. *Image and Vision Computing* [online]. 2016, **52**, p. 25-41. ISSN 0091-3286. Available from: https://doi.org/10.1016/j.imavis.2016.04.013
[18] CHANG, H., HARIHARAN, H., YI, M., KOSCHAN, A., ABIDI, B., ABIDI, M. An indoor and outdoor, multimodal, multispectral and multi-illuminant database for face recognition. IEEE Computer Society Conference on Computer Vision and Pattern Recognition : proceedings [online]. 2006. ISBN 978-0-7695-2646-1. Available from: https://doi.org/10.1109/CVPRW.2006.28
[19] ROSSIKHIN, YU. A., SHITIKOVA, M. V., LOKTEV, A. A. The analysis of thin-walled building structures subjected to impact excitation. 4th International Ph.D. Symposium in Civil Engineering : proceedings [online]. 2002. Available from: https://doi.org/10.1002/stab.200201020
[20] CHERNOYAROV, O. V., BREZNAN, M., TEREKHOV, A. V., Restoration of deterministic and interference distorted signals and images with use of the generalized spectra based on orthogonal polynomials and functions. *Communications - Scientific Letters of the University of Zilina* [online]. 2013, **15**(2A), p. 71-77. ISSN 1335-4205, eISSN 2585-7878. Available from: http://komunikacie.uniza.sk/index.php/communications/article/view/34
[21] LOKTEV, A. A., BAKHTIN, V. F., CHERNIKOV, I. YU., LOKTEV, D. A. Method of determining external defects of a structure by analyzing a series of its images in the monitoring system (in Russian). *Vestnik MGSU*. 2015, **3**, p. 7-16. ISSN 1997-0935, eISSN 2304-6600.
[22] LOKTEV, D. A., LOKTEV, A. A. Determination of object location by analyzing the image blur. *Contemporary Engineering Sciences* [online]. 2015, **8**(9), p. 467-475. ISSN 1313-6569, eISSN 1314-7641. Available from: http://dx.doi.org/10.12988/ces.2015.52198
[23] ALFIMTSEV, A. N., LOKTEV, D. A., LOKTEV, A. A. Comparison of methodologies for developing systems of intellectual interaction (in Russian). *Vestnik MGSU*. 2013, **5**, p. 200-208. ISSN 1997-0935, eISSN 2304-6600.
[24] CHERNOYAROV, O. V., KUTOYANTS, Y. A., MARCOKOVA, M. On frequency estimation for partially observed system with small noises in state and observation equations. *Communications - Scientific Letters of the University of Zilina* [online]. 2018, **20**(1), p. 67-72. ISSN 1335-4205, eISSN 2585-7878. Available from: http://komunikacie.uniza.sk/index.php/communications/article/view/48
[25] DRAKOPOULOS, V. Fractal-based image encoding and compression techniques. *Communications - Scientific Letters of the University of Zilina* [online]. 2013, **15**(3), p. 48-55. ISSN 1335-4205, eISSN 2585-7878. Available from: http:// komunikacie.uniza.sk/index.php/communications/article/view/687
[26] LOKTEV, D. A., LOKTEV, A. A. Development of a user interface for an integrated system of video monitoring based on ontologies. *Contemporary Engineering Sciences* [online]. 2015, **8**(20), p. 789-797. ISSN 1313-6569, eISSN 1314-7641. Available from: http://dx.doi.org/10.12988/ces.2015.57196
[27] LOKTEV, A. A., IZOTOV, K. A., LOKTEV, D. A. The possibility of increasing the bandwidth of fiber-optic communication lines. Moscow Workshop on Electronic and Networking Technologies (MWENT) : proceedings [online]. 2018. ISBN 978-1-5386-3497-4. Available from: https://doi.org/10.1109/MWENT.2018.8337243

Michal Titko - Jan Havko - Jana Studena

MODELLING RESILIENCE OF THE TRANSPORT CRITICAL INFRASTRUCTURE USING INFLUENCE DIAGRAMS

The article discusses the possible impact of disasters on functionality of the transport critical infrastructure elements by overcoming their resilience. The aim of the article is to provide an appropriate approach to the resilience measurement through understanding of this close relationship. It was achieved by using combination of (1) a decision-theoretical approach based on Influence Diagrams, which was used as a tool to model functionality disruption level of transportation network elements after disaster impact and (2) the time decomposition of the functionality disruption duration of these elements. Based on this approach, the transportation network element resilience assessment was conducted in form of the transportation element resilience loss. The proposed approach is intended to be applied to the critical infrastructure elements rather than to the transportation network as a whole.

Keywords: *resilience, disasters, risk reduction, critical infrastructure, transportation, influence diagrams*

1 Introduction

Over the last decades, there is a considerable research interest and ongoing discussions on the topic of the transportation network (TN) resilience from both practitioners' and academic communities. Several approaches to the TN resilience understanding and measurement have been proposed and the variety of research perspectives including those from the disaster or hazard perspective were introduced. The resilience of the TN has become an important issue in ensuring operational continuity [1] of the TN and in providing of a TN key function - to provide means to move people and goods between the origin and destination [2-3].

Importance of resilience issue increases with severity of possible consequences caused by a TN disruption. Under certain circumstances, the disruption of the TN can cause problems in ensuring the national priorities such as economic sustainability [4] and growth, human welfare [4], social development, providing security and public order [5-6], operational capability of the armed forces [5]; it plays a critical role in delivering disaster relief or facilitating mass evacuations, but plays an important role in disaster management, as well [7-9]. Those examples of consequences can be relevant only (1) in cases of the large-scale disruptions of a TN or (2) for a small part of a dense TN of every state, which can be considered as truly important. The second option results in identification of the critical infrastructure (CI) notion - a subset of the transportation infrastructure that is of the particular importance and interest, which is of interest in this article.

Based on relation of a TN element performance/functionality disruption, caused by a disaster and its resilience overcoming, this paper describes the approach to the resilience measurement suitable for the transportation CI elements. That implies focus on the resilience of TN elements in particular, rather than the TN as a whole. There are still properties of the systematic approach in form of demand change distribution after a disaster occurrence. From this reason, but not limited to, a decision-theoretical approach, based on Influence Diagrams (IDs), was used in this paper. It was used as a tool to model functionality disruption of the TN elements after disaster occurrence. It is argued that the use of IDs can address two important aspects of resilience modelling: (1) provide an improved framework for the risk and resilience assessment through more elaborate combining probabilities and measures of disruption levels after a disaster with respect to not only a direct influence (loss of capacity due to disaster) but also to often neglected an indirect influence of a disaster (change of demand distribution in TN) and (2) facilitate knowledge elicitation from human experts through a structured approach to the problem. Moreover, the approach is complemented by the time decomposition of the functionality disruption duration of the TN elements with respect to all the relevant resilience features (robustness, redundancy, resourcefulness, responsiveness, recoverability).

2 Background and rationale

The resilience concept originated from ecology [10-11] and has been continuously enhanced into other areas [12], e.g. business and economics [13], telecommunication systems [14], power systems [15-16], production systems

Michal Titko[1,*], Jan Havko[2], Jana Studena[1]
[1]Faculty of Security Engineering, University of Zilina, Slovakia
[2]Henkel Slovensko, Bratislava, Slovakia
*E-mail of corresponding author: michal.titko@fbi.uniza.sk

and supply chains [17], water distribution systems [18], health care systems [19], as well as infrastructure systems in general [20]. There are several applications and approaches to the resilience assessment in transport [21-28] and transportation systems. In technical systems, resilience is perceived as an ability of the system to absorb disturbance, to tolerate the negative changes of the system, while ensuring the basic (essential) functions, structure and identity of the system [29].

Resilience of the CI is rather new and has been intensified especially due to increasing dependency of societies on critical infrastructures services [30-31] and in terms of disasters, such as Fukushima disaster. According to Bruneau et al. [32] and O'Rourke [33], the CIs would be resilient if they were characterized by systems that are robust (robustness), redundant (redundancy), resourceful (resourcefulness) and capable of rapid response (responsiveness or rapidity). Based on the research approach of different authors and subject under analysis, there can be found other features, which characterize resilience of a system (e.g. preparedness/preparation [34-35], recoverability [34-37], absorption [38], adaptation [37-38]). In definition and description of all the mentioned features, an overlapping and similarities in explanation can be observed. For the purpose of the paper and better understanding of the main features used for the following resilience assessment, their definitions are provided:

- robustness - the inherent strength (also resistance [33]), or the ability of elements, systems and other measures of analysis to withstand a given level of stress or demand without suffering degradation or loss of function [33, 39-40],
- redundancy - the extent to which elements, systems, or other measures of analysis exist that are substitutable, i.e., capable of satisfying functional requirements in the case of disruption, degradation, or loss of functionality [15],
- resourcefulness - the capacity to identify problems, establish priorities [39], mobilize needed resources and services in emergencies [33, 39] and mobilize resources in the process of recovery [39].
- responsiveness - the capability of the system to respond to changes of an environment and activate the forces and means [36] aimed at dealing with the impacts of disaster in order to protect an CI element functionality. In this article is argued that more resilient system response activities should start before a disaster occurs (when risk determinants change), followed by elimination of the function degradation activities in time of the disaster effects.
- recoverability - responsiveness is continuously followed by renewal (recovery) of the element main function. It is the ability to recover the desired functionality level after a disaster [34, 36]. Some authors understood recovery processes as the part of responsiveness feature [33, 39], but in opinion of these authors the recovery processes differ greatly from response activities and therefore they should be assessed separately.

Apparently, all the features can be divided into two main groups: (1) features which represent inner (structural) ability of the system or element to withstand the negative effects of a disaster - robustness, absorption and redundancy; (2) features which represent external ability of responsible authorities (crisis managers or object operators) to protect and recover main function of a particular element - preparedness, responsiveness, resourcefulness, recoverability, etc. This categorisation will be address in the following assessment because it is important to consider the fact that a CI element can suffer operational disturbance (e.g. due to high snow level) but it still can be without structural damage.

Differences between resilience assessment approaches and frameworks mentioned above are basically in assessment methodology and final expression of resilience. In majority of quantitative methodologies a large number of properties are needed [41], which seems to be one of the main inconveniences within resilience evaluation that should be addressed. From disaster and hazard perspective, is very important to capture stochastic nature of disaster occurrence and its influence on resilience evaluation. Moreover, here is argued that the particularities of a system/subject under analysis (within this paper it is dealt with the TN elements and CI elements in particular) should be more precisely incorporated into resilience assessment in order to propose an appropriate approach for that system/subject assessment. In order to address all of these features in resilience assessment, a new modified approach is proposed, which is based on Influences Diagrams (IDs).

3 Methodology - approach to transportation element resilience assessment

Resilience reflects the ability of an element or a system to ensure its function(s) in conditions of effects of external and internal factors [42]. The effects of a threat can disrupt the core function(s) of the system, in this case the transport system with core function ensuring population mobility and goods movement [3, 5], by overcoming the resilience of the element. To what extent the resilience is distorted/disturbed, to a corresponding extent the functionality and operability of the CI element is disturbed too. This rate of disruption is assumed as one of variable for expression of resilience. The functionality range from 100% (full performance) to 0% (total disruption) is assumed. Moreover, there are significant differences in cases of short-term and long-term functionality disturbance and therefore it is claimed that the time factor (time variable) should be incorporated into the resilience assessment.

Following the mentioned facts, the two main variables of the TN element resilience assessment are assumed, namely:

- to what extent the functionality of an element may be disrupted (if ever) - *Disruption rate assessment*,

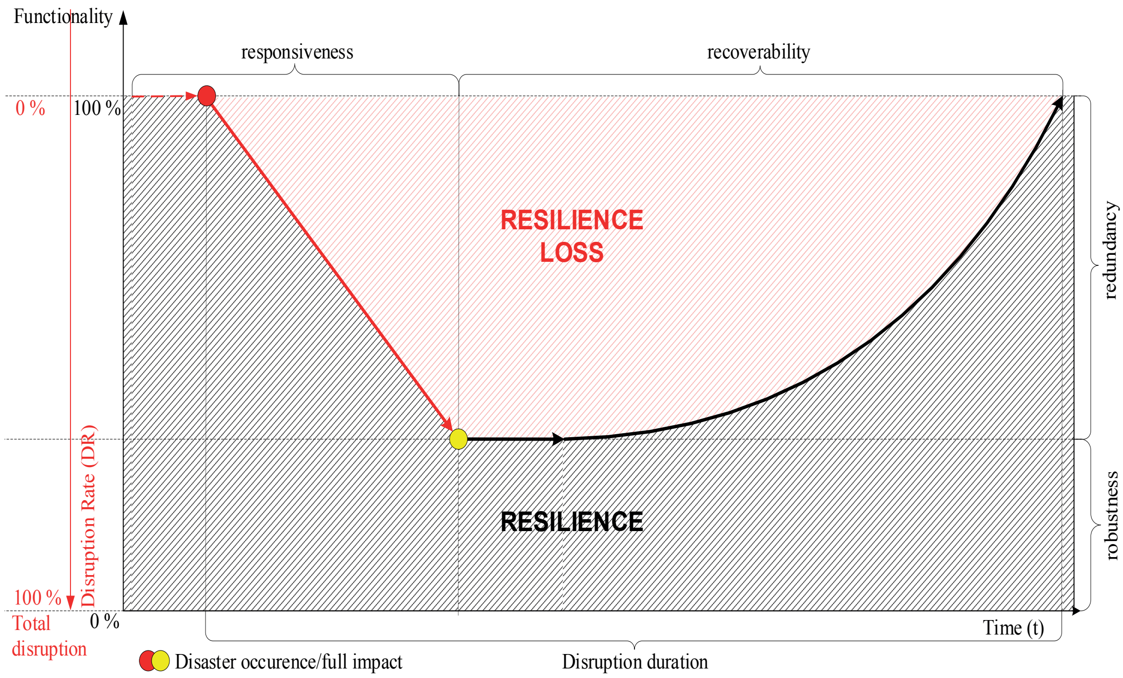

Figure 1 *Example of a TN element disruption profile with incorporating corresponding resilience features - conceptual definition*

- how long a disruption may take - *Disruption duration assessment.*

Several studies have proposed infrastructure disruption profile [34-35, 37, 41, 43-44] to capture resilience or resilience loss, each with some common (normal conditions, disruption state, recovery) and specific issues considered. Such a profile seems to be an appropriate tool to illustrate and capture the basic relations between variables which define a notion of resilience. In order to capture relation between here defined variables (disruption rate and disruption duration), taking into account all the resilience key features, the concept illustrated in Figure 1 is used as a conceptual definition of resilience notion. This concept is closely described in sections 3.2-3.6.

As shown in Figure 1, resilience is of a continuous nature (keeps the same value if nothing happens), so it will be more appropriate to evaluate the resilience of the TN element by expressing its predicted loss rate. Therefore, the loss of the CI resilience can be measured as the expected loss in quality of its provided function (*Disruption Rate - DR*) over the time (*Disruption Duration - DT)* [33], simply captured in equation:

$$Resilience\ Loss = f(DR, DT), \qquad (1)$$

The purpose is to produce a numeric measure that would quantify the notion of resilience.

3.1 Disruption rate

In order to express the Disruption rate of a TN element within resilience assessment, it should be clear what will be understood as a failure or functionality disruption. A disruption of a transportation element can be defined in terms of reliability of an element to perform its main function [7]. As an important characteristics of the CI element to perform its function is considered its capacity [9]. The possible loss of that quantity can be considered as a failure measure. Basically, the reduction or the loss of capacity can be caused by physical (structural) damage or physical obstacles on the road. Moreover, there is the second performance issue we should take into consideration - an ability of a TN element to satisfy the transportation demand. The rate of satisfaction of that need is assumed as the second failure measure. Therefore, the two main aspects of the CI elements functionality disruption are assumed:

- direct disruption, which is understood as the impact on CI element capacity - *Capacity loss*,
- indirect disruption - change in traffic distribution resulting in effects on demand on a TN element or the TN as whole - *Demand change.*

Both impacts have an effect on the main function of a TN element and therefore their combination can provide overall value for the TN element functionality loss - called the *Disruption rate.* However, while the Capacity loss is considered only in a negative perspective (only loss of the capacity is considered), Demand change can be considered in a positive perspective, as well (a positive effect on the TN element functionality) because hazard and disaster effects may result also into decreasing demand on the TN. In order to capture these different perspectives, we assume Influence Diagrams as an appropriate tool to model Disruption rate. The modelling procedure is described in subsection 3.1.3.

***Table 1** Categorisation of Capacity loss*

Levels of Capacity loss	Explanation
Nominal or no limitation	Managing the situation by common means, maintenance and management; comparing the maximum construction capacity and the utilization rate of the transportation element; some TN elements have a reserve that guarantees the required capacity despite the disaster.
Low limitation	Effect on traffic capacity is low - remaining capacity is able to handle the traffic demands with some minor delays resulting from the reduced speed limit, rescue activities, etc.
Significant limitation	Traffic demand is not fully satisfied or it is satisfied with significant delays - there are delays due to obstacles (debris) on the transport element, or due to transport route conditions; for some types of vehicles (e.g. trucks) the transition can be temporarily disabled - the alternative routes are applied (redundancy feature takes place).
Partial collapse	Complete loss of the capacity - due to structural damages (on surface, static, etc.) use of an element is forbidden and long-lasting disruption is assumed.
Total collapse	Complete loss of the capacity - in the worst cases destruction of an element without recovery option is assumed.

The Disruption rate is considered as an overall failure measure and represent a loss in quality of provided function by the TN element. A scale from 0 to 1 (with the corresponding transformation into percentage values from 0% to 100%) is assumed for the Disruption rate, with increasing values indicating higher functionality loss.

3.1.1 Capacity loss - the direct disruption of the functionality of the transport critical infrastructure

There are several reasons causing transportation element capacity reduction or loss. They are mainly external - disasters, traffic accidents, etc., or internal - incidents, maintenance and repairs. The rate of loss is dependent on the disaster type, its intensity and severity. The scope of present assessment are external triggers, especially disasters and man-made incidents (e.g. floods, earthquake damages, heavy snow load, wind storm, traffic accident, etc.), while the internal factors can also cause long-lasting capacity reduction, but the realisation is scheduled (repairs) and appropriate measures are put in place to prevent traffic complications. The capacity loss rate can be categorised as it is shown in Table 1.

3.1.2 Demand change - the indirect disruption of the functionality of the transport critical infrastructure

In addition to the direct impact of a disaster on capacity, each hazard can produce *demand* on the TN (cause people to use transportation network). Demand on a TN element can be decreased as well as increased which also depend on current situation, disaster location, the possibility of using both driving directions in case of mass evacuation and other TN links availability [6], etc. The demand factor, whether increased or decreased, has influence on the TN element performance only and causes no structural damage to a TN element. If a disaster or accident causes a decreased demand on a TN element, it could have a positive effect on the resilience rate and vice versa. To withstand negative effects of a demand change could be a case for more TN elements (due to already rising traffic intensity in normal conditions), for the CI elements in particular. Therefore, it seems to be a necessary variable to be taken into account within the resilience assessment. Basically, one understands the ability to manage demand change distribution over the TN as the redundancy feature of the TN element resilience. For the demand change factor the following levels are assumed: Lowered, Normal, Increased and Mass Evacuation. Changing demand (if one expects any level of increased demand) for a given TN element can be addressed by other elements of the network, among which the changed demand is distributed [45]. In order to ensure replacement of the disrupted element, in some cases, the element can be temporarily replaced by a makeshift element (e.g. a makeshift bridge); usually it would be an element with lower capacity serving as a temporary substitution; sufficient for the time being. Planning such a measure can increase redundancy of the whole TN and an element in particular.

3.1.3 Modelling disruption rate using influence diagrams

The influence diagram is a probabilistic decision model that is a more compact representation of a decision problem than a decision tree [46]. The ID captures dependencies between variables in the modelled domain, which seems to be appropriate to capture relationship between direct and indirect disruption of the functionality of the CI transportation element. This property allows for more compact and efficient (especially in terms of knowledge elicitation) representation of the problem, implying that it is suitable for larger scale decision problems.

There are three types of variables (nodes) in ID: (1) chance nodes that capture unknown events and relevant probabilities including probabilistic dependencies (by means of conditional probabilities), (2) utility nodes that

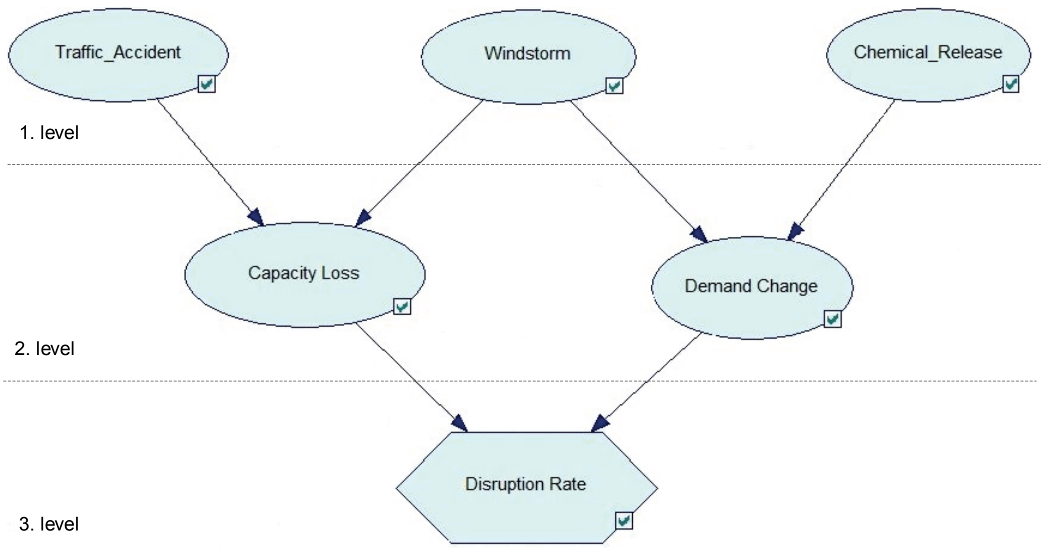

Figure 2 *A simple example of the ID model*

Table 2 *An example of model definition for the node Capacity loss*

Windstorm	Present		Absent	
Traffic accident	Present	Absent	Present	Absent
Nominal or No Limitation	0.05	0.1	0.045	1
Low Operability Limitation	0.35	0.5	0.45	0
Significant Operability Limitation	0.59	0.395	0.5	0
Partial Collapse	0.008	0.004	0.004	0
Total Collapse	0.002	0.001	0.001	0

Table 3 *An example of model definition for the node Demand using the noisy-average model*

Parent (Weight)	Chemical Release		Windstorm		LEAK(1)
State	Present	Absent	Present	Absent	
Lowered	0	0	0.3	0	0
Normal	0.2	1	0.7	1	1
Increased	0.3	0	0	0	0
Mass Evacuation	0.5	0	0	0	0

encode utilities (which can be costs, profits, etc.) that define user's preferences over the set of outcomes and (3) decision nodes that define elements of the domain over which the decision maker has the complete control [47].

To model the overall disruption of the CI element functionality it is proposed to define a measure which capture this quality (Disruption rate). In order to define this rate a structured approach, based on IDs, is proposed. We assume a fixed three-layer network structure of an ID. Nodes that correspond to threats are placed in the top layer. The middle layer of the network always includes two nodes, corresponding to the direct (Capacity loss) and indirect (Demand change) impact on the TN element functionality. In the lowest layer a single utility node (Disruption rate) would be placed that would combine the effects of Capacity loss node and Demand change node. A simple example of the ID model is shown in Figure 2.

A lot of different research approaches related to the resilience assessment are based on the subject matter experts (SMEs) (represent by relevant stakeholders) opinions, consultations, or evaluations [e.g. 48-49]. Involving the SMEs into several steps within the IDs modelling is assumed. In the first step of modelling, a list of possible threats should be produced. This can be done by the SMEs familiar with given TN and with the concept of risk assessment, or by selection of pre-defined threats, which are of particular interest. Threats are assumed to be binary (present or absent) and quantified by asking the SMEs to provide probability of the threat occurring.

It is argued, as some authors [50-51], that a system might be vulnerable to certain events but be resilient to

***Table 4** An example of definition for the utility node - Disruption rate*

Capacity	Demand			
	Lowered	Normal	Increased	Mass Evacuation
Nominal	0	0	0.2	0.7
Low Operability Limitation	0.05	0.25	0.5	0.8
Significant Operability Limitation	0.5	0.7	0.8	0.9
Partial Collapse	1	1	1	1
Total Collapse	1	1	1	1

others. Therefore, it is important to take into account the specific risk and threat profiles to the area under analysis. Moreover, the occurrence of multiple events at once is highly unlikely, of course, if one omits the possibility of a synergic effect; e.g. occurrence of the earthquake and flood at the same time is very unlikely, but combination of a snowstorm and a traffic accident is very likely. From that reason it is assumed that each threat is assessed separately and in the relevant cases combination of the two threats is assumed. That is also dictated by practical considerations, while the burden placed on the SMEs providing probabilities should be limited. In particular, nodes with a large number of parent nodes (a large number of incoming links) should be quantified with a number of exponential probability distributions. This implies that if there are 5 parent nodes (5 threats) to a node (e.g. Capacity loss node) and all of them are binary (have only two states), an SME would be required to provide $2^5 = 32$ probability distributions, what would be hardly feasible in practice.

Next step is to designate if the threat has a potential to directly affect a TN element, i.e. to block, damage or destroy road surface, etc. The SMEs would need to provide corresponding probabilities. Similarly, the SMEs would need to define if the threat can result in increased (even mass evacuation) or decreased traffic - if the demand on the TN element can be affected and provide corresponding probabilities. The states of the nodes would be as mentioned above: Nominal, Low Operability Limitation, Significant Operability Limitation, Partial Collapse and Total Collapse for the Capacity loss node and Lowered, Normal, Increased and Mass Evacuation for the Demand change node. Examples of Capacity loss node and Demand change node are illustrated in Tables 2 and 3.

As it is shown in Tables 2 and 3, there are significant differences in definition of both nodes. In order to reduce the number of parameters required to specify the ID model and properly capture relevant interactions between the variables, it is decided to set at least the Demand change node as the noisy-average node, which is available in GeNIe software and allows reducing the number of parameters required to quantify the model from exponential to linear in the number of parent nodes (the Capacity loss node does not meet the required conditions for noisy-average node because a threat cannot increased the capacity of the TN element, it can only decrease its capacity - see following conditions). The noisy-average nodes are suitable for the modelled interactions between variables (nodes) where the following conditions are met [46]: (1) the parent nodes have a state that describes the 'normal' state (there is no snowstorm, no flood, etc.), (2) the child node has a 'normal' state, as well (corresponding to typical traffic patterns or the level of traffic flow for which the road was designed), (3) for the child variable the deviation from the 'normal' state can be in both increased and decreased values. The way the influences are combined is achieved by averaging (hence the name), which means that no single parent variable is assumed to have stronger influence on the state of the child variable than the other parent variables.

The last step is to combine the direct and indirect impact of the threat(s) on the TN element functionality. The utility node (Disruption rate) merging the Capacity loss and Demand change can be defined as it is shown in Figure 2. The probability values are again required to be produced by the SMEs (e.g. in Table 4).

3.1.4 Calculation of the disruption rate

In order to understand how the approach works, an example of the ID model is considered that assumes 3 different threats: Traffic Accident, Wind Storm and Chemical Release. As it is shown in Figure 2, the three options are considered by which a threat can affect the child nodes (second level/layer):

- a threat can affect only the capacity of the TN element, e.g. a Traffic Accident has a potential to affect capacity of the TN element, but it does not produce a demand on a system;
- a threat can affect only the Demand, e.g. an incident associated with the release of chemical substance (Chemical Release) can result in forcing people to leave the threatened area (some form of evacuation) and incur heavy load on the TN, but it is assumed that the infrastructure is able to withstand such a release with no noticeable effects on it;
- a threat such as Wind Storm can affect both variables, Capacity as well as Demand, because there is a chance that some transportation links could be blocked or damaged due to trees or other obstacles and there is still a possible change in demand, in both directions, increased if evacuation is needed or decreased if people will be afraid of using the TN in such weather conditions and at the same time they will feel safe at the current position (home, work, etc.).

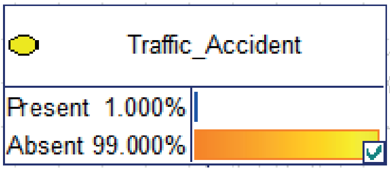

Figure 3 *Probability of a traffic accident occurrence*

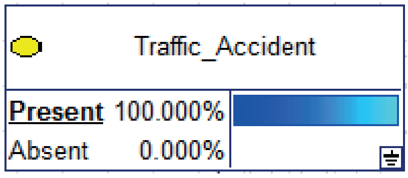

Figure 4 *The instantiated node - traffic accident is present*

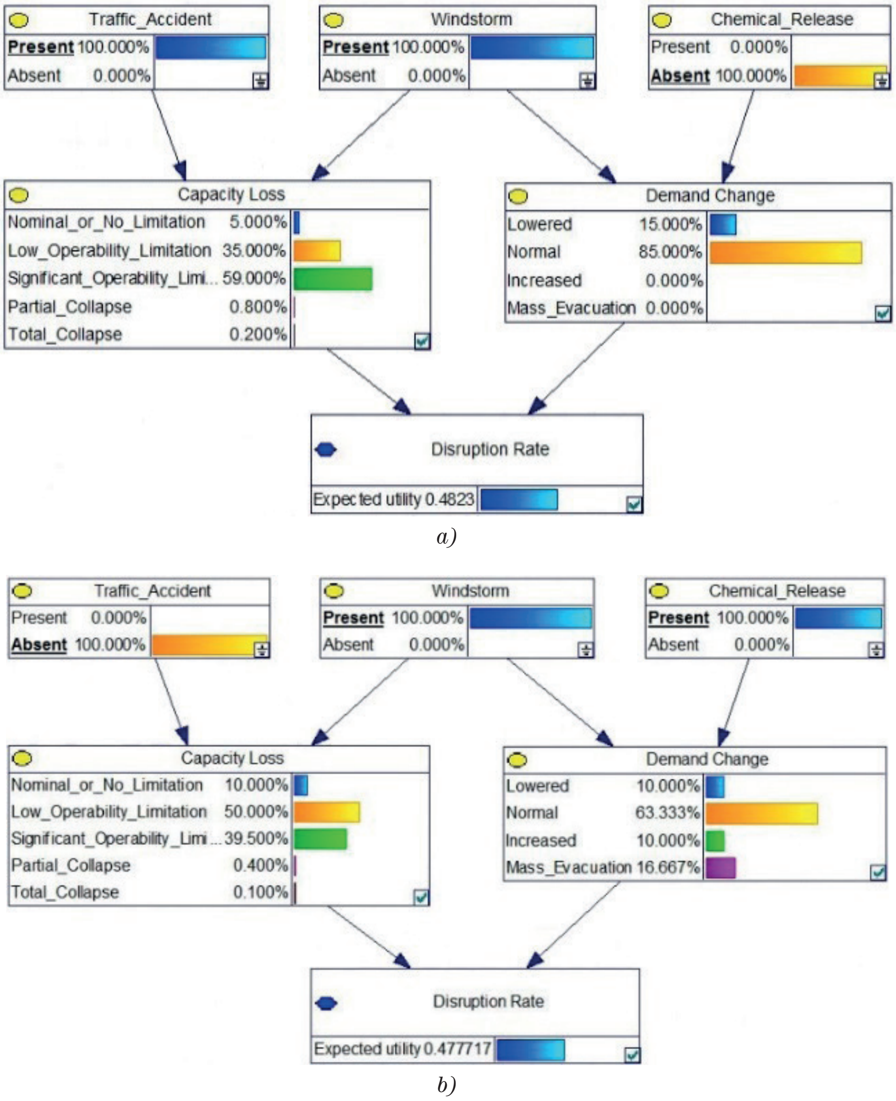

Figure 5 *The ID model for calculation of the Disruption rate for two (present) threats combination*

For each threat corresponding probabilities of occurrence are provided: e.g. Traffic Accident: 0.01, Wind Storm: 0.001, Chemical Release: 10^{-5}. In order to calculate resilience to certain events (threats) the idea that some of the events should be considered as "present" is implied, rather than to calculate with probability of their occurrence. This is dictated by the interest to assess the resilience of the TN element "when" a threat occurs rather than "if" it occurs. Using of the IDs allow for such a dynamic calculation (see example of difference in Figure 3 - probability of occurrence; and Figure 4 - the instantiated node - traffic accident is present) which can be consider as the IDs benefit. The same setting option is available for the second layer as well, e.g. it is possible to set a state of Demand change node to Mass Evacuation or to set a state of Capacity loss node to Partial Collapse, etc.

For the sake of an example, the two cases are analyzed: (1) combination of present threats Traffic Accident and Wind Storm at the same time (Figure 5a); (2) combination of present threats Wind Storm and Chemical Release at the same time (Figure 5b).

Following the values from Table 4, in the Disruption rate node will show up the probabilistic dependencies of child nodes and parent nodes, by means of conditional probabilities, so expected values will vary based on the probabilities of the child nodes. The expected utility value

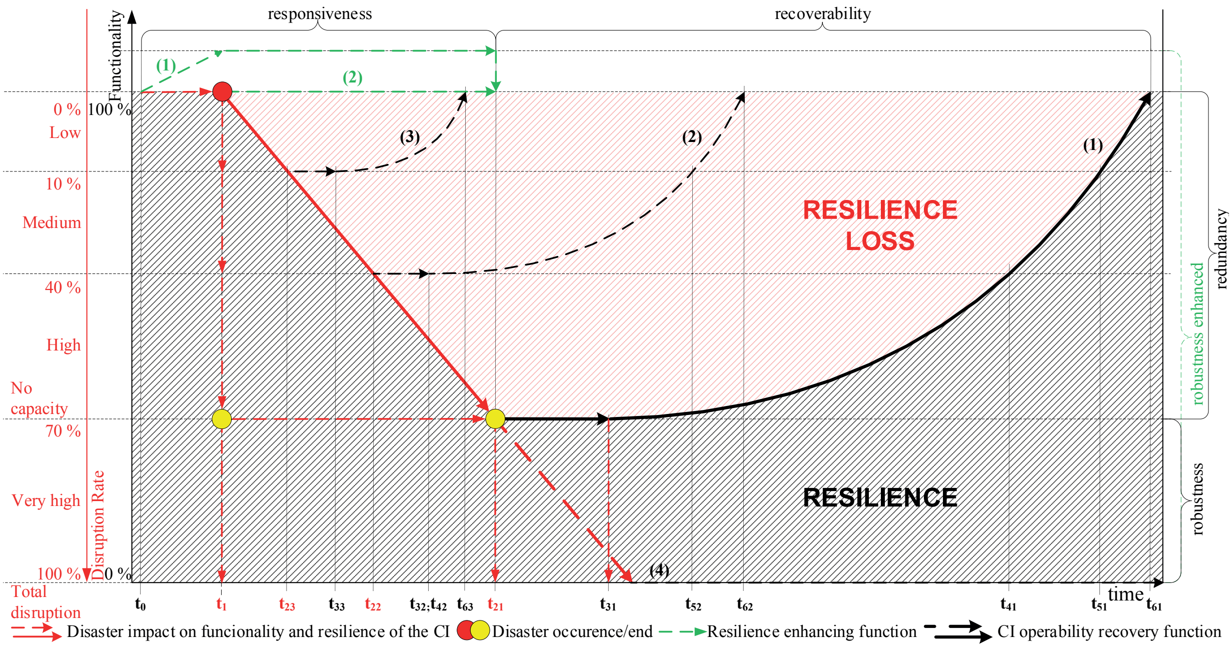

Figure 6 *The time decomposition of a CI element disruption profile in relation to overcoming its resilience*

of the Disruption rate node reflects the potential impact of an extraordinary event on the functionality of the TN element, considering only its robustness and partially absorption capacity. It does not reflect other resilience features. Therefore these features are included into resilience assessment separately and within the Disruption duration part.

3.2 Disruption duration - time decomposition of the CI element functionality disruption

Except for the extent of a TN element disruption, the time aspect related to that disruption is necessary to take into consideration [52], since with increasing duration of the disruption, resilience is lower [34]. Globally, the time aspect of a TN element resilience, in this case called the Disruption duration, will vary based on resilience features. A broad measure of the TN elements resilience which captures influence of those resilience key features and their relation to a TN element functionality can be expressed in form of the time decomposition profile illustrated in Figure 8. Basically, there are two resilience features, responsiveness and recoverability, that directly express disruption duration of a TN element. In most cases, the disruption duration of a TN element functionality is the same as the time needed to the recover element functionality. Therefore, the recovery activities decomposition towards the overall renewal of the TN element will be introduced as the most important part of Disruption duration. Of course, in cases where there is a gradual loss of functionality over disaster impact, we will also consider that time as a part of overall resilience loss assessment.

Figure 1 also shows the connection between the robustness (partially also redundancy) and the possible functionality loss (explained in section 3.1. Disruption rate), where the loss of the robustness means the loss of the functionality. From the time perspective, the dependencies are visible as well. For example, in the worst scenarios with expected great disruption of robustness (higher level of Disruption rate), the Disruption duration is expected as longer lasting and vice versa. This assumes a certain level of dependence between the Disruption rate and Disruption duration. However, there are two issues to be aware of: (1) this logic would only apply to physical damage to the element and at the same time the condition that the elements being considered are equally large (structurally similar, with similar technical conditions) must be met - this will guarantee similar robustness; (2) otherwise, in the case that only the capacity of an element is affected, the duration of the functionality reduction depends primarily on the threat, which caused the disruption - significant differences in the recovery duration after exposure to various threats (traffic accident, snow storm, wind storm, flood, etc.) are assumed. It is possible to omit the given conditions - this would imply a certain degree of the results distortion, but at the same time it will simplify the estimation of the Disruption duration.

For the better understanding of resilience loss profile (Figure 6), the following explanations of resilience features with related time periods are provided.

3.3 Responsiveness feature in resilience concept t_{2n}-t_0

Responsiveness represents the capability of the system to activate the forces and means aimed at restoring the function of the system [34, 53] and at prevention of a situation deterioration. It is expressed by the time (responsiveness period) between the occurrence of an emergency, or even before (when the event is likely to happen) and the end of degradation elimination process and consequently its renewal [36] which can be considered as an overlapping with recovery. The two main time periods within the responsiveness are assumed - "risk factors change period" and "impact period".

Risk factors change period (t_1-t_0)

Risk factors change period and the whole responsiveness period are closely interconnected and will therefore be continuously explained. Continuous monitoring of internal and external environment development supports identification of changes that could have an undesirable effect on the system functions or processes in time. Early and proper assessment of risks or risk factors change is a prerequisite for taking adequate measures to increase the level of system resilience to such effects. The process of monitoring and evaluating changes of risk factors can be carried out together with (or even rather before) a possible response to both foreseeable and accidental crises. Responsiveness is therefore dependent on the prevention measures, preparedness level of the responsible authorities, rescue forces and availability of resources in order to address the crisis.

Impact period = t_{2n}-t_1; t_{2n}-t_0

Impact period can be characterised as the time period during which the devastating and destructive features of disaster are manifested and absorption ability of a TN element is exceeded. The result is different degree of functionality loss (red arrows in Figure 6.). Depending on the exposure rate, intensity of a disaster and vulnerability of a particular TN element, two types of functionality loss can be distinguished: (1) immediate and (2) continuous.

- immediate loss of functionality - change of risk factors is rapid (t_1-t_0 can be technically 0) and often unforeseeable. In a very short time, the effects of a disaster will be present - the consequences are immediate. There is very little time to take measures to reduce the consequences before disaster. As a result, various levels of functional impairment of the TN element may occur (Disruption Rate levels) - depending on the intensity of a disaster (shown by the red vertical dashed function). In such cases, responsiveness is very limited. Rapid loss of resilience can be observed.
- continuous loss of functionality - mostly related to a known threat resulting into a disaster with cumulative impact over a longer time period (cumulative high precipitation resulting into a continuous flood) or with progressive intensity development (wind storm with increasing speed over time). It is possible to take preventive measures (green vectors) and temporary increase the level of infrastructure resilience (enhance robustness feature or redundancy). Measures can be taken also during a disaster impact period (t_{2n}-t_1) - there is a time to respond depending on the capability of rescue services and available resources. Such events can be predicted to a certain extent. Important elements, such as the CI elements, can be better protected.

As it was mentioned before, on the graph (Figure 6), possible positive changes (green vectors (1) and (2)) are also shown as an option to increase the TN element resilience level. It can be done by (a) enhancing robustness of an element (e.g. dams building against flood, adjustment of nearby surroundings, etc.); (b) enhancing redundancy of an element (e.g. prepare a plan for makeshift bridge placement and building); (c) enhancing resourcefulness - all mentioned and other actions require provision of necessary material and human resources. In order to realise such an action and use adequate resources before disaster occurs, crisis and disaster planning and procedures are required to be in place (related mainly to CI element protection). In order to facilitate subsequent recovery actions, these measures and actions may be very helpful mainly in the worst case scenarios represented by black function (3) and (2), slightly less in recovery function (1).

3.4 Recoverability feature in resilience concept t_6-t_2

The impact period is continuously followed by the recovery activities. There can be observed an overlapping of impact period with recovery period (phase) as the reaction on an emergency (saving and protecting people, property, environment, etc.) running in parallel with some recovery actions. See for example period t_{21}-t_1 followed by t_{31}-t_{21} where is difficult to set exact end of reaction and start of the recovery phase. It will vary based on a threat severity and suddenness.

The recovery period is divided into several basic steps. In practice, there can be more stages (steps) within the recovery phase, however, in order to generalize assessment for purposes of resilience measurement, these steps can be considered as valid for almost all the scenarios of recovery.

Assessment and preparatory period = t_{3n}-t_2

Period of aftermath assessment and preparatory measures related to the designation of recovery method (restoration of traffic flow, transport capacity, detour, etc.). Disruption rate level remains the same. A lower level of disruption requires a shorter assessment time as the assessment activities are easier. In the worst cases the preparatory period can be as long as preparation of project documents and selection of a contractor. The result of the assessment can be (in the time t_{31}) a rejection of any recovery efforts as well, due to high recovery expenses or due to extensive structural damage.

Temporary recovery = t_{4n}-t_{3n}

The period during which the aim is to restore the transport operability as quickly as possible. Use of the provisional measures is assumed. This phase is designated to achieve the required level of the performance (reduce the

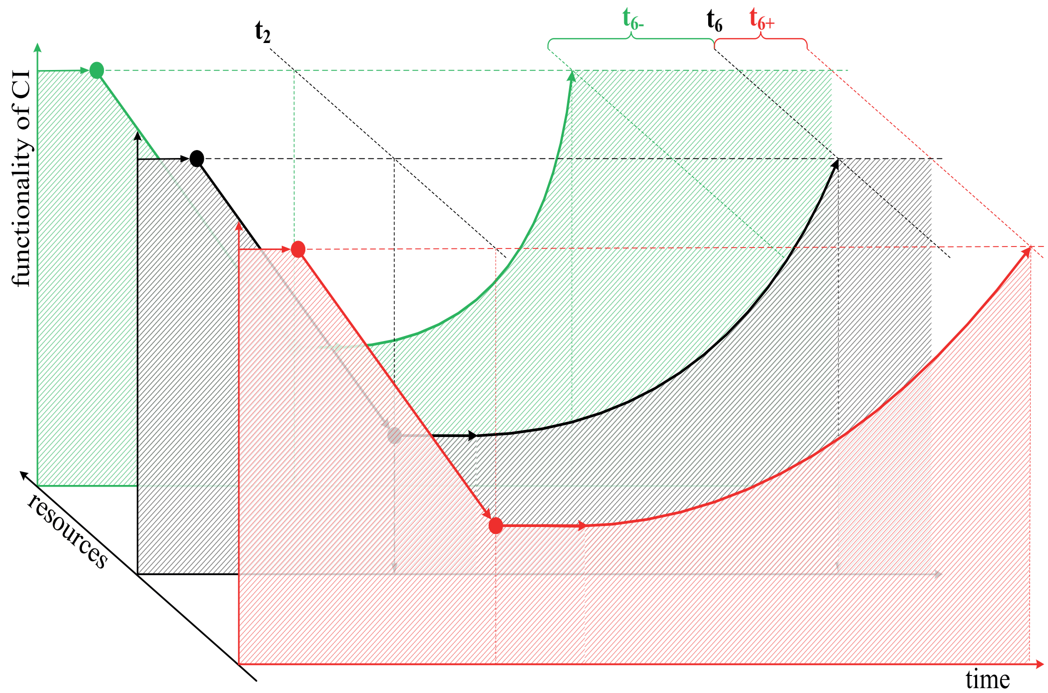

Figure 7 *Possible influence of the resourcefulness on the recovery time and the resilience of the CI (adapted from [32])*

loss of a TN element capacity). As the assumed elements are the CI elements, the common transport capacity is expected to be high and therefore achieving of the required level of performance will be more demanding. Described type of recovery is designated mainly for cases of the high transport capacity loss or in the case of malfunction.

This temporary recovery should bring the TN element into the better state but there still would remain some degree of disruption. For purposes of further calculation, this disruption state will be marked as $DR_{TR.}$

If the transport capacity of the TN element is affected, more resilient elements will be more redundant and another routes will be available to address demand on affected element. It should be stated that the estimated start of the recovery activities is immediate (in Figure 8), however, in practice it may take much more time due to preparation of the documents, inadequate policies or ineffective procedures in the preparatory phase.

Partial recovery = t_{5n}-t_{4n}

All the construction and technical deficiencies or operational obstacles must be removed during this period in order to achieve the full transport capacity. It must be achieved at a higher operating speed (e.g. for rail transport at least 60 km.h^{-1}) but some limitations are still in place.

Similarly, partial recovery should bring the TN element into the better state but there still would be some degree of disruption. For purposes of further calculation, this disruption state will be marked as $DR_{PR.}$

Full recovery = t_{6n}-t_{5n}

The TN element functionality is recovered without operation limitation with full transport capacity and with the designed maximum permissible speed.

3.5 Resourcefulness feature in resilience concept

As it was mentioned, the time necessary for keeping or restoring the functionality of the CI element is dependent on the organisational preparedness of the crisis management (crisis planning, recovery planning, policies in place, etc.). It is represented by the features responsiveness and recoverability. Implementation of prepared procedures and approaches is conditioned by resources (material as well as human resources), which we are at disposal in order to manage the impacts of a disaster. It can be illustrated by the resilience expansion into three-dimension level (Figure 7).

By appropriate allocation and use of resources, the CI functionality loss time (t_{6-}) can be reduced. The time may be reduced in period of the "impacts", as well as in "assessment" period and in all the "recovery" periods. Theoretically, if infinite resources were available, time to recovery would asymptotically approach zero [39]. If the necessary resources are not available, the time of the operability loss can increased (t_{6+}). Resourcefulness and responsiveness (and recoverability) can be seen as the complementary features because without appropriate resources in place, it is impossible to react accordingly, but even if the amount of resources was sufficient, the response or recovery time may be longer due to human limitations, missing or neglected planning, inadequate procedures, operational and organizational failures or ineffective policies [39].

To quantify and mathematically describe resourcefulness some variable can be used, as it is in [39].

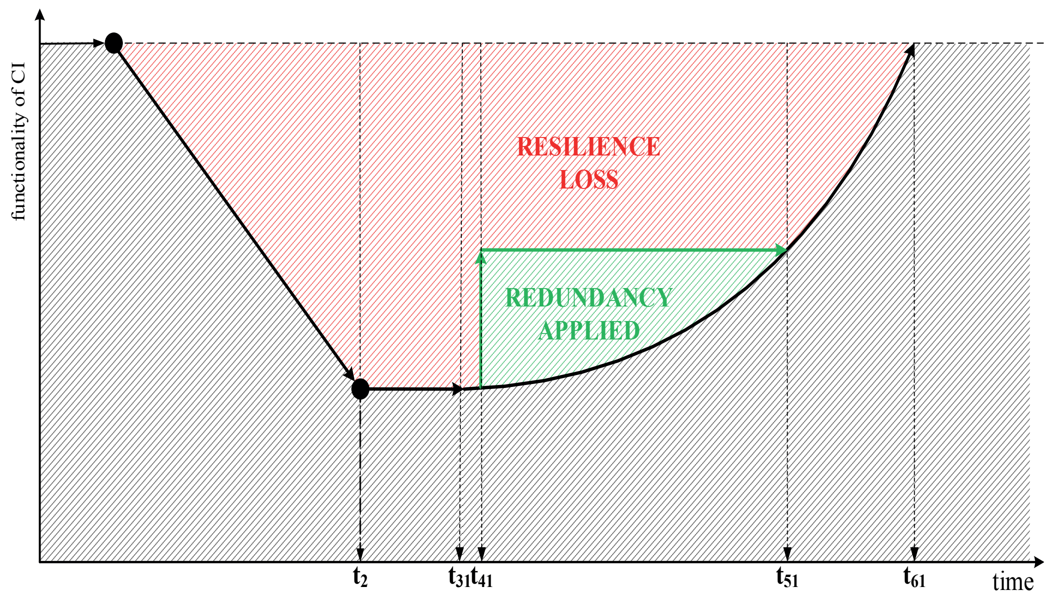

Figure 8 *Redundancy feature applied in resilience concept*

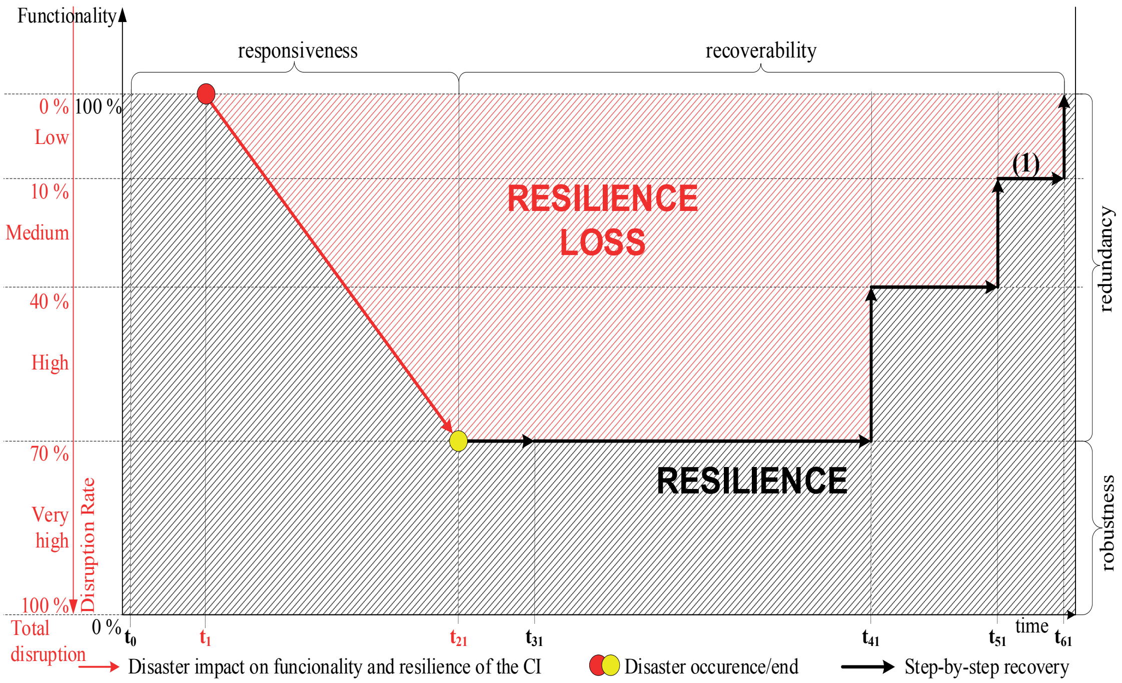

Figure 9 *Resilience profile; step-by-step recovery periods applied*

3.6 Redundancy feature in resilience concept

The TN element is redundant if it can be replaced, for example, a temporary bridge, which replaces a broken one until it is repaired (Figure 8 - green shaded area). However, it is more common in electrical networks, where, for example, in the case of a generator failure, a second one will be ready to replace it immediately. Replacement of individual TN element is not so flexible and therefore more common is use of the TN network redundancy rather than redundancy of a particular TN element. In this case, one can understand redundancy of a TN element as its possible substitution by another element or set of elements within the network - they provide connection to the original destination. This case is addressed within Demand change part, which has already been explained in subsection 3.1.2. The problem arises if such an alternative does not exist or an alternative fails to fully satisfy the demand, or only with great constraints - redundancy is very low or there is no redundancy.

According to Figure 8 redundancy does not shorten the time needed for reparation or rebuilding but it helps the network to reduce the demand for a damaged element. If such resources are at disposal to temporary cope with impacts of disaster on particular element, one can significantly reduce the functionality loss, as well as the resilience loss.

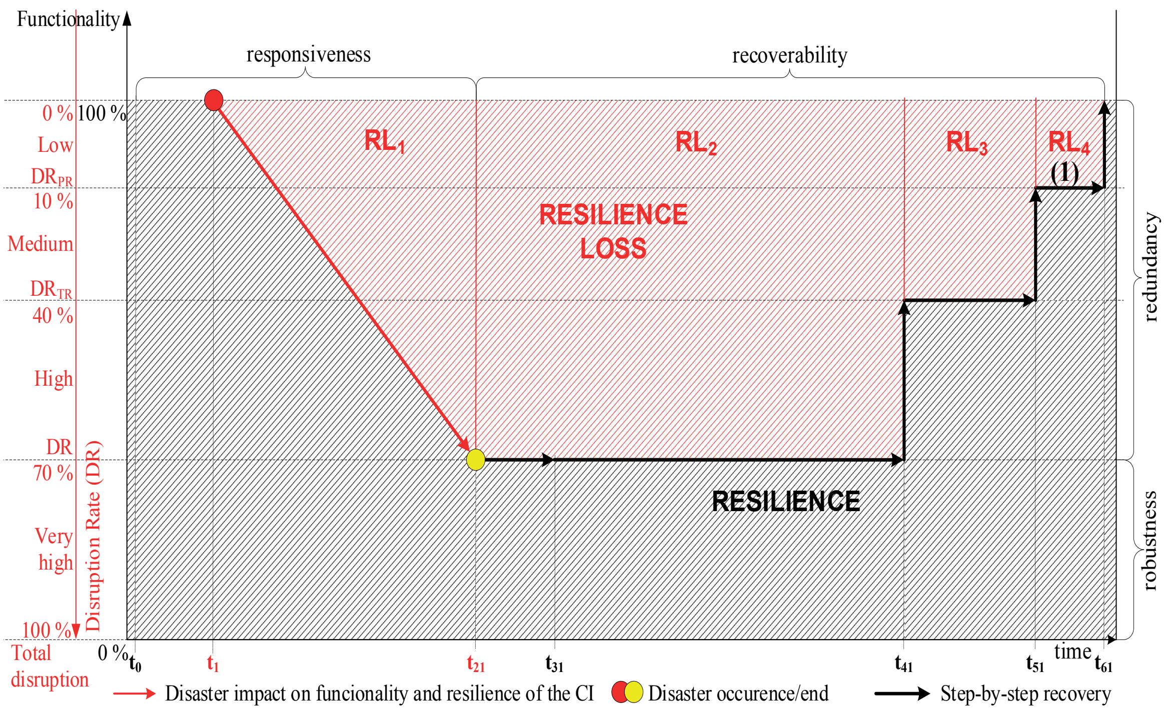

Figure 10 *Resilience profile divided into several parts (for the purpose of calculation)*

3.7 Implementation particularities of transportation system into the resilience assessment concept

Regarding to literature, the authors predominately use the option of continuous recovery function over time for different system under analysis [34, 37, 41, 44]. Here is adopted the idea that recovery of the TN functionality, or its part, or an element in particular, is in practice implemented by completing of different recovery stages, step by step (level by level) rather than continuously. For example, after damages on the road, repairing of one road lane is in progress, so the performance of such an element is let say 50%. When that lane is repaired and no further work is required, then the performance is at some point again 100%. There is no gradual rise from 50% to 100% but “a jump” from 50% to 100%. From this reason, for understanding and measurement of the recovery process duration, as well as for assessment of the resilience loss, a more suitable disruption and recovery decomposition is illustrated in Figure 9 (similarly used in [54]). Three different levels of recovery, corresponding to three defined recovery periods (plus an assessment period) are taken into consideration (see section 3.4). It is argued here that this particularity of transportation system applies for the majority of the disruption cases and it also simplifies the final calculation of the resilience loss.

Unlike the case in Figure 6, the concept illustrated in Figure 9 requires an assessment of individual recovery periods because one needs to estimate the time frame e.g. from t_{31} to t_{41}. Since the resilience assessment is conducted in the safety state, only an estimate can be made. It can be based on evidence of events that have already happened or on qualified experts’ estimates.

4 Results - the measure of the critical infrastructure resilience

As it was mentioned, it is preferred to assess the resilience of the TN element by expressing its loss rate over time (*resilience loss - RL(t)*). The measure of a TN element resilience loss can be expressed in more detailed way using Figure 10, which divides RL into several parts (RL_1, RL_2, RL_3, RL_4).

Mathematically, RL can be defined as a sum of these individual parts within the response and recovery phases:

$$Resilience\ Loss = RL_1 + RL_2 + RL_3 + RL_4\,, \tag{2}$$

In more detailed way:

$$Resilience\ Loss = \frac{1}{2}\int_{t_1}^{t_{21}} DR(t)dt + \\ + \int_{t_{21}}^{t_{41}} DR(t)dt + \int_{t_{41}}^{t_{51}} DR(t)dt + \int_{t_{51}}^{t_{61}} DR(t)dt, \tag{3}$$

where:
DR(t) = calculated Disruption rate,
$DR_{TR}(t)$ = designated Disruption rate after temporary recovery (in this case it is set on 40%),
$DR_{PR}(t)$ = designated Disruption rate after partial recovery (in this case it is set on 10%).

Basically, the first part of Equation 3 means the expected balance in quality during the disaster impact (t_{21}-t_1), the second part is the expected balance during the assessment period (t_{31}-t_{21}) and temporary recovery (t_{41}-t_{31}), the third part is the expected balance in quality over the time to partial recovery (t_{51}-t_{41}) and the fourth part is the expected balance in quality over the time to full recovery (t_{61}-t_{51}). The given equation defines the concrete example illustrated in Figure 12. We claim that it will be different for each disaster, since the intensity of a threat and recovery options will vary from case to case.

5 Discussion

Based on definition, Figure 10 illustration and calculation (Equation 3) of the resilience loss, it can be assumed that similar shaded areas would correspond to the same resilience loss. For instance, Figure 11 parts (A) and (B) represent the same resilience loss, however, in the case (A) the loss of performance provided is not significant but it takes considerably longer time as it is in the case (B). On the contrary, in the case (B), the loss of the performance is more severe, but a TN element will recover faster (e.g. trees of the road). It seems that different levels of functionality loss could be a case for some infrastructural networks [39], as well as for the transport critical infrastructure.

As it was mentioned before, it is preferred to use the resilience loss profile for the TN elements assessment illustrated in Figure 10. For the purpose of this discussion section, it is represented by Figure 12.

The question is, what is for a user or assessor considered to be a more important disruption: (1) a less disruption that takes longer time and affects a greater number of people (Figure 12A), or (2) a more serious disruption that takes less time and affects probably less people (see Figure 12B). Assuming that with increasing functionality loss, the time needed to remove this disruption will increase, the problem would be practically solved, since example B would be impossible. However, there are situations where there this assumption does not apply, such as a traffic accident that can block (full disruption) traffic for a few hours, but after that, a disrupted link will be fully

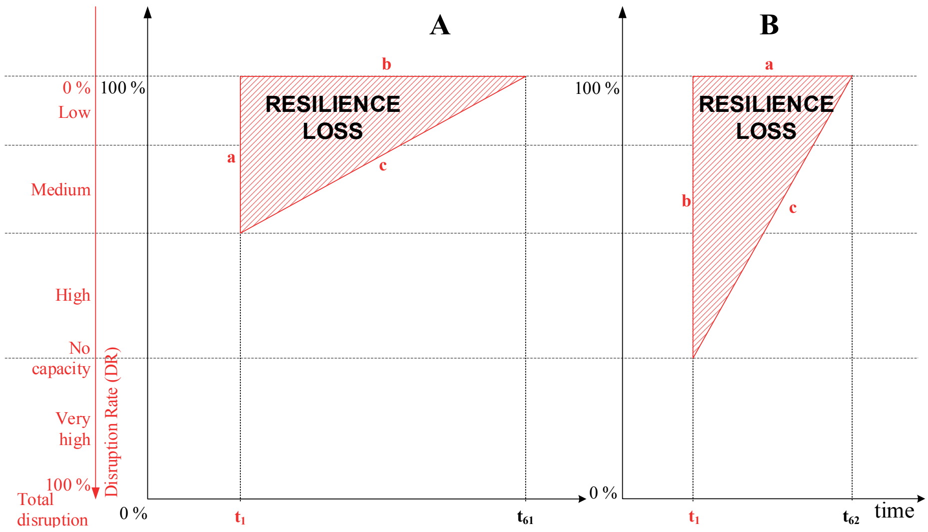

Figure 11 *Difference in resilience loss (gradual restoration of functionality assumed)*

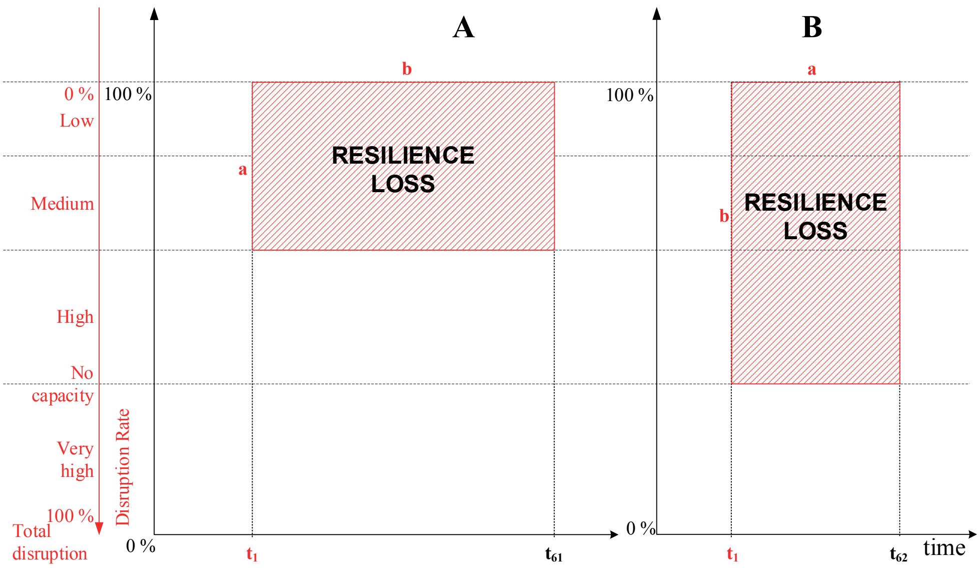

Figure 12 *Difference in resilience loss (instant restoration of functionality assumed)*

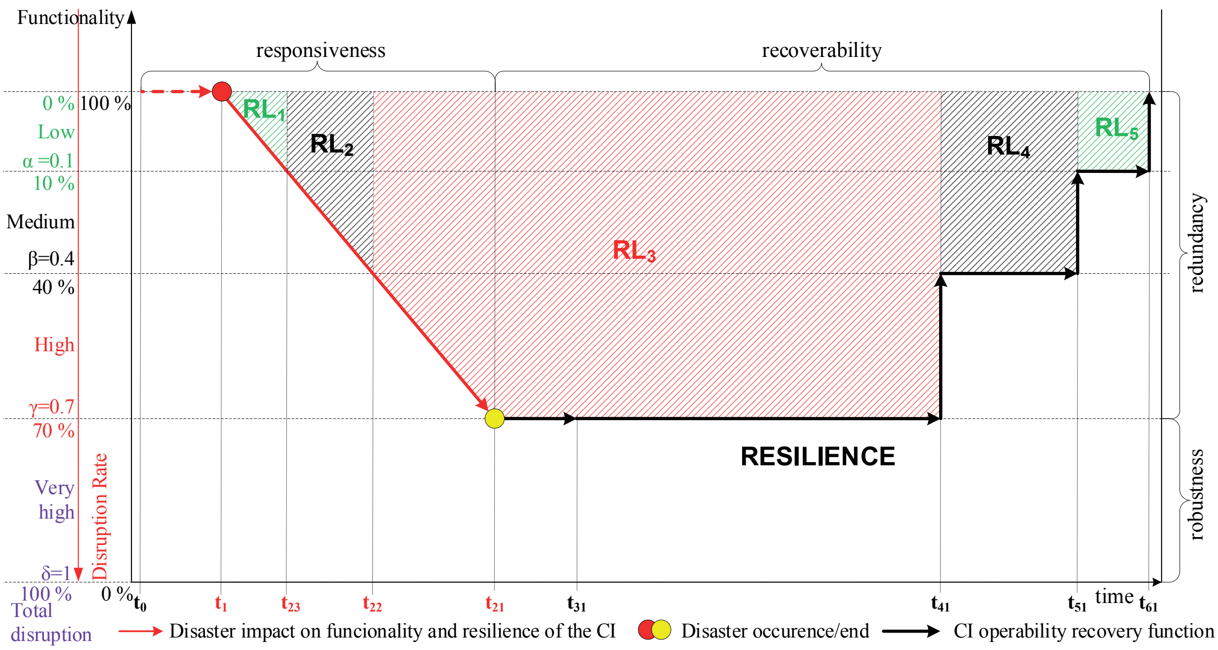

Figure 13 *Differences in disruption importance for the resilience calculation*

operable again. In order to capture these differences, use of the weighted values (e.g. α, β, γ, δ) for different levels of resilience loss is assumed, rather than performing the consequences analysis for different scenarios of disruption. With increasing Disruption rate the higher importance (higher weight value) is assumed.

To illustrate these differences in disruption importance, Figure 13 is used as an example.

In this example are used the following weights: $\alpha = 0.1$; $\beta = 0.4$; $\gamma = 0.7$; $\delta = 1$. Given weights are the same for the impact period, as well as for the recovery period (they correspond to temporary recovery level DR_{TR} and partial recovery level DR_{PR}). They can vary based on the assessor's preferences, but they should be consistent for all TN elements under analysis. Given assumptions also change the calculation of Resilience Loss final value (Equation 4):

$$\begin{aligned} Resilience\ Loss &= \alpha RL_1 + \beta RL_2 + \gamma RL_3 + \\ &+ \beta RL_4 + \alpha RL_5, \end{aligned} \tag{4}$$

As can be seen, the weight α is assigned to the green areas with low disruption of TN element functionality; similarly β is assigned for the medium disruption rate and so on. The weight δ is not used in this particular example, but it will be used if disruption rate (DR) of value more than 0.7 is predicted. The calculation could vary if e.g. immediate loss of the functionality is assumed (t_{21}-t_1 = 0).

The importance of different disruption levels, thus addresses, implies some degree of the results distortion, but if the approach and assessment are used consistently for all the network elements (or designated network part), the values can be comparable and useful in the context of the whole network.

6 Conclusions

The concept of resilience in the context of transportation network is a subject of active interest from both practitioners' and academic communities. There is a number of definitions and different understandings of resilience in transport, as well as a number of methodologies to evaluate resilience. Those methodologies need a huge number of properties and large processes to be performed to get results and this fact can be a disadvantage [41]. From that reason a proposed approach is intended to be applied to the CI elements, rather than to the transportation network as a whole. This is also dictated by the practical considerations, while burden placed on the assessors should be limited.

This paper provides an approach to the resilience measurement by expressing resilience loss. The approach is based on the IDs, which was used as a tool to model functionality disruption level (Disruption rate) and it was combined by duration of disruption (Disruption duration). The probabilistic definition of Disruption rate level used in IDs is the most important part of the assessment. It allows for quantitative expression of disruption level based on the conditional probability of variables in modelled domain. Since besides the commonly considered variable "performance loss" or disruption (called the capacity loss), a new very important variable for TN (demand change) into model is added, the IDs are very appropriate in modelling these relationships. The combination of these two properties in IDs benefits into more accurate expressing of overall resilience loss than in other approaches. It results into identifying of more and less resilient TN elements, which can be compared and appropriate measures can be made to increase the overall resilience of the particular TN element. It can be done for the all resilience features (robustness, redundancy, resourcefulness, responsiveness, recoverability). There are also several other benefits resulting from using the IDs: (1) it allows for more compact and efficient knowledge elicitation, (2) it allows for dynamic assessment of resilience, under assumption that some of the events are observed (some nodes will be instantiated in ID) - for example if there is wind storm in area, the model can result with increased Distortion rate for some elements, allowing for implementing measures that would provide situational awareness, (3) it reduces burden placed on the assessors.

As a result, the resilience loss profile and calculation of the resilience loss are introduced. Unlike in other approaches, it is argued that within the TN it is more appropriate to model and calculate recovery in a form of several separate "step-by-step" activities, rather than as a continuous (e.g. linear) function of a single recovery activity. Moreover, the disruption levels importance, in form of weights, is also discussed as an important part of an accurate resilience loss assessment.

This research indicates that understanding of the resilience distribution in the transportation network may help to identify critical components of transportation infrastructure, make the transportation infrastructure less vulnerable to effects of disasters and adopt soft or hard measures in order to enhance the resilience of transportation elements and resilience features in particular.

References

[1] ABUDAYYEH, D., NGODUY, D., NICHOLSON, A. Traffic signal optimisation in disrupted networks with re-routing. *Transportation Research Procedia* [online]. 2018, **34**, p.195-202. ISSN 2352-1465. Available from: https://doi.org/10.1016/j.trpro.2018.11.032

[2] BURWELL, D. An exchange of building U.S. road capacity: metropolitan transportation politics. In: *Moving people, goods and information in the 21st century. The cutting-edge infrastructures of networked cities*. HANLEY, R. E. (ed.). London and New York: Reutledge Taylor and Francis Group, 2004, p.127-137.

[3] Vyskumny ustav dopravny / Research Institute of Transport. *Analyza rizik sektora doprava, podsektory cestna doprava a zeleznicna doprava / Risk analysis of the transport sector, subsectors of road transport and rail transport* (in Slovak). Zilina, 2014.

[4] KAHN RIBEIRO, S., KOBAYASHI, S., BEUTHE, M., GASCA, J., GREENE, D., LEE, D. S., MUROMACHI, Y., NEWTON, P. J., PLOTKIN, S., SPERLING, D., WIT, R., ZHOU, P. J. Transport and its infrastructure. In: *Climate change 2007: Mitigation*. Contribution of working group III to the fourth assessment report of the intergovernmental panel on climate change. METZ, B., DAVIDSON, O. R., BOSCH, P.R., DAVE, R., MEYER L. A. (eds.). Cambridge University Press, 2007.

[5] SIMAK, L., DVORAK, Z., GASPIERIK, L., KAMPOVA, K., REITSPIS, J., SEIDL, M., SVETLIK, J. *Protection of critical infrastructure in sector transportation*. Zilina: EDIS, 2012.

[6] LEITNER, B., LUSKOVA, M., O'CONNOR, A., VAN GELDER, P. Quantification of impacts on the transport serviceability at the loss of functionality of significant road infrastructure objects. *Communications - Scientific Letters of the University of Zilina* [online]. 2015, **17**(1), p. 52-60. ISBN 1335-4205, eISSN 2585-7878. Available from: http://komunikacie.uniza.sk/index.php/communications/article/view/393

[7] TAYLOR, M. A. P, D'ESTE, G. M. Concepts of network vulnerability and applications to the identification of critical elements of transport infrastructure. 26th Australasian Transport Research Forum : proceedings [online]. 2003. Available from: http://search.ror.unisa.edu.au/media/digital/open/9915913443501831/12143366150001831/13143375830001831/pdf

[8] LOVECEK, T., RISTVEJ, J., SIMAK, L. Critical infrastructure protection systems effectiveness evaluation. *Journal of Homeland Security and Emergency Management* [online]. 2010, **7**(1). eISSN 1547-7355. Available from: https://doi.org/10.2202/1547-7355.1613

[9] HOLLA, K. Lessons learned from the implementation of the SEVESO III directive in the Slovak Republic. *Safety and Security Engineering VII* [online]. 2018, **174**, p. 25-31. eISSN 1743-3509. Available from: https://doi.org/10.2495/SAFE170031

[10] HOLLING, C. S. Resilience and stability of ecological systems. *Annual Review of Ecology and Systematics* [online]. 1973, **4**, p.1-23. ISSN 1545-2069, eISSN 1545-2069. Available from: https://doi.org/10.1146/annurev.es.04.110173.000245

[11] DEANGELIS, D. L. Energy flow, nutrient cycling and ecosystem resilience. *Ecology* [online]. 1980, **61**(4), p. 764-771. eISSN 1939-9170. Available from: https://doi.org/10.2307/1936746

[12] YODO, N., WANG, P. Engineering resilience quantification and system design implications: a literature survey. *Journal of Mechanical Design* [online]. 2016, **138**(11). ISSN 1050-0472, eISSN 1528-9001. Available from: https://doi.org/10.1115/1.4034223

[13] HOFFMAN, E. *Building a resilient business*. Raptor Networks Technology Inc., 2007.

[14] OMER, M., NILCHIANI, R., MOSTASHARI, A. Measuring the resilience of the transoceanic telecommunication cable system. *IEEE Systems Journal* [online]. 2009, **3**, p. 295-303. ISSN 1932-8184, eISSN 1937-9234. Available from: https://doi.org/10.1109/JSYST.2009.2022570

[15] SAURIN, T. A., CARIM JUNIOR, G. C. Evaluation and improvement of a method for assessing hsms from the resilience engineering perspective: a case study of an electricity distributor. *Safety Science* [online]. 2011, **49**(2), p.355-368. ISSN 0925-7535. Available from: https://doi.org/10.1016/j.ssci.2010.09.017

[16] OUYANG, M., DUENAS-OSORIO, L. Multi-dimensional hurricane resilience assessment of electric power systems. *Structural Safety* [online]. 2014, **48**, p.15-24. ISSN 0167-4730. Available from: https://doi.org/ 10.1016/j.strusafe.2014.01.001

[17] YODO, N., WANG, P. Resilience analysis for complex supply chain systems using bayesian networks. 54th AIAA Aerospace Sciences Meeting : proceedings [online]. AIAA SciTech Forum, 2016. eISBN: 978-1-62410-578-4, AIAA 2016-0474. Available from: https://doi.org/10.2514/6.2016-0474

[18] LUNA, R., BALAKRISHNAN, N., DAGLI, C. H. Post earthquake recovery of a water distribution system: discrete event simulation using colored Petri nets. *Journal of Infrastructure Systems* [online]. 2010, **17**(1), p. 25-34. ISSN 1076-0342. Available from: https://doi.org/10.1061/(ASCE)IS.1943-555X.0000039

[19] CIMELLARO, G. P., REINHORN, A. M., BRUNEAU, M. Seismic resilience of a hospital system. *Structure and Infrastructure Engineering* [online]. 2010, **6**(1-2), p. 127-144. ISSN 1573-2479. Available from: https://doi.org/10.1080/15732470802663847

[20] TAMVAKIS, P., XENIDIS, Y. Comparative evaluation of resilience quantification methods for infrastructure systems. *Procedia-Social and Behavioral Sciences* [online]. 2013, **74**, p. 339-348. eISSN 1877-0428. Available from: https://doi.org/10.1016/j.sbspro.2013.03.030

[21] ALIPOUR, A., SHAFEI, B. seismic resilience of transportation networks with deteriorating components. *Journal of Structural Engineering* [online]. 2016, **142**(8), p. C4015015. ISSN 0733-9445, eISSN 1943-541X. Available from: https://doi.org/10.1061/(ASCE)ST.1943-541X.0001399

[22] REGGIANI, A., NIJKAMP, P., LANZI, D. Transport resilience and vulnerability: the role of connectivity. *Transport Research, Part A: Policy & Practice* [online]. 2015, **81**, p. 4-15. ISSN 0965-8564, eISSN 1879-2375. Available from: https://doi.org/10.1016/j.tra.2014.12.012

[23] BHAVATHRATHAN, B. K., PATIL, G. R. Capacity uncertainty on urban road networks: a critical state and its applicability in resilience quantification. *Computers, Environment and Urban Systems* [online]. 2015, **54**, p. 108-118. ISSN 0198-9715. Available from: https://doi.org/10.1016/j.compenvurbsys.2015.07.005

[24] OMER, M., MOSTASHARI, A., NILCHIANI, R. Assessing resilience in a regional road-based transportation network. *International Journal of Industrial and Systems Engineering* [online]. 2013, **13**(4), p. 389-408. ISSN 1748-5037, eISSN 1748-5045. Available from: https://doi.org/10.1504/IJISE.2013.052605

[25] MATTSSON, L. G., JENELIUS, E. Vulnerability and resilience of transport systems: a discussion of recent research. *Transport Research, Part A: Policy & Practice* [online]. 2015, **81**, p. 16-34. ISSN 0965-8564, eISSN 1879-2375. Available from: https://doi.org/10.1016/j.tra.2015.06.002

[26] MILLER-HOOKS, E., ZHANG, X., FATURECHI, R. Measuring and maximizing resilience of freight transportation networks. *Computers and Operations Resea*rch [online]. 2012, **39**(7), p. 1633-1643. ISSN 0305-0548, eISSN 1873-765X. Available from: https://doi.org/10.1016/j.cor.2011.09.017

[27] TAMVAKIS, P., XENIDIS, Y. Resilience in transportation systems. *Procedia-Social and Behavioral Sciences* [online]. 2012, **48**, p. 3441-3450. eISSN 1877-0428. Available from: https://doi.org/10.1016/j.sbspro.2012.06.1308

[28] COX, A., PRAGER, F., ROSE, A. Transportation security and the role of resilience: a foundation for operational metrics. *Transport Policy* [online]. 2011, **18**(2), p. 307-317. ISSN 0967-070X, eISSN 1879-310X. Available from: https://doi.org/10.1016/j.tranpol.2010.09.004

[29] HROMADA, M. *Technologicke aspekty ochrany kritickej infrastruktury SR / Technological aspects of critical infrastructure protection in Slovakia* (in Slovak). Dissertation. Zlin: Tomas Bata University in Zlin, 2011.

[30] SHAFIEEZADEH, A., BURDEN, L. I. Scenario-based resilience assessment framework for critical infrastructure systems: case study for seismic resilience of seaports. *Reliability Engineering and System Safety* [online]. 2014, **132**, p. 207-219. ISSN 0951-8320. Available from: https://doi.org/10.1016/ 10.1016/j.ress.2014.07.021

[31] GOPALAKRISHNAN, K., PEETA, S. *Sustainable and resilient critical infrastructure systems: simulation, modeling and intelligent engineering*. Springer, 2010, p. 84-91. ISBN 978-3-642-11405-2.

[32] BRUNEAU, M., REINHORN, A. Seismic resilience of communities - conceptualization and operationalization. International Workshop on Performance Based Seismic-Design : proceedings. 2004.

[33] O'ROURKE, T. D. Critical infrastructure, interdependencies and resilience. *Bridge*. 2007, **37**(1), p. 22-29. ISSN 0077-5614.

[34] REHAK, D., SENOVSKY, P., SLIVKOVA, S. Resilience of critical infrastructure elements and its main factors. *Systems* [online]. 2018, **6**(21), p. 1-13. eISSN 2079-8954. Available from: https://doi.org/10.3390/systems6020021

[35] SHEFFI, Y. R. J. *The resilient enterprise: overcoming vulnerability for competitive advantage*. MIT Press, 2005. ISBN 978-0262693493.

[36] U. S. Department of Homeland Security. *Critical infrastructure resilience final report and recommendations*. Washington D.C., 2009.

[37] TAYLOR, M. A. P. *Vulnerability analysis for transportation networks*. Elsevier, 2017. ISBN 9780128110102, eISBN 9780128110119.

[38] KAHAN, J. H., ALLEN, A. C., GEORGE, J. K. An operational framework for resilience. *Journal of Homeland Security and Emergency Management* [online]. 2009, **6**(1). eISSN 1547-7355. Available from: https://doi.org/10.2202/1547-7355.1675

[39] BRUNEAU, M., REINHORN, A. Exploring the concept of seismic resilience for acute care facilities. *Earthquake Spectra*. 2007, **23,** p. 41-62. ISSN 8755-2930.

[40] FERRARIOA, E., PEDRONIA, N., ZIOA, E. Evaluation of the robustness of critical infrastructures by hierarchical graph representation, clustering and Monte Carlo simulation. *Reliability Engineering and System Safety* [online]. 2016, **155**, p. 78-96. ISSN 0951-8320. Available from: https://doi.org/10.1016/j.ress.2016.06.007

[41] MARTINEZ-PASTOR, B., NOGAL, M., O'CONNOR, A., CAULFIELD, B. Evaluation of resilience in traffic networks: models and characteristics. Irish Transport Research Network : proceedings. 2015.

[42] LUKAS, L., HROMADA, M. Resilience as main part of protection of critical infrastructure. *International Journal of Mathematical Models and Methods in Applied Sciences* [online]. 2011, **5**, p. 1135-1142. ISSN 1998-0140. Available from: http://www.naun.org/main/NAUN/ijmmas/20-879.pdf

[43] ASBJORNSLETT, B. E. Assess the vulnerability of your production system. *Production Planning and Control* [online]. 1999, **10**, p. 219-229. ISSN 0953-7287, eISSN 1366-5871. Available from: https://doi.org/10.1080/095372899233181

[44] BRUNEAU, M., CHANG, S., EGUCHI, R., LEE, G., O'ROURKE, T., REINHORN, A., SHINOZUKA, M., TIERNEY, K., WALLACE, W., VON WINTERFELT, D. A framework to quantitatively assess and enhance the seismic resilience of communities. *Earthquake Spectra* [online]. 2003, **19**, p. 733-752. ISSN 8755-2930. Available from: https://doi.org/10.1193/1.1623497

[45] DANG, Y. Model on transportation demand distribution. 7th International Joint Conference on Computational Sciences and Optimization : proceedings [online]. 2014. Available from: https://doi.org/10.1109/cso.2014.109

[46] HOWARD, R. A., MATHESON, J. E. Influence diagrams. In: *The principles and applications of decision analysis Vol. II*. HOWARD, R. A., MATHESON, J. E. (eds.). Strategic Decisions Group, 1984, p. 721-762.

[47] TITKO, M., ZAGORECKI, A. Modelling vulnerability of critical infrastructure of transportation network using influence diagrams. *Communications - Scientific Letters of the University of Zilina* [online]. 2013, **15**(4), p. 58-62. ISBN 1335-4205, eISSN 2585-7878. Available from: http://komunikacie.uniza.sk/index.php/communications/article/view/711

[48] CERE, G., REZGUI, Y., ZHAO, W. Urban-scale framework for assessing the resilience of buildings informed by a Delphi expert consultation. *International Journal of Disaster Risk Reduction* [online]. 2019, **36**, p. 101079. eISSN 2212-4209. Available from: https://doi.org/10.1016/j.ijdrr.2019.101079

[49] MOGHADAS, M., ASADZADEH, A., VAFEIDIS, A., FEKETE, A., KOTTER, T.A multi-criteria approach for assessing urban flood resilience in Tehran, Iran. *International Journal of Disaster Risk Reduction* [online]. 2019, 35, p. 101069. eISSN 2212-4209. Available from: https://doi.org/10.1016/j.ijdrr.2019.101069

[50] DILLEY, M., BOUDREAU, T. E. Coming to terms with vulnerability: a critique of the food security definition. *Food Policy*. 2001, **26**, p. 229-247. ISSN 0306-9192.

[51] WISNER, B., BLAIKIE, P., CANNON, T., DAVIS, I. *At risk: natural hazards, people's vulnerability and disasters*. 2. ed. London: Routledge, 2004. ISBN 0415252156.

[52] DEVANANDHAM, H., RAMIREZ-MARQUEZ. J. Generic metric and quantitative approaches for system resilience as a function of time. *Reliability Engineering and System Safety* [online]. 2012, **99**, p. 114-122. ISSN 0951-8320. Available from: https://doi.org/ 10.1016/j.ress.2011.09.002

[53] SLIVKOVA, S., REHAK, D., NESPOROVA, V., DOPATEROVA, M. Correlation of core areas determining the resilience of critical infrastructure. *Procedia Engineering* [online]. 2017, **192**, p. 812-817. 2017, p.812-817. eISSN 1877-7058. Available from: https://doi.org/10.1016/j.proeng.2017.06.140

[54] ROSE, A. Economic resilience to natural and man-made disasters: multidisciplinary origins and contextual dimensions. *Environmental Hazards* [online]. 2007, **7**(4), p. 383-398. ISSN 1747-7891, eISSN 1878-0059. Available from: https://doi.org/10.1016/j.envhaz.2007.10.001

Marica Mazurek

THE INNOVATIVE APPROACH TO RISK MANAGEMENT AS A PART OF DESTINATION COMPETITIVENESS AND REPUTATION

The aim of this paper is a critical discussion on application of a framework for tourism disaster management and the response of governments and communities to crises and disasters. Perception of danger and threat might be decisive factors, which could undermine image, reputation, and competiveness of a country. It might have also a decisive influence on the performance of a country from the economic point of view and especially influence on service provisions, for instance infrastructure (transportation), safety and security. The conceptual approach to research is based on analysis and discussion of the applied models of crisis management in tourism. Main purpose of this paper is to overview and compare methodological and conceptual approaches of academics to crises and disasters in published articles dealing with the creation of pro-active risk management models and their application.

Keywords: *models of crisis management, competitive advantage, image, reputation, service provision, transportation, cultural differences*

1 Introduction

Safety and security in tourism are important factors influencing tourists' demand. Countries, depending on tourism, experienced in a future tremendous economic consequences due to external reasons as a result of natural causes or man-made infliction. Vulnerability of tourism destinations is relatively high. Responses of different countries to these events depend on a variety of factors, especially the economic position, the model of governance, preparedness to cope a critical situation, reaction of international community, mass media and business culture. As a consequence of crises and disasters, tourism activities usually decline, the image and competitiveness are undermined. A highly competitive destination does not exist by chance [1-2]. The purpose of this paper is to overview and compare methodological and conceptual approaches of academics dealing with the topic of risk management in their studies, as well as to explore different concepts and approaches to risk management, where each concept requires different methodological approach. As an example of the approach to crises and disasters scenario, a case study of SARS outbreak in Toronto, Canada, has been used.

2 Literature review

Main conceptual framework in the studied literature could be divided into specific categories. The first group includes studies dealing with the reasons of events as crises and disasters, the second group discusses the impacts of crises and disasters on economy, tourism performance, services and infrastructure, for instance transportation, community, etc. and the last group is concerned with the attitudes and responds of stakeholders. Each concept requires different methodological approach. The authors in [3-8] discussed the models, which could be used in a case of crises and disasters predominantly in tourism destinations. The second group of authors was dealing with crises management, for example [8].

The predominant approach to research of crises and disasters was embraced by using the inductive research approach (observation, searching for some specific patterns of events and their reasons). The authors; for instance [7], used a broader amount of research and academic literature, which allowed understanding more deeply crises and disasters. The inductive approach was applied in articles [5-7, 9].

Some authors tried to develop a generic model suitable not only for tourism destinations, but for different purposes, for instance a country general with its specific requirements of safety, security, service provision (for instance transportation services, etc.). Faulkner applied a deep inductive approach in order to construct generic model of crisis and disasters [3]. Ritchie underlined a necessity of more holistic and strategic approach [9]. Hence, models are more useful for studies of the first group of conceptual approach, e. g. the reasons of crises and disasters and the roles of stakeholders during these events. However, some authors shifted further risk assessment research of crisis management to a different methodological approach by

Marica Mazurek
Faculty of Humanities, University of Zilina, Slovakia
E-mail of corresponding author: marica.mazurekova@fhv.uniza.sk

questioning particular destination stakeholders, corporate and government representatives, policy makers and planners about their preparedness to deal with crises and disasters [6]. As the authors stated, “the purpose was to produce insight rather to test theory, the study was inductive in nature and used a qualitative, interpretative approach” [10]. Their research revealed, through interviewing of experts on corporate and government security, safety, tourism policy and planning, some controversial aspects of former research approaches based on compiling of theoretical frameworks without testing the attitudes of stakeholders. A research underlined necessity of the co-operative approach of all the stakeholders, compatible jurisdiction, allocation of financial resources, etc. Thus, the pragmatic approach to the studied topic revealed important gaps between the managerial theoretical approach and practice. Similar experience was perceived after the implication of pro-active generic models in real settings, where interviews with individual tourism operators and DMOs (Destination Marketing Organizations) representatives were used, which allowed deeper insight into the topic of crises and disasters. In that case a complicated character of tourism research is visible, where knowledge in tourism could be approached from two angles. One is delineated by the multidisciplinary character of tourism studies rather than a single discipline. It causes blending of academic disciplines by implication of the statement of “knowing that” (e.g. what we know that we know) together with specific disciplines, which are close to tourism studies (sociology, psychology, geography, anthropology) [11]. However, in the case of managerial decisions in tourism, the second type of knowledge, e.g. “procedural knowledge (“knowing how”), based on professional practice of tourism management and marketing, has to be implemented.

As a consequence, if some researchers tried to understand impacts of tourism stakeholders and business environment (the second concept) to crises and disasters, or attitudes of community and stakeholders (the third concept), this approach required totally different paradigmatic approach. For example, for studies of attitudes and responds of stakeholders in the studied articles, researchers used such methods as phenomenology and interpretive approach, which are based on understanding of real experiences of participants. Moreover, in some case studies, peculiarities in the implementation of generic models into specific cultural or business environments, were described.

Some researchers applied the post-positivist approach and studied the impact of the two variables, frequency and severity of terrorist events, on decline of demand. Quantitative methods, based on survey research, have been applied in research on changing attitudes of visitors to the destination after crisis and disasters.

A case study, used in Katherine flooding research, was based on the implication of Faulkner’s generic pro-active risk management model. Prideaux, Laws and Faulkner discussed the application of forecasting methods by blending the qualitative and quantitative methods [12]. The forecasting methods could be useful to predict some developments, but not the consequences, and the authors stated. That “understanding the impact that unexpected disruption may have on tourism flows is important for forecasters, planners, investors and operators” [12].

The studied conceptual and methodological approaches to crises and disasters in the academic literature enabled to understand deeper the impediments of research of crises and disasters. The following research on the content of literature dealing with crisis and disasters managerial approaches required specific methodology and methods.

3 Methodology

The method of content analysis of articles in existing journals and the secondary sources on internet and in publications was used in research. The main focus of the article was on application of model of crisis and disasters and the specific case studies from inflicted countries. This research has a strong conceptual character. A method of the case study from Canada has been used in this study. The studied materials have been collected during the study stay in Canada at the University of Waterloo as well as in further research. This case study is based on the secondary research of the existing literature. Additional literature, which was used for the content analysis, was selected upon the required topic studied in this research. Tourism studies research is rather complicated where an influence of different epistemologies and disciplines might be visible. For this reason, research was dealing with a question how different authors approached a topic of studies from the methodological point of view.

Additionally, the strategic approaches to crisis and disasters have been studied and compared in different countries and cultures. This information was based on the studied secondary sources.

The articles were selected from different academic journals (Table 1 contains a list of studied academic journals containing a sample of 32 academic papers and 5 books). The content analysis was thoroughly focused on the methodological approaches of the authors to the studied topic.

4 Results

Drawing from the insight in academic literature, on crises and disasters, published in journals since 1999 until now, one can see that majority of published articles were trying to develop deeper understanding based on previous academic work in this field. Scholars discussed especially the applicability of models, complications with implementation, managerial tasks and application of models in culturally diverse environment. The marketing recovery strategy revealed a crucial role of mass media.

Some articles discussed the applicability of models into real situations. For example, in 2001 a generic pro-

***Table 1** Content Analysis of the articles and books*

Journal of Vacation Marketing	Tourism Management
1. Litvin and Alderson (2003) [13]	20. Faulkner and Vikulov (2001) [7]
2. Frisby (2011) [14]	21. Paraskevas and Arendell (2007) [6]
3. Fall (2004) [15]	22. Ritchie, (2004) [9]
4. Yeoman, Lennon and Black [16]	23. Faulkner (2001) [3]
5. de Sausmerez (2005) [17]	24. Quintal, Lee and Soutar (2010) [30]
6. Barton (1994) [18]	25. Prideaux, Laws, and Faulkner (2003) [12]
7. Durocher (1994) [19]	26. Pauchant and Mittroff (1992) [31]
8. Beirman (2002, [20]	
Journal of Travel Research	Crisis Management in Tourism
9. Henderson (1999) [21]	
10. Milo and Yoder (1991) [22]	
11. Pizam and Fleischer (2002) [23]	
12. Drabek (1995) [24]	27. Campiranon and Scott (2007) [32]
13. Mansfeld (1999) [25]	
14. Sonmez, Apostolopoulos and Tarlow (1999) [8]	
15. Goodrich (2005) [26]	
16. Pizam (1999) [27]	
Annals of Tourism Research	Disaster Prevention and Management
17. Okumus and Karamustafa (2005) [28]	28. Heath (1998) [4]
Current Issues in Tourism	e-Review of Tourism Research (eRTR)
18. Miller and Ritchie (2003) [5]	29. Tarlow (2004) [33]
19. Var, Brayley and Korsay (1989) [29]	30. Tarlow (2005) [34]
Books	
31. Crouch and Ritchie (2003), [2]	
32. Hall (1994) [35]	
33. Hofstede (2001) [36]	
34. Mansfeld and Pizam (2006) [37]	
35. Wall (2006) [38]	

active risk management model was used in the Foot and Mouth Disease outbreak in Great Britain and in 1998 during the flooding in Australia (Katherine floods). The academic discussions tried to divide crises and disasters into specific groups based on infliction. The goal was to generate a set of rules or managerial approaches during the crises and disasters in a form of a holistic model of disaster management strategy. As a result, Faulkner's pro-active generic risk management model or Ritchie's holistic model were generated, but the applicability of created models was disputable.

Academics predominantly expressed consensus in a matter of division of crises and disasters into two groups, but could not find a boundary between them. For example, in Figure 1 a case of Lockerbie caused by human infliction, was by Faulkner named as a disaster, but the classification of this event was a terrorist attack in the air industry [3]. This table was created before 2001 and the general knowledge on crises and disasters did not experience such events as 9/11 or Bali terrorist attacks, terrorist attack in Egypt, Tsunami in Asia, SARS outbreak in Asia and Toronto, Canada. The emerging events later, even more pointed out at the necessity to deal with this topic generally, not only in tourism context, because a tourism destination is also a place with local people and local industry.

The authors dealing with crises and disasters criticized problems of "inept management structures and practices or a failure to adapt to change" [3, 9]. Ritchie added that "a crisis implies the need for change to prevent the situation occurring again, while a disaster requires responses to limit the impacts" [9]. As the author explains, important is the ability to act or change the situation, not only to define a type of events based on infliction. Some cases could bear features of both events, as for example Foot and Mouth Disease outbreak (health care negligence with a serious ripple effect on agriculture, tourism).

The authors had a problem with a definition of crisis and disasters, for example Selbst defined crisis as "any action or failure to act that interferes with an organization's ongoing functions …. that has a detrimental personal effect as perceived by the majority of its employees, clients and constituents" [39]. The problem with this definition is that

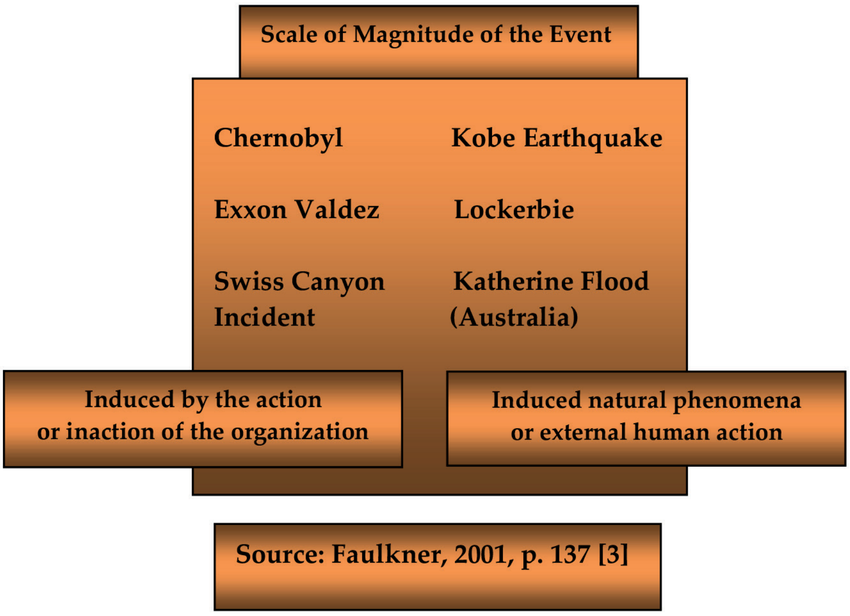

Figure 1 *Crises and disasters*

it only defines crises, and as Faulkner stated, "Selbst's definition of crisis seems to exclude situations where the survival of an organization of community is placed in jeopardy because of events over which those involved have little control [10]."

During the development of different types of crises and disasters, evident was a shift from crisis management models [38] to pro-active risk management models [3] or holistic models [9, 40-41], which was perceived as "an established management decision-making aid……for pro-active decision making that continuously assesses potential risks, prioritizes the risks and implements strategies to cope with those risks" [42]. Creation of a generic model by Faulkner underlined a necessity for the pro-active approach to tourism disaster management, continuous assessment of risks, development of scenarios in the pre-event stage and use of the forecasting techniques. His attempt to generate this type of model for tourism destinations is contributory and positive because all the former crises management models were developed for business environment, Pauchant's and Mitroff's model [31], Ritchie's model [28], Faulkner and Vikulov's models [7] etc. Faulkner's generic pro-active risk management model was used in the 2001 Foot and Mouth Outbreak in the United Kingdom, which was a case of a crisis in agriculture; however, the ripple effect on tourism industry in the United Kingdom was evident.

More discussion is needed on perception of disaster management framework of models (re-active models) and pro-active risk management models as has been stated by some academics in academic journals. The first academic, who identified these two approaches to model creation in crisis and disasters, was Heath, who mentioned the traditional crisis management approach and the risk management approach [4]. Miller and Ritchie added that "the traditional crisis management approach involves no initial (pre-crisis) planning or management (Figure 2) … and the role of risk management approach "is to respond to the crisis and manage the impacts effectively and efficiently (Figure 3) [5].

Application of the same model in different type of disaster or crises and in different countries, cultures, might be a real constraint. Almost ten years later, Campiranon and Scott (2007) revealed "that national culture has a significant impact on crisis management" [32]. To support this idea, Heath noted that "responses of different governmental representatives to crises and disasters are based on their cultural rules" [4]. Specifically, he mentioned that "after the 1995 Kobe earthquake Japanese cultural orientation towards bottom-up consensus in decision-making also affected the timeliness of the response." Eastern cultures do not react the same way as western cultures and their hierarchical approach to the decision-making process could be a strong argument that generic would not be implemented in the same way as it would be in western societies. Some form of criticism also lies in adoption of similar management methods to different management environments. For example, some authors compared the differences between reaction of American and Chinese managers while dealing with uncertain situation: "having a high uncertainty avoidance culture, Chinese managers normally lack an adventurous spirit and the sense of risk. On the other hand, low uncertainty avoidance American managers are more likely to accept risk" [43]. These examples only confirm what the other authors discussed as being in impertinent situation for implementation of models in different environments. Thus, academics as Faulkner mentioned this possibility by stating that "different internal cultures and modus operandi barriers to communication and co-operation between organizations" [3].

In addition, Campiranon and Scott discussed the influence of socio-cultural concepts on the successful

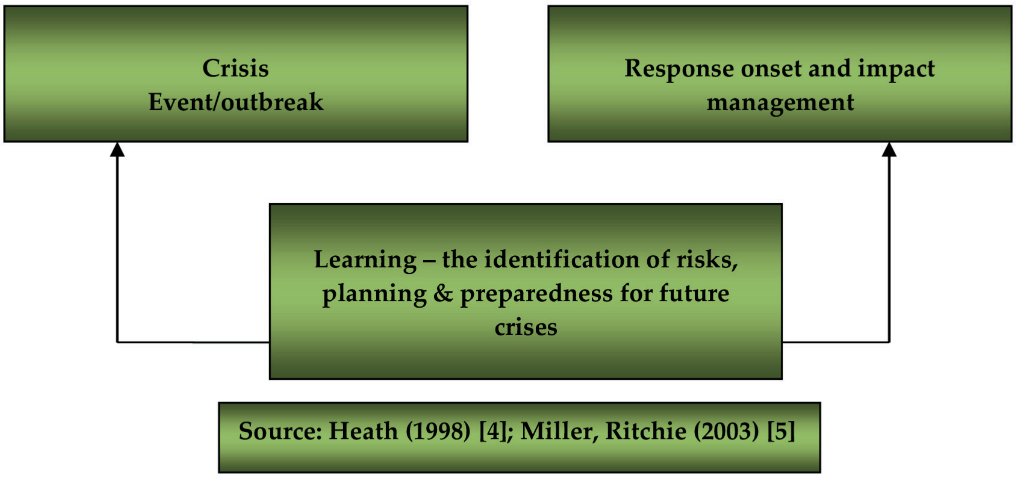

Figure 2 *A traditional approach to a crisis*

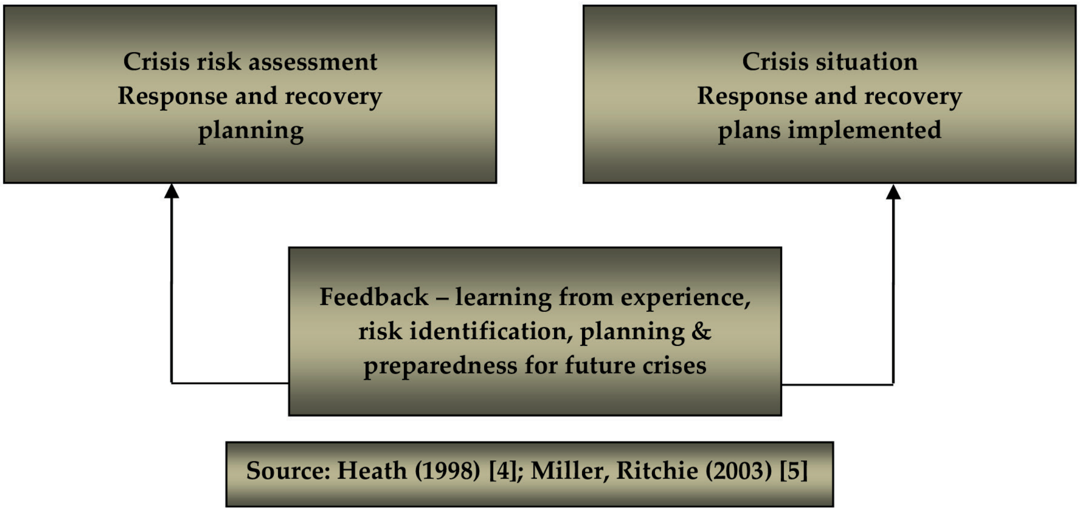

Figure 3 *A risk management approach to a crisis*

implementation of crises management strategies in organizations or different entities [32]. Johnson and Peppas mentioned that "crisis intensity varies from country to country and culture to culture, which means that it is very important that crisis response plans are developed for a specific location" [44]. Okumus and Karamustafa stated that the success of each pro-active model depends on national culture and in some cultures "despite experiencing so many severe disasters, both tourism organizations and government officials still ignore the need to employ a pro-active approach to managing crises" [29]. This is perhaps a partial reflection of the national culture in Turkey's business environment. In Turkish culture reliance on public sector interference is not identical as for example in western cultures. The existence of different approaches of governments and cultures to crises and disasters is evident and this might also influence particular stages of recovery process described in generic models.

The above stated authors (Faulkner, Ritchie, Paraskevas and Arrendell) mentioned the role of mass media during the crises and disasters. Media could become the so called double-edge sword of media involvement in crises as being a helpful factor in dissemination of information, but also a hindering factor that creates more chaos and ruins image of a destination. Frisby studied the impact of media and public relations after the outbreak of the Foot and Mouth disease in Great Britain in 2001 and 9/11 in New York in 2001 and studied the role of the BTA (British Tourist Authority), dealing with marketing and promotion of Great Britain overseas and creation of an image of Great Britain as a destination [14]. Image is crucial for destinations' competitiveness because creation of an image in the marketing concepts is a long-period process, and visitors tend to respond quickly and avoid visit problematic destinations. As Frisby commented "BTA created a public relations strategy and program to fulfill its objectives in re-establishing tourism from overseas as rapidly as possible" [14]. Similarly, Fall discussed about the role of mass media and public relations after crisis and disasters occur and stated that "crisis has the potential to impact negatively on an organization's image" [15]. Faulkner commented that "media outlets can help by dissemination warnings…however they can also hinder emergency operations by spreading false information" [3]. The recovery stage of the generic model includes the media communication strategy and the role of media and recovery marketing strategies is crucial for a success of a recovery. Faulkner added that "a media communication strategy… (is) essential in order to ensure that misleading and contradicting information". However, in some of discussed articles examples opposing the description of the media communication strategy were used and criticized their attempts to exaggerate. In some cases, the media reports have a potential to have a devastating impact on disaster-affected destinations. This scenario was confirmed for instance in the SARS outbreak in Toronto, Canada in 2003.

5 Case study in Canada

The outbreak of SARS (Severe Acute Respiratory Syndrome) did not have an extreme impact on mortality of people because only 45 people died, but an immediate effect was evident in tourism industry. Over 1/3 of 95 000 employees in tourism were laid off (based on Smith Travel Research) after the SARS outbreak and total decrease of tourism revenue due to SARS was 500 million in Toronto, Ontario in the following months. From April to June 2004, the number of international visitors declined 14%, their spending declined 13% and the travel deficit in the income from international tourism was over 1.1 billion CAD together with the decrease of employment in tourism by 2.4%, KPMG, PKF Consulting [38]. Inflicted were also businesses in Toronto, not only in tourism, but generally. For instance, restaurants experienced 20-30% decline, and other services (education, health and social services, retail, transportation) were also hit due to SARS outbreak. Additionally, at least five major conventions and events were cancelled (over 20 000 attendees, cancellation of bus tours, music concerts), etc. Ontario is one of major economic powers besides Alberta, which contributes by 40% to Canada's GDP and Toronto is a creator of 20% of GDP (1 billion CAD off in 2003). Based on the secondary research of Wall [38], KPMG, PKF Consulting sources, the Federal government invested to public sector additionally 650 million CAD on tax relief of inflicted business, discounts of prices of flight tickets, PR events, 25 million CAD marketing campaign due to the SARS outbreak. The businesses in Toronto were given 5 month tourism tax holiday and 10 million CAD was spent on business recovery strategy. The Provincial government added 118 million CAD for SARS Recovery package (66.8 CAD - global confidence in Toronto, 9 million CAD on event marketing, 8 million CAD on events. The total revenue loss in Toronto in April 2003 compared to April 2002 was 97 mil. CAD, compared to other Canadian cities as Montreal (17.1 mil. CAD), Ottawa (7.1 mil. CAD), Calgary (6.2 mil. CAD) or Vancouver (39.1 mil. CAD). The impacts of SARS on hotel market in the first quarter of 2003 compared to the same period of 2002 revealed %-age decrease in all provinces of Canada, but major decrease was indicated in Ontario (- 18.5%) compared to the total decrease (-11.0 %). The same source of information (Conference Board of Canada) discussed the impact of SARS crises on economic activity at Pearson International Airport in Toronto, where the loss in revenues in the 2nd quarter of 2003 were 403,7 mil. CAD. These outcomes testify on the importance of the phase of recovery and especially the creation of image and co-operation with media in the recovery phase.

Except the investment incentives in the process or recovery, Faulkner's pro-active management model underlined the importance of media communication strategy. The role of media has been confirmed also in the SARS outbreak case in Toronto, where the information could even undermine the fragile economic situation. It is the most sensitive case how governments approach the situation and especially how media objectively report on the crisis. Marra [45] and Ritchie [9] noted "that poor communication strategies can often make the crisis worse". Public perception during crises and disasters is crucial, and Heath stated that "crises management is as much about dealing with human perception about the crisis and the management of crisis as it is about physically resolving the crisis situation" [4]. For example, despite the devastating outcome of Izmit earthquake in Turkey in 1999, a positive lesson learned from this disaster was a strong coordinative campaign and effective communication and public relation campaign that helped to overcome the catastrophic damages.

6 Conclusions and implications

In conclusion, it is important to mention that some authors were concerned with the applicability of models and the question was not how models should be constructed, but who will bear responsibilities and how models will operate in real settings.

The authors critically approached the fact that existence of pro-active risk management models is a golden rule to solve managerial decisions. As Wall indicated "it is important to consider who should bear the risk - and the answer will vary from place to place and with the nature of the risks" [38]. Every situation and environment is different and the authors in their articles mentioned even different settings of applicability of models, for example Faulkner discussed in his article about the responsibilities of communities to act during critical situations (in this case in tourism setting) [3]. Paraskevas and Arrendell by developing discussion on terrorist events as crises in tourism setting, underlined the role of DMOs in implementation of risk management models [6].

However, those discussions revealed interesting facts and questions that before the implementation of models such problems, as sufficient authority of entities, little control, creation of financial resources, co-operation among stakeholders, role of government in external situations, lack of proper jurisdiction, etc. have to be resolved. Moreover, some authors; for instance Faulkner did not mention specifically the responsibilities of particular members in community, which are critical for the successful application of models in real settings [3]. Ritchie stated "the type of crisis and disaster and its magnitude will impact upon stakeholders in different ways" [9]. In other words, different reactions and settings will be required in the case of an air strike (with the impact on tourist and other travelers) and the large-scale disasters and crises with more devastating impacts, not only on tourism.

For this reason, it is complicated to create generic models; on the other hand, it is worthwhile to attempt to do so and to protect other entities in an affected region from the collateral damage. The generic models have been applied in typical western countries as Great Britain and Australia, but some authors expressed their hesitation of applicability of generic models in the non-western environment and eastern cultures.

The attempts to devise universal model for tourism destinations was based on life-long academic expertise of scholars and their studies. For example, Faulkner implied extremely thorough approach through explaining the definitions and former research [3]. However, even the most logical and conceptual approach could create impediments in implementation. For instance, the generic model could not be fully implemented in all environments as formally intended. One of the reason, as Hofstede indicated, was "that people from different national cultures tend to have different styles of management" [36].

Many studied articles, discussing the risk management strategies, were finished before the situation has become even more emerging, but some articles appeared in academic journals especially in the last decade and revealed a necessity to pay more attention to this problem. The authors were preoccupied with the idea of creation of the generic pro-active models, which will be useful for detrimental situations. In some case, models were simulated during the disastrous situations and revealed that human society is rather complicated.

An important fact is that creation of models shifted human's curiosity ahead and raised a necessity of further research dealing not only with the applicability of models, but reactions and attitudes of stakeholders, community, government. Body of studied literature and its review enabled to explore constraints in implementation of models or risk management, as for example complexity of human society and its multicultural character, discuss the role of mass media and public relations in the recovery process, and define the differences among crises and disasters. For tourism and its performance and competitiveness, the risk management discourse needs to be taken into consideration because tourism activities and performance are dependent on the safe and secure environment and positive image is crucial for destinations.

References

[1] VANHOVE, N. A comparative analysis of competition models for tourism destinations. In: *Progress in Tourism marketing*. KOZAK, M., ANDREU, L. (eds). Oxford, UK: Elsevier, 2006, p. 101-114. ISBN 0080450407.

[2] CROUCH, J., RITCHIE, B. The competitive destination - a sustainable tourism perspective. Wallingford, UK: Cabi, 2003. ISBN 9780519966646.

[3] FAULKNER, B. Towards a framework for tourism disaster management. *Tourism management* [online]. 2001, **22**(2), p.135-147. ISSN 0261-5177, eISSN 1879-3193. Available from: https://doi.org/10.1016/S0261-5177(00)00048-0

[4] HEATH, R. The Kobe earthquake: some realities of strategic management of crises and disasters. *Disaster Prevention and Management* [online]. 1998, **4**(5), p. 11-24. ISSN 0965-3562, eISSN 1758-6100. Available from: https://doi.org/10.1108/09653569510100965

[5] MILLER, G. A., RITCHIE, B. W. A farming crisis or a tourism disaster? An analysis of the foot and mouth disease in the UK. *Current Issues in Tourism* [online]. 2003, **6**(2), p. 150-171. ISSN 1368-3500, eISSN 1747-7603. Available from: https://doi.org/10.1080/13683500308667949

[6] PARASKEVAS, A., ARENDELL, B. A strategic framework for terrorism prevention and mitigation in tourism destinations. *Tourism management* [online]. 2007, **28**(6), p. 1560-1573. ISSN 0261-5177, eISSN 1879-3193. Available from: https://doi.org/10.1016/j.tourman.2007.02.012

[7] FAULKNER, B., VIKULOV, S. Katherine, washed out one day, back on track the next: a post- mortem of a tourism disaster. *Tourism management* [online]. 2001, **22**(4), p. 331-344. ISSN 0261-5177, eISSN 1879-3193. Available from: https://doi.org/10.1016/S0261-5177(00)00069-8

[8] SONMEZ, S. F., APOSTOLOPOULOS, Y., TARLOW, P. Tourism in crisis: managing the effects of terrorism. *Journal of Travel Research* [online]. 1999, **38**(1), p. 13-18. ISSN 0047-2875, eISSN 1552-6763. Available from: https://doi.org/10.1177/004728759903800104

[9] RITCHIE, B. W. Chaos, crises and disasters: a strategic approach to crisis management in the tourism industry. *Tourism management* [online]. 2004, **25**, p. 669-683. ISSN 0261-5177, eISSN 1879-3193. Available from: https://doi.org/10.1016/j.tourman.2003.09.004

[10] SAUNDERS, M., LEWIS, P., THORNHILL, A. *Research methods for business students*. 3. ed. Harlow: Prentice-Hall, 2003. ISBN 978-0-273-71686-0.

[11] ECHTNER, C. M., JAMAL, T. B. The disciplinary dilemma of tourism studies. *Annals of Tourism Research* [online]. 1997, **24**(4), p. 868-883. ISSN 0160-7383. Available from: https://doi.org/10.1016/S0160-7383(97)00060-1

[12] PRIDEAUX, B., LAWS, E., FAULKNER, B. Events in Indonesia: exploring the limits to formal tourism trends forecasting methods in complex crisis situations. *Tourism Management* [online]. 2003, **24**(4), p. 475-487. ISSN 0261-5177, eISSN 1879-3193. Available from: https://doi.org/10.1016/S0261-5177(02)00115-2

[13] LITVIN, S. W., ALDERSON, L. L. How Charleston got her groove back: a convention and visitors Bureau´s response to 9/11. *Journal of Vacation Marketing* [online]. 2003, **9**(2), p. 188-197. ISSN 1356-7667. Available from: https://doi.org/10.1177/135676670300900207

[14] FRISBY, E. Communication in a crisis: the British Tourist Authority´s responses to the foot-and-mouth outbreak and 11th September. *Journal of Vacation Marketing* [online]. 2003, **9**(1), p. 89-100. ISSN 1356-7667. Available from: https://doi.org/10.1177/135676670200900107

[15] FALL, I. The increasing role of public relations as a crisis management function: Empirical examination of communication re-strategizing efforts among destination organization managers in the wake of 11th September, 2001. *Journal of Vacation Marketing* [online]. 2004, **10**(3), p. 238- 251. ISSN 1356-7667. Available from: https://doi.org/10.1177/135676670401000304

[16] YEOMAN, I., LENNON, J., BLACK, L. Foot-and-mouth disease: a scenario recurrence for Scotland´s tourism industry. *Journal of Vacation Marketing* [online]. 2005, **11**(2), p. 179-190. ISSN 1356-7667. Available from: https://doi.org/10.1177/1356766705052574

[17] DE SAUSMEREZ, N. Book review: restoring tourism destinations in crisis. *Journal of Vacation Marketing* [online]. 2005, **11**(1), p. 103-104. ISSN 1356-7667. Available from: https://doi.org/10.1177/1356766705050849

[18] BARTON, L. Crisis management: preparing for and managing disasters. *The Cornell Hotel and Restaurant Administration Quarterly* [online]. 1994, **35**(2), p. 59-65. ISSN 1938-9655, eISSN 1938-9663. Available from: https://doi.org/10.1177/001088049403500219

[19] DUROCHER, J. Recovery marketing: what to do after a natural disaster. *The Cornell Hotel and Restaurant Administration Quarterly* [online]. 1994, **35**(2), p. 66-71. ISSN 1938-9655, eISSN 1938-9663. Available from: https://doi.org/10.1177/001088049403500220

[20] BEIRMAN, D. Marketing of tourism destinations during a prolonged crisis: Israel and the Middle East. *Journal of Vacation Marketing* [online]. 2002, **8**(2), p. 167-176. ISSN 1356-7667. Available from: https://doi.org/10.1177/135676670200800206

[21] HENDERSON, J. C. Managing the Asian financial crisis: tourist attractions in Singapore. *Journal of Travel Research* [online]. 1999, **38**(2), p. 177-181. ISSN 0047-2875, eISSN 1552-6763. Available from: https://doi.org/10.1177/004728759903800212

[22] MILO, K. J., YODER, S. L. Recovery from natural disaster: travel writers and tourist destinations. *Journal of Travel Research* [online]. 1991, **30**(1), p. 36-39. ISSN 0047-2875, eISSN 1552-6763. Available from: https://doi.org/10.1177/004728759103000107

[23] PIZAM, A., FLEISCHER, A. Severity versus frequency of acts of terrorism: which has a larger impact on tourism demand? *Journal of Travel Research* [online]. 2002, **40**(3), p. 337-339. ISSN 0047-2875, eISSN 1552-6763. Available from: https://doi.org/10.1177/0047287502040003011

[24] DRABEK, T. E. Disaster planning and response by tourist business executives. *The Cornell Hotel and Restaurant Administration Quarterly* [online]. 1995, Vol. 34, p. 81, 36(3), 86-96, 1995. ISSN 1938-9655, eISSN 1938-9663. Available from: https://doi.org/10.1016/0010-8804(95)96941-9

[25] MANSFELD, Y. Cycles of war, terror, and peace: determinants and management of crisis and recovery of the Israeli tourism industry. *Journal of Travel Research* [online]. 1999, **38**(1), p. 30-36. ISSN 0047-2875, eISSN 1552-6763. Available from: https://doi.org/10.1177/004728759903800107

[26] GOODRICH, J. N. Book review: restoring tourism destinations in crisis: a strategic marketing approach. *Tourism Management*. 2005, **26**(3), p. 475-476. ISSN 0261-5177, eISSN 1879-3193.

[27] PIZAM, A. A comprehensive approach to classifying acts of crises and violence of tourism destinations. *Journal of Travel Research* [online]. 1999, **38**(1), p. 5-12. ISSN 0047-2875, eISSN 1552-6763. Available from: https://doi.org/10.1177/004728759903800103

[28] OKUMUS, F., KARAMUSTAFA, K. Impact of and economic crisis: evidence from Turkey. *Annals of Tourism Research* [online]. 2005, **32**(4), p. 942-961. ISSN 0160-7383. Available from: https://doi.org/10.1016/j.annals.2005.04.001

[29] VAR, T., BRAYLEY, R., KORSAY, M. Tourism and world peace: case of Turkey. *Annals of Tourism Research* [online]. 1989, **16**(2), p. 282-286. ISSN 0160-7383. Available from: https://doi.org/10.1016/0160-7383(89)90078-9

[30] QUINTAL, V. A., LEE, J. A., SOUTAR, G. N. Risk, uncertainty and the theory of planned behavior: a tourism example. *Tourism Management* [online]. 2010, **31**(6), p. 797-805. ISSN 0261-5177, eISSN 1879-3193. Available from: https://doi.org/10.1016/j.tourman.2009.08.006

[31] PAUCHANT, T. C., MITTROFF, I. I. *Transforming the crisis prone organization: preventing individual, organizational and environmental tragedies*. San Francisco: Jossey-Bass, 1992. ISBN 978-1555424077. In: PARASKEVAS, A., ARENDELL, B. A strategic framework for terrorism prevention and mitigation in tourism destinations. *Tourism Management* [online]. 2007, **28**, p. 1560-1573. ISSN 0261-5177, eISSN 1879-3193. Available from: https://doi.org/10.1016/j.tourman.2007.02.012

[32] CAMPIRANON, K., SCOTT, N. Factors influencing crisis management in tourism destinations. In: *Crisis management in tourism* [online]. LAWS, E., PRIDEAUX, B., CHON, K. (eds). Wallingford, UK: Cabi Publishing, 2007, p. 142-156. ISBN 978-1-84593-047-9. Available from: https://doi.org/10.1079/9781845930479.0142

[33] TARLOW, P. Tourism Risk. *e-Review of Tourism Research (eRTR)*. 2004, **2**(3), p. 11-13. ISSN 1941-5842.

[34] TARLOW, P. Terrorism and Tourism. *e-Review of Tourism Research (eRTR)*. 2005, **3**(5), p. 18-21. ISSN 1941-5842.

[35] HALL, C. M. *Tourism and politics: policy, power and place*. Chicshester, New York: Wiley & Sons, 1994. ISBN 0471949191.

[36] HOFSTEDE, G. *Culture's consequences: comparing values, behaviors, institutions, and organizations across nations*. 2. ed. Thousand Oaks, CA: Sage, 2001. ISBN 0-8039-7323-3.

[37] MANSFELD, Y. *Tourism, security and safety: from theory to practice*. MANSFELD, Y., PIZAM, A. (eds.). Burlington, Mass.: Elsevier Butterworth-Heinemann, 2006. ISBN 9780750678988.

[38] WALL, G. Recovering from SARS: the case of Toronto tourism. In: *Tourism, security and safety: from theory to practice*. MANSFELD, Y., PIZAM, A. (eds.). Burlington, Mass.: Elsevier Butterworth-Heinemann, 2006. ISBN 9780750678988.

[39] SELBST, P. 1978. In: *Crisis management strategy: competition and change in modern enterprises*. BOOTH, S. New York: Routledge, 1993. ISBN 9781138183735. In: FAULKNER, B. Towards a framework for tourism disaster management. *Tourism Management* [online]. 2001, **22**(2), p. 135-147. ISSN 0261-5177, eISSN 1879-3193. Available from: https://doi.org/10.1016/S0261-5177(00)00048-0

[40] COOMBS, T. Ongoing crisis communications: planning, managing and responding. Thousand Oaks, CA: Sage, 1999. ISBN 0761913203. In: RITCHIE, B., W. Chaos, crises and disasters: a strategic approach to crisis management in tourism industry. *Tourism Management* [online]. 2003, **25**, p. 669-683. ISSN 0261-5177, eISSN 1879-3193. Available from: https://doi.org/10.1016/j.tourman.2003.09.004

[41] Crisis guidelines for the tourism industry - World Tourism Organization [online]. Available from: https://www.e-unwto.org In: CAMPIRANON, K., SCOTT, N. Factors influencing crisis management in tourism destinations. In: *Crisis management in tourism* [online]. LAWS, E., PRIDEAUX, B., CHON, K. (eds). Wallingford, UK: Cabi Publishing, 2007, p. 142-156. ISBN 978-1-84593-047-9. Available from: https://doi.org/10.1079/9781845930479.0142

[42] Pacific Asia Travel Association [online]. Available from: https://www.pata.org In: CAMPIRANON, K., SCOTT, N. Factors influencing crisis management in tourism destinations. In: *Crisis management in tourism* [online]. LAWS, E., PRIDEAUX, B., CHON, K. (eds). Wallingford, UK: Cabi Publishing, 2007, p. 142-156. ISBN 978-1-84593-047-9. Available from: https://doi.org/10.1079/9781845930479.0142

[43] FANN, P., ZIGANG, Z. In: CAMPIRANON, K., SCOTT, N. Factors influencing crisis management in tourism destinations. In: *Crisis management in tourism* [online]. LAWS, E., PRIDEAUX, B., CHON, K. (eds). Wallingford, UK: Cabi Publishing, 2007, p. 142-156. ISBN 978-1-84593-047-9. Available from: https://doi.org/10.1079/9781845930479.0142

[44] JOHNSON, V., PEPPAS, S. Crisis management in Belgium: the case of Coca-Cola. *Corporate Communications: An International Journal* [online]. 2003, **8**(1), p. 18-22. ISSN 1356-3289. Available from: https://doi.org/10.1108/13563280310458885 In: CAMPIRANON, K., SCOTT, N. Factors influencing crisis management in tourism destinations. In: *Crisis management in tourism* [online]. LAWS, E., PRIDEAUX, B., CHON, K. (eds). Wallingford, UK: Cabi Publishing, 2007, p. 142-156. ISBN 978-1-84593-047-9. Available from: https://doi.org/10.1079/9781845930479.0142

[45] MARRA, F. Crisis communication plans: Poor prediction of excellent crisis public relations. *Public Relations Review*. 1998, **24**(4), p. 461-474. ISSN 0363-8111. In: RITCHIE, B. W. Chaos, crises and disasters: a strategic approach to crisis management in the tourism industry. *Tourism management* [online]. 2004, **25**, p. 669-683. ISSN 0261-5177, eISSN 1879-3193. Available from: https://doi.org/10.1016/j.tourman.2003.09.004

COMMUNICATIONS – Scientific Letters of the University of Zilina
Author guidelines

- All papers have to deal with the topic of transport and be submitted strictly within one of the listed subtopics. Please, refer to list of topics and subtopics here and indicate it clearly when submitting your paper.
- Submitted papers must be unpublished and must not be currently under review for any other publication.
- Manuscripts written in good English must include abstract and keywords also written in English. The abstract should not exceed 10 lines.
- Submitted manuscripts should not exceed 20 pages including figures and graphs
- Submission should be sent by e-mail – as an attachment – to the following address: komunikacie@uniza.sk.
- The author‘s exact mailing address, full names, E-mail address, telephone or fax number, the name and address of the organization and workplace (also written in English) must be enclosed.
- For all manuscripts a double-blind peer review by at least two independent reviewers and language correction is mandatory.
- After reviewing and incorporating the editor‘s comments, the final draft (before printing) will be sent to authors for final review and minor adjustments.

The full author quidelines are available at:
http://komunikacie.uniza.sk/index.php/communications/guidelines

KOMUNIKÁCIE
COMMUNICATIONS

VEDECKÉ LISTY ŽILINSKEJ UNIVERZITY
SCIENTIFIC LETTERS OF THE UNIVERSITY OF ZILINA
VOLUME 22 Number 1

https://doi.org/10.26552/com.J.2020.1

Editor-in-chief:
Vladimir MOZER – SK

Associate editor:
Branislav HADZIMA – SK

Executive editor:
Sylvia DUNDEKOVA – SK

Honorary members:
Otakar BOKUVKA – SK
Jan COREJ – SK (in memoriam)
Milan DADO – SK
Pavel POLEDNAK – CZ

Editorial board:
Greg BAKER – NZ
Abdelhamid BOUCHAIR – FR
Pavel BRANDSTETTER – CZ
Mario CACCIATO – IT
Jan CELKO – SK
Andrew COLLINS – GB
Samo DROBNE – SI
Erdogan H. EKIZ – SA
Michal FRIVALDSKY – SK
Juraj GERLICI – SK
Vladimir N. GLAZKOV – RU
Ivan GLESK – GB
Mario GUAGLIANO – IT
Andrzej CHUDZIKIEWICZ – PL
Jaroslav JANACEK – SK
Zdenek KALA – CZ
Antonin KAZDA – SK
Michal KOHANI – SK
Jozef KOMACKA – SK
Matyas KONIORCZYK – HU
Tomas LOVECEK – SK
Frank MARKERT – DK
Jaroslav MAZUREK – SK
Marica MAZUREKOVA – SK
Jorge Carvalho PAIS – PT
Peter POCTA – SK
Maria Angeles Martin PRATS – ES
Pavol RAFAJDUS – SK
Che-Jen SU – TH
Giacomo SCELBA – IT
Janka SESTAKOVA – SK
Eva SVENTEKOVA – SK
Eva TILLOVA – SK
Anna TOMOVA – SK
Franco Bernelli ZAZZERA – IT

Address of the editorial office:
University of Zilina
EDIS – Publishing House
Univerzitna 8215/1
010 26 Zilina, Slovakia

E-mail: komunikacie@uniza.sk

Individual issues of the journal can be found on:
http://komunikacie.uniza.sk

Each paper was reviewed by two reviewers.

Journal is excerpted in **SCOPUS** and **EBSCO.**

Published quarterly by University of Zilina in
EDIS – Publishing House of University of Zilina

Registered No: EV 3672/09

ISSN (print version) 1335-4205
ISSN (online version) 2585-7878

ICO 00397 563

January 2020